REGULATION OF GENOME STABILITY VIA MCM2-7 ATPASE ACTIVE SITES IN SACCHAROMYCES CEREVISIAE

by

Sriram Vijayraghavan

Bachelor of Science, Ranchi University, India, 2005

Master of Science, MK University, India, 2008

Submitted to the Graduate Faculty of the

Kenneth P. Dietrich School of Arts and Sciences

in partial fulfillment

of the requirements for the degree of

Doctor of Philosophy

University of Pittsburgh

2014

UNIVERSITY OF PITTSBURGH

Kenneth P. Dietrich School of Arts and Sciences

This thesis was presented

by

Sriram Vijayraghavan

It was defended on

July 17th, 2014

and approved by

Jeffrey Brodsky, PhD, Professor, Biological Sciences

Karen Arndt, PhD, Professor, Biological Sciences

Andrew VanDemark, PhD, Associate Professor, Biological Sciences

John Woolford, PhD, Professor, Biological Sciences, CMU

Dissertation Advisor: Anthony Schwacha, PhD, Associate Professor, Biological Sciences

REGULATION OF GENOME STABILITY VIA MCM2-7 ATPASE ACTIVE SITES IN SACCHAROMYCES CEREVISIAE

Sriram Vijayraghavan, PhD

University of Pittsburgh, 2014

Genome stability is vital to the survival and health of eukaryotic organisms. Consequently, many complex mechanisms coordinate with each other in an intricate fashion to ensure that genomes are preserved during duplication and its subsequent propagation. Despite the vast number of factors involved in these processes, their coordinated regulation hinges on a few key components. One such factor is the eukaryotic replicative helicase Mcm2-7, which is a multi-subunit enzyme complex that unwinds DNA during S-phase and paves the way for nascent DNA synthesis by the polymerases. As an essential and highly versatile replisome component, Mcm2-7 is well-suited as the ideal hub for the regulation of not only DNA replication but other fork-related activities such as S-phase checkpoints and sister chromatid cohesion. While all members of the Mcm2-7 complex are highly conserved and essential in all eukaryotes, their contributions towards DNA unwinding are unequal and distinct, and the *in vivo* functions of most of the Mcm ATPase active sites has remained largely unknown. We conducted an *in vivo* analysis of a viable *mcm2* ATPase active site allele in *Saccharomyces cerevisiae* and found that under conditions of genotoxic stress it is deficient in the DNA replication checkpoint (DRC) activation, upstream of the Rad53/CHK2 effector kinase. Furthermore, this allele also exhibited a peculiar cell-cycle specific DNA damage phenotype and defective sister chromatid cohesion (SCC) under conditions

that are normally conducive to growth. Importantly, these phenotypes manifest from an apparent defect in ATP hydrolysis rather than a qualitative reduction in Mcm2 protein abundance, stability or complex integrity. Therefore, our study demonstrates for the first time that Mcm2-7 can coordinate DNA replication with genome stability through discrete ATPase active sites. Curiously, these functions appear to be separable from general replication defects as shown through a different subset of *mcm* mutants, indicating that different active sites of Mcm2-7 pleiotropically coordinate various aspects of genome integrity during S-phase.

TABLE OF CONTENTS

LIST OF TABLES

LIST OF FIGURES

PREFACE

I sincerely thank my thesis advisor Dr. Anthony Schwacha for all his guidance during this challenging and exciting project. He has always reposed his faith in my abilities and is never short of encouragement and advice whenever I need it. He has helped me identify my strengths and weaknesses as a student researcher and has always strived to steer my research in the right direction. I thank him for his immense patience, and for the liberty he provided to pursue novel ideas throughout the course of this work. His mentorship would stand me in good stead in all my future endeavors.

I thank my thesis committee Dr. Jeff Brodsky, Dr. Karen Arndt, Dr. Andy VanDemark and Dr. John Woolford for their belief in me, and for their constant support and guidance. They have always had sage advice in times of need and helped me in maintaining focus and perspective over the years.

I would like to extend my sincere gratitude towards the yeast and DNA replication research community for their advice and help with strains, reagents and protocols and resources for conducting this research especially Dr. Nancy Kleckner, Dr. William Bonner, Dr. Frank Uhlmann, Dr. Dave MacAlpine, Dr. Kara Bernstein, Dr. Angelika Amon and Dr. Charlie Boone. Additionally, I would like to thank the generous labs of Biological Sciences for all their help whenever it was needed.

I thank all current and past members of the Schwacha lab that I've had the pleasure of working with in the duration of my research, especially Dr. Emily Tsai who pioneered this project, and Dr. Nicholas Simon for being a great friend and colleague over the years.

Finally, I thank all my friends and family, especially my parents for their unconditional love and support. I would be remiss to not mention my wife, the brilliant Dr. Natalie Saini. Words are truly never going to be enough to appreciate her importance to me as a friend, a colleague and a companion for life. Without her, I would have probably never made it this far.

1.0 INTRODUCTION

The precise duplication, maintenance and propagation of genetic material are fundamental events that are indispensable for survival across all domains of life. Most organisms possess elaborate, multi-component pathways that act in a highly coordinated fashion to faithfully preserve their respective genomes. Eukaryotic organisms, in particular, have additionally evolved complex regulatory mechanisms to supervise the manipulation of their genome. Over the years, tremendous progress has been made towards the identification of various factors that play key roles during DNA replication and segregation, even as novel components are consistently being discovered and investigated. Therefore, it has become increasingly important to identify the mechanistic links that connect multiple factors, and ask if there is a unifying mechanism that connects DNA replication to its global maintenance and ultimately its accurate segregation to daughter cells.

The following sections are dedicated to reviewing our current understanding of the overall process of DNA replication in eukaryotes, with special emphasis on the eukaryotic replicative helicase Mcm2-7. Most of the research summarized in these sections focuses on studies done in the budding yeast *Saccharomyces cerevisiae*, with specific references to our knowledge of replication gathered from other model systems as indicated.

Eukaryotic DNA replication- an overview

Although the basic mechanism and components of semiconservative DNA replication are similar in prokaryotes and eukaryotes, DNA replication is a spatiotemporally regulated process in the latter and involves contributions from several additional and novel replication fork components. Additionally, owing to the large sizes of typical eukaryotic genomes, replication occurs at a much slower rate and is strictly monitored by various quality control mechanisms (discussed later). Moreover, in order to preserve genome stability, replication is coordinated with several other cell-cycle specific processes including replication checkpoints and sister chromatid cohesion.

The process of eukaryotic DNA replication can be broadly divided into three main events (details provided throughout the chapter):

1) Initiation
2) Elongation
3) Termination

1) Initiation – During the G1 phase of the cell cycle, Origin recognition complex (ORC) associates with origins of replication. Subsequently, essential factors Cdc6 and Cdt1 promote the loading of the Mcm2-7 helicase at origins through an ATP-hydrolysis dependent mechanism. The origin-loaded Mcm2-7, along with Cdt1, Cdc6 and ORC constitute the pre-replicative complex (pre-RC) (reviewed in [1], **Figure 1**). Notably, to assist in bidirectional replication, two Mcm2-7 hexamers are loaded at each replicative origin. At this stage, the helicase is catalytically inactive and therefore cannot initiate DNA unwinding during G1.

Upon entry into S-phase, the pre-RC undergoes extensive remodeling in a manner dependent on cell cycle kinases. Subsequently, helicase loaders dissociate from the pre-RC, and several additional accessory replication factors (e.g. Sld proteins, GINS, Cdc45) associate with, and aid in the activation of Mcm2-7. The helicase becomes competent to unwind double-stranded DNA at this stage (**Figure 1**).

2) Elongation –The complete replisome progression complex (RPC) is assembled by the inclusion of the replicative DNA polymerases (Pol δ and Pol ϵ), primase/Pol α, sliding clamp (PCNA), topoisomerase, and several fork-stabilizing factors (listed in **Table 1**) that coordinate with Mcm2-7 to synthesize nascent double-stranded DNA throughout replication bidirectionally.

3) Termination – Replication termination, while poorly understood, is believed to occur through several independent mechanisms, including collisions between two opposing forks, passage of forks through replication barriers, or simply by reaching the end of linear DNA molecules [2-5]. The Mcm2-7 complex, along with other replisome components presumably dissociate from DNA and are not loaded until the next cell cycle, thereby limiting replication to once per cell cycle. Additional events such as replication of ends by telomere-associated complexes and resolution of concatenated DNA by Type II-toposisomerases ensure the complete duplication of the genome [6, 7].

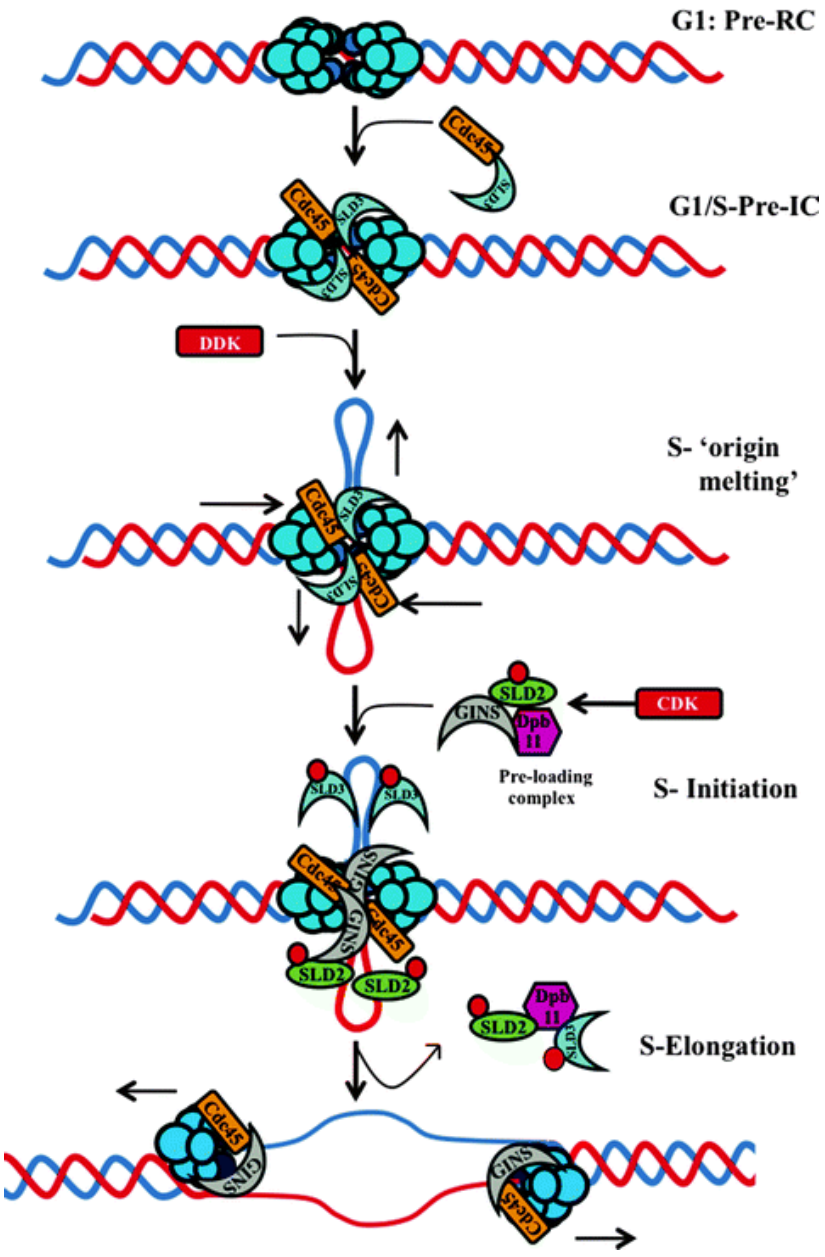

Figure 1. Schematic of eukaryotic DNA replication during initiation and elongation

Refer to text for details. (adapted with permission from [8]).

1.1 PRE-RC FORMATION AND THE MCM2-7 HELICASE

1.1.1 Origins of replication and ORC

DNA replication across all domains of life is initiated at discrete focal points within their genomes called origins of replication, which vary in composition and frequency among different organisms. Typical bacterial genomes initiate bidirectional replication from a singular *ori; E. coli* finishes replication of its 4.6 Mb genome in 20 minutes, with replication occurring at a rate of nearly 1kb/sec [9]. In contrast, the larger eukaryotic genomes replicate at a much slower rate (50 bases/sec), but are nevertheless coordinated in a highly time-regulated manner. This is made possible by the presence of numerous origins of replication interspersed throughout their genome at defined intervals. In the budding yeast *Saccharomyces cerevisiae*, there are approximately 400 origins of replication that are spaced on average 35 Kb apart throughout the 12 Mb genome. Human genomes have been reported to carry nearly a hundred times as many origins as yeast [10].

Although the simultaneous firing of all origins may appear to be the optimal mechanism to replicate chromosomes in eukaryotes, this is seldom observed. Instead, origins display a strict spatio-temporal firing pattern, with some functioning early in S-phase (early origins), while others functioning during the latter half of DNA replication (late/dormant origins). Besides the timing of their activation, this classification of origins is additionally based on several factors including the chromosomal context of the DNA regions surrounding the origins. This includes the nucleosome occupancy and the presence of transcribed genes, which evidently play a crucial role in allowing access to origins of various replication factors, and additionally coordinate with replication forks to avoid frequent replication-transcription clashes [11, 12]. Multiple origins confer distinct

advantages upon regulation of DNA replication in eukaryotes by allowing large genomes to replicate in a finite time within the normal span of the cell cycle. The presence of numerous origins offsets the slow rate of fork progression from a single origin and allows timely genome duplication. If too few origins are licensed to be activated during S-phase, certain replication forks may terminate before they could fuse with forks from such inactive origins and result in large unreplicated regions. Furthermore, in the presence of fork impediments or DNA damage at one or more regions in the genome, activation of previously dormant origins ensures the continuation of replication, thus permitting timely duplication of the genome [13, 14].

Origin structure and context: The original replicon model put forth by Jacob and Brenner suggested that replication is regulated by binding of an initiator (i.e., a trans-acting factor) to a single replicator (i.e., DNA sequence bound by initiator) [15]. Although proposed initially to explain replication of circular bacterial genomes, the subsequent extension of this model to the more complex eukaryotic genomes allowed the search for multiple such sequences that can direct replication of the entire genome as discrete, coordinated units. Although origins are typically AT-rich sequences, a broad consensus on what defines a eukaryotic origin is still a matter of debate, with significant differences observed between lower eukaryote and metazoan origins. In budding yeast, origins are referred to as Autonomous Replicating Sequences (ARS), initially named for their ability to allow yeast plasmids to stably propagate [16]. These sequences are defined by several conserved structural elements [17]. The ACS (ARS Consensus Sequence) element is AT-rich and is defined by a 11 bp consensus sequence that serves as the primary ORC-binding site (see below) [18]. There are several other proximal elements (B1-B3) that play an important, but not individually essential, role in ORC assembly as well as in binding proteins of the pre-RC

including the replicative helicase and helicase loaders (see below) [19, 20]. The multiple elements within ARS regions are also through to contribute to the efficiency of origin usage, as not all origin sequences fire during each cell cycle [21]. In contrast to yeast origins, metazoan origins do not possess any defined consensus sequences and may instead be more structurally related through either repeat elements that allow formation of unusual DNA conformers such as G-quadruplexes, or specific histone modification marks [22, 23]. In *Drosophila*, origin identity has been frequently attributed to regions of the genome that are actively transcribed and are relatively nucleosome free, or bear specific histone variants like H2A.Z [24]. Moreover, ChIP-seq analyses have also found increased abundance of proteins such as the acetylase HBO1 at these regions, which indicates these sites are the preferred choice for formation of the pre-replicative complex [25].

ORC proteins: In eukaryotes, replication origins are bound by the Origin recognition complex (ORC), which is a complex of six distinct AAA+ family ATPases (ORC1-6). ORC was initially identified in budding yeast through glycerol gradient experiments and DNase footprinting assays as a protein that binds the ACS *in vitro* [18]. Paralogs of ORC are found in both prokaryotes, e.g. DnaA [26, 27], as well as in archaea, e.g. ORC1 (reviewed in [28]). Through the course of evolution, most ORC subunits in yeast, with the exception of ORC1 and ORC5, lost the ability to bind ATP, and only ORC1 is capable of hydrolyzing ATP [29, 30]. ORC1,-2,-4 and-5 additionally contain Winged-helix (WH) domains at their C-termini that assist in DNA binding. ORC6 is the smallest protein in the complex and is related to the transcription factor TFIIB [31]. In terms of activity, ATP hydrolysis by ORC1 is crucial for the initial recruitment of licensing factors such as Cdc6 to origins [32]. Regardless of their position on the chromosomes, ORC is initially recruited to all origins in the genome and remains associated through most of the cell cycle. Although the

dynamics of ORC-DNA association are still much-debated, there is emerging evidence that ORC show a preference for negatively supercoiled DNA [33] and rely on specific chromatin cues (e.g. the presence of histone modifications) to interact with origin DNA [34].

1.1.2 The eukaryotic replicative helicase Mcm2-7

DNA replication is crucially dependent on the precise regulation of DNA unwinding, as misregulation of this process can result in the generation of excessive single-stranded DNA without any corresponding DNA synthesis and drastically hamper genome stability. The replicative helicase is the main molecular motor that drives replication fork progression. In eukaryotes, the Mcm2-7 complex acts as the core of the replicative helicase to unwind dsDNA during S-phase. The Mcm2-7 holoenzyme is a heterohexameric complex comprised of six distinct subunits arranged in a toroidal fashion, which give rise to six different AAA+ ATPase active sites at their inter-subunit junctions (**Figure 2**).

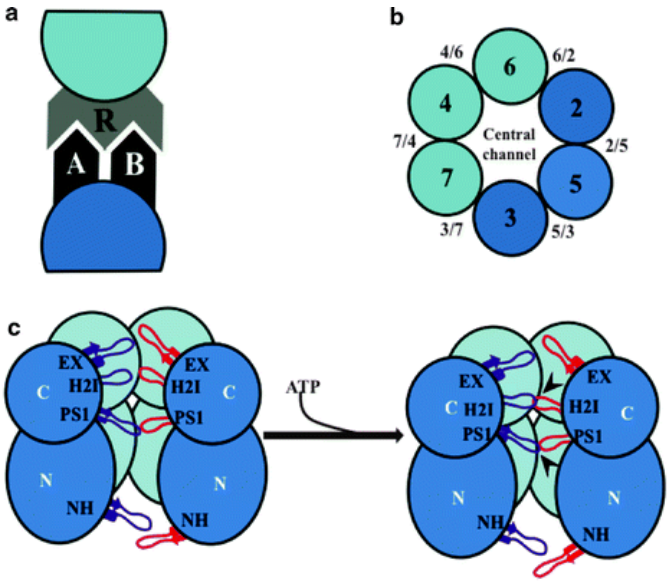

Figure 2. Mcm2-7 helicase ATPase active site organization

a, b) Canonical ATPase active site arrangement at inter-subunit junctions (R- arginine finger, A-Walker A,B-Walker B). c) Cross section of Mcm2-7 showing β-hairpins in the Mcm2-7 central channel. EX- External hairpin, H2I-Helix-2 insert, PS1-pre-sensor 1, NH- N-terminal hairpin. (adapted with permission from [8]).

Discovery and organization - Many of the genes comprising Mcm2-7 were initially discovered in a yeast genetic screen to find mutants defective in plasmid stability (hence the name ***M***ini***c***hromosome ***m***aintenance) [35]. The primary motivation for the screen was to search for replication proteins that can act as *initiators* and participate in the usage of replicative origins (*replicators*). The screen additionally revealed other *MCM* factors that are not a part of the core replicative helicase but are associated with various aspects of replication (*e.g.*, Mcm1, Mcm10). While Mcm2, 3 and 5 were identified from the initial screen, subsequently, other members of the complex were identified in a screen for *cdc* mutants (Mcm 4, 5, 7 as *cdc* mutants *cdc54, cdc46* and *cdc47*, respectively) or in *S. pombe* as segregation mutants (Mcm6 (*mis5+*), reviewed in [36]). These genes were eventually related as members of the same complex by comparing conserved structural motifs (Mcm box) within their sequences, and because of their ability to cause minichromosome maintenance and S-phase defects. Additionally, Mcms were identified as the key replication licensing components in *Xenopus* egg extracts by their ability to associate with and support replication of salmon sperm DNA in a cell cycle specific manner [37, 38]. The interactions among the six proteins has been determined in numerous ways, both genetically through suppression analyses and two-hybrid assays, as well as biochemically through immunoprecipitation and affinity chromatography. Gel filtration experiments have shown that the proteins co-migrate as a hexameric complex of ~600kDa, and additionally as several smaller subcomplexes [39, 40](see below). The precise order of the proteins in the complex was deduced

in later biochemical studies through pairwise dimer-association analyses, the arrangement being Mcm 2-6-4-7-3-5, with Mcm2 and Mcm5 positioned adjacently in the closed ring (**Figure 2**. [41, 42]).

Structure of Mcm2-7- All proteins of the Mcm2-7 complex belong to the diverse AAA+ ATPase family of nucleotide hydrolases (reviewed in [43, 44]). Several other replicative factors including Cdc6, ORC, bacterial DnaA, and the clamp loader RF-C belong to the same class of proteins [45-47]. Member of the AAA+ ATPase family are characterized by a conserved P-loop domain containing Walker A and Walker B motifs in the C-terminal region, which assist in ATP binding and positioning of a nucleophilic water molecule for ATP hydrolysis, respectively [44]. Additionally, the Arginine finger element, present C-terminal to the P-loop contacts the γ-phosphate of ATP and mainly assists in ATP hydrolysis. Some additional features of the Mcm proteins include a zinc finger motif N-terminal to the Walker boxes as well as conserved pre-sensor 1 (PS-1) and pre-sensor-2 (PS-2) loops that are involved in various aspects of MCM-DNA association, including moving the duplex through the central channel (**Figure 2**). Characteristic of ring-shaped AAA+ proteins, ATPase active sites within Mcm2-7 are formed at dimer interfaces; one subunit contributes the Walker A and B motifs, while the adjacent subunit provides the arginine finger to constitute a fully functional active site at inter-subunit junctions. The active sites follow the nomenclature Mcm X/Y, with Y being the subunit providing the Walker A and B motifs to the active site, and X being the arginine finger-contributing subunit (e.g. Mcm6/2).

1.1.3 Mcm2-7 loading and pre-RC assembly

In eukaryotes, the assembly of multi-protein complexes such as the Mcm complex and ORC at origins commences towards the end of telophase and during early G1, whereby replication origins are bound by ORC-Cdc6 (ORC refers to the six subunit ORC complex) [48]. Following this association, origins become competent to recruit the replicative helicase Mcm2-7. This process additionally depends on the association of Mcm2-7 with Cdt1 [49, 50]. Together, these events assist in the loading of inactive Mcm2-7 head-to-head double hexamers to origins of replication that encircle double stranded origin DNA with opposite polarities. The final Cdc6-ORC MCM2-7 assembly at origins in G1 phase is referred to as the pre-replicative complex (pre-RC, see below). It should be noted that helicase loaders such as Cdc6 are AAA+ proteins homologous to the bacterial DnaC [51]. The temporal separation of pre-RC formation and initiation of replication is crucial to ensure that Mcm complexes are not repeatedly loaded during the same cell cycle and trigger re-replication. Details of the above steps are presented below (**Figure 3**).

Formation of the OCM complex - In order to function in replication as a processive helicase, Mcm2-7 rings must be stably loaded on DNA so that they can participate in DNA unwinding over an extended period of time. This process is mediated by a group of closely related proteins including ORC, Cdc6 and Cdt1 (**Figure 3**). In early G1 phase, multiple molecules of the helicase loader Cdt1 associate with individual Mcm2-7 hexamers and assist in their loading at replicative origins [50, 52]. A survey of the role of Cdt1 from multiple systems has demonstrated that Cdt1 is critical for the recruitment of the double hexamers to origins, a role that requires the C-terminal of Cdt1 [53-55]. While initially identified in *S. pombe*, the conserved role of Cdt1 in replication has been studied in various eukaryotes, including *Drosophila*, where *DUP* (*double*

parked) encodes the Cdt1 homolog [56], and *Xenopus* [53]. This initial loading requires the association of ORC-Cdc6 complex with the replicative origins. Cdt1 is crucial in this process as depletion of Cdt1 from cell extracts eliminates Mcm loading at origins without affecting ORC or Cdc6 loading on origin DNA [29, 57, 58]. However, the formation of stable double hexamers on the origin is a complex process that requires ATP hydrolysis by Cdc6 and release of Cdt1 [29]. It should be noted ATP hydrolysis by ORC or Cdc6 is not required for the mere *association* (defined biochemically as salt-sensitive Mcm complexes) of Mcm2-7 complex with origins. However, ATP hydrolysis is required for the stable *loading* of the helicase, with a 'loaded complex' biochemically defined as a salt-resistant protein-DNA complex [57, 59, 60]. The resulting DNA-associated OCM (ORC-Cdc6-Mcm2-7) complex is biochemically resistant to high-salt washes and is capable of forming stable Mcm2-7 double hexamers on origin DNA [32, 61]. This group of origin-bound proteins that are stably loaded on DNA during G1 is referred to as the pre-replicative complex (pre-RC) (**Figure 1,3**, reviewed in [1]). Notably, both ORC and Cdc6 are critically dependent on ATP in order to bind the origin and initiate pre-RC formation [62]. Eliminating Cdc6 ATP hydrolysis stabilizes Mcm2-7–Cdt1 complexes and precludes their loading at origins [29].

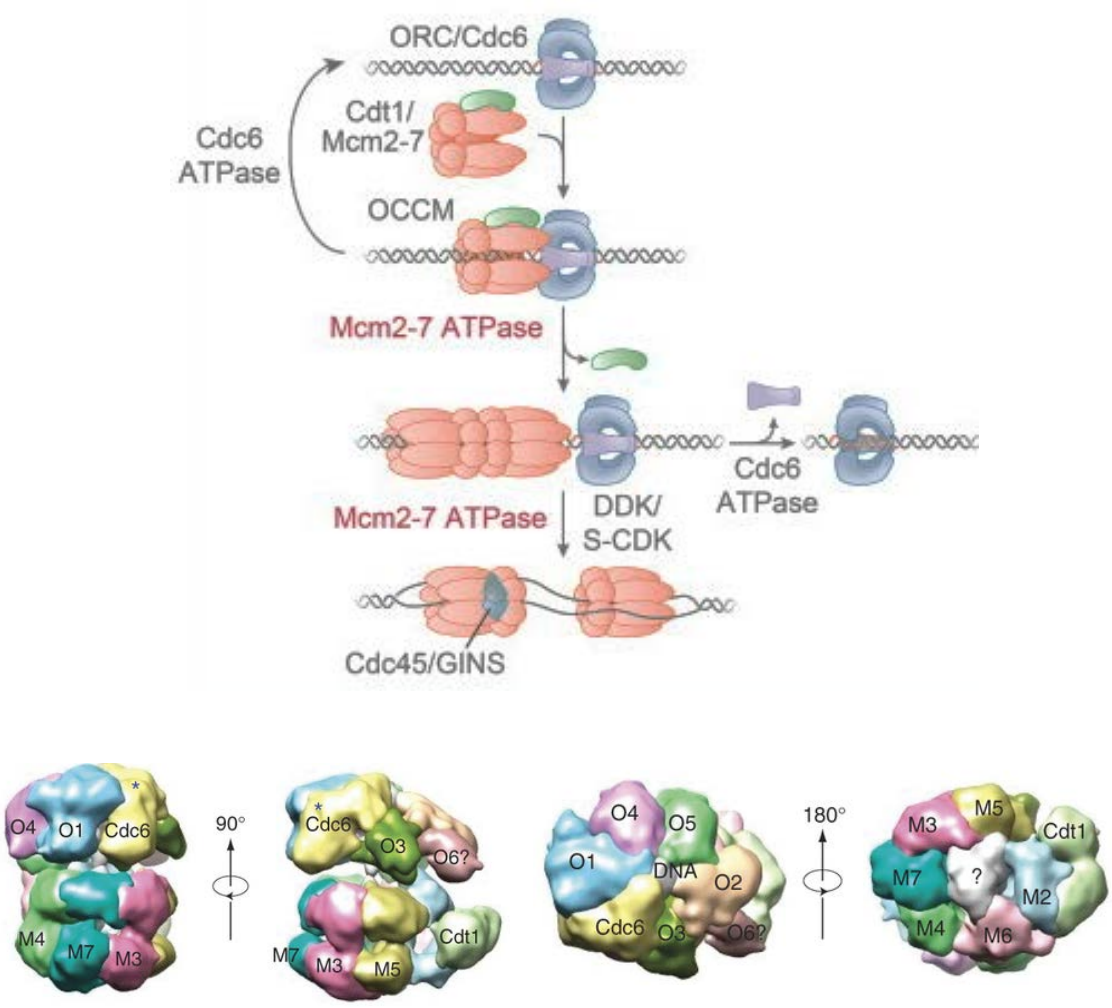

Figure 3. Current model of Mcm2-7 during licensing and pre-RC formation

(Top) Schematic of pre-RC formation. OCCM- ORC/Cdc6/Cdt1/Mcm2-7. See text for details. Adapted with permission from [63]. (Bottom) Cryo-EM reconstruction of the OCCM complex from yeast. Mcm subunits are labeled M2-M7, ORC subunits are denoted as O1-O5. Question mark indicates unknown density that likely corresponds to DNA within the central channel. Adapted with permission from [64].

Stable loading of Mcm double hexamers: Upon departure of Cdc6 and Cdt1 from the initial pre-RC complex, Mcm2-7 loads on double stranded DNA as double hexamers that are aligned in a head-to-head fashion through their N-terminal regions [59, 65]. Because single Mcm2-7 hexamers

have not been observed on DNA, the double hexamers likely load in a concerted manner, with ORC-Cdt1 interactions possibly mediating this loading. Once loaded, these hexamers retain the ability to slide non-directionally on dsDNA and were found to be resistant to salt and DNase, indicating that loaded double hexamers are highly stable [65]. Analogous to the archael double-hexameric Mcm complexes, the N-terminal zinc finger domains of Mcm2-7 are proposed to play a potential role in stabilizing interactions between the double hexamers [66]. The double hexameric Mcm2-7 configuration on DNA has been observed in other eukaryotic systems, including *Xenopus* [67]. While the double hexamers serve an obvious purpose in bidirectional replication via uncoupled sister replisomes, other groups have also proposed the notion of loading several hexamers on origins, which are subsequently shifted away from origins as replication progresses (see **Figure 1**, [65]). Such molecules do not disassemble from DNA but rather have been proposed to come in handy during replicative stress, possibly to aid in fork restart, obviating the need to re-load Mcms [57]. It is worth noting that both the helicase loading factors (Cdc6 and Cdt1) are inactivated prior to S-phase entry, and therefore cells can no longer use them to reload Mcm complexes onto collapsed forks. Therefore, extra pre-loaded Mcm2-7 complexes might be a mechanism to obviate the need for helicase loaders during replication stress, once S-phase is in progress.

How Mcm2-7 complexes transform from being merely associated with origin DNA to being stably loaded double hexamers has been a long-debated issue in the field. However, recent biochemical and structural studies of pre-RC formation has shed new light on the mechanism of Mcm loading. Using an *in vitro* system to study DNA-protein complexes in the presence of various salt concentrations, researchers found that the loading of two Mcm2-7 complexes at origins could

be a sequential process [61]. Initially only a single Cdt1-complexed Mcm2-7 hexamer is loaded on to ORC-Cdc6 bound origins. Cdt1 release upon Cdc6 ATP hydrolysis makes this initial hexamer competent for binding a second Mcm2-7 hexamer. It is currently assumed that this process requires a conformational change within ORC–Cdc6–Mcm2-7 that may arise from DDK-dependent phosphorylation (discussed below, **Figure 3**). Subsequently a second Cdt1-bound Mcm complex may then be recruited to the origin where it stably loads on DNA and associates tightly with the first hexamer possibly after another round of ORC/Cdc6 ATP hydrolysis and Cdt1 release. Similar to the initial loading reaction, the absence of Cdc6 ATP hydrolysis does not preclude the *association* of the second hexamer with origins but prevents its stable *loading*. The various intermediate complexes described above that are formed during the pre-RC assembly have also been recently observed structurally through cryo-EM studies of the yeast OCCM complex (**Figure 3**, [64]) The process of replication initiation (discussed below) is also contingent upon Cdt1 recruitment to ORC, as ablating this association results in the failure of Mcm2-7 recruitment to origins [50]. This interaction also requires Cdc6; it has been suggested that Cdc6 binding imparts a conformational change within ORC6 which allows it to bind Cdt1 and subsequently recruit Mcm2-7.

Despite the above studies, the current model of Mcm2-7 loading remains a contentious subject. In slight contrast to the above reported role of Cdt1 for licensing, it has been recently demonstrated that the initial recruitment of Mcm2-7-Cdt1 to ORC-Cdc6 at origins is mediated through the C-terminus of Mcm3, an event that also promotes ORC-Cdc6 ATP hydrolysis [68]. Moreover, this interaction plays a significant role in detecting incomplete Mcm-Cdt1 complexes and restricts the assembly of non-productive pre-RCs. According to this idea, any sub-optimal

Mcm complexes interacting with ORC-Cdc6 still triggered ATP hydrolysis, which in turn mediated disassembly of such Mcm complexes. Therefore, ATP hydrolysis during origin licensing acts as an internal quality control mechanism that ensures that only fully assembled components participate in pre-RC assembly.

Several recent studies have identified the precise roles of ORC, Cdc6 and Mcm2-7 ATP hydrolysis at various steps in pre-RC formation [63, 69]. While Mcm2-7 ATP hydrolysis being important for the final stages of pre-RC assembly such as double hexamers formation and Cdt1 release [63, 69], Cdc6 ATP hydrolysis helps release non-productive intermediates in the licensing process [69]. A recent model of origin licensing and pre-RC assembly is shown in **Figure 3 (top)**.

1.2 MCM2-7 ACTIVATION AND THE BEGINNING OF S-PHASE

S-phase is triggered by cell cycle specific kinases that activate numerous replication factors and make them competent for participation in replication. Two basic processes that mark S-phase are the unwinding of double stranded DNA by Mcm2-7, which provides the single-stranded templates for the leading and lagging strand polymerases for DNA synthesis. CDK (cyclin-dependent kinase) and DDK (Dbf4-dependent kinase) activate a plethora of factors including the replicative helicase Mcm2-7 [70-72] and several additional initiator proteins such as Sld2 and Sld3 (see below, 'regulation of replication section'). Another key feature of S-phase is the dramatic transformation of Mcm2-7 into a higher order structure called the CMG complex, which is characterized by the association of Cdc45 and the GINS complex with the Mcm2/5 subunits (**Figure 4**,see section on

gate below). The CMG helicase functions as a very robust helicase compared to Mcm2-7 alone and likely functions as the *in vivo* replicative helicase.

1.2.1 Discovery of the CMG helicase

While Mcm2-7 from at least some organisms has demonstrable DNA unwinding activity in the absence of additional factors, it is a weak helicase in isolation [73]. Therefore, it was proposed that additional factors may be required to enhance the robustness of Mcm2-7. The focus of the replication field subsequently centered on Cdc45 and the heterotetrameric GINS complex (**G**o-**i**chi-**n**i-**s**an, Japanese for 5-1-2-3, and refers to Sld5, Psf1-3) [74, 75]. Preliminary studies in yeast demonstrated the importance of these factors to the formation of stable replisome progression complexes (RPC) and S-phase progression, as inactivation of either component led to considerable delays in fork progression, thereby prolonging S-phase [74, 76]. Similarly, depletion of Cdc45 from *Xenopus* extracts was observed to impair elongation [76-80]. While initial attempts at isolating the CMG complex from yeast were precluded by modest protein yields [74], subsequent work with *Drosophila* embryonic extracts successfully led to the isolation of a stable 11-member complex comprising of Mcm2-7 complexed with Cdc45 and GINS through stringent immunoaffinity and fractionation approaches (**Figure 4**) [81]. Biochemical analysis of recombinant mutant CMG complexes also confirmed that the helicase activity of the complex specifically required Mcm2-7 [73]. Overall, these experiments clearly demonstrated a universal requirement for Cdc45 and GINS for replication progression during S-phase.

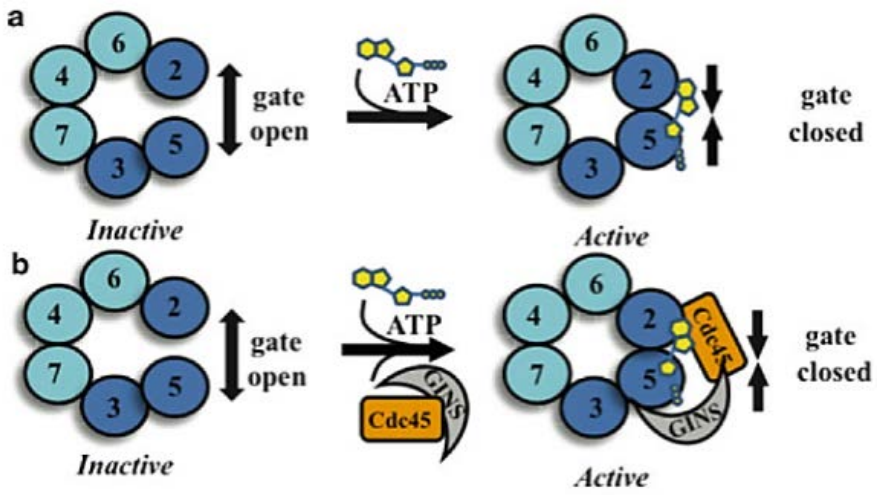

Figure 4. Mcm/5 ATP-dependent gate and CMG helicase

Mechanism of Mcm2-7 gate regulation by ATP binding, Cdc45 and GINS (refer text for details). Adapted with permission from [8].

1.2.2 Mcm2/5 gate opening and closing– implications for helicase loading and activation

Non-equivalence of McmATPase active sites–implications for helicase activity regulation

Although similar in organization to bacterial DnaA and archaeal Mcm helicases, which are also hexameric AAA+ATPase complexes, the eukaryotic Mcm2-7 has several unique qualities that make it a particularly interesting enzyme complex. At present, Mcm2-7 is the only known heterohexameric replicative helicase, while both bacterial and archael replicative helicases are formed from six identical copies of the same protein. Though Mcm2-7 is comprised of six active sites that are formed by a group of very similar proteins, the active sites are not functionally identical (reviewed in [41]). If bacterial, viral and archael replicative helicases are fully capable of unwinding dsDNA using six copies of the same subunit, then why does Mcm2-7 have six different subunits? Extensive mutational analysis of budding yeast Mcm2-7 complexes outlined the nonequivalence of Mcm ATPase active sites.

Using ATP hydrolysis and ssDNA association analyses as a metric for Mcm biochemical activity, it was determined that Mcm2,3,5 make very little contributions to these activities(reviewed in [43]). Furthermore, Mcm3/7 and 7/4 were observed to make the largest contribution to ATP hydrolysis within the complex [41]. Although only two out of the six active sites contribute significantly to the bulk ATP hydrolysis, there is functional inter-dependence among all active sites, as mutating the ATP binding motif (Walker A) in any of the six active sites completely inactivates ATP hydrolysis in Mcm2-7 [82]. On the other hand, DNA unwinding by Mcm2-7 primarily centers on the Mcm4, 6 and 7 subunits, with Walker A mutations in any of these subunits completely eliminating helicase activity [82]. A subcomplex made of Mcm467 was biochemically shown to be able to unwind duplex DNA with a 3'→5' polarity in an ATP-dependent manner [83], an activity that was surprisingly found absent from Mcm2-7 holocomplexes in initial biochemical studies. Therefore, it was inferred that Mcm2,3 and 5 were involved in some unknown regulatory aspect of DNA unwinding. Consistent with this notion, addition of either the Mcm5/3 dimer or Mcm2 monomer was shown to negatively affect the helicase activity of Mcm467 [84]. Furthermore, Mcm4 and 7 were found to be sufficient for DNA unwinding by analysis of Mcm4/7 hexameric complexes [85]. Analysis of Mcm complexes with Walker A mutations in Mcm6 and 7 from *Xenopus* have also been shown to display elongation defects [86], further corroborating the involvement of these subunits in DNA binding. The biochemical studies presented above were paradoxical to several in vivo studies proposing the requirement for all the six subunits throughout replication [78, 87-89].

Discovery of Mcm2-7 helicase activity– The functional differences between Mcm467 and Mcm2-7 biochemical activities were a puzzle in the field for a long time. To solve this issue, the effect of ATP on ssDNA association rates were analyzed for the two complexes. It was found that the Mcm467 and Mcm2-7 complexes significantly differ in their on-rate towards circular ssDNA, with the Mcm2-7/ssDNA association occurring much more slowly [90]. Interestingly, in the case of Mcm2-7 this slow association rate can be relieved by pre-incubation with ATP, resulting in an increase of the on-rate to levels identical to that observed for Mcm467 [90]. In addition, pre-incubation with ATP abolished Mcm2-7 binding to circular ssDNA completely, while simultaneously incubating the purified complex with ATP and DNA drastically increased the association rate [90]. Other groups have also demonstrated that Mcm 467 has >20 times lesser affinity for circular ssDNA than Mcm2-7 [85]. Based on the above DNA binding studies, and by analogy to studies done with archael Mcms [66, 91, 92], it was inferred that Mcm2-7 complex binds DNA via the regulation of a specific active site only present in the holocomplex (discussed below, [90]).

Biochemical and structural analysis of the Mcm 'gate' - The Mcm2/5 gate was biochemically identified based on differences in ATP incubation-dependent DNA binding between Mcm467 and Mcm2-7 [90]. Because Mcm467 poorly bound circular ssDNA regardless of ATP pre-incubation, it was proposed that the differences in Mcm-circular ssDNA association involve the regulation of the remaining subunits Mcm2, 3 and 5. Subsequently, ATPase active site mutations in Mcm2 (*mcm2RA*) and Mcm5 (*mcm5KA*) were found to abolish the ATP incubation dependence of Mcm2-7 for circular ssDNA binding, albeit with opposite effects– the *mcm5KA* mutation causes Mcm2-7 to bind circular ssDNA regardless of ATP pre-incubation, while the *mcm2RA* mutation was seen

to completely block Mcm-7 circular ssDNA association [90, 93]. These results hinted at a putative regulatory 'switch' controlling the open and closed topologies of the Mcm complex. Additionally, dimer association studies showed weak association between Mcm2 and 5 [41, 42]. In combination, these studies provided the primary confirmation for an ATP-dependent 'gate' within Mcm2-7 at the Mcm2/5 junction (**Figure 4**).

With regards to DNA unwinding, Mcm2-7 activity is strongly augmented by large anions such as acetate and glutamate [94]. Addition of these anions seemed to mimic the effects of ATP pre-incubation on Mcm2-7–circular ssDNA association. The fact that this effect was anion-dependent suggested that it most likely occurred through a change within the Mcm2-7 complex and not through an alteration of poly-anionic DNA. The stimulation of helicase activity in the presence of these anions *in vitro* possibly mimics subtle conformational changes that lead to helicase activation *in vivo*, such as the association of Mcm2-7 with accessory factors such as GINS and Cdc45 (**Figure 4**, see below), or those imparted by CDK/DDK phosphorylation of Mcm2-7.

The observation of an ATP-dependent gate within the Mcm complex clearly suggested a mechanistic basis for helicase regulation. While Mcm complexes with an open gate are incapable of unwinding DNA, helicase activity is restored by shutting the gate in an ATP-dependent manner. How is the status of the gate communicated to the Mcm4/7 motor domain? Analysis of the ATPase active sites immediately flanking the Mcm2/5 gate provided important clues towards solving this problem. While the 5/3 and 6/2 (and additionally, the Mcm4/6) active sites have low intrinsic ATP turnover rates, conserved ATPase mutations within these active sites differentially affect the ability of the Mcm complex to interact with ssDNA [93]. Similar to Mcm2/5 mutations, some arginine

finger and Walker B mutations within the 6/2 and 5/3 active sites affect, albeit weakly, the ability of Mcm 2-7 to interact with closed DNA substrates and the ssDNA association rate [93]. Additionally, a *MCM2* Walker B mutation (*mcm2DENQ*) has defective ATP hydrolysis, but is nevertheless viable, suggesting that the 6/2 active site probably lacks a catalytic role towards DNA unwinding [41]. Rather, these sites could potentially be important for communicating the status of the gate to the motor domain allosterically through subtle conformation changes [93].

Because regulation of DNA unwinding is a critical feature of eukaryotic replication, the control of Mcm2-7 activation through an ATP-dependent gate is an attractive model. This has several vital implications– a) Gate opening and closing is directly tied to helicase activation, as mutants that interfere with these directly misregulate DNA unwinding *in vitro*, b) The presence of such a gate may allow the helicase to load on dsDNA during pre-RC formation. This has been recently observed via biochemical analysis of Mcm2-7 complexes in which Mcm2 and 5 were artificially linked to block the gate and analyzed for pre-RC assembly and initiation [95], c) Temporary opening and closing of the gate may allow subtle remodeling of the helicase that would allow it to transition from a dsDNA-bound to its 3→5' unwinding competent ssDNA-bound complex (**Figure 1**), d) Gate regulation is likely involved in unloading of the complex from DNA upon termination of replication, and stalling of the replication fork upon encountering replicative stress or DNA damage.

Structural validation of the Mcm2/5 gate was obtained from EM reconstruction studies of Mcm2-7 in the presence or absence of ATP analogs (**Figure 5**, [96]). While addition of the ATP analog ADP.BeF_3 was seen to cause a subtle shift in the population of Mcm2-7 hexamers to a

constricted gate form (notched), this effect was significantly more pronounced in the context of the CMG helicase. Cdc45 and GINS were found to bind at the Mcm2/5 active site and constrict the opening to more significant degree than was observed with the Mcm2-7 hexamer alone (**Figure 5**). These observations provide a persuasive mechanistic explanation for why the CMG complex functions as a more robust helicase compared to Mcm-7 alone. The interaction of Cdc45 and GINS with the 2/5 gate allows the complex to bind more stably to DNA and likely activates the helicase in S-phase (**Figure 5**). The presence of the gate was more recently confirmed in a recent structural and biochemical analysis of the yeast Mcm2-7 complex, in which Rapamycin-induced Mcm2-Mcm5 fusions were assayed for their ability to participate in pre-RC formation, Mcm loading, cell cycle progression [95].

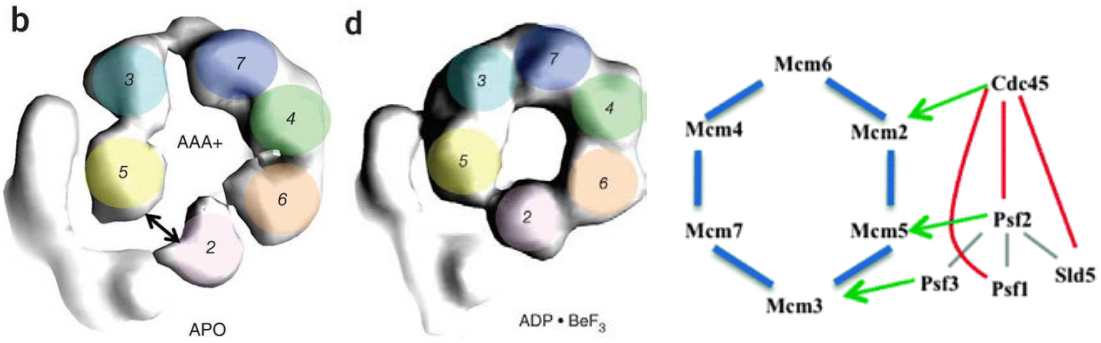

Figure 5. Structural analysis of the CMG complex from *Drosophila*

EM 3D reconstructions showing open and locked forms of the MCM complex in presence and absence of an ATP analog. White density at Mcm2/5 gate correspond to Cdc45 and GINS. Interactions between Mcm subunits, GINS subunits and Cdc45 are shown on the right. Adapted with permission from [8, 97].

Physical contacts among various components of the CMG complex were defined from the above EM studies (**Figure 5**). Both GINS and Cdc45 are situated at the Mcm2/5 gate, where they physically contact Mcm2,3 and 5 subunits [96]. Specifically, GINS associates with Mcm3 and 5

through its Psf2 and Psf3 subunits while contacting Cdc45 through Sld5 and Psf2. While initial contacts between GINS and Mcm2-7 are limited to the N-termini of the Mcm subunits, addition of an ATP analog was seen to extend these interactions to the C-terminal halves of Mcm3 and Mcm5. Together, Cdc45 and GINS serve to bridge the Mcm2-5 gate within Mcm2-7 and in the presence of ATP, shut the gate and activate the helicase (**Figures 4, 5**).

1.2.3 Mechanism of DNA unwinding by Mcm2-7

Various mechanisms have been proposed for the mode of DNA unwinding by Mcm2-7. Analysis of replicative helicases from various prokaryotic and viral replication systems have brought forth three general models (reviewed in [98]):

1) The *strand-exclusion* model, which proposes the extrusion of one strand of the duplex DNA through the outside of the ring and tracking of the helicase ring along the complementary strand. The papillomavirus helicase E1 is an example of such a mechanism where single bases are extruded in a stepwise fashion through the central channel of the complex. This model is supported by the observation that most hexameric helicases tend to prefer binding ssDNA over dsDNA (also see **Figure 1**).

2) A derivation of the strand exclusion model is the *ploughshare* model, that proposes that an element within the helicase acts like a wedge or a 'ploughshare' to separate two strands of DNA ahead of the replication fork as the helicase tracks along single stranded DNA. The evidence for this mechanism can be found in the recBCD helicase of *E. coli* which functions during recombinational repair.

3) *Double stranded pump* model, which proposes that when double hexamers are loaded on DNA, the torsional force generated by the helicases pulls dsDNA through their central channel and the resulting unwound ssDNA is extruded laterally from between the helicases. EM studies carried out with the well-studied SV40 T-Antigen (Tag) helicase support such a model, with micrographs displaying the characteristic 'bunny ears' conformation of the extruded DNA between helicase hexamers [99].

Elegant single molecule studies have recently provided valuable insight into the putative mechanism of DNA unwinding by Mcm2-7. Using the established *Xenopus* cell free replication system, embryo extracts were incubated with flow-cell bound lambda DNA to analyze DNA replication at the single molecule level [100]. By monitoring fluorescently-labeled replicated molecules through TIRF microscopy, the authors were able to effectively rule out the pump model. When both ends of the DNA molecule were tethered to the flow cell, thereby disallowing 'pumping' through the helicase, efficient DNA replication could still be observed, as measured by UTP-digoxigenin incorporation. Under the pump model, no replication would have been possible if both ends of the DNA remain tethered to a surface, which would prevent active pumping of DNA towards and through the helicase. Additionally, shortening of the unreplicated DNA would be observed. Thus, it was effectively demonstrated that sister replisomes, while initially held together, can functionally uncouple during bidirectional eukaryotic replication, which favors the strand exclusion model as the likely mechanism of action for Mcm2-7. Therefore, the requirement for the double hexameric Mcm configuration during replication elongation is unlikely (refer to **Figure 1**).

On a similar theme, subsequent single molecule assays utilizing strand-specific blocks to fork progression unequivocally demonstrated that Mcm2-7 operates as a 3'→5' helicase through strand displacement [101]. *Xenopus* extracts were incubated with DNA substrates containing inter-strand crosslinks to monitor converging replication forks. Specific 'roadblocks' to fork progression were either placed on the leading or lagging strands in the form of either Biotin-SA molecules or Q-Dots on either side of the crosslink and both replication and helicase movement were tracked. In good agreement with earlier studies, Mcm2-7 was found to specifically stall in the presence of the leading strand roadblocks, while preferentially bypassing lagging strand blocks, clearly demonstrating that it functions as a leading strand helicase. Moreover, it further strengthens the case for Mcm2-7 being a strand displacing helicase because a dsDNA pump would be unable to track on DNA in the presence of blocks, regardless of whether they are placed on the leading or the lagging strand.

How are ATP binding and hydrolysis coordinated with DNA unwinding? Although the mechanistic basis of this process is obscure, sequence comparison of Mcm2-7 with other closely related helicases such as the archeael MCM complex suggests that this process may involve several positively charged β-hairpin 'fingers' that extend from each subunit into the Mcm2-7 central channel ([102, 103], **Figure 2**)). In particular, the pre-sensor1(PS1) hairpin and the helix-2 insert (H2I) hairpin that reside within the Mcm C-terminal ATPase active site domain are thought to play a likely role in coupling ATP binding and hydrolysis to DNA binding by the Mcm complex within its central channel ([103, 104], **Figure 2**). In fact, studies with the closely related helicase SV40 Large T-Antigen indicates that pre-sensor 1 hairpin can undergo a striking (~17A°) conformational change in the presence of ATP [102, 105].

Despite the substantial progress made toward understanding the unwinding mechanism of Mcm2-7, it is unclear whether unwinding is solely dependent on the helicase or whether additional replisome components assist the helicase in the process. Some recent studies have closely analyzed the contribution of Cdc45 to active DNA unwinding. Structurally, Cdc45 shows close homology to the bacterial protein RecJ which is a 5'→3' exonuclease [106]. Though Cdc45 does not possess any demonstrable nuclease activity, recent biochemical investigations have shown that Cdc45 has a predilection for long ssDNA tracts (>80 nt), apparently with little sequence specificity [107, 108]. This feature of Cdc45 is particularly important in replication stress where it can bind ssDNA and help the helicase to stall. Cdc45 mutants have been reported to uncouple CMG from the polymerase, resulting in long RPA-coated ssDNA tracts [107]. Moreover, Cdc45 can efficiently bind ssDNA-dsDNA junctions as are observed in branched replication intermediates. Additionally, Cdc45 is capable of sliding on DNA with a 3'→5' polarity, akin to the polarity of CMG [108]. These data imply that Cdc45 may contribute to DNA unwinding by acting as a wedge to pry apart ssDNA tracts generated by the ATP-dependent motor activity of Mcm2-7.

Role of the Sld proteins in helicase activation- From studies in budding yeast, it was found that one of the earliest events in S-phase is phosphorylation of the Sld2 and Sld3 proteins by the cyclin dependent kinase CDK, also known as Cdc28 in budding yeast [109]. During helicase activation, the Sld proteins essentially play the role of chaperones to assist in the assembly of the pre-initiation complex consisting of the CMG helicase and several other proteins needed for elongation. Sld3 is a homolog of the Treslin/Ticrr protein found in vertebrates [110]. Sld3, along with its partner Sld7 binds Cdc45 and initially recruits it to Mcm2-7 in form an intermediate complex called CMS (Cdc45/Mcm2-7/Sld3) (**Figure 1**) [111]. The Sld2 protein on the other hand interacts with GINS.

Upon phosphorylation, both Sld2 and Sld3 undergo similar conformational changes that expose domains which are bound by tandem BRCT repeats of the protein Dpb11, which is a homolog of the human TopBP11 protein [112-114]. While this interaction disrupts Sld3-Cdc45 binding, it helps guide Sld2-GINS to the Cdc45-bound Mcm2-7 and promotes assembly of the CMG replicative helicase. Additionally Dpb11 further binds additional factors such as the leading strand polymerase Polε. The quarternary complex formed by Sld2, Dpb11, GINS and Polε is also referred to as the pre-loading complex (pre-LC) (**Figure 1**) [115]. In combination with Sld3-Cdc45-Mcm2-7, this multi-protein assembly constitutes the pre-initiation complex (pre-IC) (**Figure 1**) [116]. CDK phosphorylation of Sld3-Sld7 and Sld2 lead to their dissociation from this complex and the assembly of CMG (**Figure 1**, see below).

Biochemically, Sld2 and Sld3 have ssDNA binding activities, which have important implications in their role during initiation of DNA unwinding in the following manner: Sld2 and Sld3 bind with high affinity to ssDNA at early origins of replication *ARS* and *ARS305*, and importantly, they bind to complementary DNA strands [117]. *In vitro*, Sld3-ssDNA association weakens the interactions between Sld3 and Cdc45 and Mcm2-7 which may help destabilize CMS and allow CMG formation, since the dissociation of Sld3 from CMS is a pre-requisite for GINS binding. Therefore, Sld2 and Sld3 seemingly play key roles in Mcm2-7 remodeling during S-phase, allowing both assembly of the active CMG helicase, and limited unwinding at origins (origin melting, **Figure 1**) that permits the helicase to transition from a dsDNA-bound form to an ssDNA-bound form.

A unifying model for DNA unwinding by Mcm2-7- In light of the above recent findings, it is necessary to revisit the mechanism of DNA unwinding by the Mcm complex. Though strand exclusion is the most likely mechanism for helicase progression, the mechanism that converts the dsDNA bound CMG to its ssDNA-bound unwinding competent form remains under investigation. The intriguing possibility is that CMG assembly occurs on partially melted origin DNA which may be generated through a particular conformation of Mcm2-7 within alternative complexes like the pre-LC. Alternatively, it can be speculated that the initial phosphorylation and activation of Mcm2-7 may briefly allow it to unwind origin DNA (origin melting) by a limited, pump-like mechanism, which then generates two complementary single DNA strands (**Figure 1**). It should be mentioned that in the *E. coli* replication system, limited origin unwinding is initially performed by the activity of the origin-binding DnaA initiator proteins themselves [118], whereas a similar role for ORC-Cdc6 has not been observed in eukaryotes. Sld2 and Sld3 might associate with their respective complementary ssDNA strands and help to laterally extrude them. This produces additional conformational changes that allow CMG assembly and, ultimately, separation of the double hexamers. During this process, the Mcm2-7 complex presumably opens and reseals its 'gate' active site transiently to encircle ssDNA (**Figure 1**). Newer studies have also linked other proteins to the limited DNA unwinding activity observed during origin firing, such as Mcm10 which is an essential replisome component that is required to stabilize Polα/primase at the replication fork [119, 120].

1.2.4 Additional members of the eukaryotic replisome

Eukaryotes additionally assemble a vast number of proteins at active replication forks, which all closely coordinate with the DNA unwinding components discussed above (reviewed in [1]). The eukaryotic replisome consists of leading and lagging strand polymerases, the clamp and clamp loader, PCNA and RFC, respectively, topoisomerases I and II, primase/Polα, ssDNA binding protein RPA, DNA ligase and numerous other factors. Notably, many factors with roles beyond replication also closely associate with replication forks, such as proteins involved in the intra-S phase checkpoint Mrc1,Tof1 and Csm3 (Claspin, Tim, Tipin in higher eukaryotes) [121-124], the cohesin complex that is involved in sister chromatid cohesion [125], and DNA repair factors such as Fen1 that help in fork recovery when DNA damage is encountered during elongation [126]. Although there is broad conservation among eukaryotes with regards to the main replisome components, higher eukaryotes have evolved additional factors which help in replisome maintenance and stability. A summary of various factors involved at the different steps of eukaryotic replication can be found in **Table 1.** While most of the proteins found in yeast are conserved across Eukarya, additional factors that are only found in higher metazoans are also listed in **Table 1**.

Yeast	Higher eukaryotes	Function	Selected references
Mcm2-7	MCM2-7	Core of the replicative helicase, unwinds DNA in S-phase	[39, 43, 94]
pre-RC formation			
ORC 1-6	ORC1-6	Origin-binding, pre-RC formation	[18, 127]
Cdc6	CDC6	Helicase loading,	[29, 61, 128, 129]
Cdt1	CDT1	Mcm2-7 recruitment to origins	[49, 50, 54]
	Geminin	Cdt1 inhibition	[130, 131]
Dia2	?	F-box protein, binds to origins and regulates S-phase entry	[132]
Initiation and Elongation			
Sld2	RECQ4?	Interacts with GINS and Pol E through Dpb11 and recruits them to site of initiation, activated by CDK	[112, 114, 133]
Sld3	Treslin/Ticrr	Interacts with Cdc45 and recruits to Mcm2-7, activated by CDK	[107, 134, 135]
Sld7	?	Partners Sld3 in recruiting Cdc45 to Mcm2-7	[136, 137]
Dpb11	TOPBP1	Interacts with Sld2 and Sld3 through BRCA repeats	[138-140]
Pre-initiation complex and fork progression			
GINS	GINS	Accessory subunit of helicase, binds to Mcm2-7 and activates it	[74, 80, 141, 142]

Cdc45	CDC45	Accessory subunit of helicase, binds to Mcm2-7 and activates it	[77, 142, 143]
Pol ε	POLϵ	Leading strand polymerase	[144, 145]
Pol δ	POLδ	Lagging strand polymerase	
Primase/Polα	POLα	Synthesis of short RNA primers during replication	[146]
	DUE-B	pre-IC formation	[147]
	GEMC1	TopBP1 loading	[148]
Mcm10	MCM10	Bridges primase and helicase, potentially involved in helicase unloading at the end of S-phase	[119, 149-151]
	Mcm8-9	Implicated in helicase loading, elongation	[152, 153]
Ctf4	AND-1	Recruits primase to DNA along with Mcm10, assists in primase-helicase interaction	[154, 155]
S-phase regulatory kinases			
Cdc28	CDK1	Main S-phase cyclin (CDK), activates many replication factors	[109, 114, 139, 156, 157]
Clb5	Cyclin B2/B1	B-type cyclin, activates Cdc28 during initiation	[158, 159]
Cdc7	CDC7	Kinase subunit of DDK, involved in Mcm2-7 activation in S-phase	[70, 160-165]
Dbf4	DBF4	Regulatory subunit of DDK, involved in Mcm2-7 activation in S-phase	
Additional elongation factors			
Yra1	THOC4	Interacts with Pol δ, Dia2.	[166]

		Required for S-phase entry	
RPA (RFA1-3)	RPA 70,32,14	Single-stranded DNA binding protein	[167]
Pol30	PCNA	Sliding clamp for replicative polymerases	[168-170]
RF-C	RFC	Clamp loader	
Elg1	ELG1	Clamp 'unloader'	[171]
Ctf18	CTF18	alternative clamp loader, also functions in SCC and checkpoint	[172, 173]
Top1,2	TOPO1,2	Topoisomerases, relieve torsional stress during unwinding, function during elongation and termination	[6, 174, 175]
Mcm10	MCM10	Bridges primase and helicase, potentially involved in helicase unloading at the end of S-phase	[119, 149, 150]
	Mcm-BP	Implicated in helicase unloading	[176]
Fen1	FEN-1	Flap endonuclease, processes Okazaki fragments	[177, 178]
Checkpoint factors			
Mrc1	Claspin	Part of the MTC mediator complex that senses replication stress, also bridges Pole and Mcm2-7	[121, 123, 179, 180]
Tof1	Tim	Part of the MTC mediator complex that senses replication stress	
Csm3	Tipin	Part of the MTC mediator complex	

Mec1	ATR	Sensor kinase in checkpoint response, takes part in Mcm2-7 activation during S-phase, mediates replication fork termination	[3, 181]
Sister chromatid cohesion			
SMCs/cohesin (Smc1,3)	SMCs	Maintenance of sister chromatid cohesion during S- and G2 phase	[182-186]
α-Kleisin (Scc1)	SCC1	Connects Smc1 and 3 to make the tripartite cohesin ring	
Scc2,4	SCC2,4	Loading of cohesin on chromosomes in G1	
Eco1	Esco1	Acetylates Smc3 and establishes cohesion	

Table 1. Eukaryotic replication factors

1.3 REGULATION OF DNA REPLICATION

1.3.1 Replication regulation by CDK and DDK

A strict temporal regulation of eukaryotic DNA replication is compulsory for avoiding genomic instability. The bacterial replication machinery initiates the next round of nucleoid duplication before completion of cytokinesis [187]. In contrast, eukaryotes carefully separate DNA replication (S-phase) from chromosome segregation (M-phase) to prevent errors in either process and ensure that each daughter cell receives one and only one complete genome per cell cycle.

Accordingly, Mcm2-7 activity is heavily targeted by multiple regulatory mechanisms due to its vanguard role at the replication fork.

As previously stated, eukaryotes harbor complex genomes distributed across multiple chromosomes, with each of these units containing several active origins of replication. Cells are only allowed to load pre-RCs on origins during the G1 phase and 'fire' these origins in S-phase. This temporal sequestration of loading and activation events ensures that multiple replication factors work in perfect synchrony in a mutually exclusive manner and restrict replication to only one round per cell cycle. How do cells maintain this temporal order of events? S-phase specific cyclin-dependent kinases (CDKs) and the Dbf4-dependent kinases (DDK) play a major role in implementing this temporal program (**Figure 1**).

In eukaryotes, an increase in cyclin-dependent kinase activity signals the start of S-phase and triggers DNA replication. In yeast, Cdc28 is the predominant S-phase CDK. Along with cyclin Clb5, it primarily phosphorylates Sld2 and Sld3, which promotes their interaction with Dpb11 and assists in the subsequent assembly of the CMG and other replicative factors such as Polε on DNA (Refer to **Figure 1**) [112]. The association of the S-phase CDK with specific cyclins precludes RPC assembly in G1. A similar mode of S-CDK action is also observed in the fission yeast *S. pombe* [188]. As a further means to prevent reloading of Mcm complexes on origins during S-phase, CDK associates with ORC6 via a conserved RXL motif which prevents recruitment of Cdt1-Mcm2-7 in a phosphorylation-independent manner, possibly through steric interference [189]. Subsequent phosphorylation of Orc2 and Orc6 then leads to inhibition of Mcm2-7 loading [190]. CDK mediated phosphorylation of Cdc6 results in its degradation, mediated by the SCF

family of E3 ubiquitin ligases [191]. Moreover, CDK phosphorylation also occurs on unbound Mcm2-7, which leads to their nuclear export [192]. Therefore, CDK utilizes multiple means to control replication timing and activation (also see [190, 193]).

Phosphorylation of specific pre-RC components by the Dbf4-dependent kinase (DDK) represents an indispensable step in S-phase initiation. DDK is a heterodimeric enzyme complex consisting of Cdc7 and Dbf4 [161, 162, 194]. In budding yeast, various DDK-phosphorylation sites have been described on the N-terminal tails of Mcm2, Mcm4 and Mcm6, which become phosphorylated in S-phase [195, 196]. Interestingly, there are additional phosphorylation sites on these proteins which are required for pre-RC 'priming' by different kinases prior to DDK activation. Although the identity of such priming kinases is still under investigation, the ATR homolog Mec1 as well as CDK are the prime candidates for this regulatory event [181]. In terms of its role in helicase activation, DDK phosphorylation likely produces conformational changes within Mcm2-7 that either alleviate inhibitory interactions or promote favorable association of the helicase with other replisome components such as Cdc45 and GINS (**Figure 1**, [70, 165]). To ensure DDK activation is limited to S-phase, the regulatory Dbf4 subunit is specifically targeted for ubiquitylation and subsequently, proteasomal degradation by APC/C in G2/M [197].

In summary, CDK and DDK-mediated phosphorylation of various replication factors in S-phase prevent re-replication and ensures genomic stability through multiple means.

1.3.2 S-phase DNA replication checkpoints

The replication fork frequently encounters impediments during the process of elongation. These are typically in the form of fork stress such as nucleotide depletion, or because of physical damage to the DNA ahead of the replication fork, which may be in form of ssDNA– or dsDNA breaks. Misregulated replication through such types of damage would be detrimental to the repair process and likely lead to the irreversible loss of genetic information. Eukaryotic cells have evolved various mechanisms to deal with such fork impediments. First and foremost, fork progression must be completely halted so as to prevent it from continuing past a lesion or another fork obstacle. Secondly, repair mechanisms that process the challenge(s) presented to fork progression and repair them before replication restart must be activated in a timely manner. If left unrectified, fork-related damage is severely detrimental to the integrity of the genome. Genomic instability and segregation errors arising from fork misregulation are often the underlying source for a wide range of human diseases, including cancer.

How are these processes coordinated? Our best understanding of this process comes from *S. cerevisiae*, where genotoxic signals are sensed by an intra-S phase checkpoint mechanism. Upon encountering replication stress, a signaling cascade is activated that senses stress through a concerted kinase activation cascade. Stress signals in this pathway are initially sensed and relayed downstream by phosphoinositide-3'-kinases (PI3K) Mec1–which is the yeast homolog of the well-known metazoan protein ATR, as well as the closely related Tel1–the yeast homolog of the mammalian ATM kinase [198, 199]. In budding yeast, the intra-S-phase checkpoint is further divided into two partially redundant sub-pathways that differentially sense replication fork stress (**Figure 6**): a) the DNA replication checkpoint (DRC) is specifically involved in sensing stress

arising from nucleotide shortage, such as that induced by drugs like hydroxyurea (HU)[200], b) the DNA damage checkpoint (DDC) monitors DNA lesions that are generated by endogenous forces, or through exogenous stressors such as the DNA alkylating chemical methyl methanesulfonate (MMS) [201, 202]. The DRC pathway involves activation of Mrc1 (Claspin in vertebrates) [203], which once phosphorylated triggers downstream factors that eventually activate the effector kinase Rad53 (CHK2 in mammals). Hyperphosphorylated Rad53 can, in turn, activate numerous factors related to cell cycle control, transcription and DNA repair, in addition to stabilizing replication forks [204, 205]. For its role in transducing the signal between Mec1 and Rad53, Mrc1 is considered a mediator protein in the checkpoint signal transduction cascade. Similarly, the DDC pathway utilizes a mediator protein called Rad9 which binds to and activates Rad53, leading to analogous downstream responses seen with the DRC pathway (**Figure 6**, [206]).

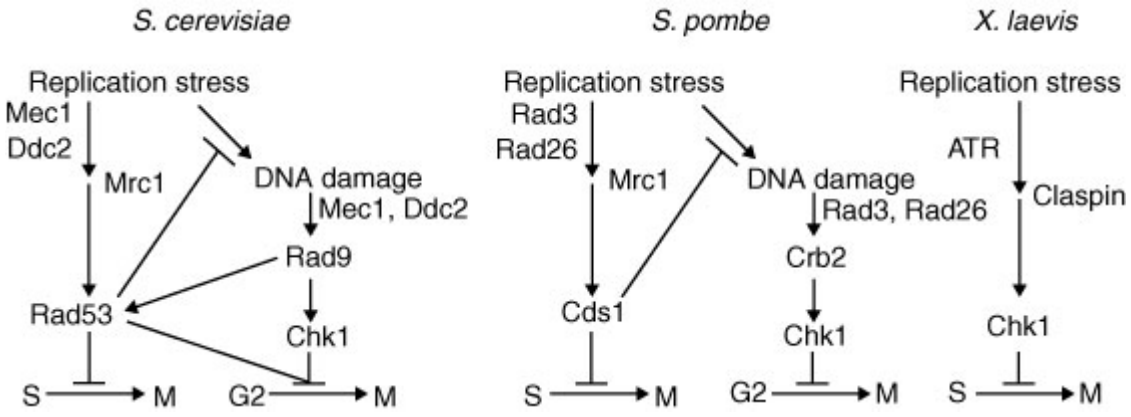

Figure 6. Intra-S phase checkpoints in different organisms

(Adapted with permission from [203]).

Mrc1- dual role in replication and checkpoint activation– Despite their overlapping roles in the checkpoint response, there is a key difference between the mediators of DRC and DDC. Unlike Rad9, Mrc1 also travels with the replication fork as part of a heterotrimeric complex

consisting of Mrc1, Tof1 and Csm3 [179]. As part of this complex, Mrc1 associates with key components of the replisome such as Mcm2-7 and the leading strand polymerase Polε [121]. In fact, Mrc1 is required to couple the helicase and polymerase, because absence of *MRC1* results in continued unwinding in the absence of DNA synthesis, which eventually results in fork collapse [123]. Importantly, the role of Mrc1 during normal DNA replication and during checkpoint activation are separable, as was demonstrated by mutating Mec1 phosphorylation SQ/TQ sites on Mrc1 [123]. Although this mutant (*mrc1AQ*) failed to activate Rad53, it associated with replication forks normally and progressed through S-phase with wild type kinetics, clearly showing that Mrc1 plays a checkpoint-independent role during unchallenged growth conditions. Regardless of the role of Mrc1 in replication, Mec1-dependent phosphorylation of Mrc1 is necessary for an appropriate response to replication stress; *mrc1AQ* mutants not only lack phosphorylation but additionally fail to recruit Mec1 to replication forks during replication stress [207]. While this indicates that phosphorylated Mrc1 somehow manages to stabilize Mec1 at replication forks, these observations imply additional roles for Mec1 during replication other than simply acting as a sensor kinase (refer to section on replication termination).

Analysis of checkpoint mutants under challenging growth conditions with HU or MMS treatments typically demonstrates aberrant fork structures, accumulation of ssDNA tracts, and failure to complete replication, all of which cumulatively contribute to elevated cell death in such mutants [200, 208]. Under these conditions, failure to activate the Rad53 effector kinase severely affects replication due to an inability to mount a checkpoint response; Rad53 in part seems to primarily stabilize replication forks through a mechanism that depends on the DSB repair exonuclease Exo1 [209, 210], as deleting *EXO1* in a *rad53*-null background can completely

suppress the lethality of this strain over a wide range of DNA-damaging treatments [211]. Importantly, this effect is not observed in the presence of HU, with *exo1rad53* double mutants exhibiting an inability to restart stalled forks similar to *rad53* alone. Therefore, Rad53 additionally has an Exo1-independent function at replication forks.

On the other hand, Mec1 serves a more important role in replication fork dynamics in the presence of exogenous stress, as is evident with the more severe phenotypic defects seen with *mec1* mutants. While *mec1* mutants fail to finish replication in the presence of HU much like *rad53* mutants, they display much more severe fork defects and are more sensitive to genotoxic agents compared to *rad53* mutants. Moreover, in contrast to *rad53*, deletion of *exo1* does not rescue *mec1* lethality in the presence of DNA damaging agents [211]. These observations further supports a Rad53-independent role for Mec1 at the replication fork.

Multiple targets of Mec1 in replication- Even though certain targets of Mec1-dependent phosphorylation are well-characterized (*e.g.*, Mrc1), it is conceivable that additional replisome components are subject to Mec1 and/or Rad53-mediated phosphorylation under different genotoxic challenges. Various proteome-wide searches have been conducted to identify targets of checkpoint kinases in yeast [212, 213], with specific studies focusing on Mec1 targets having identified >300 putative substrates that carry the canonical SQ/TQ phosphorylation sites [214]. Further functional classification of these targets identified multiple putative Mec1 (and Tel1) substrates at the replication fork [215], which supports a broader role for Mec1 in stabilizing the replication fork during challenged growth. A list of the various targets of Rad53 and Mec1-mediated phosphorylation is reviewed in [216].

1.3.3 The role of Mcm2-7 in replication checkpoint

As described above, the main purpose of the checkpoint machinery is likely to halt replication fork progression in the presence of replication stress or DNA damage. Therefore, it is conceivable that such regulation involves interaction of checkpoint factors with the molecular motors that power fork progression. A prime candidate for regulation is the replicative helicase Mcm2-7, as unregulated DNA unwinding can lead to the generation of long tracts of ssDNA which may potentially give rise to DNA damage. However, the involvement of Mcm2-7 in checkpoint response is only marginally understood. Many studies support the idea that Mcm2-7 and its associated factors are directly regulated by checkpoint kinases. Mec1 can specifically phosphorylate Mcm4, which is important for S-phase activation of Mcm2-7 and is potentially crucial for regulating replication in the event of DNA damage or fork stalling [217]. Furthermore, *in vitro* phosphorylation of Mcm3 and Mcm4, as well as the GINS subunit Psf2 by Chk2 (yeast Rad53 homolog in metazoans) in *Drosophila* was seen to inhibit CMG helicase activity, indicating that the mechanism of helicase regulation by checkpoint kinases could be conserved among yeast and higher eukaryotes [218].

Previous studies have shown association between Mcms and checkpoint factors Mrc1, Tof1 and Csm3 (MTC complex, refer to **Table 1**) both in the presence and absence of replication stress [179]. In particular, a detailed analysis of Mcm-Mrc1 interaction in budding yeast identified Mcm6 as the major binding partner of Mrc1 [219]. This interaction is physiologically important, as *mcm* mutants ablated for the Mrc1-interacting domain were found to poorly mount the checkpoint response in the presence of DNA damaging chemicals, in addition to displaying multiple cell cycle defects. It could be inferred from these observations that Mcm2-7 may have a

role in sensing DNA damage and/or coordinating an appropriate checkpoint response through interactions with specific checkpoint mediators. Mrc1 has been further documented to stabilize Polε during replication stress through direct interactions with the C-terminus of Pol2, which is the largest subunit of Polε [220]. Furthermore, a recent study suggested that components of the DNA repair machinery can regulate the temporary dissociation and reassembly of the CMG complex during replicative stress, particularly through their interactions with GINS [221]. Overall these studies suggest that proper checkpoint response relies on the coordination between DNA unwinding and synthesis through precise protein-protein interactions at the replication fork.

1.4 REPLICATION ELONGATION AND TERMINATION

1.4.1 Replication elongation and Mcm2-7

Replication progression requires coordination among the different molecular motors at the replication fork to ensure synchronous unwinding and DNA synthesis. As a *bona fide* member of the replisome progression complex, Mcm2-7 is precisely coordinated during S-phase to ensure proper elongation. Initial insights into the role of Mcm2-7 in elongation emerged from chromatin immunoprecipitation (ChIP) studies of Mcm4 that demonstrated association with intra-origin regions in a cell cycle specific manner (reviewed in [1, 222]. Additionally, CMG constituents have been found associated with artificially paused replication forks using the *Xenopus* replication system, and the **R**eplisome **P**rogression **C**omplex (RPC) that includes Mcm2-7, isolated from yeast was shown to be obligatorily dependent on all its constituents for fork progression [74, 87, 223]. Moreover, inactivation of Mcm2-7 using *mcm* degron alleles during initiation was sufficient to

block replication fork progression in yeast, further demonstrating that Mcm2-7 plays a vital role in elongation [88]. Such observations imply that Mcm2-7 likely coordinates with other replisome components such as polymerases to control fork progression. An inter-dependence between polymerases and replicative helicases has been studied biochemically in many other systems including T7 phage and *E. coli* [224, 225], and has been recently elucidated through a structural analysis of different replisome components in yeast [226]. It is conceivable that coupled motors would be more processive on DNA in comparison to individual ones. For example the DnaB helicase unwinds dsDNA at a ~20-fold faster rate as a part of the PolIII-DnaB-Tau complex than DnaB alone [227].

As mentioned earlier, Mcm2-7 and the leading strand polymerase Polε are coupled through Mrc1. Removal of Mrc1 physically compromises replication forks, which manifests as DNA double strand breaks during S-phase (see below, [203]). The CMG complex and the leading strand polymerase Polε have also been shown to directly interact via binding of the Dpb2 subunit of Polε to the Psf1 subunit of GINS [228]. It is less clear whether there is a similar association between the lagging strand polymerase Polδ and the CMG complex; addition of purified Polε but not Pol δ to the CMG complex significantly increases its processivity [229].

Additionally, the helicase is coupled to the primase/Polα via Mcm10 [149]. In addition to stabilizing primase-helicase association by interacting with the catalytic subunit of Polα, along with Ctf4, Mcm10 has been proposed to play a limited but important role during initiation, possibly by contributing to origin unwinding [150]. However, Mcm10, while associated with loaded Mcm2-7 complexes during initiation, is not associated with the replisome progression complex (RPC)

during elongation, as demonstrated by using degron alleles of Mcm10 in yeast and subsequently analyzing RPC components. Additional evidence for the role of Mcm2-7 in elongation comes from the analysis of Mcm10-Polα interactions, as an elongation defect in a *mcm10* mutant was shown to be suppressed by an *mcm7* mutation [149].

1.4.2 Replication termination and Mcm2-7 regulation

Despite the advances made in elucidating the molecular mechanism of the early steps of replication and elongation, termination in eukaryotic replication remains a poorly-understood process. Unlike *E. coli*, where specific Tus-ter sites mediate replication termination from bidirectional forks emerging from a single origin [230], there are no consensus eukaryotic termination sites. Early studies in yeast identified a limited number of genomic loci corresponding to termination sites, *e.g.*, the rDNA locus on Chr XII, which tends to make replication forks unstable [231]. Such stretches of DNA can inherently act as replication fork barriers (RFBs) and may also represent sites of converging replication forks [232]. In addition, forks are frequently seen to stall at other chromosomal regions such as CEN sequences present at centromeres, and Ty elements [233, 234]. Other groups have identified Replication slow zones (RSZs) that halt replication forks passing through them. Mec1, which is the ATR homolog of yeast, is proposed to play an important role in regulating fork passage through such RSZs, as *mec1* mutants accumulate considerable replication-dependent DNA damage at these loci, presumably from an inability to stall forks at RSZs [3]. However, the nature of the relationship between putative fork-pausing sites and replication termination remains controversial.

A recent genome-wide survey of replication fork stalling loci revealed a number of potential termination regions in the yeast genome [2]. By monitoring convergent BrdU peaks from neighboring origins in synchronized yeast populations, researchers were able to estimate the extent of termination events throughout the yeast genome. These potential termination sites spanned an average of 5kb of DNA. More than half of the sites identified corresponded to previously-recorded replication pause sites, as observed by Polε occupancy, and many sites were frequently associated with high transcriptional activity. The latter could represent another mode of replication termination, mediated by collisions between the replication forks and the transcription machinery.

Merging replication forks would result in the formation of distinct X-shaped DNA structures, which represent replicated catenanes, structures that are considered obligatory intermediates for termination [7, 235]. In order to resolve these structures and separate the newly replicated molecules, additional factors are involved during termination. Such catenated double stranded structures are exclusively resolved by Type-II topoisomerases [6, 236]. In yeast, Top2 is an essential Type II topoisomerase that travels with the replication fork to relieve supercoils generated from DNA unwinding and has been shown to play a role in resolution of catenated DNA molecules during replication termination [6]. Top2 was found to be necessary for the fork breakage observed in *mec1* mutants at Chromosome III fragile sites/RSZ [236]. Through analysis of replication intermediates via 2D gel electrophoresis, Top2 mutants were further found to accumulate X-shaped structures at numerous putative termination sites [2]. Furthermore, *top2* mutants arrest in G2, accumulate catenated DNA in S-phase that progresses into mitosis and accrues significant chromosome segregation defects [175]. Together, these experiments strongly

imply a crucial role for Top2 in replication termination and fork pausing, possibly by coordinating with additional fork-related factors such as the replicative helicases and checkpoint proteins.

How may Mcm2-7 be regulated during termination? In this context, the Mcm2/5 gate plays an obvious role. As discussed earlier, the 2/5 gate acts in an ATP-dependent manner to close the toroidal Mcm ring and activate the helicase in S-phase (**Figure 4**). It is conceivable that at the end of replication, Mcm2-7 hexamers undergo similar conformational changes that allow them to re-open the ring and unload from merging replication forks. It is currently unclear if there are additional factors that assist in Mcm2-7 unloading during termination. Studies in higher eukaryotes have shown that MCM-BP is a novel Mcm-interacting factor that plays a role during helicase unloading at the end of replication [237, 238]. Alternatively, it is possible that the torsional forces generated upon the merger of two convergent forks somehow destabilizes the helicases and cause them to unload. Because Mcm2-7 hexamers tend to stall ~40 nucleotides from inter-strand crosslinks [101], Mcm2-7 hexamers would probably be incapable of unwinding unreplicated DNA at the junction of converging forks. In this scenario, it is possible that additional helicases might perform the residual unwinding after unloading of Mcm2-7. The DNA helicase Rrm3 might be an obvious candidate, as *Δrrm3* mutants have been shown to accumulate X-shaped structures [239, 240].

1.5 COORDINATING REPLICATION WITH SISTER CHROMATID COHESION

In addition to precisely duplicating chromosomes, cells have the added responsibility of segregating the newly-replicated genome equally between their daughter cells. Any errors in this process can create genomic instability, as is frequently observed in cancer cells. Therefore, genomes rely upon special factors that oversee the distribution of duplicated genomes.

Two key processes need to be coordinated with DNA replication in order to maintain ploidy – sister chromatid cohesion (SCC), a process by which the newly replicated chromosomes are held together via cohesin proteins through S- and G2 phases of the cell cycle, followed by chromosome segregation in the M-phase of the cell cycle (reviewed in [241]). While physically restraining sister chromatids during replication, SCC additionally creates a force opposite to that generated by spindle attachment to centromeres [242]. Such forces are indispensable for the proper bi-alignment of sister chromatids at the metaphase plate, as premature termination of SCC invariably results in genome mis-segregation.

The precise coordination of these events is necessary to divide the replicated genome equally between two daughter cells. Most of our current understanding of these processes is derived from elegant studies done in budding yeast using clever and informative genetic assays. Results demonstrate that cohesins and replication factors often show a regulatory inter-dependence.

1.5.1 Factors involved in sister chromatid cohesion

In yeast cohesion is mediated by conserved proteins that belong to the group known as the SMCs (Structural maintenance of chromosomes). Of these Smc1 and Smc3 form the core cohesin ring that encircle DNA [182, 243]. This structure is comprised of antiparallel coiled coils that fold upon itself to generate a hinge point and two free termini that juxtapose to give rise to the ATPase domain (Nucleotide-binding domain, NBD), with the final 'ring' essentially being a V-shaped structure (**Figure 7**, [244]). A smaller protein termed kleisin, or Scc1 forms a bridging subunit within the cohesin ring, binding between the two NBDs of the cohesin ring [245]. While cohesins are not present in bacteria, similar complexes are observed [246]. Finally, an additional protein Scc3 is required for stable association of the cohesin rings with DNA to complete the core cohesive structure [182]. Biochemical studies provide direct evidence that the cohesins can bind and hold together sister chromatids through direct topological interaction between DNA and cohesins (**Figure 7**, reviewed in [183]).

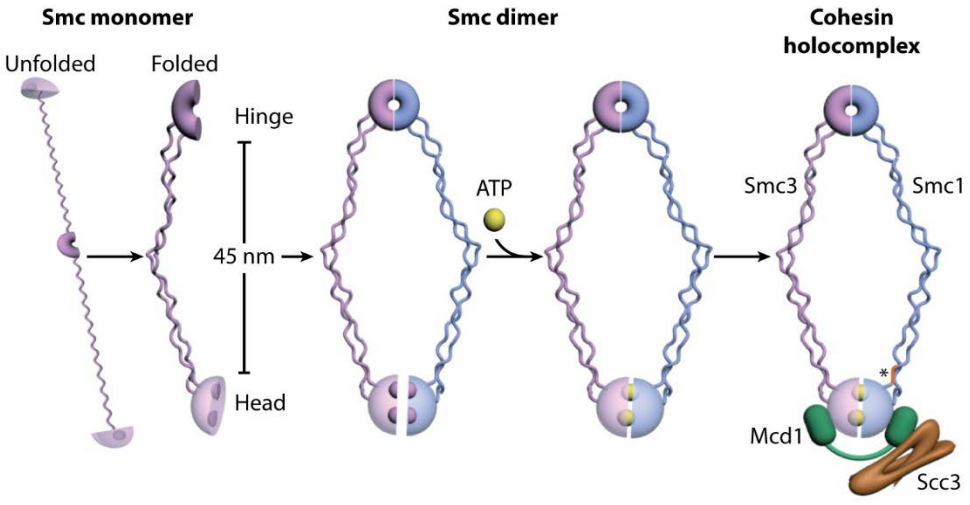

Figure 7. Cohesin ring architecture

(adapted with permission from [247])

A complex of Scc2/Scc4 is necessary to initially recruit and load cohesins on DNA [186, 248]. Importantly, the loading of cohesins seems to be site-specific, with preferred loading at numerous, regularly spaced 1-4kb regions termed cohesion-associated regions (CARs) [248]. Although found at an interval of every 20-25 kb, CARs are particularly abundant around centromeres, which leads to an enrichment of cohesins at this region. CARs do not, however, represent the final binding sites for the cohesins, which slide into neighboring regions once loaded on to DNA. The timing of cohesin loading is controlled by the availability of Scc1 only during late G1, which can then associate with and trigger the ATP hydrolysis at the NBDs of cohesins (**Figure 8**, [249, 250]). This is an important step, as it results in a conformational change at the distal hinge domain of the cohesion ring that allows the ring to open and entrap DNA. Additionally, certain kinetochore components such as Ctf19 are also known to play a role in cohesin loading, especially in the pericentromeric regions [251].

1.5.2 Cohesion establishment and timing

Another critical event in the proper association of cohesion with the replicating DNA is the 'establishment' of cohesion, which further stabilizes cohesin-DNA binding at sister chromatids (**Figure 8**). The Eco1 acetyltransferase acts on Smc3 by adding acetyl marks to conserved lysine residues in its NBD [184, 252, 253]. Mutations in *ECO1* lead to severe loss of cohesion, implying that this establishment activity is critical for the proper generation of cohesion on replicating DNA [184]. Mechanistically, Eco1-mediated acetylation is thought to close the DNA exit gate on the cohesin ring, as artificial fusion constructs of Scc1 and Smc3– subunits participating in closing the

DNA exit and entry gate–can rescue the deleterious effects of *eco1* mutations. Interestingly, mutations in certain genes such as the cohesion antagonist *WPL1* can rescue the cohesion defects of *eco1*, suggesting that Wpl1 acts as to destabilize cohesion, mainly through increased Smc3 turnover [254, 255].

So how is the precise timing of cohesion determined? Eco1 is active during S-phase, during which it is presumed to travel with the replication fork. Through cell-cycle arrest experiments, Eco1 has been shown to be dispensable during G2/M, which is consistent with the timing of sister chromatid separation [184]. At the same time, high Wpl1 activity in G2 assists in the destabilization of cohesins, and concomitantly counteracts the establishment of other loaded cohesin complexes. Moreover, the loaded cohesin complexes are deacetylated through the activity of Hos1 and are recycled to be used in the subsequent cell cycle (**Figure 8**, [256]).

1.5.3 Condensins and the Spindle Assembly Checkpoint (SAC)

In addition to cohesins, special factors help in the compaction of metaphase chromosomes and prepare them for spindle orientation and subsequent segregation to daughter cells. Condensins are another class of SMC proteins that perform this function. In yeast, a single condensin complex (Condensin I) composed of Smc2 and Smc4, the kleisin subunit Brn1 and Ycs4/Ycs5 subunits participate in chromosome condensation [257-259]. Condensins are primarily thought to assist in chromosome compaction via topological induction of positive supercoils in the newly replicated chromatids, as well as by compaction of additional structures such as chromatin loops. Finally, the correct resolution of the duplicated genome into compacted metaphase structures relies on

Topoisomerase II (Top2 in yeast), as inactivation of Top2 results in hemicatenated structures and anaphase bridges during anaphase that ultimately lead to ploidy defects [236, 260].

Importantly, SCC is required for chromosome bi-orientation at the metaphase plate, through which spindles from the opposite poles of the cell attach to each sister chromatid and generate correct tension on the chromosomes. Cohesin complexes loaded both at the centromeric region, and the surrounding (pericentromeric) regions are thought to contribute to bi-orientation. Improper attachment of spindles to kinetochores from a single spindle pole body (Syntely) or non-attachment of microtubules to kinetochores can both trigger the spindle assembly checkpoint (SAC) which blocks mitosis, corrects the chromosome orientation, restores tension at the centromeres and helps in correct chromosome segregation (reviewed in [261]).

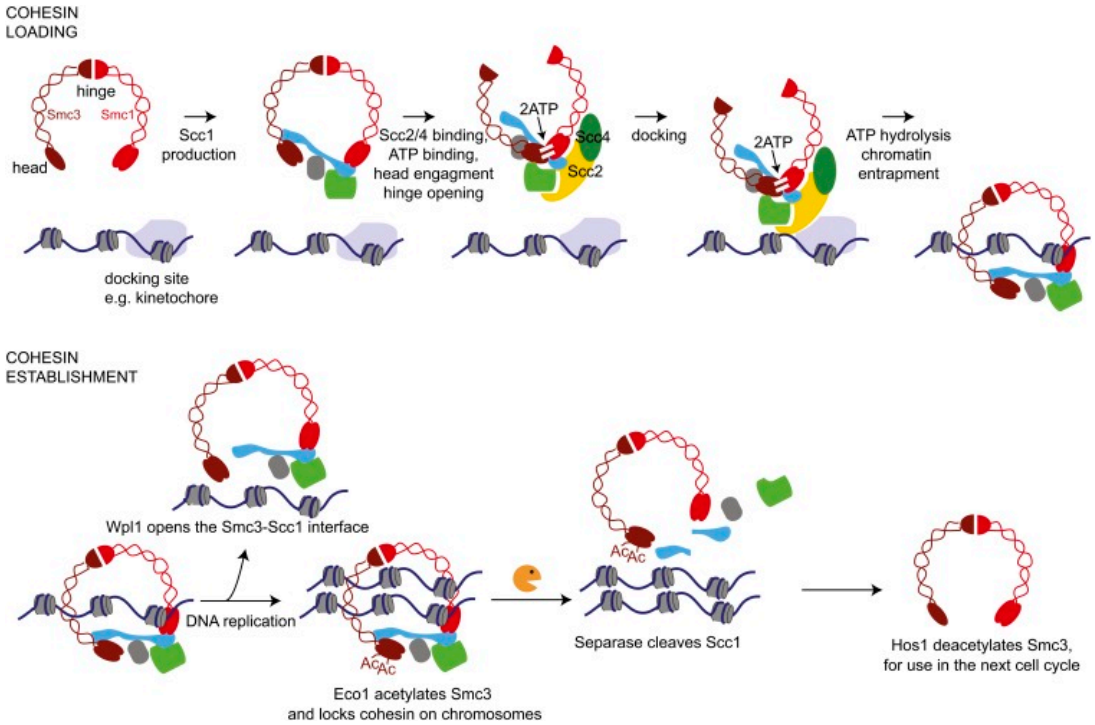

Figure 8. Mechanism of sister chromatid cohesion

(adapted with permission from [241]).

1.6 OVERVIEW OF THESIS GOALS

Although Mcm2-7 has six unique ATPase active sites, in principle, mutations in each of these sites can be tested *in vivo* for specific defects to elucidate their functions. As described earlier, while this approach has been successfully used for the biochemical analysis of these active sites, a majority of these ATPase active site mutations are lethal in yeast, including all Walker A substitutions. Therefore, we are limited to three viable mutants for our *in vivo* analysis.

Among the viable mcm mutants, *mcm4RA* and *mcm6DENQ* both contain mutations within the Mcm4/6 active site. Similarly, the *mcm2DENQ* mutant, which is the focus of chapters 3 and 4 resides within the Mcm6/2 active site. Notably, both these active sites reside between the Mcm2/5 'gate' and the Mcm7/4 'motor' domain of the Mcm2-7 helicase, and presumably play roles in either regulating the gate and the motor, or facilitating communications between these domains by transmitting conformational changes across the complex. These *mcm* mutants, therefore, potentially provide a great tool to elucidate the *in vivo* functions of regulatory Mcm active sites.

This dissertation primarily focuses on the *in vivo* analysis of the *mcm2DENQ* mutant with limited comparison to other *mcm* mutants. The purpose of the dissertation is to identify novel features associated with Mcm2-7 regulation, and to expand the knowledge of Mcm2-7 participation in processes beyond DNA replication. Additionally, this study aims to explore whether specific ATPase active sites within Mcm2-7 have overlapping or distinct *in vivo* functions. Besides DNA replication, two other processes closely coordinate with the replisome— intra S-phase checkpoints (see next chapter) and sister chromatid cohesion (SCC).

We limited our analyses of *mcm* mutant phenotypes to these processes for several reasons. First, like DNA replication, replication checkpoints and SCC are primarily observed during S-phase, where they closely interact with many replication factors. Secondly, there are several well-established assays to study these processes in detail using budding yeast. This allowed us to quickly test several factors under a variety of different conditions within a reasonable time span.

Lastly, it is known that several human diseases are inherently associated with defects in genome stability, including most types of cancer. As Mcm2-7 misregulation is commonly observed in many proliferative diseases, this study provides a rationale to explore the mechanistic link between replication and processes that govern genome stability such a checkpoints and SCC. We sought to test whether Mcm2-7 is the key factor whose regulation lies at the heart of all of these processes. Above all, we have aimed to elucidate precise functions of some of the lesser-known Mcm active sites *in vivo*, which would provide us deeper insight into the mechanism, and physiological relevance of a complex enzyme with multiple functionally distinct ATPase active sites.

The main thesis is formally divided into three subsections. The first one (**Chapter 3**) details the discovery of a novel *in vivo* regulatory function for the Mcm6/2 active site through genetic analysis of the *mcm2DENQ* mutant. Here, we show that the Mcm2-7 complex is a part of the DNA replication checkpoint, whereby it mediates a response to replicative stress through the Mcm6/2 active site. In the second part (**Chapter 4**), we describe how the Mcm complex is involved in the maintenance of genome stability, focusing mainly on DNA damage phenotypes of the *mcm2DENQ* mutant under conditions that generally support normal growth. Lastly, we discuss some intriguing

observations from the *in vivo* analysis of the Mcm4/6 active site mutants (**Appendix A&B**), and show that the multiple roles associated with Mcm2-7 are genetically separable through distinct ATPase active sites.

2.0 MATERIALS AND METHODS

2.1 LIST OF STRAINS AND PLASMIDS

Unless mentioned otherwise, all strains listed below are isogenic derivatives of W303 [262]

2.1.1 Yeast strains

strain	genotype	reference
UPY110	*MATa, ade2-1, ura3-1, his3-11, 15, leu2-3, 12, can-100, trp1-1, Δmcm2::hisG/pAS404 (ARS/CEN URA+ P_{MCM5}-MCM2).*	This study
UPY464	*MATa, ade2-1, ura3-1, his3-11,15, trp1-1, leu2-3,112, can1-100,bar1::hisG*	This study
UPY499	*MATa, ade2-1, ura3-1, his3-11,15, trp1-1, leu2-3,112, can1-100,bar1::hisG,mcm2DENQ*	This study
UPY525	*MATa, ade2-1, ura3-1, his3-11,15, trp1-1, leu2-3,112, can1-100, bar1::hisG, mcm6DENQ*	This study
UPY529	*MATa, ade2-1, ura3-1, his3-11,15, trp1-1, leu2-3,112, can1-100, bar1::hisG, mcm4RA*	This study
UPY537	*MATa, ade2-1, ura3-1, his3-11,15, trp1-1, leu2-3,112, can1-100, bar1::hisG, mcm4RA, ade3Δ*	This study
UPY541	*MATa, ade2-1, ura3-1, his3-11,15, trp1-1, leu2-3,112, can1-100, bar1::hisG, mcm6DENQ, ade3Δ*	This study
UPY553	*MATa his1*	N.Kleckner
UPY554	*MATα his1*	N.Kleckner
UPY606	*MATa, ade2-1, ura3-1, his3-11,15∷HIS3-LACI-GFP, trp1-1, leu2-3,112, can1-100, bar1::hisG, mcm2DENQ, ade3Δ, lacO-ChrIV(932137)*	This study
UPY 610	*MATa, ade2-1, ura3-1, his3-11,15, trp1-1, leu2-3,112, can1-100, bar1::hisG,, ade3Δ*	This study

UPY613	*MATa, ade2-1, ura3-1, his3-11,15::HIS3-LACI-GFP, trp1-1, leu2-3,112, can1-100, bar1::hisG, ade3Δ, lacO-ChrIV(932137)*	This study
UPY630	*MATa, ade2-1, ura3-1, his3-11,15, trp1-1, leu2-3,112, can1-100, bar1::hisG, Δrad9::HIS3-lox*	This study
UPY634	*MATa, ade2-1, ura3-1, his3-11,15, trp1-1, leu2-3,112, can1-100, bar1::hisG, Δrad9::HIS5+-lox, mcm2DENQ*	This study
UPY638	*MATa, ade2-1, ura3-1, his3-11,15, trp1-1, leu2-3,112, can1-100, bar1::hisG, mcm4Chaos3*	This study
UPY646	*MATa, ade2-1, ura3-1, his3-11,15, trp1-1, leu2-3,112::LEU2-MRC1-3XHA, can1-100, bar1::hisG*	This study
UPY647	*MATa, ade2-1, ura3-1, his3-11,15, trp1-1, leu2-3,112::LEU2-MRC1-3XHA, can1-100, bar1::hisG, mcm2DENQ*	This study
UPY648	*MATa, ade2-1, ura3-1, his3-11,15, trp1-1, leu2-3,112, can1-100, bar1::hisG, LEU2::RAD9-3XHA*	This study
UPY649	*MATa, ade2-1, ura3-1, his3-11,15, trp1-1, leu2-3,112::LEU2-RAD9-3XHA, can1-100, bar1::hisG, mcm2DENQ*	This study
UPY666-1	*MATa, cdc6-1, ade2-1, ura3-1, his3-11,15, trp1-1, leu2-3,112, can1-100, bar1::hisG, ade3Δ*	This study
UPY667-1	*MATa, cdc9-1, ade2-1, ura3-1, his3-11,15, trp1-1, leu2-3,112, can1-100, bar1::hisG, ade3Δ*	This study
UPY670	*MATα can1::P_{STE2}-HIS3, lyp1,his3-1,leu2-0,ura3-0 (S288C)*	This study
UPY706	*MATa, ade2-1, ura3-1, his3-11,15, trp1-1, leu2-3,112, can1-100, bar1::hisG, bub1::HIS5+-lox*	This study
UPY707	*MATa, ade2-1, ura3-1, his3-11,15, trp1-1, leu2-3,112, can1-100, bar1::hisG, bub1::HIS5+-lox,mcm2DENQ*	This study
UPY713	*MATa, ade2-1, ura3-1, his3-11,15, trp1-1, leu2-3,112, can1-100, bar1::hisG, mrc1::HIS5+-lox*	This study
UPY715	*MATa, ade2-1, ura3-1, his3-11,15, trp1-1, leu2-3,112, can1-100, bar1::hisG, rad9::HIS5+-lox, sml1::URA3-lox, mrc1Δ*	This study
UPY739	*MATa, ade2-1, ura3-1, his3-11,15, trp1-1, leu2-3,112, can1-100, bar1::hisG, cdc15-2*	This study
UPY740	*MATa, ade2-1, ura3-1, his3-11,15, trp1-1, leu2-3,112, can1-100, bar1::hisG, cdc15-2, mcm2DENQ*	This study
UPY744	*MATa, ade2-1, ura3-1, his3-11,15::HIS3-LACI-GFP, trp1-1, leu2-3,112, can1-100, bar1::hisG, ade3Δ, mrc1::URA3-lox, lacO-ChrIV(932137)*	This study

UPY811	*MATa, ade2-1, ura3-1, his3-11,15::HIS3-LACI-GFP, trp1-1, leu2-3,112, can1-100, bar1::hisG, ade3Δ , mcm4RA, lacO-ChrIV(932137)*	This study
UPY812	*MATa, ade2-1, ura3-1, his3-11,15::HIS3-LACI-GFP, trp1-1, leu2-3,112, can1-100, bar1::hisG, ade3Δ , mcm6DENQ, , lacO-ChrIV(932137)*	This study
UPY826	*MATa, ade2-1, his3-11,15, trp1-1, leu2-3,112, can1-100,cdc16-123, GAL, psi+CFIII(CEN3.L.YPH278)URA3-SUP11*	This study
UPY827	*MATa, ade2-1, his3-11,15, trp1-1, leu2-3,112, ura3, can1-100, smc3-42,GAL,psi+*	Kim Nasmyth
UPY828	*MATa, ade2-1, his3-11,15, trp1-1, leu2-3,112, ura3, can1-100, scc2-4, GAL, psi+*	Kim Nasmyth
UPY831	*MATa, ura3::3XURA3tet O-112, leu2::LEU2-tetR-GFP, his3-11,15, eco1-1, trp1-1::PDS1-myc18-TRP1*	Kim Nasmyth
UPY837	*MATa, ade2-1, ura3-1, his3-11,15, trp1-1, leu2-3,112, can1-100, bar1::hisG, sml1::loxP-HIS5+-loxP, mec1::loxP-URA3-loxP*	This study
UPY838	*MATa, ade2-1, ura3-1, his3-11,15, trp1-1, leu2-3,112, can1-100, bar1::hisG, sml1::loxP-HIS5+-loxP, rad53::loxP-URA3-loxP*	This study
UPY860	*MATa, ade2-1, ura3-1, his3-11,15::HIS3-LACI-GFP, trp1-1, leu2-3,112, can1-100, bar1::hisG, cdc15-2 , lacO-ChrIV(932137)*	This study
UPY865	*MATa, ade2-1, ura3-1, his3-11,15::HIS3-LACI-GFP, trp1-1, leu2-3,112, can1-100, bar1::hisG, cdc15-2, mcm2DENQ, , lacO-ChrIV(932137)*	This study
UPY888	*MATa, ade2-1, ura3-1, his3-11,15, trp1-1, leu2-3,112, can1-100, bar1::hisG, mcm6DENQ- HYG MX4*	This study
UPY889	*MATa, ade2-1, ura3-1, his3-11,15, trp1-1, leu2-3,112, can1-100, bar1::hisG, mcm4RA-HYGMX4*	This study
UPY902	*MATa, ade2-1, ura3-1, his3-11,15, trp1-1, leu2-3,112, can1-100, bar1::hisG, CPY*-3XHA*	This study
UPY909	*MATa, ade2-1, ura3-1, his3-11,15, trp1-1, leu2-3,112, can1-100, bar1::hisG, SMC1-HIS3MX-3XHA*	This study
UPY910	*MATa, ade2-1, ura3-1, his3-11,15, trp1-1, leu2-3,112, can1-100, bar1::hisG, mcm2DENQ*	This study
UPY911	*MATa, ade2-1, ura3-1, his3-11,15, trp1-1, leu2-3,112, can1-100, bar1::hisG, SCC1-3XHA-KANMX*	This study
UPY912	*MATa, ade2-1, ura3-1, his3-11,15, trp1-1, leu2-3,112, can1-100, bar1::hisG,mcm2DENQ, SCC1-3XHA-KanMX*	This study

UPY918	*MATa, ade2-1, ura3-1, his3-11,15, trp1-1, leu2-3,112, can1-100, bar1::hisG, mcm4RA, rad9::loxP-HIS5+-loxP*	This study
UPY919	*MATa, ade2-1, ura3-1, his3-11,15, trp1-1, leu2-3,112, can1-100, bar1::hisG, mcm6DENQ, rad9::loxP-HIS5+-loxP*	This study
UPY920	*MATa, ade2-1, ura3-1, his3-11,15, trp1-1, leu2-3,112, can1-100, bar1::hisG, mcm4RA, mrc1::loxP-HIS5+-loxP*	This study
UPY921	*MATa, ade2-1, ura3-1, his3-11,15, trp1-1, leu2-3,112, can1-100, bar1::hisG, mcm6DENQ, mrc1::loxP-HIS5+-loxP*	This study
UPY925	*MATa, ade2-1, ura3-1, his3-11,15, trp1-1, leu2-3,112::LEU2-mrc1AQ, can1-100, bar1::hisG, mcm6DENQ, mrc1::loxP-HIS5+-loxP*	This study
UPY926	*MATa, ade2-1, ura3-1, his3-11,15, trp1-1, leu2-3,112::LEU2-mrc1AQ, can1-100, bar1::hisG, mcm4RA, mrc1::loxP-HIS5+-loxP*	This study
UPY936	*MATa, ade2-1, ura3-1, his3-11,15::HIS3-LACI-GFP, leu2-3,112,lys2::hisG can1-100, mcm6DENQ, cdc15-2, pUP1108 (LEU2, lacO-ChrIV)*	This study
UPY937	*MATa, ade2-1, ura3-1, his3-11,15::HIS3-LACI-GFP, leu2-3,112,trp1-1, can1-100, mcm4RA, cdc15-2, pUP1108 (LEU2, lacO-ChrIV)*	This study
UPY938	*MATa. bar1::LEU2, trp1-1, RAD52-YFP , ura3-1, his3-1,2*	Kara Bernstein
UPY956	*MATa, ade2-1, ura3-1, his3-11,15, leu2-3,112,can1-100, bar1::hisG, sml1::loxP-HIS5+-loxP, mec1::loxP-URA3-loxP, leu2-3,112::MRC1-3XHA-LEU2*	This study
UPY967	*MATα, ade2-1, ura3-1, his3-11,15, leu2-3,112, can1-100, TRP1, bar1::hisG, mcm2DENQ, tel1::loxP-LEU2-loxP, leu2-3,112::MRC13XHA-LEU2, sml1::loxP-HIS5+-loxP*	This study
UPY968	*MATa, ade2-1, ura3-1, his3-11,15, leu2-3,112, can1-100, bar1::hisG, tel1Δ::loxP-LEU2-loxP,leu2-3,112::MRC1-3XHA-LEU2, sml1Δ::loxP-his3-loxP*	This study
UPY980	*MATa, ade2-1, ura3-1, his3-11,15, trp1-1, leu2-3,112::LEU2-P_{GAL1}-MRC1-3XHA, can1-100, bar1::hisG, mcm2DENQ*	This study
UPY981	*MATa, ade2-1, ura3-1, his3-11,15, trp1-1, leu2-3,112::LEU2- P_{GAL1}-MRC1-3XHA, can1-100, bar1::hisG*	This study

UPY982	*MATa, ade2-1, ura3-1, his3-11,15::HIS3-LACI-GFP, leu2-3,112,lys2::hisG can1-100, mcm4RA, cdc15-2, pUP1108 (LEU2, lacO-ChrIV)*	This study
UPY983	*MATa, ade2-1, ura3-1, his3-11,15::HIS3-LACI-GFP, leu2-3,112,lys2::hisG can1-100, mcm6DENQ, cdc15-2, pUP1108 (LEU2, lacO-ChrIV)*	This study
UPY985	*MATa, ade2-1, ura3-1, his3-11,15, trp1-1, leu2-3,112, can1-100, bar1::hisG, sml1Δ::loxP-HIS5+-loxP, tel1Δ::loxP-leu2-loxP, mec1Δ::loxP-URA33-loxP, leu2-3,112::MRC1-3XHA-LEU2*	This study
UPY988	*MATα, ade2-1, ura3-1, his3-11,15, trp1-1, leu2-3,112, can1-100, bar1::hisG, sml1::loxP-HIS5+-loxP, mcm2DENQ-NATMX4*	This study
UPY998	*MATa, ade2-1, ura3-1, his3-11,15::HIS3-LACI-GFP, trp1-1, leu2-3,112, can1-100, bar1::hisG, mcm2DENQ, ade3Δ, lacO-ChrIV(932137), cdc16-123*	This study
UPY1014	*MATa, trp1-1,RAD52-YFP, ura3-1, his3-1,2,bar1::LEU2, mcm2DENQ*	This study
UPY1017	*MATa,ade2-1, Rad52-YFP mcm6DENQ, ura3-1,his3-1,2, lys2:;hisG, trp1-1, bar1::LEU2*	This study
UPY1020	*MATa, ade2-1, ura3-1, his3-11,15, trp1-1, leu2-3,112, can1-100, bar1::hisG, mcm2DENQ, pGAL-MRC1:KANMX*	This study
UPY1022	*MATa, RAD52-YFP, ura3-1, his3-1,2, lys2::hisG, trp1-1, mcm4RA*	This study
UPY1042	*MATa, ade2-1, ura3-1, his3-11,15::HIS3-LACI-GFP, trp1-1, leu2-3,112, can1-100, bar1::hisG, mcm2DENQ, ade3Δ, lacO-ChrIV(932137), sml1::loxP-LEU2-loxp*	This study
UPY1044	*MATa, ade2-1, ura3-1, his3-11,15, trp1-1, leu2-3,112::LEU2- P_{GAL1}-MRC1-3XHA, can1-100, bar1::hisG, MCM4-3XFLAG-KANMX*	This study
UPY1045	*MATa, ade2-1, ura3-1, his3-11,15, trp1-1, leu2-3,112::LEU2- P_{GAL1}-MRC1-3XHA, can1-100, bar1::hisG, mcm2DENQ Mcm4-3XFLAG-KANMX*	This study
UPY1046	*MATa, trp1-1,RAD52-YFP , ura3-1, his3-1,2,bar1::LEU2, sml1::loxP-URA3-loxP*	This study
UPY1048	*MATa, ade2-1, his3-11,15, trp1-1, leu2-3,112, can1-100, smc3-42, GAL, psi+, SMC1-3XHA-HIS3MX*	This study

UPY1049	*MATa, ura3::3XURA3-tet O-112, leu2::LEU2 tetR-GFP, his3, eco1-1, PDS1myc18::TRP(K.lactis), SMC13XHA-HIS3MX*	This study
UPY1053	*MATa, ade2-1, ura3-1, his3-11,15, trp1-1, leu2-3,112::LEU2- P_{GAL1}-MRC1-3XHA, can1-100, bar1::hisG, MCM4-3X FLAG-KANMX, tof1::loxP-HIS5+-loxP*	This study
UPY1054	*MATa, ade2-1, ura3-1, his3-11,15, trp1-1, leu2-3,112::LEU2- P_{GAL1}-MRC1-3XHA, can1-100, bar1::hisG, MCM4-3X FLAG-KANMX, csm3::loxP-HIS5+-loxP*	This study
UPY1057	*MATa, ade2-1, ura3-1, his3-11,15, trp1-1, leu2-3,112:: P_{GAL1}-CSM3-3XHA-LEU2, can1-100, bar1::hisG*	This study
UPY1058	*MATa, ade2-1, ura3-1, his3-11,15, trp1-1, leu2-3,112::pGal-CSM3-3XHA-LEU2, can1-100, bar1::hisG,mcm2DENQ*	This study
UPY1060	*MATa ura3-1,his-1,2,trp1-1,leu2-3,112,bar1::LEU2, mcm2DENQ,RAD52-YFP, sml1Δ::loxP-His5-loxP*	This study
UPY1064	*MATα can1::P_{STE2}-HIS5+, lyp1,his3-1,leu2-0,ura3-0, met15-0, mcm2DENQ-NATMX4 (S288C)*	This study
UPY1077	*MATa, bar1:LEU2, RAD52-YFP,trp1-1,ura3-1, mrc1::loxP-HIS5+-loxP*	This study
UPY1079	*MATa, bar1:LEU2, RAD52-YFP,trp1-1, ura3-1,mcm2-1*	This study
UPY1085	*MATa, ade2-1, ura3-1, his3-11,15, trp1-1, leu2-3,112, can1-100, bar1::hisG, MCM7-3XFLAG-HIS3*	This study
UPY1087	*MATα can1::P_{STE2}-HIS5+, lyp1Δ, mcm4RA-NATMX4 (S288C)*	This study
UPY1089	*MATa, ade2-1, his3-11,15, trp1-1, leu2-3,112, can1-100, smc3-42, GAL, psi+, SCC1-3XHA-KANMX*	This study
UPY1090	*MATa, ade2-1, his3-11,15, trp1-1, leu2-3,112, can1-100, scc2-4, GAL, psi+, SCC1-3XHA-KANMX*	This study
UPY1091	*MATa, ura3::3XURA3-tet O-112, leu2::LEU2 tetR-GFP, his3, eco1-1, PDS1myc18::TRP(K. lactis), SCC1-3XHA-KANMX*	This study
UPY1092	*MATa, ade2-1, ura3-1, his3-11,15, trp1-1, can1-100, bar1::LEU2*	This study

UPY1094	*MATα can1::P_{STE2}-HIS5+, lyp1,his3-1,leu2-0,ura3-0, met15-0, mcm6DENQ-NATMX (S288C)*	This study
UPY1101	*MATa, ade2-1, ura3-1, his3-11,15, trp1-1, leu2-3,112::LEU2- P_{GAL1}-MRC1-3XHA, can1-100, bar1::hisG, MCM4-3XFLAG-KANMX, CDC45-3XHA-HIS3MX*	This study
UPY1102	*MATa, ade2-1, ura3-1, his3-11,15, trp1-1, leu2-3,112::LEU2- P_{GAL1}-MRC1-3XHA, can1-100, bar1::hisG, MCM4-3XFLAG-KANMX, CDC45-3XHA-HIS3MX, mcm2DENQ*	This study
UPY1103	*MATa, ade2-1, ura3-1, his3-11,15, trp1-1, leu2-3,112, can1-100, bar1::hisG, mcm4Chaos3, MCM7-3XFLAG-HIS3*	This study
UPY1114	*MATa cdc14-3 ura3, trp1,leu2,his3*	This study
UPY1119	*MATα, ade2-1, ura3-1, his3-11,15, trp1-1, leu2-3,112, can1-100, bar1::hisG, sml1::loxP-HIS5+-loxP, rad53::loxP-URA3-loxP, mcm2DENQ-NATMX4*	This study
UPY1124	*MATa, ade2-1, ura3-11, his3-11,15, leu2-3,12, can-100, trp1-1, sml1::His-lox, mcm2Δ::hisG, pAS404 (ARS/CEN, URA3 P_{MCM5}-MCM2, rad53::loxP-LEU2-loxP*	This study
UPY1125	*MATa, ade2-1, ura3-11, his3-11,15, leu2-3,12, can-100, trp1-1,sml1::His-lox, mcm2::hisG/pAS404 (ARS/CEN URA+ MCM5promoter-MCM2wt, mec1::loxP-LEU2-loxP*	This study
UPY1135	*MATa, ade2-1, ura3-1, his3-11,15, trp1-1, leu2-3,112, can1-100, bar1::hisG, sml1::loxP-HIS5+-loxP, mec1::loxP-URA3-loxP, RAD52-YFP*	This study
UPY1137	*MATa, ade2-1, ura3-1, his3-11,15, trp1-1, leu2-3,112, can1-100, bar1::hisG, sml1::loxP-HIS5+-loxP, rad53::loxP-URA3-loxP, RAD52-YFP*	This study
UPY1141	*MATα, bar1::LEU2,lys2Δ, RFA1-8ala-RFP, RAD5,ura3-1*	Kara Bernstein
UPY1148	*MATa, ade2-1, ura3-1, his3-11,15, trp1-1, leu2-3,112, can1-100, bar1::hisG, wpl1::loxP-URA3-loxP*	This study
UPY1149	*MATa, ade2-1, ura3-1, his3-11,15, trp1-1, leu2-3,112, can1-100, bar1::hisG, mcm2DENQ, wpl1::loxP-URA3-loxP*	This study
UPY1150	*MATa, ade2-1, ura3-1, his3-11,15::HIS3-LACI-GFP, trp1-1, leu2-3,112, can1-100, bar1::hisG,*	This study

	mcm2DENQ, ade3Δ, lacO-ChrIV(932137), wpl1::loxP-URA3-loxP	
UPY1151	*MATa, ade2-1, ura3-1, his3-11,15::HIS3-LACI-GFP, trp1-1, leu2-3,112, can1-100, bar1::hisG, ade3Δ, lacO-ChrIV(932137), wpl1::loxP-URA3-loxP*	This study
UPY1152	*MATa. bar1::LEU2, trp1-1,RAD52-YFP , ura3-1, his3-1,2, wpl1::loxP-URA3-loxP*	This study
UPY1153	*MATa. bar1::LEU2, trp1-1,RAD52-YFP , ura3-1, his3-1,2, wpl1::loxP-URA3-loxP, mcm2DENQ*	This study
UPY1154	*MATa, ura3::3XURA3tet O 112, leu2::LEU2 tetR-GFP, his3, eco1-1, PDS1myc18::TRP(K. lactis), wpl1::loxP-HIS5+-loxP*	This study
UPY1157	*MATa, ade2-1, ura3-1, his3-11,15, trp1-1, leu2-3,112, can1-100, bar1::hisG, mcm2DENQ, MCM7-3XFLAG-HIS3*	This study
UPY1168	*MATa RFA1-YFP, his3-11,15, mcm2DENQ, leu2-3,112, lys2Δ, trp1-1, ura3-1, bar1::hisG*	This study
UPY1169	*MATa RFA1-YFP, leu2-3,112, his3,lys2Δ, bar1::LEU2, trp1-1, ura3-1*	This study
UPY1172	*MATa, ade2-1, ura3-1, his3-11,15::HIS3-LACI-GFP, trp1-1, leu2-3,112, can1-100, bar1::hisG, cdc15-2, lacO-ChrIV(932137)*	This study
UPY1174	*MATa. bar1::LEU2, trp1-1,RAD52-YFP, ura3-1, his3-11,15, sac3::KANMX*	This study
UPY1177	*MATa. bar1::LEU2, trp1-1,RAD52-YFP , ura3-1, his3-11,15, sac3::KANMX, mcm2DENQ*	This study
UPY 1239	*MATa, RFA1-YFP, leu2-3,112,bar1::LEU2, trp1-1, ura3-1, sac3::KANMX*	This study
UPY1240	*MATa, RFA1-YFP, leu2-3,112,bar1::hisG, trp1-1, lys2Δ, ura3-1, sac3::KANMX, mcm2DENQ*	This study

Table 2. List of yeast strains used in this study

2.1.2 Plasmids

Plasmid name	Alternate name	*Description*	Reference
pUP169	pAS436	*Amp, TRP1, ARS/CEN, P_{MCM5}. C-term HA/His10*	[82]
pUP207.2	2534-1	*Amp, TRP1(ARS/CEN) P_{MCM5}-mcm4RA-His10/HA*	[82]
pUP215	pAS823	*Amp, TRP1(ARS/CEN) P_{MCM5}-mcm6DENQ-His10/Ha*	[82]
pUP223	pAS787	*Amp, LEU2 (Integrating vector) P_{GAL1}-mcm2DENQ*	[82]
pUP233.2	2535-1	*Amp, LEU2(Integrating vector) P_{GAL1}-mcm4RA-3xHA*	[82]
pUP240	pAS813	*Amp, LEU2(Integrating vector) P_{GAL1}-mcm6DENQ-FLAG*	[82]
pUP464	pDK368-1	*LEU2 ARSH4*	[263]
pUP465	pDK368-7	*LEU2 ADE3 ARSH4-7X*	[263]
pUP577	pAG25	*Amp, NATMX4*	[264]
pUP607	pFA6a-*KANMX6*	*Amp, G418*	[265]
pUP608	pFA6a-*3XHA-KANMX6*	*Amp. G418 C-term 3XHA*	[265]
pUP616	pFA6a-*3XHA-HIS3MX6*	*Amp, HIS3 C-term 3XHA*	[265]
pUP618	pFA6a-*13MYC-His3MX6*	*Amp HIS3 C-term 13XMYC*	[265]
pUP622	pFA6a-*KANMX- P_{GAL1}*	*Amp, N-terminal P_{GAL1}-KANMX*	
pUP641	pAG32	*Amp, HPHMX, tef*	[264]
pUP650	pUG27	*Amp HIS5+, lox*	[266]
pUP652	pUG72	*Amp URA3, lox*	[266]
pUP653	pUG73	*Amp LEU2, lox*	[266]
pUP809	619-*3XFLAG-LEU2*	*Amp, LEU2 (K. lactis) 3XFLAG*	This study
pUP951	pCM46	*Amp, NAT lacO-ChrIV(932137)*	Doug Koshland
pUP954	pDB030	*Amp,HIS3,KANMX, LACI-GFP*	Doug Koshland
pUP985	176 961	*Amp, LEU2 MRC1-3XHA*	This study
pUP986	176 966	*Amp, LEU2 RAD9-3XHA*	This study

pUP987	147 197	*Amp, URA3, P_{GAL1}-MCM2*	This study
pUP988	162 197	*Amp, TRP1, P_{GAL1}-MCM2*	This study
pUP989	147 199	*Amp, URA3 P_{GAL1}-mcm2DENQ*	This study
pUP990	162 199	*Amp, TRP1 P_{GAL1}-mcm2DENQ*	This study
PUP991	169-1 new	*Amp, TRP1 mcm4Chaos3*	This study
pUP1106	*CPY** yeast shuttle vector, ERAD	*Amp,URA3 CPY**	Jeff Brodsky
pUP1127	pFA6a-6xGLY-*3XFLAG-HIS3MX6*	*Amp,HIS3 C-terminal 3X-FLAG*	[267]
pUP1143	*P_{GAL1}-MRC1-3XHA*	*Amp, LEU2 P_{GAL1}-MRC1-3XHA*	This study
pUP1163	*P_{GAL1}-mcm4RA TRP1* integrating	*Amp,TRP1 mcm4RA*	This study
pUP1165	*P_{GAL1}-mcm6DENQ TRP1* integrating	*Amp,TRP1 mcm6DENQ*	This study
pUP1167	*P_{MCM5}-MCM4 TRP1* integrating	*Amp,TRP1 MCM6*	This study
pUP1169	*P_{MCM5}-MCM6 TRP1* integrating	*Amp,TRP1 MCM6*	This study
pUP1172	*P_{GAL1}-CSM3-3XHA*	*Amp, LEU2 P_{GAL1}-CSM3-3XHA*	This study

Table 3. List of plasmids used in this study

2.2 METHODS

2.2.1 Yeast methods

All the yeast strains used in this study are isogenic to the W303 background [262], unless specified otherwise. Strains were grown at 30°C for all experiments, unless specified otherwise.

Cell cycle synchronization- Mid-log phase yeast were treated with α-factor (5mg/mL in DMSO) at a final concentration of 30nM and grown at 30°C for 3 hours. For temperature sensitive strains, a similar scheme was followed, except that strains were arrested at either permissive (typically

25°C) or non-permissive (typically 37°C) temperatures. Cells arrested in α-factor were monitored periodically for the unbudded 'shmoo' phenotype, with >95% G1 arrest considered as optimal.
To release G1-arrested cells, cells were spun down and washed thrice in culture volume of YP without dextrose, with 50ug/mL Pronase E included in the first wash to degrade excess α-factor. Cells were then resuspended in the desired volume of YPD and monitored for progress through the cell cycle.

S-phase arrest- Cells were arrested in G1 as described above and after the requisite washes, released into YPD supplemented with 200mM hydroxyurea and grown for two hours at 30°C. The arrest was monitored by counting the proportion of cells with small buds, which is typical of cells in S-phase.

G2/M arrest- Cells arrested in α-factor were washed and released into YPD supplemented with 15ug/mL nocodazole, which is a microtubule-depolymerizing drug, and grown for 2 hours at 30°C (unless specified otherwise). Arrest was monitored by counting the proportion of cells with large buds and through DAPI staining of large budded cells with a single nucleus, typical of cells entering metaphase.

2.2.2 Double strand break assay

Depending on the experiment, log phase (asynchronous) or synchronized cells were used for immunofluorescence-based analysis of phosphorylated histone H2A as a marker for DNA double strand breaks. The assay has been previously described in [268].

Fixing and spheroplasting cells: To fix cells, 3.7% formaldehyde was added to cells and tubes were incubated for 10 minutes with gentle rolling. Cells were subsequently spun and resuspended in 1mL of KPO_4 buffer containing 3.7% formaldehyde and further roller-incubated for an hour at room temperature. Thereafter, cells were washed twice in KPO_4 buffer and resuspended in 0.1mL sorbitol buffer. Cells were then spheroplasted by the addition 6uL of 2mg/mL Zymolyase 20T and 1μL β-mercaptoethanol followed by a 15 minute roller incubation at room temperature. Spheroplasts were gently washed twice in sorbitol buffer and finally resuspended in 50 μL of the same buffer.

Permeablizing and immunostaining cells: Cells were spotted on to poly-L-lysine coated slides, and excess cells were aspirated from the slide. Slides were then immediately immersed in methanol for 6 minutes and transferred to acetone for 30 seconds at -20°C to permeablize cells. Once the acetone dried off, spots were incubated with 40-50μL blocking buffer (1.5% BSA, 0.5% Tween-20, 0.1% TritonX-100 in PBS) for 15-30 minutes in a humid container. Thereafter, cells were treated with 12-15μL anti-phosphoH2A antibody (Personal gift from W.Bonner) overnight. After 4-5 washes with blocking buffer, cells were treated with 12-15uL secondary antibody (Alexa Fluor 546. Anti-rabbit), followed by a room temperature incubation for an hour in dark. Slides were washed as above, treated with 1μg/mL DAPI for a minute and mounted with Slowfade antifade (Life Technologies). Coverslips were applied and sealed with nail polish and slides were observed using the Zeiss AxioSkop 40L epifluorescence microscope.

2.2.3 Additional fluorescence microscopy

For the analysis of strains bearing GFP or YFP-tagged proteins of interest, cells were collected at appropriate timepoints, washed once in double the cell volume of distilled water, and resuspended in distilled water for microscopy. For each sample, ~5-10 µL of the cell suspension was spotted on slides and analyzed as above.

To observe cell nuclei, cells from appropriate timepoints were fixed with an equal volume of 100% cold ethanol, and DAPI (4',6-diamidino-2-phenylindole) was added to the fixed cells at a final concentration of 1µg/ml . Cells were washed, resuspended in water and analyzed as above.

2.2.4 Sister chromatid cohesion assay

To analyze sister chromatid cohesion during metaphase, strains were built so as to contain centromere-proximal Lac-operator construct on Chromosome IV containing 256 tandem arrays of the Lac operator sequence [269]. Additionally these strains were engineered to express a GFP-tagged LacI repressor protein that has high affinity for the Lac operator array. The above strains were synchronized and released into media containing 15µg/ml nocodazole to arrest cells at the G2/M junction and conditionally block chromosome segregation. Samples were analyzed for the presence of GFP-dots by fluorescence microscopy as described above. Cells that erroneously missegregated chromosome IV despite the nocodazole block displayed two GFP dots in close proximity in the mother bud, whereas cells that maintained cohesion only display a single GFP dot that likely represents overlapping/tightly adherent sister chromatids.

2.2.5 Co-immunoprecipitation analysis of the Mcm2-7 complex

Immunoprecipitation assays were carried out via modifications of the methods described in [150, 154]. For all Mcm complex immunoprecipitation experiments, 3mM ATP was included in the lysis and wash buffers, as it stabilizes the Mcm complex. Cultures were grown to roughly $2X10^7$ cells/ml in 100-200mL rich media, harvested at 5500rpm using a GSA rotor and resuspended in lysis buffer for subsequent steps. Recipe for lysis buffers were adopted from [150] and consist of 100mM HEPES-KOH pH 7.9, 100mM potassium glutamate, 10mM Magnesium acetate, 10% glycerol, 0.1% NP-40. Immediately prior to lysis, the buffers were supplemented with 3mM ATP, 1M DTT, protease inhibitors, 2mM NaF, 2mM, β-glycerophosphate. Lysis steps were carried out in the cold room by mixing the cell suspension with an equal amount of pre-chilled, acid washed glass beads and vortexing 6-8 times , with each cycle consisting of 30s pulses followed by 30s ice incubations. The resulting lysate was separated from cell debris by a low speed spin, and clarified twice by centrifugation at 14000 rpm for 10 minutes each. To increase the probability of isolating 'loaded' Mcm complexes, lysates were treated with ~500-600 Units of DNase I for one hour and subsequently centrifuged to pellet the digested chromatin. Lysates containing 600μg-1mg protein were subsequently used for immunoprecipitations. All steps were performed at 4°C.

For analyzing the interactions between Mcm2-7 and Mrc1, an Mrc1-3XHA construct was expressed under the *GAL1* promoter and immunoprecipitations were carried out using either anti-HA (mouse monoclonal, Covance) or anti-MCM (rabbit polyclonal, AS 1.1) antibody treatment for two hours followed by incubation with protein G beads for an additional hour. A similar approach was used for testing Mcm-Csm3 interactions, whereby strains were engineered to express

a Csm3-3XHA construct under the *GAL1* promoter. In order to get optimal culture growth for Csm3 induction, 2% raffinose was included in all the growth media.

In order to test protein-protein interactions between the members of the Mcm complex, strains were engineered to express either Mcm4-3XFLAG or Mcm7-3XFLAG, and immunoprecipitations were conducted using M2 FLAG agarose beads (Mouse, Sigma) for two hours at 4°C. GammaBind Sepharose beads (GE Healthcare) from all the above IP experiments were ultimately washed thrice in lysis buffer (unless noted otherwise), resuspended in 20µL 2X SDS sample buffer (20% glycerol, 0.01% bromophenol blue, 6% SDS, 0.1MTris-HCl pH6.8, 0.2 volume β-mercaptoethanol) and boiled for 3 minutes. Proteins of interest were analyzed by western blot as described below.

To test the integrity of the CMG complex throughout the cell cycle, wildtype and *mcm2DENQ* mutant strains were engineered to express a 3XHA-tagged copy of Cdc45. Cultures were synchronized in G1 with α-factor, and subsequently released into fresh media containing either α-factor, 0.2M HU or 15-30µg/ml nocodazole, and incubated with shaking for 2 hours at 30°C. IPs were essentially conducted as described above, with the following exceptions. The lysis buffer included 300mM potassium acetate in place of potassium glutamate, whereas the wash buffer contained 150mM potassium acetate, and lacked any glycerol.

2.2.6 TCA extraction of proteins

Extraction of proteins was carried out as previously described [270] . ~10^8 cells were harvested and resuspended in 1mL ice cold water. After adding 25µL of 10N NaOH and 12µL of β-

mercaptoethanol , the cell suspension was incubated in ice for 15 minutes. Thereafter, 85µL of trichloroacetic acid (TCA) was added to cell suspension followed by a 10 minute ice incubation. Cells were pelleted and washed with ice cold acetone and resuspended in 100-150µL of HU Buffer mix (6M Urea, 3.75%SDS, 150mM Tris pH6.8, 0.75mM EDTA, 1X SDS sample buffer, 80mM DTT, 80mM Tris-Cl, pH 8.0). Samples were boiled for 5 minutes and spun down, and the clear supernatant was run on SDS-PAGE gels.

2.2.7 Quantitative western blotting

Cultures were synchronized using α-factor and released into fresh YPD, and samples were collected at indicated timepoints. Samples were TCA prepped as described above and western blotting was performed using antibodies against Mcm4 (AS 6.1) or Mcm6 (AS3.1). Blots were imaged using a Fujifilm imager with a CCD camera and quantified using the ImageJ software (NIH). Mcm signals were normalized to the loading control G6PDH to obtain the relative density of the Mcm signal for each sample. For quantitative analysis of the difference in protein levels between wildtype and mutant strains, normalized densities of Mcm signals from mutant samples were adjusted relative to those of the corresponding wildtype samples.

2.2.8 Cycloheximide chase assay

Assay was conducted as described earlier [271]. Cultures grown overnight were treated with cycloheximide at a final concentration of 200µg/ml, and samples were withdrawn at desired timepoints for subsequent western blot analyses. Prior to TCA precipitation, 0.01% sodium azide

was added to samples, and subsequently samples were pelleted, resuspended in ice-cold distilled water with protease inhibitors and flash frozen.

2.2.9 Western blot to detect Rad53 phosphorylation

Strains were asynchronously grown in the absence or presence of 0.2M HU or 0.033% MMS for 2 hours and processed for western blots using the TCA extraction method as described above. Rad53 phosphorylation was detected with an overnight incubation of the blot in anti-Rad53 (Santa Cruz) at a 1:1000 dilution in TBST with 5% milk at 4°C with gentle agitation. The primary antibody detects both unphosphorylated Rad53 as well as its multiple phosphorylated, super-shifted species. Subsequently, the blot was incubated for 30 minutes at room temperature with anti-goat secondary antibody at 1:10000 dilution in TBST with 1% milk. The inclusion of milk in the secondary antibody dilution was observed to be highly effective in drastically reducing the excessive background signal normally associated with the anti-Rad53 antibody, and resulted in significantly cleaner blots.

2.2.10 Chromatin extraction for analysis of DNA-bound proteins

The assay was conducted essentially as described in [184]. ~10^8 cells were harvested for each sample and resuspended in pre-spheroplasting buffer (100mM PIPES-KOH pH 9.4, 10 mM DTT). After a 10-minute incubation at 30°C, samples were spun down and pellets were resuspended in spheroplasting buffer (50mM KPO_4, 10mM DTT, 0.6M Sorbitol). 200-300U of Zymolyase 20T (2mg/mL) was added to spheroplast cells for 15 minutes at 30°C. Spheroplasts were gently washed

thrice in lysis buffer (150 mM potassium acetate, pH7.5, 0.4M Sorbitol, 2mM Magnesium acetate, 20mM PIPES-KOH pH 6.8, protease inhibitors) with 4000 rpm spins in between. After the final wash, pellets were resuspended in 250μL lysis buffer and treated with Triton X-100 at a final concentration of 1%. The suspensions were incubated on ice for ~10 minutes, after which the suspension was overlaid on a 30% sucrose cushion and spun at 13000 rpm for 10 minutes at 4°C. Prior to the spin, an aliquot was taken from the sample to serve as the input. After the spin, the supernatant was saved and the pellet resuspended in an equal volume of lysis buffer. At this step, the supernatant should contain mostly cytosolic proteins, whereas chromatin-associated proteins should stay in the pellet fraction. To confirm this, the pellet fraction was further treated with ~300U of fresh DNase I (20mg/mL in 50% glycerol, 20mM sodium acetate, 5mM calcium chloride, 0.5M PMSF) for 15 minutes on ice, and spun down. The resulting supernatant fraction should contain solubilized proteins that have been liberated from chromatin after the DNase I treatment. All fractions were analyzed for the proteins of interest by western blot.

2.2.11 Plasmid loss assay

The assay was conducted as described earlier [263].Yeast strains bearing an *ade2 ade3* double mutation and/or the test *mcm* mutation were transformed with CEN plasmids carrying either a single (p*ARS1*) or seven copies (p*ARS7*) of an early origin *ARSH4*. The plasmids additionally carry *LEU2* and *ADE3* markers for selection and colony color analysis, respectively. To test for plasmid stability, plasmid-bearing *LEU+* strains were non-selectively grown in rich media by adding 200 cells from a selectively grown early log culture (~1X 10^7 cells/ml) to 2ml YPD, for ~18 generations

and plated to rich media (~500 cells/plate) and selective media (~2500 cells/plate) , followed by 2-3 day incubation at 30°C. Thereafter, plasmid loss was calculated according to the formula

L= 1-[(S/C)(1/n)÷2], where,

L= plasmid loss rate per generation

n= number of generations

S= number of cells in the 2mL YPD culture that contain the plasmid.

C= number of cells added to the 2mL YPD culture.

For an accurate determination of n, the formula n = (ln (F/C)) ÷ (ln 2) was used, where F is the number of cells after growth in 2ml YPD.

2.2.12 Construction of *mcm* mutant strains for Synthetic gene array (SGA) analysis

For *mcm4RA* and *mcm6DENQ* mutant strains, *mcm4RA* and *mcm6DENQ* mutant constructs were amplified from a corresponding W303 strain and integrated into the SGA 'magic marker' strain [272] in the S288C genetic background via two-step gene replacement. The latter aids in scoring of *MAT*a haploids during the genetic screen as it contains a *SpHIS5* gene under the *MATa* specific *STE2* promoter integrated at the *CAN1* locus. The mutant genes were subsequently C-terminally tagged with a *NATMX* cassette for selection of the mutant gene of interest in the SGA analysis. The *mcm2DENQ* strain was built by backcrossing a *mcm2DENQ-NATMX4* strain with an S288C strain carrying the magic marker four times, as we were unable to generate this strain via gene replacement for unknown reasons. The SGA screen was performed in the Boone lab at the

University of Toronto, whereby the mutants were tested against the yeast knockout collection as well as a temperature-sensitive mutant collection.

Genetic interactions were determined from a quantitative estimate of colony sizes. An epsilon score (ϵ-score) was assigned to each interaction for measuring the extent of the deviation in observed and expected colony sizes in double mutant combinations. Interactions were categorized as either negative (indicating putative synthetic lethality/sickness) or positive (potential genetic suppression or epistasis), with the strength of these interactions inferred from the magnitude of the epsilon score. A p-value<0.05 and epsilon score >0.08 were chosen as the default cutoff values for scoring the interactions (Michael Costanzo, Boone lab, personal communication). For each mutant analysis, functional annotations of the screen hits were performed using GO Slim-Mapper (Saccharomyces Genome Database). The analysis was restricted to a few closely related processes for the sake of presentation.

2.2.13 Fluorescent plasmid segregation assay

Assay was conducted as described previously [273]. To visually assay plasmid replication and segregation in budded cells, the *cdc15-2* allele was incorporated into the test strains, which disrupts mitotic exit and causes a telophase arrest upon shift to non-permissive temperature (37°C). Strains were engineered to express LacI-GFP from an integrated construct and transformed with an ARS/CEN plasmid bearing the Lac-operator array on a part of Chromosome IV. Cells were synchronized with α-factor and released into fresh media at the non-permissive temperature to induce arrest and grown or 2 hours. G1 and telophase-arrested cells were then monitored by

fluorescence microscopy as described above to assess the distribution of plasmids among the dividing cells.

2.2.14 Genomics analysis

For ChIP-seq analyses, ChIP was performed as described [87, 180] using yeast that has the ability to uptake BrdU from the media [274]. For determining Mcm localization, either the pan-Mcm2-7 antibody (UM174, S.P. Bell, MIT) or anti- Mcm2 (Santa Cruz SC6680) was used. DNA ChIP-Seq was performed to analyze origin firing across the genome, using an anti-BrdU antibody (555627 BD Bioscience). The rest of the sample processing and statistical data analysis was performed in collaboration with Dr. David Mac Alpine (Duke University). Briefly, libraries were prepared using Illumina Sample prep kit, multiplexed, and sequenced on a GAII Illumina sequencer. The resulting data were processed, assembled, and normalized using SCS2.6 software, with roughly five million reads per experiment. All genomic experiments were performed with replicates, which were subsequently combined via quantile normalization for presentation purposes.

3.0 MCM2-7, VIA THE 6/2 ATPASE ACTIVE SITE, LINKS REPLICATION TO THE DNA REPLICATION CHECKPOINT UPSTREAM OF *RAD53*

This chapter gives an overview of the DNA replication checkpoint (DRC) and describes the checkpoint phenotypes observed with the *mcm2DENQ* mutant under conditions of replication stress. The DNA damage checkpoint is discussed to analyze the specificity of the checkpoint defects.

3.1 CO-AUTHORSHIP DISCLAIMER

The work presented below is a collaborative effort between Sriram Vijayraghavan, Dr. Emily Tsai (former graduate student, Schwacha lab), and Dr. David MacAlpine (Associate Professor, Duke University). Data in the following figures and panels have been obtained by Dr. Emily Tsai and have been reproduced here with permission from Dr. Emily Tsai and Dr. Anthony Schwacha: Figures 5, 6, 7, 8a,b, 10a-c, 11 a, b ,d. Samples for Figure 9 were prepared by Dr. Tsai, whereas the analysis and images were provided by Dr. MacAlpine's lab. The above data are being presented here for the sake of continuity of the discussion. A manuscript detailing the experiments listed in this chapter is currently being prepared for submission, with Emily Tsai as the primary author, Sriram Vijayraghavan as the second co-author, and Dr. Anthony Schwacha as the principal corresponding author.

3.2 OVERVIEW OF THE INTRA S-PHASE CHECKPOINTS

3.2.1 Intra-S phase checkpoints sense different types of genotoxic stress during replication

The replication machinery often encounters various impediments during fork progression in S-phase. These include either exposure to genotoxic agents which may cause DNA damage, topological constraints resulting from excess DNA unwinding causing accumulation of large amounts of single stranded DNA at forks, or depletion of nucleotides which impairs the ability of the replicative polymerases to carry out DNA synthesis. To deal with such events cells are equipped with an elaborate mechanism to guard genome stability and ensure replication fidelity – the intra-S phase checkpoint pathway. This pathway is divided into two related but distinct sub-networks, one termed the DNA replication checkpoint (DRC) that specifically senses replication stress such as nucleotide depletion [123, 275]. The other pathway is referred to as the DNA damage checkpoint (DDC) which, as the name implies, senses physical damage to the DNA at or ahead of the replication forks [276]. The relevance of these mechanisms lies in the fact that unrepaired or unstable forks are highly fragile structures that either fall apart (fork collapse), engage in illegitimate recombination events that severely compromise genome integrity (reviewed in [216]). Key checkpoint factors are frequently mutated in a variety of human diseases, including several types of cancer [277]. Therefore, understanding the mechanisms that govern checkpoint response and the factors that underlie checkpoint regulation are fundamental from a human health perspective.

3.2.2 Initial sensing of stress and checkpoint activation

Initiation of the checkpoint response in cells usually takes place through activation of the sensor kinase Mec1 (ATR in mammals), a member of the PI3K family of kinases that phosphorylates a variety of replisome components [181, 278]. The related Tel1 (ATM in mammals) kinase can act as the apical sensor kinase under certain conditions as well [279]. Once activated these kinases kick start a signal transduction pathway that features mediator proteins such as Mrc1 (Claspin) and Rad9, which amplify the Mec1 signal in the phosphorylation cascade (**Figure 6**, [203, 206]). Other additional factors such as Ddc2 (ATRIP in mammals), and the ssDNA binding protein RPA assist in the recruitment and activation of Mec1 at replication forks [280, 281]. The pathway leads to the activation of the Rad53 (CHK2) effector kinase, which has multiple downstream targets including DNA repair proteins, cell cycle factors and several fork-associated proteins [205]. Other counter-mechanisms observed as part of the checkpoint response involve prevention of aberrant firing of dormant replication origins (late origins) [282] and increased dNTP production through upregulation of the RNR (ribonucleotidyl reductase) genes, and also via the corresponding downregulation of the nucleotide biosynthesis inhibitor *SML1* (discussed below) [283]. Therefore, checkpoint activation is a kinase cascade that involves an ordered sensing of damage or replication stress, transduction of the signal via mediators and, ultimately, the activation of effectors to carry out repair.

3.3 RESULTS AND DISCUSSION

3.3.1 Preliminary considerations— possible role for Mcm2-7 in the DNA Replication Checkpoint (DRC)

Being one of the chief molecular motor of the eukaryotic replisome, Mcm2-7 must be carefully regulated during the checkpoint response. Misregulated helicase activity could result in uncoupling of the helicase from polymerases, resulting in generation of long ssDNA tracts without corresponding DNA synthesis. Such an event could potentially destabilize replication forks and give rise to several of the defects mentioned above. Therefore, Mcm2-7 is a target of checkpoint proteins. Mec1 has been reported to phosphorylate Mcm6 and Mcm4 [181], and several mediator proteins including Mrc1, Tof1 and Csm3 bind to one or more subunits of the Mcm complex [179]. Additionally, Rad53 also targets the Mcm complex [213].

To investigate the role of Mcm2-7 in DRC, a specific ATPase-deficient *mcm* allele– *mcm2DENQ*– was analyzed *in vivo.* This allele was generated via mutation of two conserved acidic residues in the Walker B box of Mcm2 to their amide counterparts (DE→NQ). Biochemically, the *mcm2DENQ* mutation has been shown to ablate ATP hydrolysis at the Mcm6/2 active site, thereby affecting Mcm2/5 gate opening, predominantly shifting it to a more closed conformation ([41, 284], Simon *et. al* (in preparation). Importantly, the *mcm2DENQ* mutation displays normal Mcm2-7 *in vitro* helicase activity. Importantly, unlike a majority of biochemically-tractable *mcm* ATPase active site mutations, the *mcm2DENQ* mutation is viable in yeast despite altering ATP hydrolysis at an essential active site *in vitro*. Therefore, the allele was further investigated for any *in vivo* defects that may result from impaired active site function.

In examining this allele, it was noticed that *mcm2DENQ* mutants grew slightly slower than the corresponding wildtype strains, albeit with no appreciable differences in colony size and morphology. However, the *mcm2DENQ* mutants exhibited sensitivity to moderate concentrations of the drug hydroxyurea (HU), which inhibits nucleotide biosynthesis, forming smaller colonies. Such a phenotype is characteristic of mutant alleles of the DRC including *mec1* and *mrc1*. Interestingly, the mutant was relatively resistant to DNA damaging agents such as methylmethane sulfonate (MMS) **(Figure 9)**, unlike mutant alleles of *rad9*, which is specifically involved in a parallel branch of the intra S-phase checkpoint that monitors DNA damage (DNA damage checkpoint (DDC) [285].

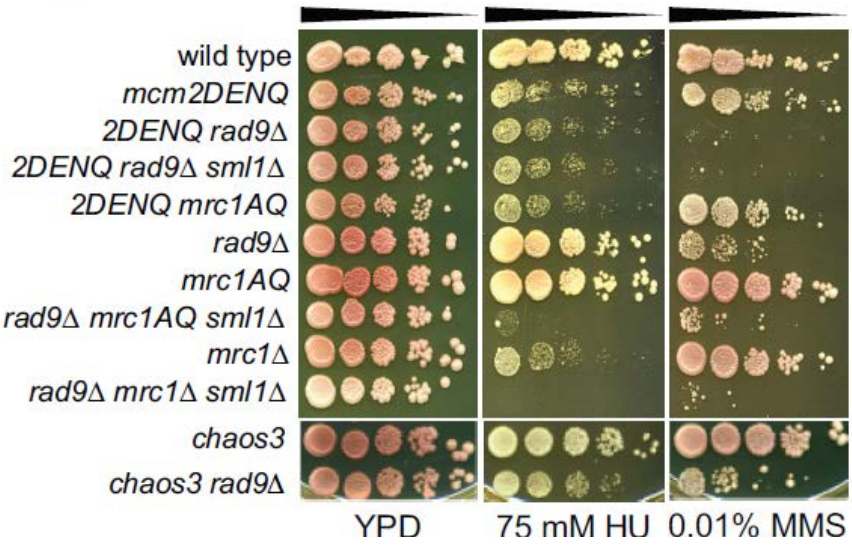

Figure 9. The *mcm2DENQ* mutant is sensitive to HU but not MMS

Wild type, (UPY464), *mcm2DENQ* (UPY499), *rad9*Δ (UPY630), *mrc1*Δ (UPY713), and *rad9*Δ *mrc1*Δ *sml1*Δ (UPY715), *mcm2DENQ rad9*Δ(UPY634), *mcm2DENQ rad9*Δ *sml1*Δ (UPY732), *mcm2DENQ mrc1AQ* (UPY758), *mrc1AQ* (UPY773), *rad9*Δ *mrc1AQ sml1*Δ (UPY745), *mcm4Chaos3* (UPY638), and *mcm4 Chaos3 rad9*Δ (UPY788) were spotted onto YPD as 10-fold serial dilutions (± HU or MMS) to assay viability.

3.3.2 The *mcm2DENQ* mutant is specifically deficient in DNA replication checkpoint signaling but not the DNA damage checkpoint

The DRC phenotype of *mcm2DENQ* was further investigated. As mentioned above, the DRC is partially redundant with the DDC, so that loss of either one of the specific mediator factors Mrc1 or Rad9 can be partially compensated by the other factor. Δ*mrc1* or Δ*rad9* mutants are individually resistant to moderate concentrations of MMS or HU. However, double mutants that ablate both DRC and DDC (Δ*rad9*Δ*mrc1*) grow poorly and are extremely sensitive to replication stress or DNA damaging agents. If *mcm2DENQ* is a DRC mutant allele, a *mcm2DENQ*Δ*rad9* double mutant should conceivably behave like the Δ*rad9*Δ*mrc1* mutant. This was found to be the case, as the double mutant was observed to be heavily MMS-sensitive **(Figure 9)**.

Furthermore, in the presence of MMS, checkpoint activation ensures that cell cycle progression is halted until damage can be alleviated. Consequently, in the complete absence of checkpoint activation, cells continue progressing through the cell cycle, inappropriately undergo cell division and lose viability. Using FACS analysis to monitor cell cycle progression, and spindle elongation as a metric of cell division, it was observed that *mcm2DENQ*Δ*rad9* double mutants exhibit a significant loss of checkpoint activation. The double mutants progressed through the cell cycle in the presence of MMS, had elongated spindles and exhibited considerable loss of viability upon prolonged exposure to MMS (**Figure 10)**. Interestingly, the *mcm2DENQ* mutant alone exhibited a normal block to cell cycle progression in the presence of MMS, further suggesting that this allele does not have a discernable DDC defect but has a specific defect in the DRC **(Figure 11)**.

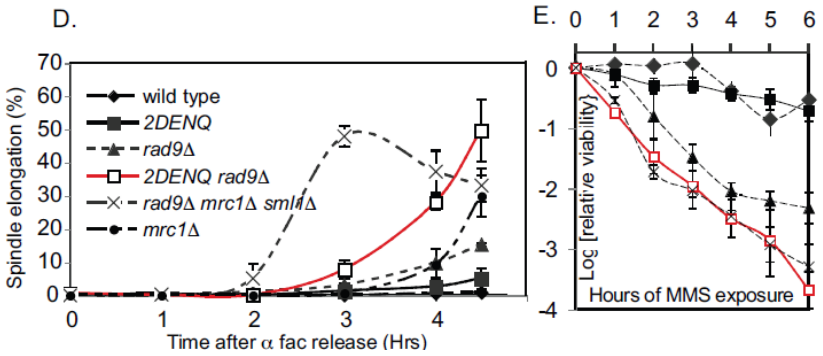

Figure 10. The *mcm2DENQ rad9*Δ mutant exhibit DRC-specific phenotypes

Cells undergoing inappropriate nuclear segregation, spindle elongation and loss of viability. (Left) The indicated strains from Figure 9 were arrested in G1 with α-factor, released into rich media + 0.01% (v/v) MMS, and spindle formation was assayed using tubulin immunofluorescence after incubation with MMS for 4.5 hours, with the graph representing the percentage of long spindles from cells at the indicated intervals. (Right) Viability following MMS exposure. Strains and growth conditions are identical to those in the left panel, and the cultures plated at the indicated intervals on YPD without drug to measure viability. Data plotted as mean ±SD of n≥3 experiments.

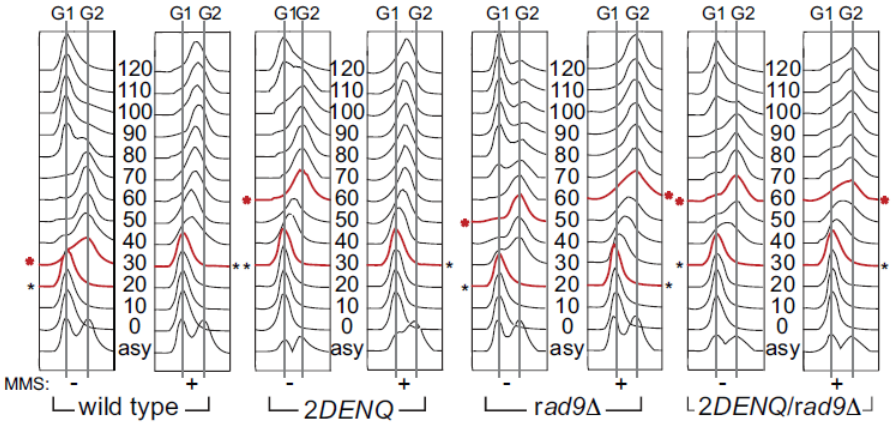

Figure 11. The *mcm2DENQ* mutant exhibits normal cell cycle block in the presence of DNA damage

FACS analysis of the indicated strains from Figure 5. Briefly, synchronized cultures were released into fresh YPD ± 0.033% MMS, and aliquots withdrawn at the indicated times were processed for FACS. After 45 (wild type) or 55 (*mcm2DENQ*) minutes α-factor was re-added to restrict analysis to a single cell cycle. Asterisks denote timepoints that represent either the apparent start (black) or end (red) [286] of S phase.

3.3.3 The *mcm2DENQ* mutant shows synthetic lethality with many DRC mutant alleles

The *mcm2DENQ* allele was examined in synthetic combinations with various DRC alleles such as *mrc1*, *tof1* and *csm3*. These three factors are known to function both as replication factors, interacting with core replisome components such as the helicase and the leading strand polymerase, and as mediators in the DRC [121, 179]. Double mutant combinations of either of these alleles with *mcm2DENQ* was found to be synthetically lethal (**Figure 12**). As noted above, Δ*rad9 mcm2DENQ* double mutants did not exhibit such synthetic lethality **(Figure 10)**. Synthetic lethality among checkpoint alleles is often suppressed by the deletion of *SML1*, an inhibitor of the nucleotide biosynthesis factor *RNR1* [287]. A common example is the Δ*mrc1*Δ*rad9* double mutant which is inviable unless combined with an additional deletion of *SML1*. Interestingly, the deletion of *SML1* was unable to rescue the synthetic lethality of *mcm2DENQ* with either Δ*mrc1*, Δ*tof1* or Δ*csm3*, indicating the loss of some essential function outside of the DRC, such as replication. This was further corroborated by the observation that a separation-of-function allele of *mrc1*- *mrc1AQ*- which has a compromised checkpoint function but normal replication [123], is viable in combination with *mcm2DENQ* **(Figure 12)**. The *mrc1AQ mcm2DENQ* double mutant exhibits the same phenotypic characteristics as either of the single mutants, further indicating that the DDC function is likely intact and thereby able to substitute for the loss of function of DRC components such as Mrc1 and Mcm2-7. Interestingly, the *mcm2DENQ* mutant was found to exhibit synthetic lethality with the sensor kinase mutant *mec1*Δ despite the presence of an *sml1*Δ, but not with the effector kinase mutant *rad53*Δ (**Figure 12)**.

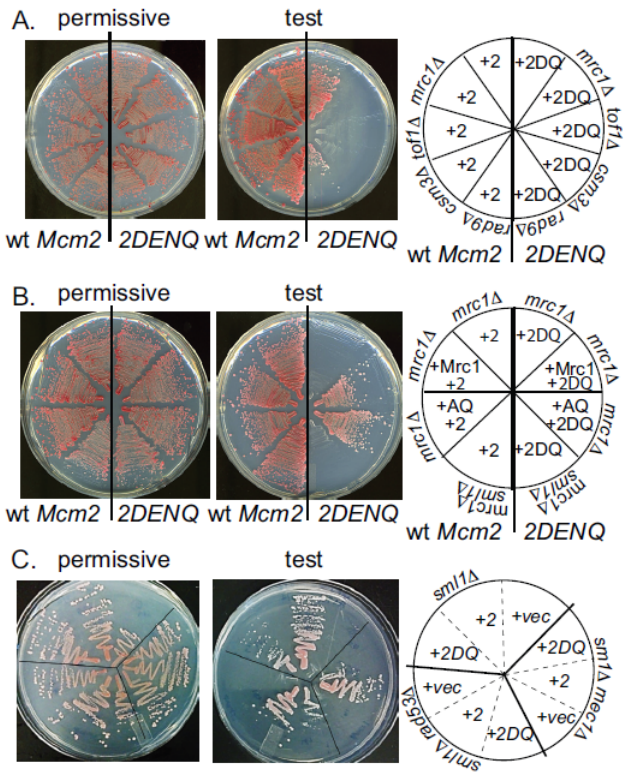

Figure 12. Synthetic lethality between DRC alleles and the *mcm2DENQ* mutant

A basic plasmid shuffle system was used. All strains used are *mcm2*Δ complemented a wildtype *MCM2*/*URA3* plasmid (pUP191) in addition, one of the following *TRP1* test plasmids: empty vector (vec, pUP169), *MCM2* (+2, pUP197) or *mcm2DENQ* (+2DQ, pUP199). Growth of these strains was compared under permissive conditions (left, media lacking uracil) with the pUP191 providing Mcm2 function, or under non-permissive conditions (right, media contains 5-fluoroorotic acid (5-FOA)) with either pUP197 (*MCM2*, left side of plate) or pUP199 (*mcm2DENQ*, right side of plate) providing the Mcm2 function. (A) Synthetic lethal interactions between the *mcm2DENQ* allele and checkpoint mediator alleles: wild type (UPY110); *mrc1*Δ (UPY428.1); *tof1*Δ (UPY631); *csm3*Δ (UPY632); *rad9*Δ (UPY421). (B) Test of *mrc1AQ* and *sml1*Δ to suppress the synthetic lethality between *mcm2DENQ* and *mrc1*Δ. The analysis is similar to (A), except the parent strains contain a deletion of both Mcm2 and of Mrc1. Three additional derivatives of these strains that contain the following relevant genotypes were also tested: *LEU2::MRC1* (+Mrc1, UPY781), *LEU2::mrc1AQ* (+AQ, UPY676), and *sml1*Δ (UPY636). These four strains in addition carry a TRP1+ plasmid containing either wild type *MCM2* or *mcm2DENQ* as in (A). (C) Synthetic lethality between *mcm2DENQ*, *mec1Δ* and *rad53Δ*. The wild type strain (UPY629) contains a chromosomal deletion of both *MCM2 and SML1*, and a complementing *MCM2+*/*URA3+* plasmid (pUP191). The *rad53Δ* (UPY1124) and *mec1Δ*

(UPY1125) strains were made by deletion of the corresponding genes using the wild type strain. The nine indicated strains were tested for synthetic lethality as in (A).

3.3.4 The *mcm2DENQ* mutant exhibits aberrant late origin firing under replication stress

In the presence of replication stress, the DRC acts to suppress late replication origins from firing inappropriately, possibly as a mechanism to reduce further depletion of the cellular nucleotide pool [288]. The specific loss of DRC components such as Mrc1 leads to widespread late origin firing despite the presence of HU. In contrast, the loss of DDC components (*rad9Δ*) does not lead to late origin firing defects. To examine whether the *mcm2DENQ* exhibits a similar defect, genome wide origin firing was analyzed via a ChIP-seq approach **(Figure 13)**. We initially tested for Mcm-origin association in *mcm2DENQ* to determine whether the mutant has any defects in general replication such as insufficient origin loading. Using ChIP with an Mcm2-7 specific antibody, it was observed that *mcm2DENQ* and the wildtype strains exhibited similar levels of Mcm-origin loading in G1-arrested cells, with >90% overlap between Mcm-association peaks of wildtype and *mcm2DENQ* samples, suggesting that there was no defect in pre-RC formation (**Figure 13**). We next sought to measure origin firing in the presence of HU, using BrdU to enrich for nascent DNA synthesis. This was followed by anti-BrdU ChIP and subsequently massively parallel sequencing of the BrdU-enriched DNA. As a control, origin firing was concordantly measured in a Δ*mrc1* strain. DRC mutants have been previously published to exhibit inappropriate firing of a large set of late dormant replication origins [180, 289]. While there was no significant difference in BrdU enrichment at early origins of replication between wildtype, *mcm2DENQ* and Δ*mrc1*, there was a marked increase in the proportion of late origin firing in the Δ*mrc1* mutant.

Interestingly, the *mcm2DENQ* mutant exhibited a somewhat intermediate level of late origin firing relative to Δ*mrc1* (**Figure 13**).

Overall, these observations further substantiate the role Mcm-7 in the DNA replication checkpoint, suggesting that the roles of Mcm2-7 in replication and DRC are separable through the Mcm6/2 active site.

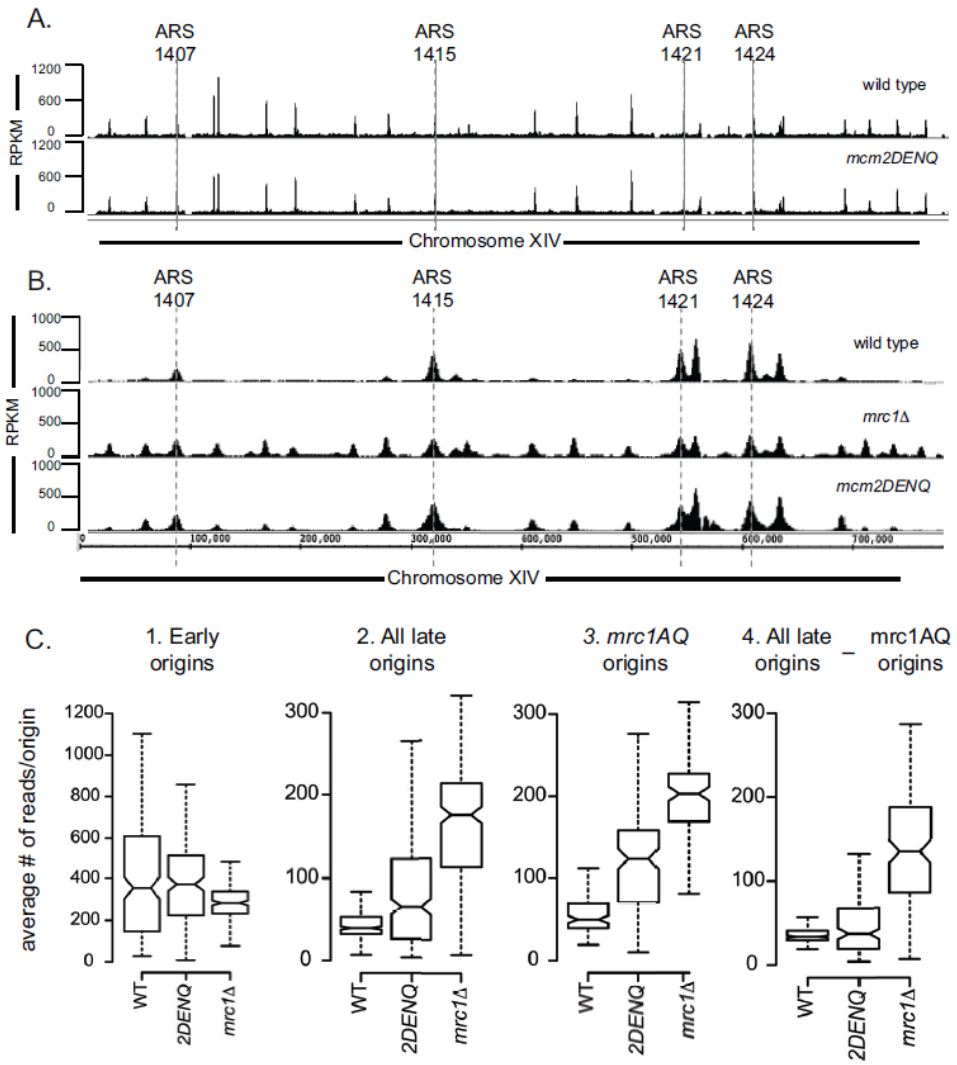

Figure 13. The *mcmDENQ* mutant shows inappropriate late origin firing

(A) Mcm2 ChIP-seq analysis of wild type (UPY493) and *mcm2DENQ* (UPY524) strains during α-factor arrest. A representative region of Chromosome XIV is shown, and RPKM are plotted. (B) BrdU ChIP-seq data are

shown for HU arrested wildtype (UPY493), *mcm2DENQ* (UPY524), and *mrc1*Δ (UPY722) and the data are plotted similar to (A). (C) Box and whisker plots describing the median and quartiles of BrdU enrichment for wild type (UPY493), *mcm2DENQ* (UPY524), and *mrc1*Δ (UPY722) at different subsets of origins. Significance was determined by a one-tailed Wilcoxon rank sum test to examine if the mutants have differences that are greater than wild type. Results for *mrc1AQ* are from [290].

3.3.5 The *mcm2DENQ* mutant places Mcm2-7 upstream of Rad53 in the DRC pathway

We sought to establish the position of Mcm2-7 in the DRC pathway. While Δ*mec1 mcm2DENQ* combinations were synthetically lethal, as observed both through plasmid shuffle experiments and tetrad analyses, *mcm2DENQ* Δ*rad53* double mutant combinations are viable, albeit slightly sick (**Figure 12**). As mentioned previously, Mec1 acts as the initial sensor of replication stress and/or DNA damage in the DRC pathway, with Rad53 phosphorylation serving as the readout of checkpoint activation. Therefore, we sought to test whether the *mcm2DENQ* allele has any effect on Rad53 phosphorylation. Cultures of different DRC and DDC mutants were subjected to acute treatments of HU or MMS for two hours and analyzed for Rad53 phosphorylation using a polyclonal anti-Rad53 antibody. As expected, most of the single mutants had normal relative levels of phosphorylated Rad53 in the presence of drugs, indicating the partial overlap between the DRC and DDC (**Figure 14)**. However, there was a marked reduction in Rad53 phosphorylation in *mcm2DENQ* Δ*rad9* double mutants in the presence of either HU or MMS. This is similar to that observed in the Δ*mrc1*Δ*rad9*Δ*sml1* mutant, which lacks any checkpoint activation owing to the complete loss of both the DRC and DDC. In contrast, *mcm2DENQ mrc1AQ* double mutants exhibited relatively normal Rad53 phosphorylation, lending further proof to the notion that Mcm2-7 functions in the same pathway as Mrc1. We further checked the status of Rad9 and

Mrc1 phosphorylation in the *mcm2DENQ* mutant **(Figure 14)**. Neither Rad9 nor Mrc1 phosphorylation was compromised in the presence of HU or MMS in the *mcm2DENQ* mutant, indicating that the *mcm2DENQ* mutation does not interfere with the relaying of signals between Mec1 and the checkpoint mediators, and therefore, likely functions parallel to Mrc1 and/or Rad9.

It is known that in addition to Mec1, Tel1 (ATM in mammals) functions as a parallel sensor to activate downstream mediators under certain conditions [279] . To determine whether or not the observed Mrc1 phosphorylation was occurring via Tel1, Mrc1 phosphorylation was analyzed in *tel1*Δ mutants. We observed that while deletion of *TEL1* had no apparent effect on Mrc1 phosphorylation, a Δ*tel1*Δ*mec1*Δ*sml1* triple mutant lost Mrc1 phosphorylation, suggesting strongly that the phosphorylation of Mrc1 occurs through Mec1 **(Figure 14)**.

Overall, the above observations imply that Mcm2-7 functions upstream of Rad53 activation, and possibly in parallel with Mrc1 in the DRC pathway.

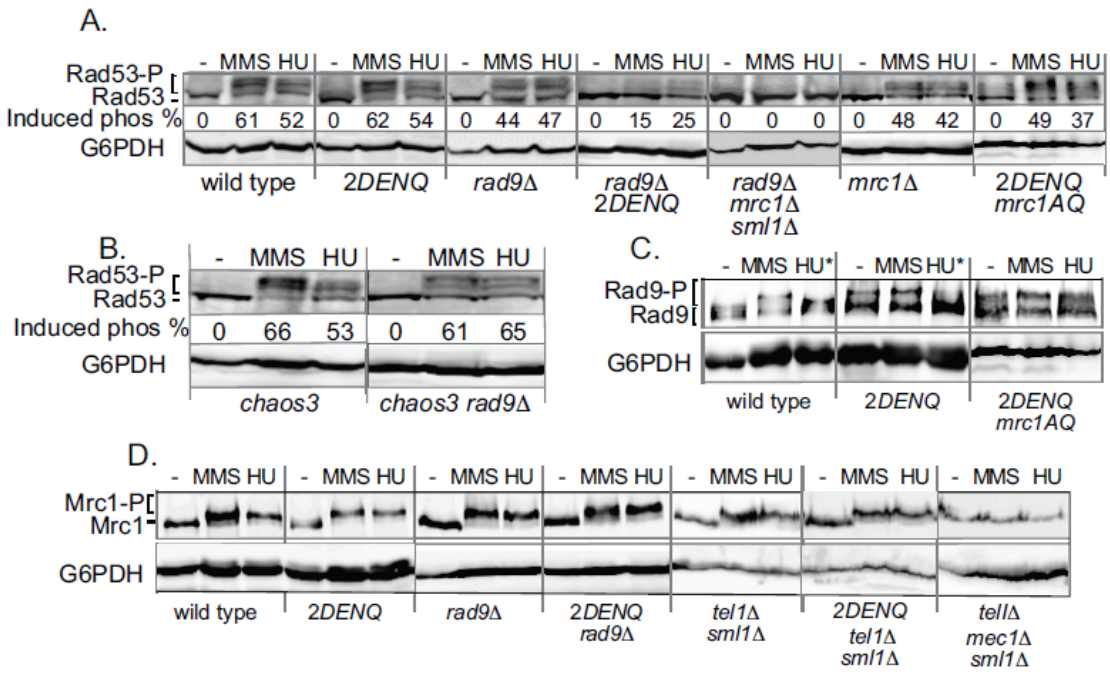

Figure 14. Mcm2-7 is a part of the DRC phosphorylation cascade

(**A-B**) Rad53 phosphorylation. Representative quantitative Western blots of Rad53 are shown from asynchronous cultures using the indicated strains from Figure 5 grown ± 200 mM HU or 0.033% MMS for 90 minutes as indicated. Induced phosphorylation % = ((slow mobility Rad53p) ÷ (total Rad53p)) X 100. Values were corrected for any phosphorylation observed in the absence of exogenous DNA damage (**C**) Rad9 or (**D**) Mrc1 phosphorylation was measured (Rad9-3xHA: wild type (UPY648), and *mcm2DENQ* (UPY649); and Mrc1-3xHA: wild type (UPY646), *mcm2DENQ* (UPY647), *rad9*Δ (UPY659), *mcm2DENQ rad9*Δ (UPY660), *tel1*Δ *sml1*Δ (UPY968), *mcm2DENQ tel1*Δ *sml1*Δ (UPY967) and *tel1*Δ *mec1*Δ *sml1*Δ (UPY985) as in (**A)** except that a C-terminal 3xHA epitope tag was engineered into each protein, and anti-HA (HA11, Covance) was used for Western blots. The epitope-tagged Mrc1 and Rad9 are functional and partially alleviate the MMS sensitivity of a *rad9*Δ *mrc1*Δ *sml1*Δ strain (data not shown). *As previously observed [203], HU causes minimal Rad9 phosphorylation in wild type and *mrc1*Δ (and apparently *mcm2DENQ*).

3.3.6 The *mcm2DENQ* mutation has minimal secondary effects on Mcm2 protein or Mcm2-7 complex stability

Because the *mcm2DENQ* mutation interferes with ATP hydrolysis at the Mcm6/2 active site, the defects observed with this mutant strongly imply that regulation of this active site is critical for the role of Mcm2-7 in the DRC pathway. However, it formally remains possible that the *mcm2DENQ* mutation results in some gross conformational change that leads to either a decrease in Mcm2 expression or stability, or may cause the whole complex to become unstable. In other words, *mcm2DENQ* could behave as a hypomorphic mutation. Such a *mcm* allele has been previously isolated from a genetic screen in mice, and characterized both *in vivo* and biochemically (*mcm4Chaos3*) [291, 292]. In order to test this, Mcm2 protein levels were assayed in the *mcm2DENQ* mutant and were found to be comparable to wildtype, indicating that the mutation does not simply result in reduced Mcm levels. Similarly, protein stability was also tested by

treating cells with cycloheximide to arrest protein synthesis, followed by a timecourse analysis of Mcm2 levels **(Figure 15, panel B)**. Again, no significant difference in Mcm2 stability was observed between wildtype and *mcm2DENQ* strains. Limited proteolysis of purified Mcm2-7 complexes containing wildtype Mcm2 or *Mcm2DENQ* mutant subunit, either in the presence or absence of ATP yielded similar profiles, suggesting that the *mcm2DENQ* mutation does not cause gross structural changes within the Mcm complex **(Figure 15, panel D)**. Finally, through co-immunoprecipitation experiments with yeast lysates using Mcm4-3XFLAG as the bait, it was further determined that the *mcm2DENQ* mutation had a minimal effect on the integrity of the Mcm complex, as we were able to pull down the remaining five subunits in both wildtype and *mcm2DENQ* strains **(Figure 15, panel C)**. These data strongly suggest that *mcm2DENQ* is not merely a hypomorphic allele, but rather represents a specific change that selectively misregulates the Mcm6/2 active site.

As mentioned above, many DRC factors are *bona fide* replication proteins that travel with the replication fork and physically interact with core members of the replisome. Notably the MTC (Mrc1/Tof1/Csm3) has been shown to directly bind to both Mcm2-7 and Polε, and likely serves to couple the two molecular motors during fork progression [179, 220]. The physical proximity of these factors to replication proteins likely assists in an expedited checkpoint response in event of replication stress, allowing stalling of forks and recruitment of additional checkpoint and/or repair factors. Therefore, a checkpoint defect could possibly arise from loss of physical association between the Mcm complex and one or more members of the MTC complex. To test this, we first checked interactions between Mcm2-7 and Mrc1 in wildtype and *mcm2DENQ* strains, using either a 3XHA-tagged Mrc1 or the Mcm2-7 complex as baits and probing for co-precipitation of the

other protein. We noticed that Mrc1-Mcm2-7 interactions were intact in both wildtype and mutant strains. Csm3 was also found to interact with Mcm2-7 similarly between *mcm2DENQ* and wildtype strains, using a similar approach as the one adopted for Mrc1 co-immunoprecipitations **(Figure 15)**.

It has been reported that Tof1 and Csm3 are both required for Mrc1 to interact with the Mcm complex [179]. We confirmed this by checking Mcm-Mrc1 interactions in Δ*tof1* and Δ*csm3* backgrounds. Mrc1-Mcm2-7 interactions were lost in the absence of Tof1 as reported earlier, suggesting that in both wildtype and *mcm2DENQ* strains, Tof1 is likely interacting normally with the Mcm complex. However, we noted that in our hands the loss of Csm3 had no effect on Mcm-Mrc1 interactions **(Figure 15)**, suggesting, contrary to previous observations [219], that Mrc1 binding to the Mcm complex does not necessarily rely on Csm3–Mcm2-7 interactions.

Overall, these results strongly imply that the DRC defects observed in the *mcm2DENQ* mutant likely result from a specific ATP hydrolysis-related defect, not from off-target effects of either decreased protein expression, stability or complex integrity.

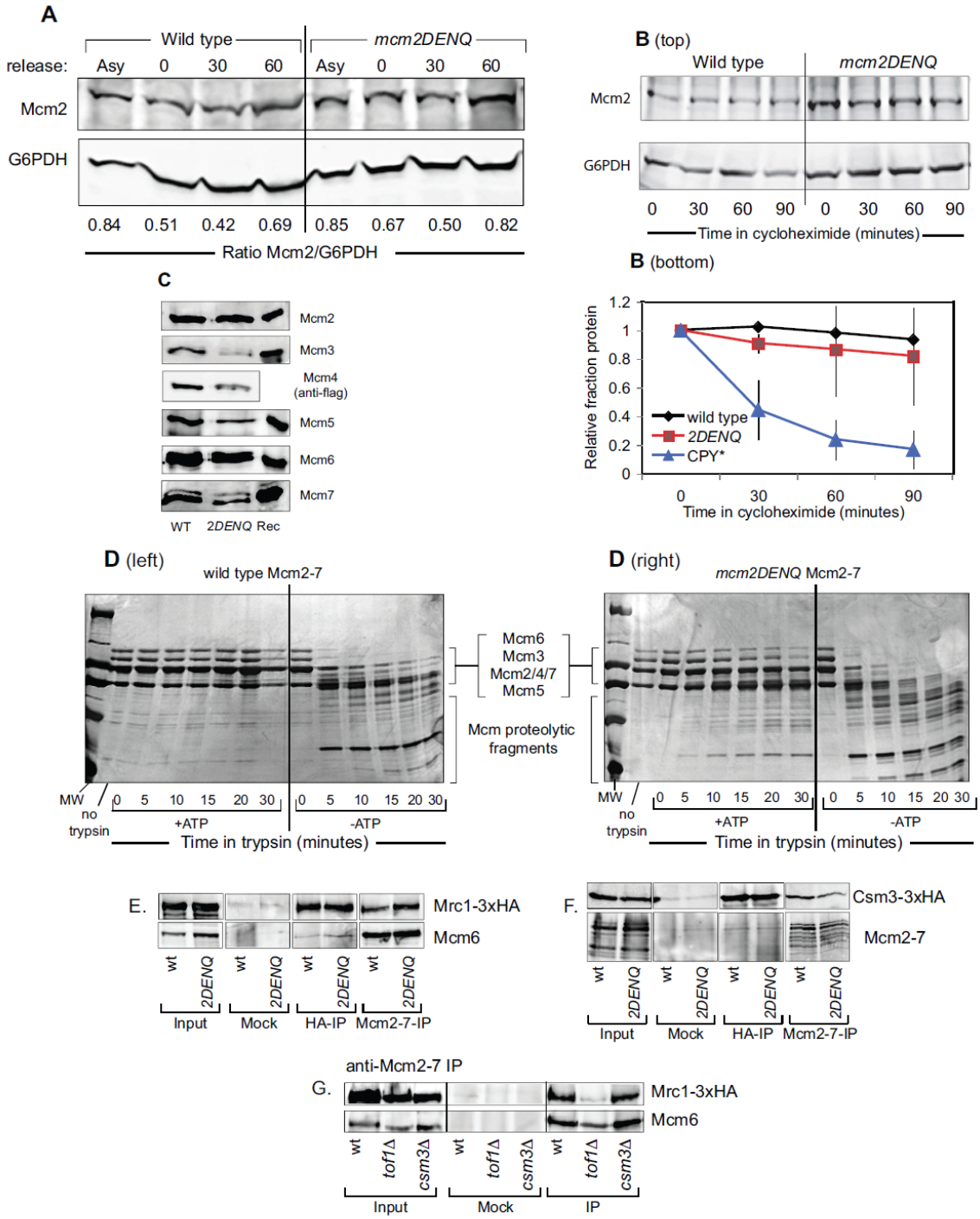

Figure 15. The *mcm2DENQ* mutant shows minimal off-target defects

(A) Wildtype or *mcm2DENQ* cell extracts were analyzed by quantitative Western blotting using antibodies either to Mcm2 or to the loading control G6PDH. **(B)** *In vivo* Mcm2 stability. Cycloheximide was added to asynchronous cultures of wild type and *mcm2DENQ* strains from (A), and the wildtype strain transformed with an

ARS/CEN plasmid encoding carboxypeptidase Y (CPY*) (pUP1106) fused to a 3XHA epitope tag (CPY* is a well-characterized ER associated degradation substrate [271]). Protein extracts were analyzed by Western blotting similar to (A**)**, except that anti-HA antibodies were used to probe for CPY*. (C) Co-IPs of Mcm subunits. UPY1044 (wild type) and UPY1045 (*mcm2DENQ*) each contain the Mcm4-3xFlag epitope tag. Western blots were probed with the indicated Mcm subunit-specific antibodies. Rec = recombinant purified Mcm2-7. (D) Limited proteolysis of Mcm2-7 complexes. Silver stained SDS-PAGE of both purified wild type [293] and *mcm2DENQ* (bottom) Mcm2-7 hexamers treated with trypsin; numbers represent minutes digested in the presence of active trypsin. Note that the Mcm2, 4, and 7 subunits co-migrate in the *S. cerevisiae* Mcm2-7 complex on SDS-PAGE. MW= molecular weight. ATP makes wild type Mcm2-7 relatively resistant to proteolysis as shown, and the digests shown were conducted in both the presence (+) and absence (-) of 10 mM ATP. **(**E**)** Mcm2-7-Mrc1 co-IPs. Yeast cell extracts of wild type (UPY1044) or *mcm2DENQ* (UPY1045) strains were immunoprecipitated using antibodies specific to either Mrc1-3xHA or Mcm2-7 as indicated. Mrc1 and Mcm6 are visualized by Western blotting using either anti-HA or anti-Mcm6. (F) Similar to (E), interactions between Mcm2-7 and Csm3 were tested by reciprocal pulldowns using strains carrying C-terminally 3XHA tagged Csm3 in a wildtype (UPY1057) or *mcm2DENQ* background (UPY1058). Mcm2-7 in this experiment was visualized using antibody UM174. (G) Immunoprecipitation experiments analogous to (E) were conducted on wild type (UPY1044), *tof1*Δ (UPY1053) and *csm3*Δ (UPY1054) strains that all contained the Mrc1-3xHA construct.

3.3.7 Discussion

We have presented evidence supporting a *bona fide* role for Mcm2-7 in the DNA replication checkpoint (DRC) pathway. The DRC pathway is complex with numerous participating factors. Although the checkpoint machinery has been known to interact with replication factors, the molecular details of many of these interactions have remained obscure. Through this work, we have shown that Mcm2-7 is involved in the regulation of a part of the checkpoint response through one of its discrete ATPase active sites.

Other groups have previously reported that specific *mcm* alleles can give rise to checkpoint defects, similar to the ones observed with the *mcm2DENQ* mutant. Particularly, the *mcm4Chaos3* mutant, which was obtained from a forward genetic screen in mice, has been associated with a high incidence of mammary adenocarcinomas in mice, with the corresponding yeast mutation giving rise to genomic instability [291, 292]. Similarly, a mutation in Mcm6 (*mcm6IL*) has been shown to disrupt the interactions between Mcm2-7 and Mrc1 in yeast, and additionally makes the strains sensitive to genotoxic agents such as MMS [219]. Other *mcm* alleles (*mcm2-1*) have also been shown to have defects in Rad53 phosphorylation (Emily Tsai, data not shown). However, these alleles are hypomorphic, whereby the defects likely arise from a significant change in the protein structure or stability, rather than from a specific loss of a specific enzymatic function.

The *mcm2DENQ* allele on the other hand disrupts the Walker B motif of the Mcm6/2 active site. In AAA+ ATPases, the active site is typically constituted *in trans* between two subunits, with one of the subunits contributing the Walker A and Walker B motifs, while the adjacent subunit contributes an Arginine finger motif. Walker B boxes play a crucial part in coordinating the nucleophilic water molecule necessary for ATP hydrolysis at these active site junctions [44]. *In vitro*, the *mcm2DENQ* mutant complexes lack ATPase activity, but are relatively efficient at DNA unwinding. Biochemically, *mcm2DENQ* mutant complexes have the propensity to force the complex into a more closed conformation by narrowing the Mcm gate, an observation that is further supported by EM analyses (Simon *et. al.*, in preparation). *In vivo*, the *mcm2DENQ* mutation does not seem to have any noticeable defects in complex oligomerization and stability, or protein expression, allowing us to rule out that it could be a hypomorphic allele like other *mcm* mutants mentioned above. Combined with the biochemical data, we propose that the Mcm6/2 active site

plays a vital role during checkpoint responses by temporally controlling Mcm gate dynamics, thereby allowing the helicase to slow down/pause when the replication fork encounters downstream obstacles.

Furthermore, the *mcm2DENQ* mutant exhibits a wide variety of classical DRC defects, including slow progression through S-phase, heightened drug sensitivity and loss of drug induced cell cycle block in combination with Δ*rad9*, and misregulated late origin firing. These observations suggest that ATP hydrolysis at Mcm6/2 active site is required for proper checkpoint regulation. As mentioned earlier, this active site is located adjacent to the Mcm2/5 'gate'. The opening and closing of this gate in an ATP-dependent manner is directly linked to helicase activation [94, 97]. Through electron microscopy, it has been demonstrated that in the context of the CMG complex, Cdc45 and GINS have been shown to bind Mcm2-7 around the gate and constrict it [97]. Assuming a similar role for the gate *in vivo*, it is not difficult to envision various circumstances under which gate regulation would be vital. For example, during a checkpoint response, the helicase must be prevented from carrying out spurious unwinding. ATP hydrolysis at the Mcm 6/2 active site may serve to modulate the gate under such circumstances by forcing it to stay open, thereby temporarily inactivating the helicase. This seemingly small change could therefore have vital *in vivo* implications. Under more normal circumstances, for instance upon completion of replication, similar mechanisms might be utilized to inactivate and/or unload the helicase from DNA.

Also, we observed normal association between various DRC mediators and Mcm2-7, clearly suggesting that the DRC phenotypes do not simply appear due to compromised physical interactions among checkpoint and replisome factors. While, we have not tested a direct

association between Mec1 and/Tel1 and Mcm2-7, we think that this association is probably also maintained similarly in the *mcm2DENQ* mutant and wildtype strains, because normal Mrc1 phosphorylation is observed under checkpoint activating conditions in both these strains. Combined with the observation that the *mcm2DENQ* mutants have normal pre-RC formation, these results further underscore the notion that the involvement of Mcm6/2 active site in the DRC is likely specific and presumably, separate from the role of Mcm2-7 during DNA replication.

While ATP hydrolysis at the Mcm6/2 active site is seemingly involved in modulating the checkpoint response, we are still speculative about factors that in turn modulate ATP hydrolysis at Mcm6/2. The mediator proteins that travel with replication forks seem like good candidates, as they directly interact with the Mcm complex. We have shown that Mrc1 is still able to bind the Mcm complex even in our ATPase-defective mutant, which implies that perhaps Mrc1 binding itself is not sufficient to regulate the helicase. Rather, factors such as Mrc1 probably modulate ATP turnover at this active site, possibly through less-understood allosteric mechanisms. Alternatively, the Mcm active sites may be regulated directly by Mec1. It is worth noting that Mcm2-7 is phosphorylated on various subunits by Mec1 during replication initiation, and much like *mrc1*, *tof1* and *csm3*, *mec1* mutations are synthetically lethal with *mcm2DENQ*, indicating that Mcm2-7 is playing an essential role in the DRC. Other groups have shown that many checkpoint mutants exhibit changes in the phosphorylation status of many replisome components, rather than physical alterations of forks [294]. Such observations lend further credence to the assumption that discrete factors could regulate the Mcm6/2, and possibly other regulatory active sites, not just by physically interacting with Mcm2-7, but through temporal modulation of their enzymatic activity.

Based on our observations, there are a couple of different scenarios for how Mcm2-7 may be involved in the DRC. First, it is possible that much like Mec1, Mcm2-7 may be acting early in the DRC pathway as a sensor of replication stress. Because Mcm2-7 is physically connected to the replication fork, it is ideally suited to sense any changes that occur in its immediate vicinity. Moreover, with six distinct ATPase active sites that have variable rates of ATP turnover, Mcm2-7 can potentially undergo subtle conformational changes under conditions that physiologically stress replication forks. Such changes could alter its interactions with, or even create novel interactions with additional checkpoint factors and may assist in mounting a swift checkpoint response. However, it is unlikely that Mcm2-7 acts redundantly as a primary sensor like ATM/ATR kinases, as Mrc1 phosphorylation was found to be relatively normal in the *mcm2DENQ* mutant (**Figure 14**).

Alternatively, Mcm2-7 may be acting as a modulator of the checkpoint signals transmitted through Mec1. In such a role, Mcm2-7 may specifically interact with activated Mrc1 during a checkpoint response, which in turn could influence ATP hydrolysis at the 6/2 active site and help stall the helicase during a checkpoint response **(Figure 16)**. The stalling of the helicase would then stabilize the replication fork and could in turn, help in the stable recruitment of other checkpoint factors like Rad53. We favor this model, as it provides a logical explanation for many of our observations. In the absence of Mcm6/2 ATP hydrolysis, the checkpoint response, although active, probably loses its robustness, which explains why the *mcm2DENQ* mutant DRC phenotypes are similar but weaker than other checkpoint mutants like *Δmrc1* or *mrc1AQ*. Because the combination of different DRC alleles and *mcm2DENQ* are synthetic lethal, it suggests that these factors likely interact to facilitate the downstream activation of Rad53. Therefore, we propose that Mcm2-7 acts

within the DRC pathway to potentiate signals transmitted to Mrc1 through Mec1, and amplify the Rad53 response.

We have shown that Mcm2-7 is an active participant in activating the DRC pathway when cells are placed under a genotoxic environment, such as those used for assaying checkpoint responses in a majority of experiments. What may be the role of the DRC and the contribution of Mcm2-7 to this pathway under physiological growth conditions? As previously mentioned, replication forks locally encounter a multitude of barriers to fork progression even during unchallenged growth conditions. These range from nucleotide exhaustion, excessive ssDNA accumulation, collisions with transcription bubbles and replication fork barriers such as genes tethered to the nuclear pore (gene gating, see next chapter [295]). When faced with such obstacles, the Mcm2-7 and other checkpoint factors likely coordinate to temporarily pause DNA unwinding but might not immediately mount a full-fledged checkpoint response. However, if such events occur genome-wide, a complete checkpoint response is warranted, which involves robust Rad53 activation. Similar models have been proposed for the regulation of DNA polymerase during S-phase by Mrc1 [296].

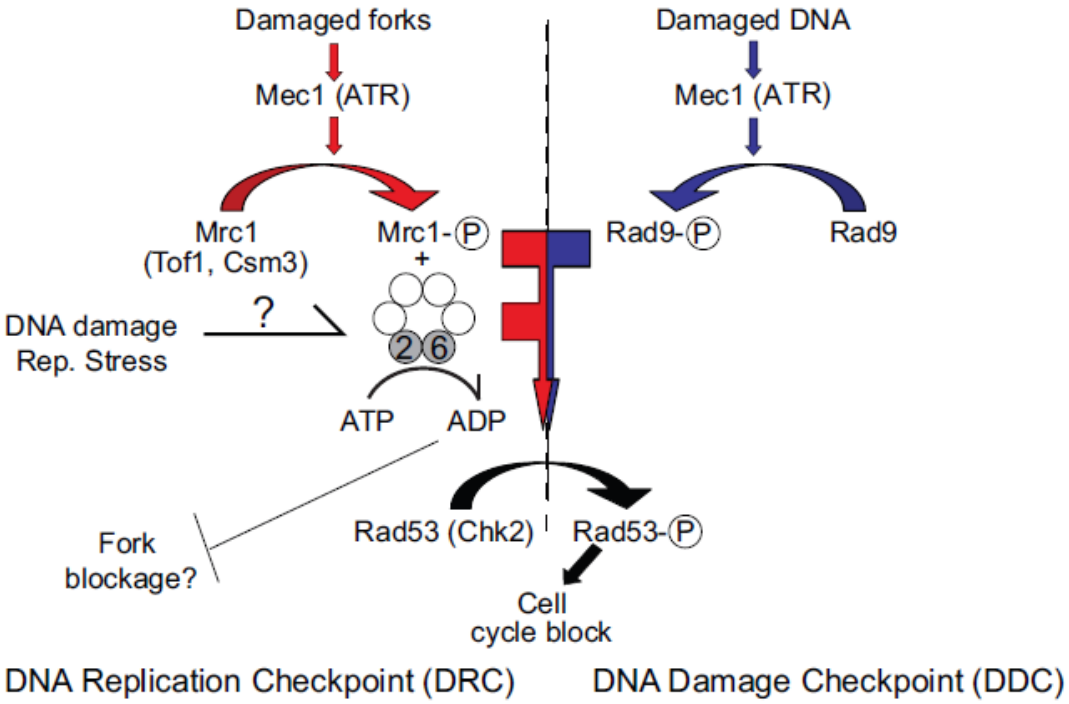

Figure 16. Model for Mcm2-7 role in DRC activation.

Refer to text for details.

4.0 REGULATION OF MCM2-7 VIA A SPECIFIC ACTIVE SITE IS A KEY DETERMINANT OF GENOME STABILITY DURING NORMAL GROWTH

This chapter describes the role of the Mcm2-7 complex in the maintenance of genome stability. The discussion is based on the phenotypic analysis of primarily the *mcm2DENQ* mutant under unchallenged growth conditions, mainly focusing on its peculiar DNA damage phenotypes. Additionally, we present evidence here describing the involvement of the Mcm2-7 complex in the establishment of proper sister chromatid cohesion (SCC). To assist in the interpretation of the data, an overview of the DNA double strand break (DSB) repair pathway in yeast is included, with special emphasis on homologous recombination. For the same purpose, we also briefly review specific aspects of SCC in the context of DNA replication.

4.1 CO-AUTHORSHIP DISCLAIMER

The work presented below is a collaborative effort between Sriram Vijayraghavan and Dr. Emily Tsai (former graduate student, Schwacha lab). A manuscript detailing the experiments listed in this chapter is currently being prepared for submission, with Sriram Vijayraghavan as the primary author, Emily Tsai as the second co-author, and Dr. Tony Schwacha as the principal corresponding author. Data in the following figures and panels have been obtained by Dr. Emily Tsai and have been reproduced here with permission from Dr. Emily Tsai and Dr. Anthony Schwacha: Figures 13 (upper panel) and Figure 25. As with the previous chapter, the above data are being presented here for the sake of continuity.

4.2 OVERVIEW OF DOUBLE STRAND BREAK REPAIR IN YEAST

4.2.1 Two pathway choices are commonly available for DSB repair in yeast

Double strand breaks (DSBs) present a potent threat to genome integrity in eukaryotes. If left unattended, DSBs can be lethal, owing to their ability to spawn wide-ranging genome aberrations including mutations, large deletions, and chromosome segregation errors. Interestingly, certain types of DSBs are physiologically relevant, like the ones mediated by Spo11 during meiosis to initiate homologous recombination [297]. Therefore, the timing and occurrence of DSBs are critical to the well-being of the genome.

Eukaryotes have evolved elaborate mechanisms to counter DNA damage. Homologous recombination (HR) is one of the well-studied processes that mediate DNA double strand break repair occurring during DNA replication and in the later stages of the cell cycle (reviewed in [298]). As the name implies, this process relies on repairing damage by utilizing a homologous DNA substrate in a series of steps that involve searching for the correct template, strand invasion and DNA synthesis, and finally correct ligation and separation of newly synthesized molecules (**Figure 17**). This is the preferred mode of DNA damage repair because the sequence information of the repaired substrate is conserved. In certain cases, eukaryotic cells repair DSBs through a mechanism called non-homologous end joining (NHEJ), which involves the re-ligation of the broken ends present at a DSB [299]. This process is heavily mutagenic, as it occurs at the expense of substrate information; joining of the broken ends occurs after initial processing of the ends by exonucleases, although it is much more common in higher eukaryotes with larger genomes [300].

4.2.2 Homologous recombination-mediated DSB repair

The process of HR relies on a precise sequence of interactions between checkpoint and recombination proteins at the site of break. Together, these proteins constitute ‘foci’ or localized areas of DNA repair [301, 302]. The focus-based repair module is important in several ways. Firstly, a single focus can represent the simultaneous processing of more than one DSB within any given cell. This means that multiple DNA damage events can be concomitantly repaired using the same set of proteins within a short time span, thereby increasing the efficiency of this process. Secondly, by maintaining a high local concentration of repair proteins at the site of the DSB, the machinery ensures that spurious recombination events do not occur elsewhere in the genome at undamaged templates, thereby greatly reducing the likelihood of random mutagenesis. Additionally, the presence of many redundantly acting factors in this process, both in yeast and humans, ensures that the broken DNA ends are properly tethered before undergoing recombinatorial repair, because failure to do so can potentially hamper proper homology search and the subsequent strand invasion processes [303]. Because many of the factors involved in HR-based DSB repair are only active in S- and G2 phases of the cell cycle [304], the system is biased towards repair using a duplicate template as opposed to non-homologous sequences within the genome. Therefore, HR permits the cells to carry out DSB repair in a streamlined and efficient manner.

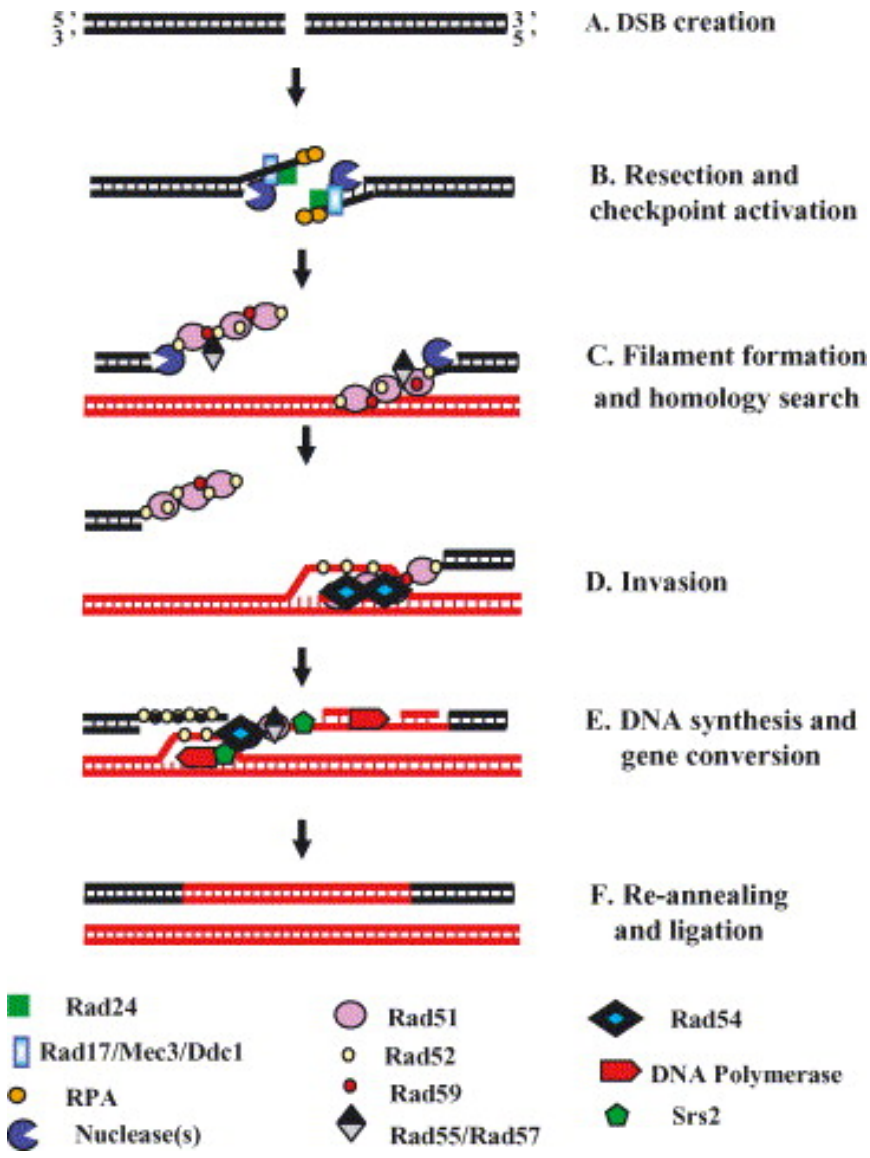

Figure 17. Mechanism of DSB repair by homologous recombination

Refer to text for details. Adapted with permission from [305].

4.2.3 DSB repair foci form in multiple waves of protein recruitment and dissociation at the sites of DNA damage

The first step in DSB repair is recognition of the broken DNA ends, which in yeast is carried out by the Mre11-Rad50-Xrs2 (MRX) complex (MRE11-RAD5-NBS1 (MRN complex) in humans)[306-308]. This represents an important first step in DSB repair, as factors involved in NHEJ often compete for the same DNA ends. In yeast, yKu70-yKu80 heterodimers bind to broken DNA ends and initiate NHEJ-based repair [309], and the ability of MRN to outcompete these factors is what biases the repair in favor of HR. In order to initiate DNA repair during HR, the 5' ends on either side of the DSB must first be chewed away, a process termed as end resection, with many redundant nucleases participating in this process including Mre11, Exo1 and Dna2 and Sae2 [303, 310, 311]. In many cases, the nucleolytic activities of these proteins are capable of acting on many different types of DNA substrates, including branched structures such as cruciform DNA [308]. Additionally, the Sgs1 (BLM in human) helicase assists nucleases such as Exo1 in this process [311]. The resulting exposed single stranded 3' end overhangs act as substrate to load additional repair factors (see below, **Figure 17**).

Additionally, Mre11 binding to the DNA ends helps to recruit the Tel1 kinase (ATM in humans) to the DSB site, where it phosphorylates the histone variant H2A (H2AX in humans) on a conserved serine residues to yield the so-called γH2A mark [312]. The γH2A signal can be spread over many kilobases of DNA surrounding the break site and facilitates binding of the Rad9 (53BP1 in humans) mediator protein to other nearby chromatin marks such as histone H3 methylated at lysine 79 [313]. As mentioned in the previous chapter, Rad9 is a constituent of the S-phase DNA damage checkpoint, whereby it can activate the effector kinase Rad53 (CHK2) upon

phosphorylation. Once resection is complete, the MRX complex can dissociate from DNA, allowing the single stranded DNA binding protein RPA to coat the ssDNA carrying exposed 3'ends [314]. RPA binding acts as a signal to recruit additional checkpoint factors such as Mec1-Ddc2 (ATR-ATRIP in humans) and the Rad24-RF-C clamp loaders at the sites of breakage [281, 315]. As a sensor kinase, Mec1 can additionally phosphorylate Rad9 similar to Tel1 and contribute to the activation of the DNA damage response through the subsequent activation of Rad53. A complex of Ddc1-Mec3-Rad17 (RAD9-HUS1-RAD1, the so-called 9-1-1 complex in humans) is also seen to load at the sites of Mec1-Ddc2 recruitment, probably as a means to stabilize the binding of Ddc2 to DNA [316].

Finally, RPA can direct the recruitment of the Rad52 protein to the repair foci (**Figure 17**). This multifaceted factor is crucial in HR repair, as it mediates the annealing of strands after strand exchange and recombination [317]. Rad52 activity is temporally controlled by cell cycle specific kinases such as CDK, and also checkpoint kinases like Mec1, which can phosphorylate Rad52 during S-phase [318]. Furthermore, Rad52 additionally recruits the recombinase Rad51 and the strand annealing factor Rad59 to damage sites [301, 319]. Higher eukaryotes have additional factors that are involved in Rad51 recruitment to ssDNA such as BRCA2. Many additional factors such as Rad54 and Rad55 are further required for the proper formation of the Rad51 nucleoprotein filament that eventually facilitates pairing between the ssDNA and the homologous dsDNA template and the subsequent strand exchange [320].

While the mechanism described above is sufficient to repair most cellular DSBs arising either spontaneously or through exogenous sources such as ionizing radiation, it is possible that certain cells may acquire breaks that remain unrepaired. Recent work has further shown that sites of the genome carrying rDNA (ribosomal DNA) have a tendency to localize to nuclear pores as extra-chromosomal elements in a checkpoint-dependent manner [321]. Such DNA elements also have a high tendency to accumulate DNA damage owing to a large number of damage-prone repetitive elements within these regions. Interestingly, during cell division, the nuclear pores from the mother cell are actively prevented from diffusing to the daughter cells via septin-mediated barriers, and as such the daughter cells establish *de novo* nuclear pores. Therefore, the rDNA, at the pre-existing nuclear pore complexes, and by extension DNA damage, have the potential to act as markers for the age of mother cells and be important determinants of replicative senescence [322].

4.3 SISTER CHROMATID COHESION AND GENOME STABILITY

4.3.1 SCC timing is carefully coordinated with the DNA replication machinery

How does the replication machinery modulate sister chromatid cohesion? Through work in budding yeast, although it is known that Eco1 plays an important role in the establishment of cohesion, yeast *eco1wpl1* double mutants can still carry on relatively normal cohesion, suggesting that the process of SCC may not be completely Eco1-dependent (also refer to Chapter1, section 1.5). In fact, many factors that constitute the replisome have been associated with varying levels of cohesion defects, including the PCNA clamp loader Ctf18, members of the MTC

(Mrc1/Tof1/Csm3) complex, and the Chl1 DNA helicase, with Ctf18 and Chl1 acting in an Eco1-independent manner [323, 324]. While their exact role in cohesion is still under investigation, it has been proposed that these factors possibly help in remodeling the cohesin complex or modulating cohesin-DNA interactions when the replication fork passages through the cohesin rings, and additionally to reconfigure the cohesion apparatus in wake of the replication fork.

4.3.2 Damaged-induced cohesion

It is worth mentioning that under special circumstances, cohesion can be established outside S-phase. This is most commonly observed if DNA damage occurs during G2/ M phase through a process termed as damage-induced cohesion (DIC) [325, 326]. Surprisingly, this process involves Eco1-mediated acetylation of Scc1, and establishes cohesion not just at the site of the DNA damage, but in a genome wide manner, possibly to limit segregation errors. Eco1 activation in this situation depends on the activation of the DNA damage checkpoint, which by the means of Rad53 activation, inhibits factors such as CDK and DDK that counteract Eco1. DIC therefore not only helps prevent improper chromosome segregation, but possibly serves to increase the efficiency of HR-mediated repair of damaged DNA by keeping sister chromatids in close proximity in a proper orientation.

Furthermore, this coordination between cohesion on damaged as well as unbroken chromosomes is dependent on the sensor kinases Mec1 and Tel1, as well as repair proteins such as Mre11 [325-327]. It has frequently been suggested that cohesion merely requires the passive movement of the replication fork through cohesin rings. However, DIC contradicts this notion by showing that not only is it possible to generate cohesion outside S-phase, cells can do so without

the need for a replication fork. Induction of just one double strand break through targeted HO endonuclease expression was found to be sufficient to establish cohesion even on undamaged chromosomes [325]. To further demonstrate that replication forks are dispensable for this process, deletion of Rad52, which is necessary for homologous recombination, was found to cause no apparent defects in DIC [325]. This is surprising, as homologous recombination-mediated repair involves the generation of replication forks, and therefore knocking out Rad52 should eliminate this process.

4.3.3 Cohesin disassembly

How are cohesins removed from DNA upon the onset of anaphase? The multi-subunit Anaphase Promoting Complex / cyclosome (APC/C) is the chief regulator of this process (reviewed in [328]), that ubiquitylates several substrates, including Securin (Pds1) for proteasomal destruction. Pds1 is an inhibitor of separase (Esp1 in yeast), which once activated, can cleave Scc1 and physically unload cohesin rings from chromatin. Separase cleavage of Scc1 requires prior phosphorylation of the cleavage site by the polo-like kinase Cdc5 [329]. Additionally, Cdc20 acts as a co-activator of APC/C in this process. In the event of improper spindle attachment and bi-orientation errors, the APC/C is inhibited by the **S**pindle **A**ssembly **C**heckpoint (SAC), which in yeast consists of many different members including Bub1, Bub3, Mad1-3 and Mps1, with initial inputs from the yeast Aurora B kinase homolog Ipl1 [330]. These factors influence spindle attachment by either preventing securin inhibition, or by directly sequestering APC/C activators, and possibly by enabling recruitment of other checkpoint factors at the kinetochore that aid in kinetochore-microtubule attachment.

4.4 RESULTS AND DISCUSSION

As previously discussed, the ATPase-deficient *mcm2DENQ* allele exhibits a wide variety of checkpoint defects when presented with challenging growth conditions, such as treatment with HU or MMS. However, based on the hypothesis that the replication checkpoint has probably evolved to monitor replication forks during S-phase even under normal growth, we asked whether this allele has any characteristic phenotypes during unchallenged growth conditions. This may provide further insight into how Mcm2-7 can participate in coordinating diverse processes during replication. Specifically, if Mcm2-7 participates as a Mec1-dependent checkpoint factor, then misregulation of Mcm2-7 may lead to defects in processes that are regulated by Mec1 during unchallenged growth conditions, including replication progression through fragile sites, replication termination, and post-replicative DNA damage repair.

4.4.1 The *mcm2DENQ* mutant exhibits several abnormal phenotypes under unchallenged growth conditions

In a preliminary analysis of growth defects of the *mcm2DENQ* mutant, we previously observed that this mutant exhibited a roughly 2.5 fold higher cell death than the corresponding wildtype strain, in addition to the slow growth phenotype (also observed as slightly prolonged S- and G2-phases as measured by FACS) mentioned in the previous chapter. Additonally, the *mcm2DENQ* mutant exhibited a significant increase in gross chromosomal rearrangements (>100-fold) over wildtype, indicating that the mutation is associated with considerable genomic instability (data not shown). Most of these phenotypes are often shared by a variety of checkpoint mutants such as Δ*mrc1*, and the hypomorphic *mcm* allele *mcm4Chaos3* [123, 291].

4.4.2 The *mcm2DENQ* mutant has multiple double strand breaks

To investigate the molecular basis of these defects, we assayed the *mcm2DENQ* mutant for the presence of DNA double strand breaks (DSBs), which are a common occurrence underlying many of the above phenotypes. As noted above, DSBs are accompanied by phosphorylation of histone H2A (γH2A) around the site of damage, and is therefore a well-established marker of DSBs both in yeast and mammalian cells. Using indirect immunofluorescence assays, it was observed that ~25% cells had γH2A foci in asynchronously growing cultures of the *mcm2DENQ* mutant, while less than 1% of wildtype cells had the same phenotype (Emily Tsai, data not shown). This DNA damage phenotype was also independently observed through Rad9 phosphorylation western blots (**Figure 14, Rad9 phosphorylation panel**); as mentioned previously, Rad9 gets phosphorylated as a part of the DNA damage checkpoint. A similar level of defect is observed in Δ*mrc1* mutants, likely as a result of damage resulting from the collapse of replication forks (see below).

4.4.3 The *mcm2DENQ* DSB phenotype is cell-cycle specific

To investigate the DSB phenotype more thoroughly, a timecourse analysis was carried out, whereby cultures were synchronized in G1, and released into fresh media with samples withdrawn at roughly every 15 minutes up to 2 hours for the analysis of γH2A foci.We observed that the levels of DSBs peaked at a time corresponding to entry into G2 in the *mcm2DENQ* mutant (**Figure 18**). This was surprising because if DSBs were arising simply as a consequence of replication defects, then the phenotype would be expected to overlap with S-phase. The latter phenotype was observed, as expected, for the Δ*mrc1* mutant (see below, **Figure 22**), in which replication forks

collapse as a consequence of losing an essential replisome component [123]. This observation further demonstrated that the DNA damage foci appear as soon as damage occurs, therefore the G2 DSBs do not merely represent persistent foci that appeared during S-phase. The presence of phosphorylated histone H2A in *mcm2DENQ* samples was additionally confirmed via western blot analysis (data not shown).

To further explore the timing of DSBs, synchronized cells were released into media containing 200mM HU and grown for two hours, with regular sampling throughout the time course for DSB analysis. As expected, the Δ*mrc1* mutant accumulated γH2A foci in HU, possibly due to a combination of an unstable fork and a concomitant depletion of nucleotides (**Figure 22)**. In contrast, HU completely suppressed the formation of γH2A foci in the *mcm2DENQ* mutant (**Figure 18)**. This phenotype was further dissected by the following means– Sml1 is an inhibitor of the ribonucleotide reductase enzyme, and therefore downregulates dNTP production. Accordingly, deletion of *sml1* drastically upregulates dNTP prodution. Furthermore, an *sml1* deletion is necessary to rescue the lethality of several checkpoint mutants such as *mec1*Δ and *rad53*Δ (see previous chapter). We tested whether deleting *sml1* had any effect on the DSBs observed with the *mcm2DENQ* mutant (**Figure 18**). We observed no change between DSB levels upon this treatment, suggesting that low nucleotide levels are probably not a contributing factor towards this particular type of DNA damage.

The above observations suggests two things– firstly, the DSBs associated with the *mcm2DENQ* mutant are unlikely to result from a mere instability of the replication fork, as is seen with Δ*mrc1* mutant. Secondly, it suggests that DSBs in the *mcm2DENQ* mutant rely on replication

fork progression. Therefore, DNA damage in the *mcm2DENQ* mutant is likely to be of post-replicative origin.

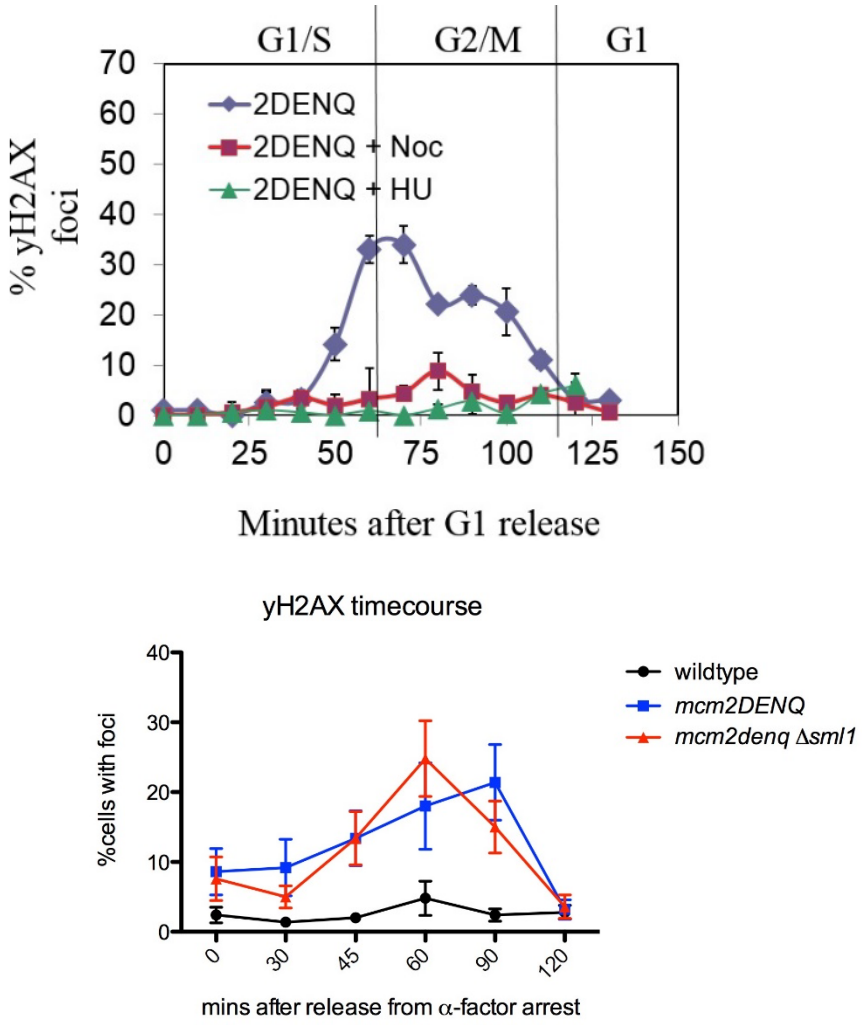

Figure 18. The *mcm2DENQ* mutant displays G2 DSBs

Cultures of *mcm2DENQ* (UPY499), *mrc1Δ* (UPY713), or *mcm2DENQ sml1Δ* (UPY948) were synchronized with α-factor, released into fresh YPD ± nocodazole or HU as indicated, and samples were processed for γ-H2AX immunofluorescence. Cell cycle transitions noted are derived from a parallel FACS analysis of the indicated strains (data not shown). Data plotted as mean ±SEM of n≥3 experiments.

4.4.4 Late breaks in the *mcm2DENQ* mutant are correlated with entry into G2, not spindle tension

To further investigate the cause of G2 breaks, several additional possibilities were explored. In order to test whether these breaks occur from the tension of the spindles on duplicated chromosomes during metaphase, synchronized cultures were released into media containing the microtubule-depolymerizing drug nocodazole. It was observed that this treatment suppressed the formation of DSBs in the *mcm2DENQ* mutant, but not in Δ*mrc1*. While this experiment suggests that the metaphase spindle may be playing a role in the appearance of the breaks, additional explanations were considered. nocodazole not only destabilizes microtubules, but also blocks entry into anaphase by triggering the spindle assembly checkpoint (SAC) as mentioned earlier . Therefore, we checked whether inactivating this pathway would continue to suppress breaks in the presence of nocodazole (**Figure 19)**. In cells lacking the critical SAC factor *BUB1*, both the presence and absence of nocodazole had minimal effects on the generation of DSBs. However in an *mcm2DENQ*Δ*bub1* double mutant, DSBs reappeared in the presence of nocodazole, suggesting that the generation of DSBs in *mcm2DENQ* is independent of spindle tension but correlated with entry into the G2/M phase of the cell cycle.

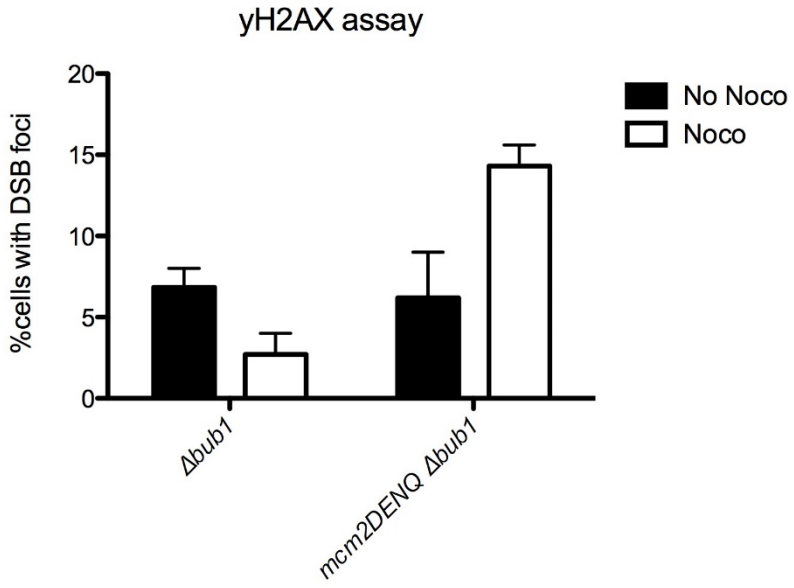

Figure 19. *mcm2DENQ* DSBs are not caused by spindle forces

γH2AX immunofluorescence of *bub1Δ* (UPY706) and *mcm2DENQ bub1Δ* (UPY 707) + nocodazole (2 hours) after α-factor release. Data plotted as mean ±SEM of n≥3 experiments.

4.4.5 G2 breaks in the *mcm2DENQ* mutant are preceded by excessive ssDNA formation in late S-phase

Although the formation of γH2A foci is among the primary response to DSBs, it does not allow us to properly determine whether the lesions arise from an earlier precursor, such as ssDNA lesions. As mentioned previously, the DSB response in yeast primarily relies on homologous recombination, which involves the temporal binding and dissociation of many different factors at the site of damage. We first checked the localization of Rad52 in our mutant strains. For this purpose, a previously-described fluorescently tagged construct of Rad52 (Rad52-YFP, [301]) was chosen, as it forms distinct subnuclear foci during DNA damage. We found that in the *mcm2DENQ*

mutant, the timing of appearance of the Rad52 foci was similar in timing to that of γH2A **(Fig 20)**, with levels peaking around 60-80 minutes after release from α-factor mediated G1 arrest. Notably though, the number of cells with Rad52 foci was considerably higher (peak at ~70%) than the corresponding percentage of cells with yH2A foci. This could result from differences in the sensitivity of the basic fluorescence assays (indirect IF vs GFP analysis). However, it is also possible that the Rad52 phenotype is at least partially separable from that of γH2A, insofar as the type of damage being reported could be different (discussed below).

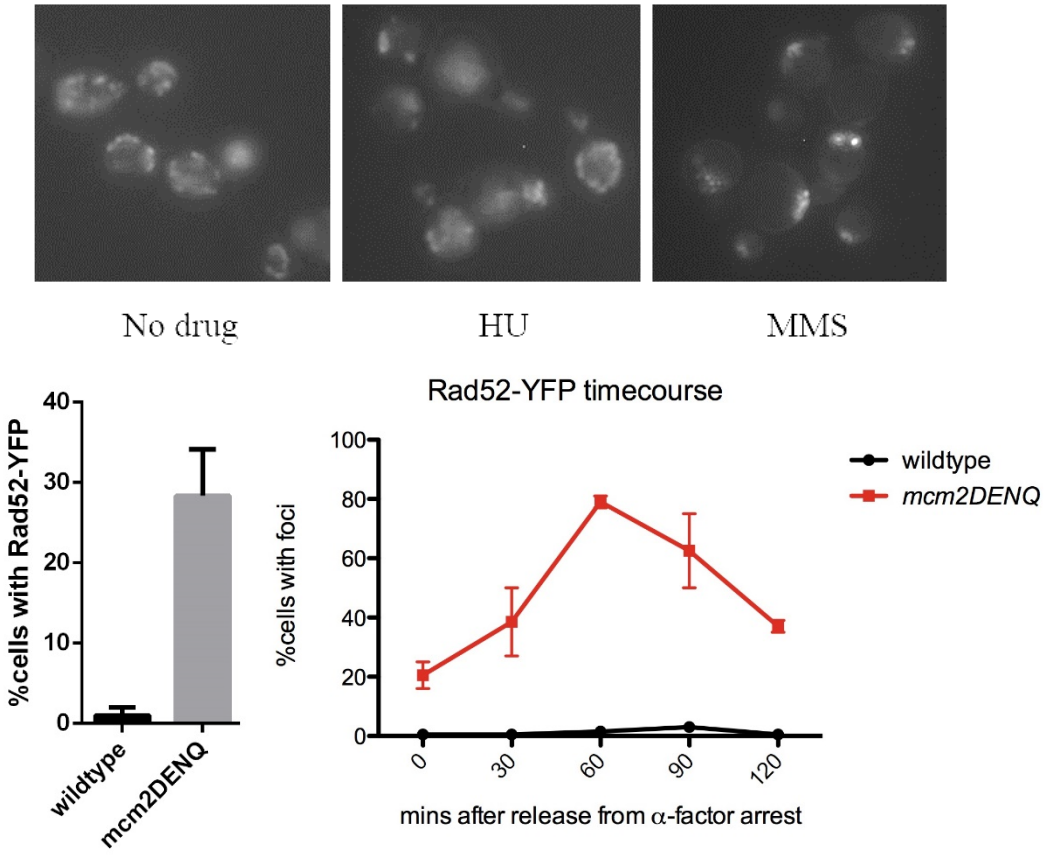

Figure 20. The *mcm2DENQ* mutant displays multiple Rad52 foci

Cultures of wild type (UPY938) treated with various drugs to show induction of Rad52-YFP fluorescence. (Bottom panel) Wildtype and *mcm2DENQ* (UPY1014) were either grown asynchronously (left panel) or synchronized with α-factor, released into fresh YPD, and samples were processed for Rad52-YFP fluorescence. Data plotted as mean ±SEM of n≥3 experiments.

To further explore the cell-cycle dependencies of Rad52-YFP appearance, synchronized cells were monitored for the appearance of foci after treatment with HU or nocodazole **(Figure 21)**. Similar to the γH2A experiment, HU treatments considerably reduced the number of observable Rad52-YFP foci, indicating that the *mcmDENQ* mutant accrues DNA damage only later in the cell cycle. However, in contrast to the earlier γH2A analysis, nocodazole treatment had a much less drastic effect in reducing the number of Rad52-YFP foci in the *mcm2DENQ* mutant. Therefore, although DSBs seem to depend on passage through G2 in order to manifest, they are likely preceded by an appearance of a different lesion, possibly ssDNA.

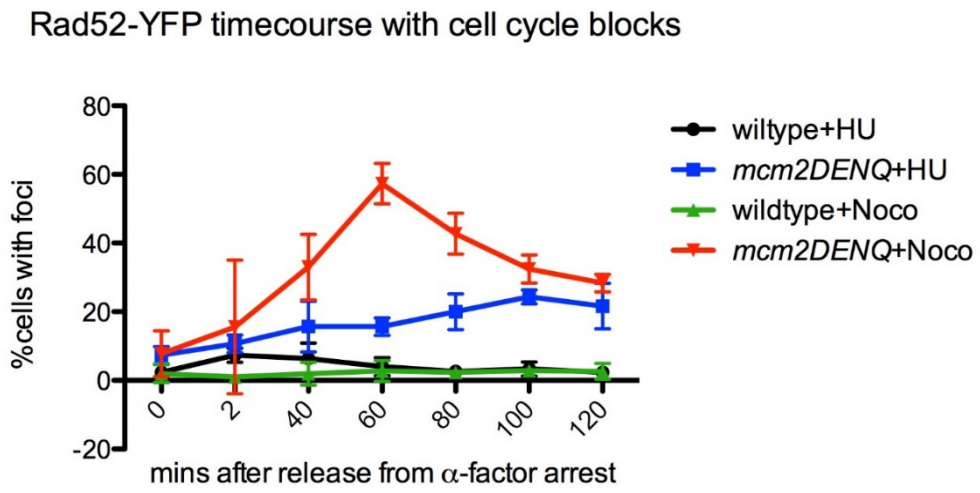

Figure 21. Rad52 foci in the *mcm2DENQ* mutant are reduced by HU but not nocodazole treatment

Strains from Figure 15 were synchronized as earlier indicated and released into YPD containing either 0.2M HU or 15μg/ml nocodazole and samples were analyzed at indicated timepoints for Rad52-YFP foci. Data plotted as mean ±SEM of n≥3 experiments.

Similar to our analysis of γH2A foci, we asked whether the *mcm2DENQ* mutant has a different pattern of expression of Rad52-YFP compared to the *mrc1Δ* mutant. As expected , we noticed a surge in the appearance of Rad52 foci early in S-phase in the *mrc1Δ* mutant (**Figure 22**). Interestingly, the absolute levels of this defect remained lower compared to the *mcm2DENQ*

mutant. We further analyzed th *mrc1Δ* mutant for Rad52-YFP foci in the presence of cell cycle blocking drugs. However, in contrast to the IF analysis, *mrc1Δ* mutants showed a significant decrease in the percentage of Rad52-YFP+ cells both upon HU and nocodazole treatments (**Figure 22**). This suggests several things: firstly, it appears that *mrc1* mutants fail to properly signal Rad52 recruitment to stalled/damaged forks under replication stress, resulting in a reduction of Rad52 foci. Similarly, *mrc1* mutants either fail to properly recruit Rad52 to sites of DNA damage in nocodazole, or the breaks observed in this mutant in nocodazole are repaired independent of the Rad52-mediated HR pathway. Despite the presence of DSBs, it is worth noting that the pattern of appearance of Rad52-YFP foci look similar in the presence or absence of nocodazole treatments, although the magnitude of the effect seems significantly different. This bears resemblance to the appearance of γH2A foci under similar treatment conditions for the *mrc1Δ* mutant (Compare 'no drug' and nocodazole data in top and bottom panels of **Figure 22**). This might also reflect a difference in the relative stabilities of Rad52 on DNA under different treatment conditions in the Δ*mrc1* mutant. Therefore, although *mcm2DENQ* and *mrc1Δ* mutants both negatively affect genome stability, their phenotypes probably differ in the underlying mechanistic basis.

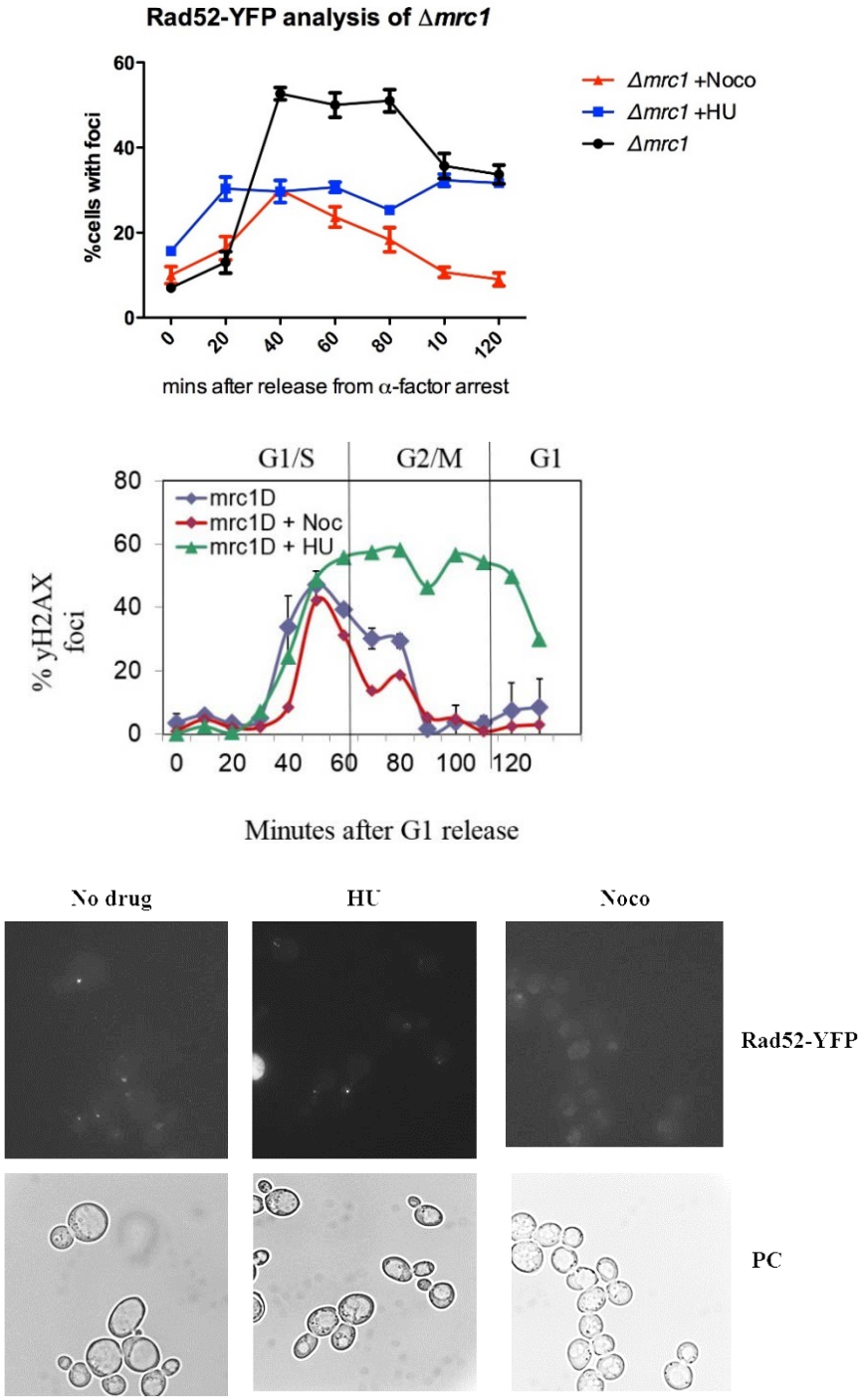

Figure 22. The *mcm2DENQ* mutant DNA damage likely has a different basis than *mrc1Δ*

Top left panel- *mrc1Δ* (UPY 1077) cultures were processed for Rad52-YFP foci analysis as described earlier in the presence of either no drug, 0.2M HU or 15µg/ml nocodazole. Data represents Mean and SD of 3 independent samples. Top right panel- *mrc1Δ* (UPY713) cultures were analyzed in a similar manner to Panel A, except that samples

were processed for γH2A IF. Data plotted as mean ±SEM of n≥3 experiments. Bottom panel- representative images from the Rad52-YFP analysis of *mrc1Δ*. Images were acquired at 120 minutes after release from α-factor arrest under the various conditions listed. PC-Phase contrast.

To determine whether there is excessive ssDNA generation in the *mcm2DENQ* mutant, strains were analyzed for the appearance of RPA foci. Rfa1 is a subunit of the heterotrimeric RPA complex of single stranded DNA binding proteins in yeast, and is normally associated with replication forks during DNA unwinding to protect ssDNA from unwarranted processing [331]. However, upon induction of DSBs, or during events where the polymerase gets uncoupled from the helicase, there is excessive generation of ssDNA either through 5' resection (in case of DSBs) or from futile DNA unwinding without any corresponding DNA synthesis (uncoupling) [122]. Under these circumstances, RPA accumulates at high concentrations on single stranded DNA . Similar to Rad52, an RFA1-YFP construct was used to fluorescently monitor RPA foci during different parts of the cell cycle, as previously described [304]. We noticed a sharp increase in the incidence of RPA foci in the *mcm2DENQ* mutant, concordant with the end of S-phase **(Figure 23)**. We further noted that the proportion of cells with RFA1-YFP foci was generally lower compared with Rad52-YFP, with levels peaking at roughly 30%. We think that this difference may be due to the dynamic nature of processing of ssDNA within cells, as RPA is generally displaced by Rad52 during HR-mediated repair (see previous chapter). As mentioned previously, RPA accumulation signals the further recruitment of additional repair factors inluding Mec1/Ddc2, and eventually Rad51/Rad52 (**Figure 17**). Interestingly, the proportion of RPA-positive cells remained similar upon nocodazole treatement but substantially decreased with HU, similar in kinetics to the appearance of Rad52 foci **(Figure 24, compare with Figure 21).** The correlation between these observations could be interpreted as follows: while G2/M entry is required for the *mcm2DENQ*

mutant cells to generate DSBs, it is not necessary for the production of ssDNA lesions, which explains why nocodazole fails to lower the levels of Rad52 and RPA accumulation despite suppressing γH2A foci.

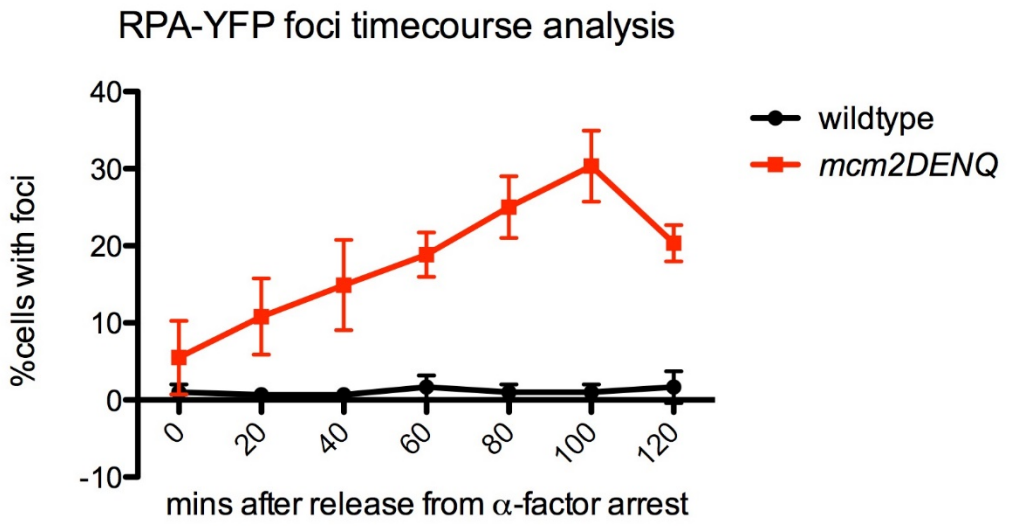

Figure 23. The *mcm2DENQ* mutant accumulates substantial ssDNA

Synchronized wildtype (UPY1169) and *mcm2DENQ* (UPY1168) cells were analyzed for the presence of RFA-YFP foci to monitor ssDNA generation during the cell cycle. Data plotted as mean ±SEM of n≥3 experiments.

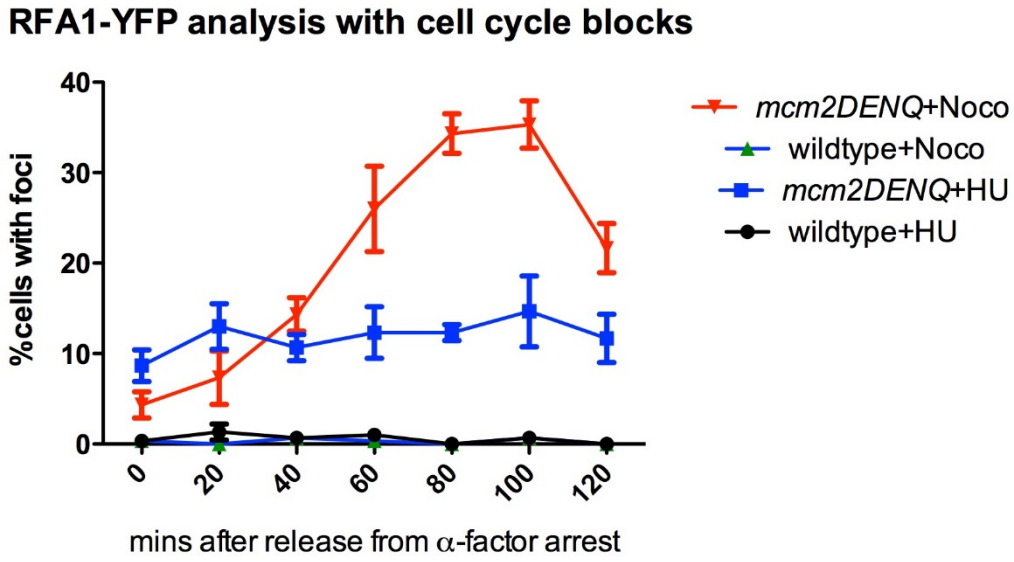

Figure 24. RPA accumulation during cell cycle arrests

Indicated strains (same as Figure 17) were synchronized and released into YPD containing 0.2M HU or 30μg/ml nocodazole. Samples were analyzed at indicated timepoints for the appearance of RFA1-YFP foci. Data plotted as mean and SEM of n≥3 experiments.

4.4.6 The DNA damage phenotype in *mcm2DENQ* is likely independent of Rad53 effector kinase activity

We previously demonstrated that the *mcm2DENQ* mutant has intrinsic defects in the DNA replication checkpoint. Within the DRC pathway, we proposed that Mcm2-7 was probably working upstream of Rad53 during a checkpoint response. Because Rad53 is the primary effector kinase in this pathway, ablation of Rad53 function could be expected to give rise to many of the phenotypes associated with its activators, even during unchallenged growth conditions. To test whether Rad53 also functions similar to Mcm2-7 during unchallenged growth conditions, we tested a *rad53*Δ*sml1*Δ for a variety of DNA damage-related phenotypes. In the absence of drugs, *rad53*Δ*sml1*Δ mutants exhibited moderate levels of Rad52-YFP foci, with similar kinetics as the *mcm2DENQ* mutant **(Figure 25)**. A similar effect was seen with the analysis of γH2A foci, with levels peaking at ~18%. In both analyses (**Figure 26)**, however, the frequency of foci appearance seemed lesser than the *mcm2DENQ* mutant, suggesting that not all of the breaks seen with the *mcm2DENQ* mutant are related directly to its role as an upstream modulator or Rad53 in the checkpoint pathway. A similar analysis of *mec1*Δ*sml1*Δ mutants for Rad52-YFP foci under unchallenged conditions yielded almost identical profiles as the *rad53*Δ*sml1*Δ mutant **(Figure 25)**, further highlighting the phenotypic similarities between various DRC alleles. *mec1* mutants have previously also been observed to give rise to multiple Rad52 foci throughout the cell cycle [301]. Unlike the *mcm2DENQ* mutant, *rad53* mutants displayed elevated levels of DNA damage

regardless of cell cycle blocks, as measured by both γH2A and Rad52-YFP analyses (**Figure 26**), likely due the role of Rad53 in stabilizing stalled replication forks along with it several other checkpoint-specific roles.

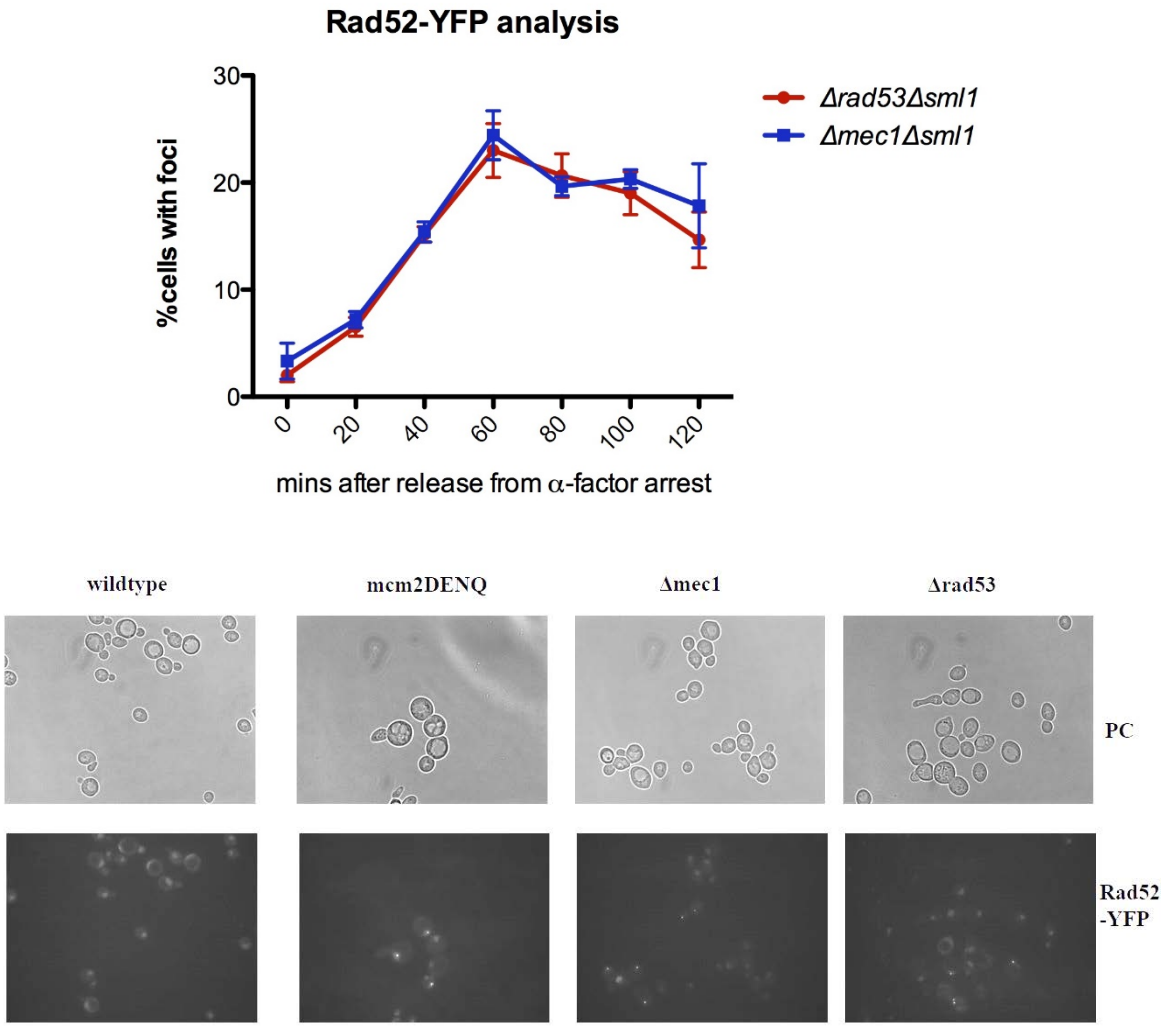

Figure 25. *rad53*Δ*sml1*Δ mutants also exhibit DNA damage phenotypes

*rad53*Δ*sml1*Δ (UPY 1137) and *mec1*Δ*sml1*Δ mutants (UPY 1135) were synchronized and released into fresh YPD for a timecourse analysis of Rad52-YFP foci. Representative images of wildtype (UPY938), *mcm2DENQ* (UPY1014), *mec1*Δ*sml1*Δ and *rad53*Δ*sml1*Δ are shown. PC- phase contrast. Data plotted as mean and SEM of n≥3 experiments.

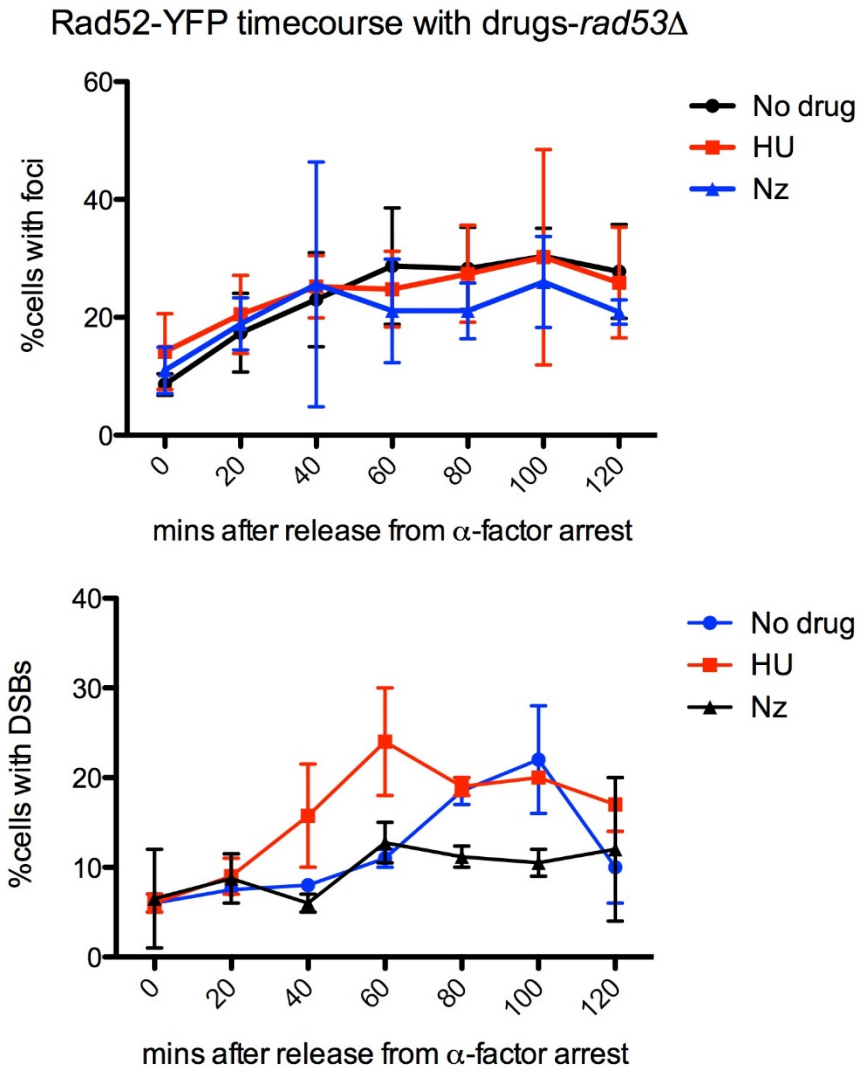

Figure 26. DNA damage analysis of the Δ*rad53* mutant

Similar to the analysis in Figure 19, *rad53*Δ*sml1*Δ mutants were synchronized and released into YPD±HU or nocodazole and samples were analyzed at indicated time points for appearance of γH2A foci(top) and Rad52-YFP (bottom). Data plotted as mean and SEM of n≥3 experiments.

We then asked if the *mcm2DENQ* DSB phenotype is directly linked to a checkpoint-dependent activation of Rad53. We tested *mcm2DENQ*Δ*sml1*Δ as well as *mcm2DENQ rad53*Δ*sml1*Δ mutants for the appearance of Rad52 foci, and found that both strains had strikingly

similar levels of Rad52-YFP induction, albeit the kinetics of the triple mutant seemed to be faster than the *mcm2DENQ sml1*Δ double mutant, possibly resulting from subtle differences in their cell cycle progression rates **(Figure 27)**. We conclude that Rad53 activity is not a significant determinant of the cell-cycle specific DNA damage phenotype of the *mcm2DENQ* mutant. Rather, events in the *mcm2DENQ* mutant seem to be correlated with a Rad53-independent progression through the cell cycle.

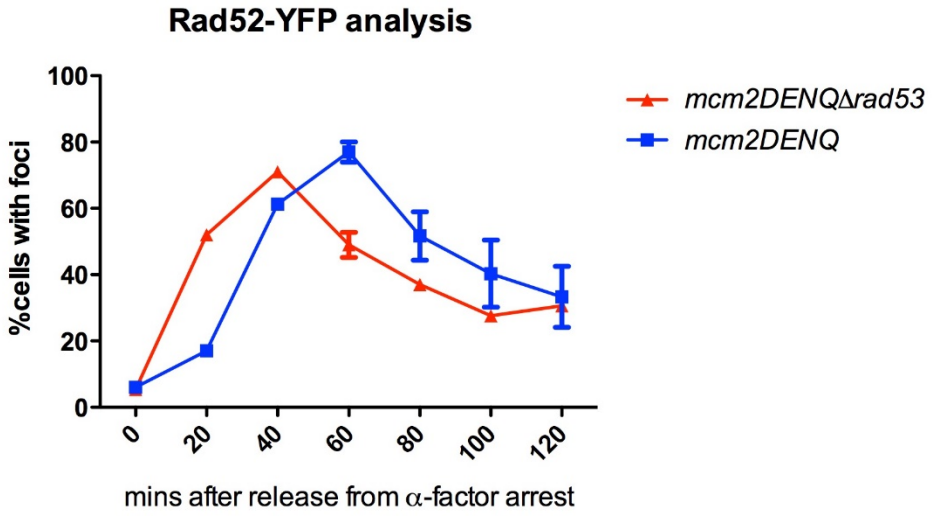

Figure 27. *mcm2DENQ* DSBs are independent of Rad53

*mcm2DENQ sml1*Δ (UPY1060) and *mcm2DENQ rad53*Δ*sml1*Δ (UPY1179) mutants were tested for Rad52 foci appearance similar to the analysis in Figure 20, albeit in the absence of any drugs. Data is represented as mean and SEM of >3 independent experiments. Data plotted as mean ±SEM of n≥3 experiments.

4.4.7 *mcm2DENQ* DNA damage is unlikely to arise from misregulated CMG dynamics during the cell cycle

While Mcm2-7 loads on DNA during G1, it is not activated for DNA unwinding until early S-phase when cell cycle specific kinases phosphorylate Mcms and allow additional factors to bind to it. Of these, the GINS complex and Cdcd45 associate directly with the Mcm2/5 gate, allowing

it to close more tightly, and increasing the robustness of the helicase [96]. This CMG complex (Cdc45/Mcm2-7/GINS) acts as the principal unwinding machine during DNA replication. Previous work has shown that the CMG complex dissociates at the end of S-phase, possibly inactivating the helicase and allowing it to unload from DNA upon replication termination [74]. Because the *mcm2DENQ* mutation has the propensity to force the Mcm complex into a closed conformation (Simon et. al., in preparation; [93]), we hypothesized that the DNA damage phenotype seen with this mutant may result from the activity of an intact, hyperactive CMG complex in G2 phase. To test this, we checked the integrity of the Cdc45-Mcm2-7 association throughout the cell cycle via co-immunoprecipitation analysis. Cultures for these experiments were synchronized in G1, and were either maintained in G1 arrest or released into either HU or nocodazole, for arresting cultures in S-phase or G2/M, respectively **(Figure 28)**. From these samples,we performed Mcm pulldowns and checked for co-precipitating Cdc45 (Cdc45-3XHA), and found that an intact Mcm2-7-Cdc45 association was only observed in HU-arrested cultures in both wildtype and *mcm2DENQ* samples. Although we did not test interactions among GINS and Mcm2-7, we infer that CMG dynamics during the cell cycle are normal and likely make little or no contribution to the DNA damage phenotypes seem with the *mcm2DENQ* mutant.

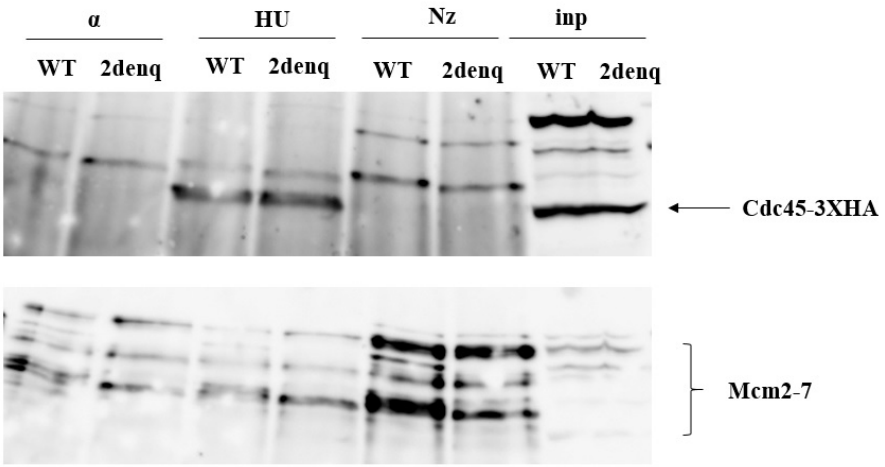

Figure 28. CMG integrity is maintained in the *mcm2DENQ* mutant

Wildtype (WT, UPY1101) and *mcm2DENQ* (UPY1102) were synchronized and either maintained in α-factor arrest or released into YPD ± HU or nocodazole for 2 hours to arrest cells in either G1, S- or G2 phases, respectively. CoIPs were performed as described in methods, using anti-MCM polyclonal to pull down the Mcm complex and test for co-precipitating Cdc45-3XHA.

4.4.8 A gene gating factor partially contributes to *mcm2DENQ* DNA damage phenotypes

Transcriptionally active regions within the genome are often tethered to the Nuclear Pore Complexes (NPCs) through scaffolding proteins that aid in the contranscriptional export of mRNA into the cytoplasm. This phenomenon, termed gene gating, poses a challenge to any replication forks that approach tethered genes, as it increases the probability of collisions between an incoming replication fork and transcription 'bubbles' at the tethered regions [295, 332]. Additionally, such a mechanism is predicted to act as a hindrance to the free rotation of DNA molecules, which makes it difficult to accommodate any torsional stress generated by polymerase-or helicase-mediated

supercoiling [5]. In yeast, checkpoint proteins such as Rad53 have been reported to play a role in gene gating during a checkpoint response, possibly by allowing the temporary dissociation of gated genes to allow the completion of replication, and additionally, to assist in the repair of any DNA damage that may occur near the tethered regions [5]. In support of this, the sensitivity of *rad53* mutants to replication stress was shown to be alleviated by mutants of the the THO/TREX-2 complex that constitute the gene gating/mRNA export machinery [5].

We hypothesized that if gene gating is contributing to the *mcm2DENQ* breaks, then analogous to the *rad53* mutant experiments described above, THO/TREX-2 mutants should suppress the DNA damage phenotype. We tested several combinations of *mcm2DENQ* with gene gating complex mutants of *THP2, SAC3* and *MFT1* (the choice of mutants was based on an SGA screen of *mcm2DENQ* mutant carried out in collaboration with Dr. Charlie Boone's lab. Refer to Appendix B for details). In our preliminary analysis, under asynchronous conditions only *sac3Δ* was seen to significantly suppress the appearance of Rad52 foci in *mcm2DENQ* mutants. Furthermore, *sac3Δ* was seen to significantly reduce the percentage of Rad52 foci^{+} cells at several points within the cell cycle. Similarly, *Δsac3mcm2DENQ* had significantly lower levels of RPA foci, indicating that the *sac3* deletion likely suppresses generation of ssDNA in the *mcm2DENQ* mutant through a gene gating-related mechanism (**Figure 29**). However, we could not see an appreciable reduction in the number of DSBs, as measured by γH2A immunofluorescence experiments, with *sac3Δ* mutants themselves accruing significant DNA damage (**Figure 29**, bottom panel).

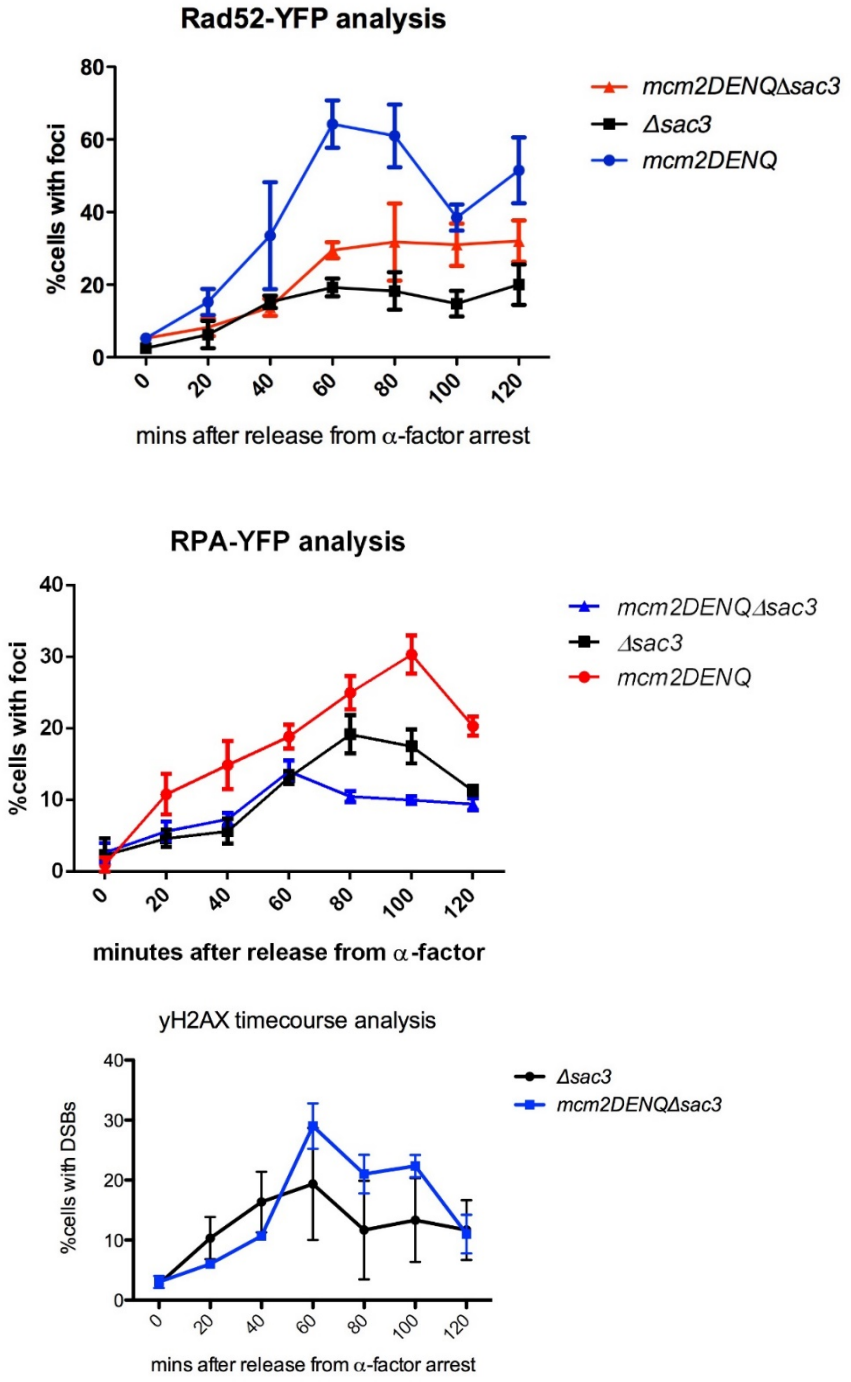

Figure 29. Gene gating partially contributes to *mcm2DENQ* lesions

sac3Δ (UPY1174), *mcm2DENQ* (UPY104), and *mcm2DENQsac3Δ* (UPY1177) were synchronized and released into the cell cycle to analyze Rad52-YFP foci. Additionally, *sac3Δ* (UPY1239), *mcm2DENQ* (UPY1168),

and *mcm2DENQsac3Δ* (UPY1240) were synchronized and released into the cell cycle to analyze RPA-YFP foci. Bottom panel- corresponding γH2A analysis. Data plotted as mean and SEM of n≥3 experiments.

We conclude that gene gating at least partially contributes to the DNA damage phenotype in *mcm2DENQ* mutants, possibly as a function of a checkpoint-related defect in this *mcm* mutant.

4.4.9 The *mcm2DENQ* mutant displays sister chromatid cohesion defects

As mentioned earlier, the replication machinery interfaces with cohesins during S-phase in order to ensure smooth fork progression and promote proper cohesion establishment. We therefore asked whether there are SCC defects in the *mcm2DENQ* mutant. Using the well-established SCC cytological assay (see Methods), we observed a significant loss in SCC in the *mcm2DENQ* mutant, at levels ~4-fold higher than wildtype **(Figure 30)**. This defect seems unrelated to Mcm2DENQ protein level, as overexpression of *mcm2DENQ* from a *GAL1* promoter failed to suppress the SCC defect (**Figure 30**). Several other checkpoint factors have been known to play a role in the establishment of cohesion. Consistent with these observations, we also noticed a significant SCC defect in many checkpoint mutants including *mrc1*Δ and *mec1*Δ*sml1*Δ strains. Interestingly, we failed to observe any SCC defects in *rad53* mutants, suggesting that SCC can occur in a Rad53-independent manner.

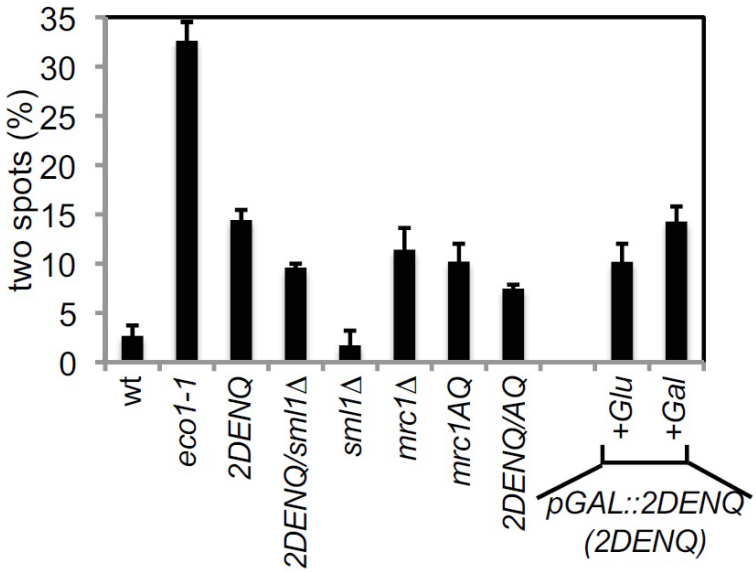

Figure 30. The *mcm2DENQ* mutant has SCC defects

SCC was assayed in synchronized cells arrested in G2 for 120 minutes with nocodazole for the following strains: wild type (UPY613), *eco1-1* (K7542), *mcm2DENQ* (UPY606), *mcm2DENQ sml1Δ* (UPY1042), *mrc1Δ* (UPY744), *mrc1AQ* (UPY822), *mcm2DENQ mrc1AQ* (UPY951), and *mcm2DENQ/ pGAL1-mcm2DENQ* (UPY884). For UPY884, results are shown following growth in glucose (+Glu, normal *Mcm2DENQ* levels) and galactose (+Gal, over-expressed *mcm2DENQ*).

We further asked if the appearance of the SCC defect in the *mcm2DENQ* mutant correlated with timing of cohesin establishment or maintenance. To assay this, cultures were synchronized and released into nocodazole for a timecourse analysis of SCC **(Figure 31)**. We observed that the characteristic 2-dot phenotype starts to appear as early as 30 minutes into the cell cycle, suggesting that a significant population of cells start to incorrectly segregate their chromosomes as soon as they replicate their DNA. The early occurrence of the SCC defect points towards a likely defect in cohesion establishment in the *mcm2DENQ* mutant. On the other hand, the Δ*mrc1* mutants showed a late onset of the SCC phenotype that correlated with entry into G2, which indicates that *mrc1* mutants fail to maintain cohesion as they approach the end of S-phase. However, the magnitude

of the defect seen with *mcm2DENQ* and other other checkpoint mutants was was much lower in comparison to the establishment-deficient *eco1-1* mutant, which, as previously reported, displayed a large SCC defect (in ~50% cells) **(Figure 30)**.

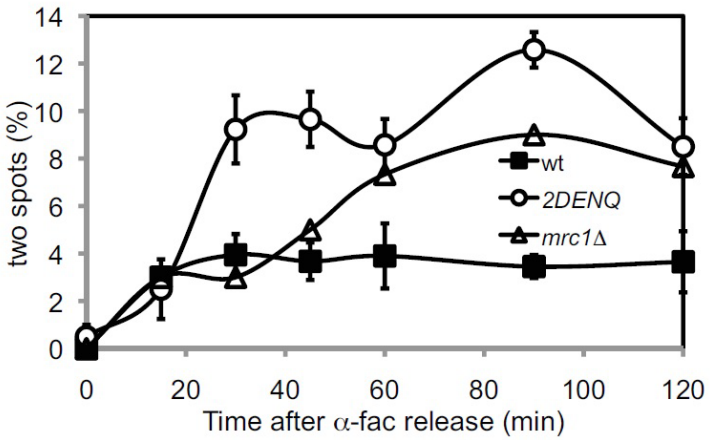

Figure 31. SCC defect of *mcm2DENQ* correlates with defective cohesion establishment

The assay was conducted with indicated strains (same as listed in Figure 25) similar to the previous figure, except SCC was assayed at specific timepoints after nocodazole arrest. Data plotted as mean ±SEM of n≥3 experiments.

4.4.10 The *mcm2DENQ* SCC defect does not arise from insufficient cohesin loading

While the SCC defect likely appears to arise from an establishment problem during S-phase, another possible interpretation of the early SCC defect could be failure to load cohesins properly in G1. To test this, we carried out a modified chromatin extraction assay to look for DNA bound cohesin ring subunits, as previously described [184]. For this assay, chromatin pellets were treated with Dnase I to release any chromatin-associated proteins into the supernatant, thereby confirming that the pellet is indeed enriched in chromatin. Using a Smc1-3XHA construct, we

were able observe equal amounts of loaded Smc1 between wildtype and *mcm2DENQ* strains in both G1 and G2/M arrested cultures **(Figure 32)**.

Having determined that the nuclear extraction method works efficiently, we then additionally tested for binding of a different cohesin subunit-Scc1, to DNA using an Scc1-3XHA construct. In this assay, pre-Dnase I treatment chromatin pellet and supernatnant fractions were tested to compare the amount of chromatin loaded vs soluble Scc1 among different strains. Once again, no observable differences could be found between wildtype and *mcm2DENQ* samples **(Figure 32)**. The *scc2-4* mutant has been previously demonstrated to be defective in cohesin loading, and we confirmed this in our assay, thereby validating the assay conditions. Similarly, the *eco1-1* mutant, although defective in SCC establishment, was found to be normal for cohesin loading, as reported previously[184]. Therefore, the *mcm2DENQ* SCC defect likely emanates from faulty cohesin establishment, probably during passage of the replication fork through loaded cohesins. We additionally observed synthetic lethality between *mcm2DENQ* and *eco1* but not *smc3* mutants (defective in loading) through genetic analyses, indicating that Mcm2-7 is likely involved in establishing cohesion in a parallel pathway with Eco1 **(Figure 33)**. Furthermore, deletion of *wpl1* failed to rescue the SCC defect or DNA double strand breaks in the *mcm2DENQ* mutant (data not shown). As mentioned earlier, *wpl1* deletions have been previously shown to suppress the SCC defect in *eco1-1* mutants [253, 333], which suggests that the SCC defect in *mcm2DENQ*, although likely to be an establishment problem, is independent of Eco1, and hints towards a parallel pathway.

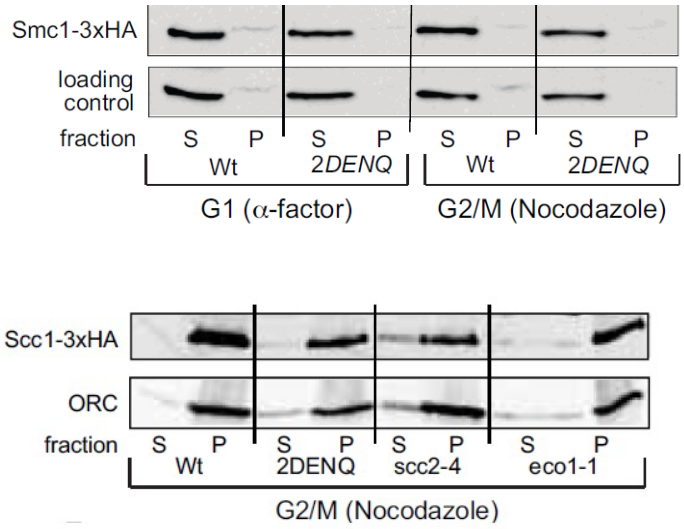

Figure 32. The *mcm2DENQ* mutant has normal cohesion-DNA association

(Top panel) Chromatin enrichment assay of Smc1-3xHA in wildtype (UPY909) and *mcm2DENQ* (UPY910) backgrounds. Supernatant and pellet fractions of initial pellet extensively treated with DNase I. Samples shown were grown at 24°C, and treated with either α-factor or nocodazole as indicated. (Bottom panel) Chromatin enrichment assay of SCC1-3xHA in wildtype (UPY911), *mcm2DENQ* (UPY912), *scc2-4* (UPY1090) and *eco1-1* (UPY1091) backgrounds. Supernatant (S) and pellet (P) fractions from initial spin are shown (refer to Methods for details). Samples shown were grown at 25°C, arrested with α-factor for 3 hours, then released into nocodazole at 35.5°C for 2.5 hours and extract made as described previously [128]. Scc1-3xHA was visualized by Western blot analysis using the HA-11 antibody, ORC refers to a doublet of ORC2 and ORC3 subunits following similar visualization using an ORC polyclonal antibody.

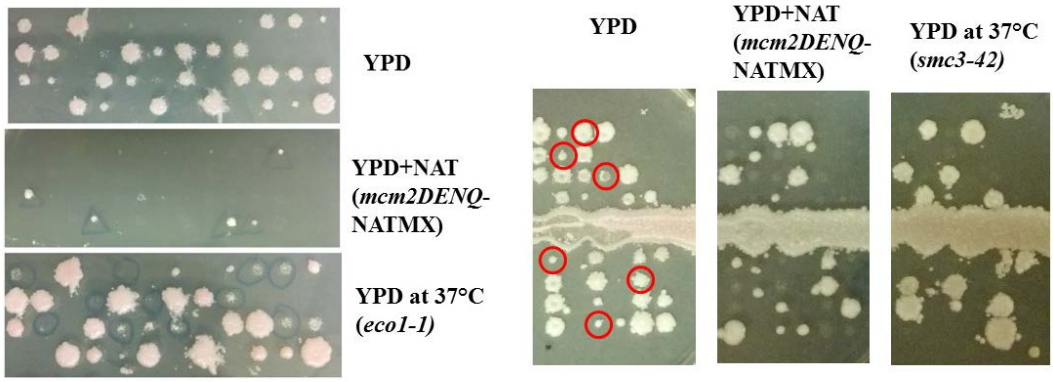

Figure 33. The *mcm2DENQ* mutation is synthetically lethal with the *eco1* mutation

Tetrad analysis from crosses between *mcm2DENQ*-NATMX (UPY627) and *eco1-1* (UPY831, left) and *smc3-42* (UPY1089, right) are shown. Red circles denote viable double mutant spore clones.

4.4.11 Discussion

In this study we further described the *in vivo* characteristics of an *mcm2* mutation that biochemically biases the Mcm2-7 complex into an open conformation. We demonstrate that during unchallenged growth conditions, this mutant exhibits a wide variety of defects related to genomic instability. This includes gross chromosomal rearrangements, cell-cyle specific spontaneous DNA damage, and sister chromatid cohesion defects. A subset of these phenotypes has previously been observed in a hypomorphic *mcm4* allele (*mcm4Chaos3*, [291, 292]) that was isolated from a mouse forward genetics screen, and correlated with a high incidence of mammary adenocarcinomas. In general, the range of genomic defects seen in the *mcm2DENQ* mutant are often observed in a variety of cancers (refer to Conclusions section).

In the previous chapter, we proposed that the Mcm2-7 complex can function as a modulator of the checkpoint response upstream of Rad53, and possibly in parallel with Mrc1. In the current study, we investigated the role of the Mcm complex in the maintenance of genomic integrity as a part of the normal replication machinery. First, we show that misregulating a specific ATPase active site within the Mcm complex can lead to cell cycle specific DNA damage and increase in gross chromosomal rearrangements. Furthermore, the same *mcm* allele concommitantly affects other processes that are important for genome stability, such as sister chromatid cohesion. Cell

cycle-specific DNA damage has similarly been observed previously with several checkpoint factors, suggesting that there may be a common basis for these phenotypes [334].

Mcm2-7 acts as the chief molecular motor of the CMG replicative helicase in all eukaryotes. While DNA unwinding is its primary role, its precise coordination with many other factors is required during replication to ensure the stability of replication forks. For instance, uncoupling between the replicative helicase and DNA polymerases can result in excessive generation of single-stranded DNA, which makes replication forks asymmetrical, highly unstable and susceptible to varying degrees of damage [335, 336]. Furthermore, a steady inflow of nucleotides is required by rapidly replicating forks during S-phase. Checkpoint-defective mutants often fail to finish replication due to insufficient nucleotide production [287]. Addtionally, the timing of DNA unwinding is also subject to precise regulation to ensure that DNA replication can only occur during S-phase. Beyond this point in the cell cycle, the helicase needs to be inactivated and unloaded from DNA, either through the dissociation of its activators (Cdc45,GINS)(K.Labib, unpublished observations), or through topological impediments such as the merging of forks from opposing directions [337]. Therefore, failure to regulate the helicase during the cell cycle can lead to several defects. When unrepaired, such genome stability issues are often highly deleterious.

We have explored several of the above possibilities to tease apart the DNA damage phenotype associated with the *mcm2DENQ* mutant. In contarst to *mrc1* mutants, the *mcm2DENQ* mutant does not seem to generate breaks as a result of collapsed forks, as the presence of HU seems to suppress the DNA damage phenotype. Additionally, we have shown that DSBs do not seem to depend on spindle forces, as forced entry into G2 in the absence of spindles was also able to

generate DSBs in our mutant. There are several regions of the genome that inherently slow down replication forks (RSZs), and are thought to represent sites of potential replication termination [3]. We failed to observe a break phenotype at one such RSZ (Schwacha, data not shown), which has previously been shown to accumulate DSBs in a *MEC1*-dependent manner [3]. The *mec1* mutant used in this study showed some of the same phenotypes as the *mcm2DENQ* insofar as it accumulated G2 DNA damage which seemed to be independent of spindle tension [236]. However, it remains to be tested whether DNA damage occurs at other such sites spread throughout the genome [2], and it remains likely that the G2 DSBs observed in the *mcm2DENQ* mutant emanate from termination errors. Furthermore, in contrast to the DSB phenotypes seen with several checkpoint mutants such as *mec1* and *rad53*, *mcm2DENQ* breaks do not seem to be correlated with insufficient nucleotide levels, as we were unable to see a change in the frequency of DSBs in the *mcm2DENQ* mutant upon the deletion of *SML1*.

The lag in S-phase passage of the *mcm2DENQ* mutant, as well as its slow growth phenotype likely have their molecular basis in DNA damage and SCC defects. Both of these defects can significantly impede normal passage of the replication fork and trigger the activation of checkpoint responses in S-phase or G2 phase. Furthermore, the SCC defect seen with *mcm2DENQ* is frequently observed with other replication factors such as *mrc1* and *ctf18* [323]. These factors serve to couple the helicase with replicative polymerases physically, and have been shown to lack any enzymatic activity. Therefore one possible function for these factors may be to coordinate sister chromatid cohesion with replication forks via the regulation of Mcm2-7. Other groups have also demonstrated the coordination between lagging strand replication and

establishment of SCC. Therefore, we hypothesize that Mcm2-7 may also be playing a role in this process by helping in reestablishing SCC in the wake of replication forks.

Additional *mcm* mutants were analyzed to check whether the defects listed above result as a general consequence of *mcm* mutations. Significantly, we found that the various genome stability defects are separable–an *mcm6DENQ* mutant, which is an ATPase defective allele of Mcm6, residing in the 6/2 active site, does not display a DNA damage phenotype. However, it shows an enhanced sister chromatid cohesion defect, suggesting that DNA damage is not obligatorily linked to Mcm misregulation (See Appendix A). Similarly, we found that the *mrc1AQ* allele also has a significant SCC defect without a corresponding DSB defect, suggesting that checkpoint misregulation does not necessarily lead to chromosome instability.

Various groups have demonstrated that DNA damage acquired during G2 promotes sister chromatid cohesion in an Eco1-dependent manner. This process, termed damage-induced cohesion (DIC), occurs genome-wide even in reponse to localized DNA damage. DIC also seems to operate independently of the DNA damage checkpoint (DDC), as *rad9* mutants lack an obvious SCC defect. We observe both G2 DSBs and an SCC defect in the *mcm2DENQ* mutant, with the magnitude of the SCC defect much lesser than that of establishment mutants such as *eco1*. It is, therefore, possible that the DSBs partially mask the SCC defect in the *mcm2DENQ* mutant on a genome-wide scale. However, as mentioned above, an *mcm6DENQ* mutant also possesses an SCC defect without any corresponding DSBs, which suggests that these processes are genetically separable to a certain extent.

Mechanistically we propose that both DSB production and SCC misregulation are linked to defective ATP hydrolysis at the Mcm6/2 active site. As previously mentioned, the heterohexameric Mcm2-7 complex has functionally distinct ATPase active site, with some playing a role in actively unwinding DNA, (Mcm4/7), and others regulating the motor activity. Of the latter, the Mcm2/5 site has been proposed to act as an ATP-dependent gate, which can directly determine the activity of the complex based on its topological state, with an open gate resulting in an inactive complex, and a closed gate activating the helicase. Additonal factors such as GINS and Cdc45 further aid in closing the gate and activating the helicase during elongation.

While biochemical and structural studies have confirmed the presence of a gated complex in both yeast and *Drosophila* Mcm complexes, much less is understood about the true *in vivo* implications of the gate [95, 97]. Initial biochemical studies and more recent EM analysis (Simon *et.al.*, in preparation) have indicated that the *mcm2DENQ* complexes have a propensity to close the Mcm 2/5 gate. We propose that *in vivo*, the *mcm2DENQ* mutation might have a similar effect on the Mcm complex. This has several interesting implications: if gate regulation is necessary during a checkpoint response or during temporary fork stalling, then failure to do so may result in a hyperactive Mcm complex. In such a conformation, the Mcm complex might initiate rounds of futile DNA unwinding without associated DNA synthesis. This would explain the generation of excess ssDNA seen during S-phase in this mutant. Additonally, helicase inactivation is a likely prerequisite for replication termination, and a hyperactive complex may associate with DNA for a prolonged amount of time. In this scenario, the helicase may pose a barrier to factors such as TopII that play a role in catenane resoluion and proper termination [175]. Such topological impediments could potentially impose structural constraints on DNA, which may result in DNA damage.

Likely scenarios for DNA damage in *mcm2DENQ* –different avenues for genome regulation

There are several interesting possibilities regarding the origin of G2 DSBs in the *mcm2DENQ* mutant. As previously mentioned, fork passage is inherently slow at certain regions within the genome (Replication Slow Zones (RSZs)), notably fragile sites, which are large regions of DNA consisting of sequences such as palindromic repeats that inherently tend to form secondary structures. Replication passage through such regions has been previously shown to rely on Mec1-dependent mechanisms [3]. Following from our previous findings that the Mcm2-7 complex is a part of the DRC pathway downstream of Mec1, we speculate that defective checkpoint control might result in the failure of the *mcm2DENQ* mutants to slow down sufficiently at RSZs. This in turn could be putting a topological constraint on the DNA at these regions, resulting in DNA damage.

Furthermore, we observed that gene gating can at least partially contribute to DNA damage observed with *mcm2DENQ.* While we have not tested the effects of the *sac3Δ* mutation on other checkpoint-related phenotypes of *mcm2DENQ,* we presume that as replication forks approach tethered genes, misregulated Mcm activity results in the failure to mount a checkpoint response in a timely manner. Presumably, a combination of misregulated DNA unwinding and opening of chromatin structures near transcription bubbles creates a local area of negative supercoiling, generating excess single stranded DNA. This would explain why *sac3Δmcm2DENQ* double mutants have considerably less Rad52 accumulation, but stll retain the DSB phenotype. Rad52 is capable of binding ssDNA without an obvious prior need for a DSB lesion, and once associated with ssDNA is capable of initiating an HR-mediated DNA synthesis. Our results hint at a novel

role for the Mcm complex in the control of replication fork progression through highly transcribed genes.

Because we observe DNA DSBs specifically towards the end of replication but rarely in the earlier stages of the cell cycle, it is tempting to speculate that some factor that is specifically active during G2/M might be responsible for physically creating breaks. The structure-specific endonuclease Mus81 is a strong candidate for such a role. Mus81 complexes with the Mms4 subunit and is responsible for cleaving a variety of structures including branched DNA, Holliday junctions and D-loops that are frequently formed during homologous recombination [338]. Importantly, to ensure integrity of replication forks, Mus81 is usually only active in G2/M. Work in *S. pombe* has demonstrated that the checkpoint kinase Cds1 (homolog of *S. cerevisiae* Rad53) regulates Mus81 to preserve the genome by aiding in the removal of chromatin-bound Mus81 from regions of stalled forks upon HU treatment in a phosphorylation-dependent manner [339], which could also explain why HU suppresses the γH2A phenotype in the *mcm2DENQ* mutant. The abundance of Rad52 and RPA foci late in the cell cycle in the *mcm2DENQ* mutant indicates frequent homologous recombination, which would be expected to generate structures that can act as substrates for Mus81. More interestingly, *S. pombe* Mus81 is also associated with DSBs in checkpoint-defective mutants[340]. Inability to enter G2/M during a nocodazole arrest then presumably blocks Mus81 activation, and therefore gets rid of DSBs but not ssDNA (as indicated by Rad52 and RPA foci). Alternatively, other nucleases such as Exo1, which play a role in cleaving ssDNA at telomeres and stalled forks may also contribute to *mcm2DENQ* DNA DSBs. As mentioned in the first chapter, *exo1* deletion suppresses the growth defects of checkpoint mutants such as *rad53.* It would be interesting to test for similar effects in our *mcm* mutant.

How then is excess ssDNA being generated specifically late in the cell cycle? As mentioned earlier, many regions of the genome are replicated late in the cell cycle. Of particular significance are the telomeres, which are one of the last segments of the genome to be replicated. Telomere maintenance requires capping proteins, as well as formation of special secondary structures called T-loops in order to prevent end-to-end fusions and to protect telomeres from being recognized by repair proteins as regular DNA damage (reviewed in [341]). Capping proteins including Cdc13/Tem1/Stn1, helicases Pif1 and Rrm3, and additional telomere-binding proteins such as Trf1 and Trf2 play various roles in this process. It is not improbable that misregulated Mcm complexes may invade telomeric regions, generating excess DNA unwinding, leading to ssDNA-binding proteins such as RPA and later, Rad52 to recognize and bind them. This potentially also makes telomeres susceptible to nucleases such as Mus81 and Exo1. It should be mentioned that double mutants of the checkpoint factor *mrc1* and capping protein *cdc13* often accumulate excessive ssDNA at telomeres [342]. From our SGA analysis of the *mcm2DENQ* mutant (Appendix B), we noted synthetic lethality between *cdc13* and *mcm2DENQ*, raising the possibility that Mcm2-7 is also somehow connected to the stability of telomeres. Future work would address how Mcm 2-7 can specifically interact with the telomere-regulating machinery and contribute to their maintenance. Given the extreme importance of telomere maintenance in the process of cellular aging, such studies would also be extremely valuable from a human health perspective.

APPENDIX A– IN VIVO ANALYSIS OF MCM4/6 ACTIVE SITE MUTANTS

A.1 INTRODUCTION

A biochemical survey of helicase activity associated with various mcm ATPase mutants previously revealed that the *mcm4RA* and *mcm6DENQ* mutant complexes fail to unwind DNA *in vitro*. Intriguingly, these mutant complexes tested normal or relatively normal for various other biochemical attributes, including ssDNA binding and ATPase activity [41]. Although, these studies suggest that the Mcm4/6 active site plays an important role in DNA unwinding, *in vivo* analyses present a slightly more complex view. When introduced into yeast, not only are *mcm4RA* and *mcm6DENQ* mutants viable, they exhibit fairly wildtype growth characteristics. Similar to the *mcm2DENQ* mutant, these mutants have changes to conserved residues within their ATPase active site domains. Specifically, *mcm4RA* was created by mutating a conserved arginine within the Arginine finger domain of Mcm4 to alanine (*mcm4*R→A), and *mcm6DENQ* has two conserved acidic residues substituted for their amide counterparts within the Walker B domain of Mcm6 (*mcm6*DE→NQ).

It is also worth mentioning that the Mcm4/6 active site is situated adjacent to the Mcm6/2 active site within Mcm2-7, and both these active sites are situated between the Mcm2/5 'gate' and the Mcm7/4 'motor' domains in the complex. It is imaginable that similar to the Mcm6/2 site, Mcm4/6 may play a role in the regulation of Mcm2-7 by relaying signals from the gate to the motor. Therefore, ablation of the Mcm4/6 active site may result in at least a subset of the defects seen with the *mcm2DENQ* mutant. Presumably, such defects are partially obscured in a simple

growth analysis and by some functional redundancy among various active sites. Both the *mcm4RA* and *mcm6DENQ* mutants additionally allow us to compare the *in vivo* functions of different Mcm ATPase active sites and check if they behave similarly or differently.

A.2 RESULTS

We conducted a limited comparative phenotypic analysis of *mcm4RA* and *mcm6DENQ* yeast mutants. The results are presented below.

A.2.1 *mcm4RA*, but not *mcm6DENQ* has a replication defect

We first checked these mutants for any defects during normal replication. Using the plasmid stability assay [263], we found that, the *mcm4RA* had a high rate of plasmid loss that could not be suppressed by additional origins of replication, indicating defective replicative initiation **(Figure 34)**. This was an interesting observation, considering the lack of any obvious growth phenotypes for this mutant. In contrast, the *mcm6DENQ* mutant exhibited intermediate to low levels of plasmid loss, implying that replication is largely normal in this mutant **(Figure 34)**. Both these observations were further corroborated in our plasmid segregation analysis (discussed below), with the small plasmid loss defect in the *mcm6DENQ* mutant appropriately explained as a segregation problem rather than a defect in replication (see below).

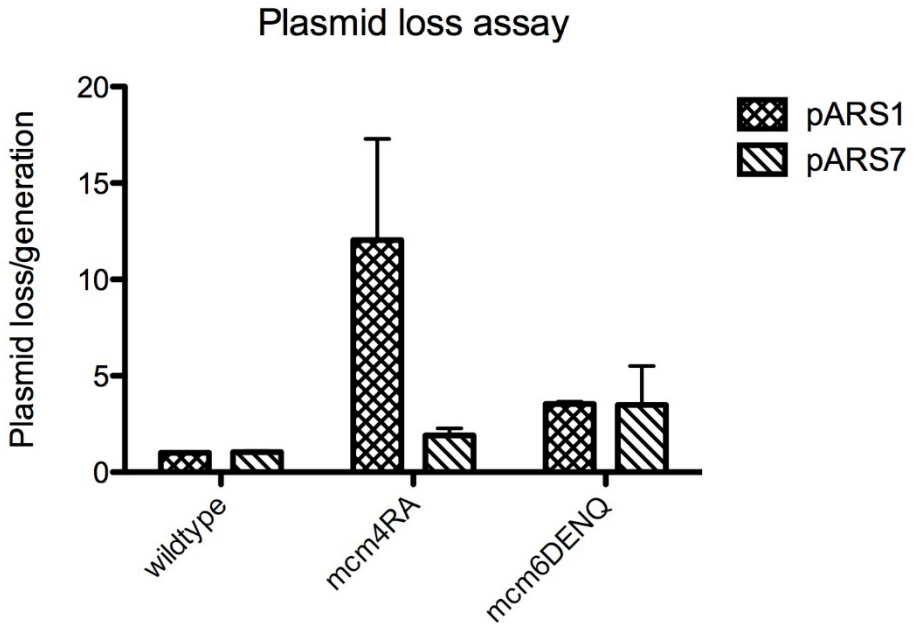

Figure 34. The *mcm4RA* mutant exhibits defective replication initiation

Wildtype (UPY610), *mcm4RA* (UPY537) and *mcm6DENQ* (UPY541) transformed with a single origin ARS/CEN plasmid (pARS1/pUP464) or multi-origin ARS/CEN plasmid (pARS7/pUP465) were tested for plasmid loss per generation.

A.2.2 The *mcm4RA* plasmid loss phenotype results from defective initiation rather than defective segregation

Although the plasmid stability assay is a standard metric of replication defects, it is insufficient to distinctly tell the difference between replication and segregation problems. To circumvent this problem, we used a previously-described assay to directly monitor plasmid segregation in daughter cells [273], whereby our mutant strains were engineered to carry CEN plasmids with integrated *lac* operator arrays, which bind with high affinity to LacI-GFP molecules expressed from a

separate construct integrated in the same strain [343]. Additionally, strains for this assay carried a background *cdc15-1* mutation that arrests cells in telophase under non-permissive conditions (37°C), and therefore allow us to monitor plasmid division and segregation from G1 to the end of M-phase without cytokinesis. In G1, most cells should have a single copy of the plasmid, and should therefore have one visible GFP dot in each cell. Subsequently, after DNA replication and plasmid segregation, each of the buds in telophase arrested double budded cells should carry a copy of the replicated plasmid (counted as 1:1 species in our assay). A significant proportion of *mcm4RA* cells (~35%) exhibited a 1:0 ratio in telophase, indicating defective replication (**Figure 35**). In contrast, a large proportion of *mcm6DENQ* cells had a 2:0 distribution of plasmids in telophase, suggesting that although plasmids were able to replicate, they failed to properly segregate into daughter cells (**Figure 35**). This was further corroborated in our assay for monitoring sister chromatid cohesion (**Figure 36,** see below).

Therefore, *mcm4RA* mutants, but not *mcm6DENQ* have defects in DNA replication. Intriguingly, the *mcm6DENQ* mutant, despite being an ATPase-defective mutant of the same active site (Mcm4/6) exhibits qualitative phenotypic differences from *mcm4RA*.

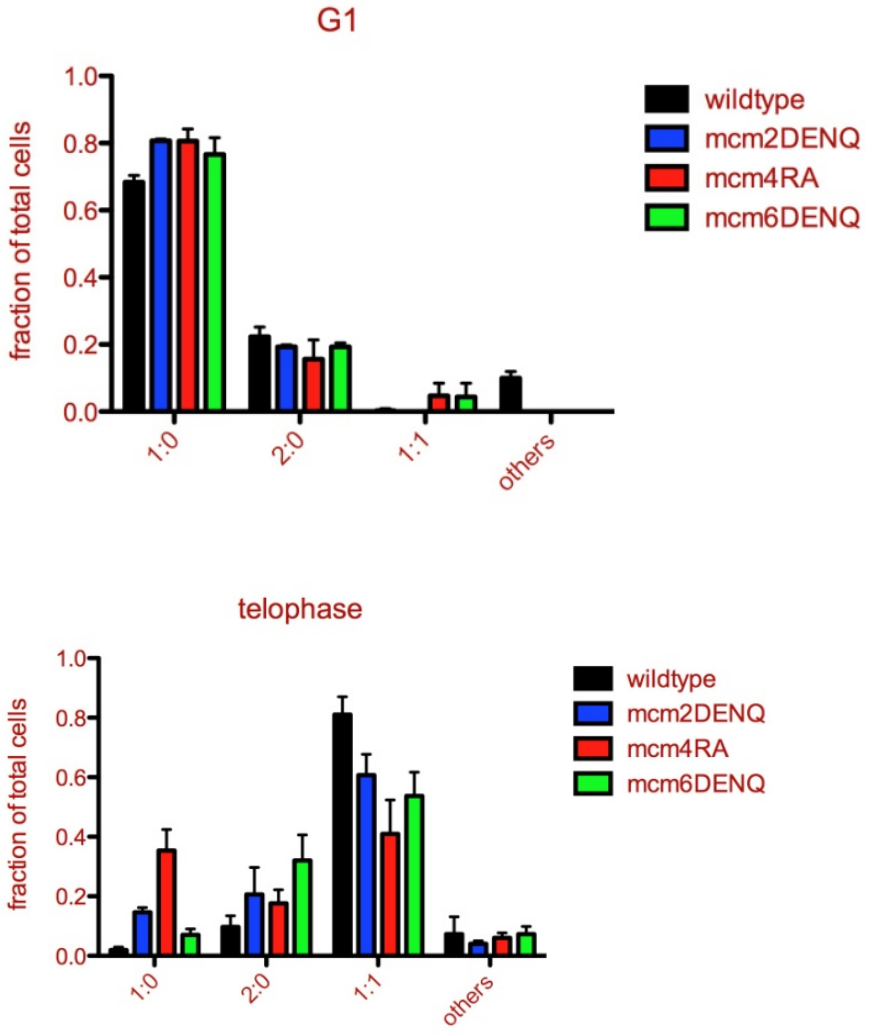

Figure 35. The *mcm4RA* mutant has defective initiation while the *mcm6DENQ* mutant has errors in segregation

Wildtype (UPY 860), *mcm2DENQ* (UPY865), *mcm4RA* (UPY 937), and *mcm6DENQ* (UPY935) strains were monitored for plasmid loss by visual analysis of plasmid-bound LacI-GFP in G1 and in telophase as described in Methods. 'Others' category includes all non-typical plasmid segregation patterns such as 3:0, or 1:2. Data plotted as mean and SD of n≥3 experiments.

A.2.3 The *mcm6DENQ* mutant has defective sister chromatid cohesion

We further explored the apparent segregation defects in the *mcm6DENQ* mutants by asking if mutants also had a corresponding defect in normal chromosome segregation. We hypothesized that segregation errors would probably result from errors in the process of sister chromatid cohesion (SCC). We monitored cells for SCC defects using the assay described earlier, we observed that the *mcm6DENQ* has a significant cohesion defect **(Figure 36)**. The magnitude of the defect seen in the *mcm6DENQ* mutant seemed similar to that observed in the *mcm2DENQ* mutant described earlier, as well as to that seen in a Δ*mrc1* mutant. In contrast, we could not observe an appreciable change in SCC in the *mcm4RA* mutant **(Figure 36)**. The above results further confirm the earlier observations made from our plasmid-based assays, indicating that the *mcm4RA* and *mcm6DENQ* mutations differentially affect DNA replication and chromosome segregation.

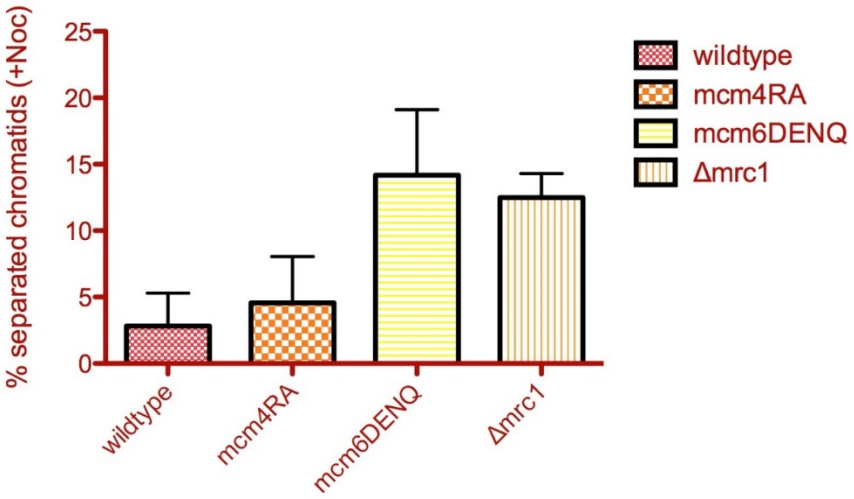

Figure 36. The *mcm6DENQ* mutant has defective SCC

Wildtype (UPY 613), *mcm4RA* (UPY 811), and *mcm6DENQ* (UPY812) and *mrc1*Δ(UPY744) strains were monitored for plasmid loss by visual analysis of chromosome-bound LacI-GFP in metaphase after nocodazole arrest for two hours, as described in Methods. Data plotted as mean and SD of n≥3 experiments.

A.2.4 The *mcm4RA* mutants have varying sensitivity to genotoxic agents

As mentioned earlier, intra-S-phase checkpoints monitor replication in events of unwarranted fork stalling or DNA damage via two parallel and partially redundant pathways. As shown earlier, the *mcm2DENQ* mutant implicates the Mcm complex in the DNA replication checkpoint (DRC) upstream of Rad53.

To check if the *mcm4RA* and *mcm6DENQ* mutants have similar checkpoint phenotypes, we tested combinations of *mcm4RA* and *mcm6DENQ* with several mutant checkpoint alleles including Δ*rad9*, Δ*mrc1* or *mrc1AQ*. In contrast to the *mcm2DENQ* mutant, we did not observe any synthetic lethality or synthetic sickness between *mcm4RA* and the *mcm6DENQ* mutants and other checkpoint alleles. We then tested double mutants on media containing either 0.01% methyl methanesulfonate (MMS) or 50mM hydroxyurea (HU). We did not observe any appreciable increase in sensitivity of the *mcm6DENQ* mutants to either treatment (**Figure 37**). In contrast, *mcm4RA* mutants show varying degrees of sensitivity to both HU and MMS treatments. While the *mcm4RAΔrad9* and *mcm4RAmrc1AQ* mutants displayed appreciable sensitivity to HU, they seem to be fairly tolerant to MMS; the *mcm4RA Δmrc1* displayed heightened MMS sensitivity **(Figure 37)**.

Sensitivity to genotoxic agents such as HU and MMS generally reflects a failure to properly initiate a checkpoint response. As mentioned earlier, the standard metric of checkpoint activation is the phosphorylation of the effector kinase Rad53. Asynchronous cultures of the above mutants were treated with either 0.033% MMS or 0.2M HU for two hours and tested for Rad53 activation **(Figure 38)**. Surprisingly, all of the *mcm4RA* and *mcm6DENQ* mutants showed Rad53 phosphorylation in the presence of HU or MMS. However, we noted that the levels of phosphorylated Rad53 differed considerably between the single mutants and the various double mutants, suggesting that perhaps the double mutants are partially defective in activating the checkpoint response **(Figure 38)**. In summary, the above analyses indicate that *mcm4RA*, and to a limited extent the *mcm6DENQ* mutant might be defective in checkpoint activation, although it is undetermined whether it functions specifically in the DRC or the DNA damage checkpoint (DDC).

This raises the possibility that perhaps replication forks are less stable in *mcm4RA*, and knocking out specific components of the checkpoint pathway in these mutants further exacerbates this defect in the presence of replicative stress. The data also seem to be consistent with a previous studies that have suggested Mcm4 as a target for checkpoint control in HeLa cells [344, 345].

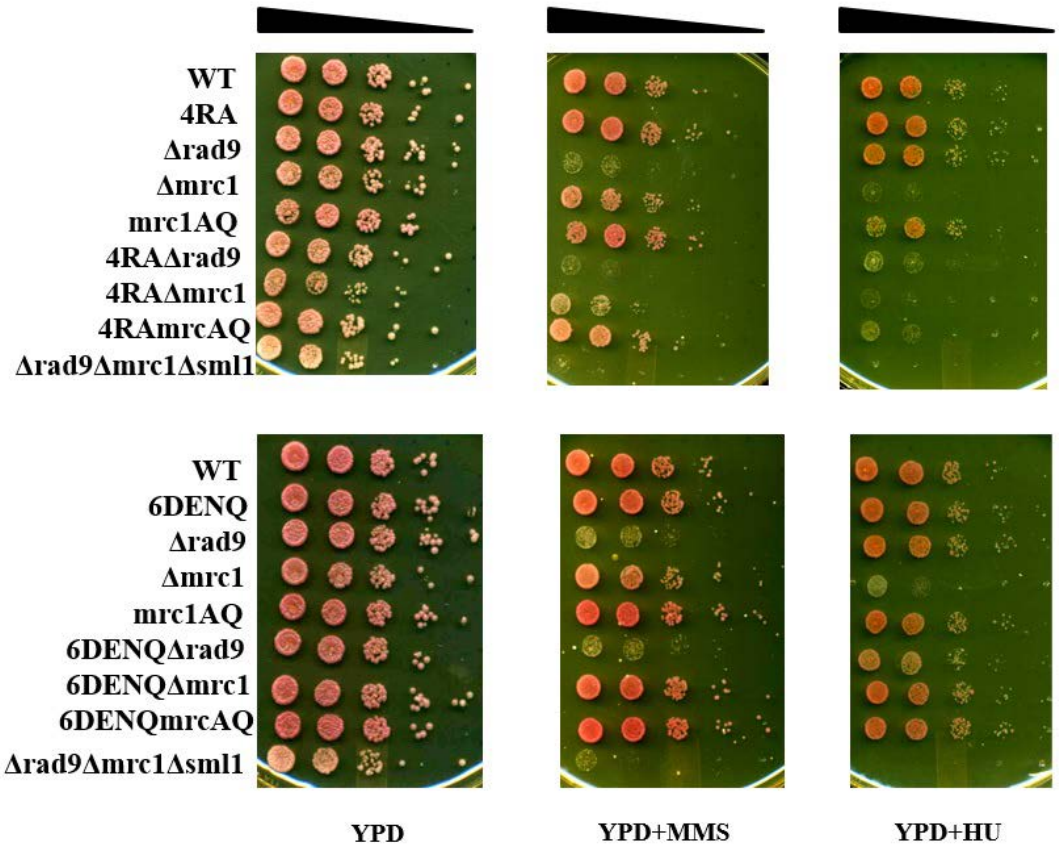

Figure 37. Sensitivity of the *mcm4RA* and *mcm6DENQ* mutants to genotoxic agents

Log phase cultures of the indicated strains were spotted on YPD± 40mM HU or 0.01% MMS in 10-fold dilutions. Images were taken after two days of incubation at 30°C. Strains used are wildtype (UPY464), *mcm4RA* (UPY529), *mcm6DENQ* (UPY525), *rad9*Δ (UPY 630), *mrc1*Δ (UPY 713), *rad9*Δ*mrc1*Δ*sml1*Δ (UPY 715), *mcm4RArad9*Δ (UPY 918), *mcm4RAmrc1*Δ (UPY 920), *mcm4RAmrc1AQ* (UPY924), *mcm6DENQrad9*Δ (UPY 919), *mcm6DENQmrc1*Δ (UPY 921), and *mcm6DENQmrc1AQ* (UPY925).

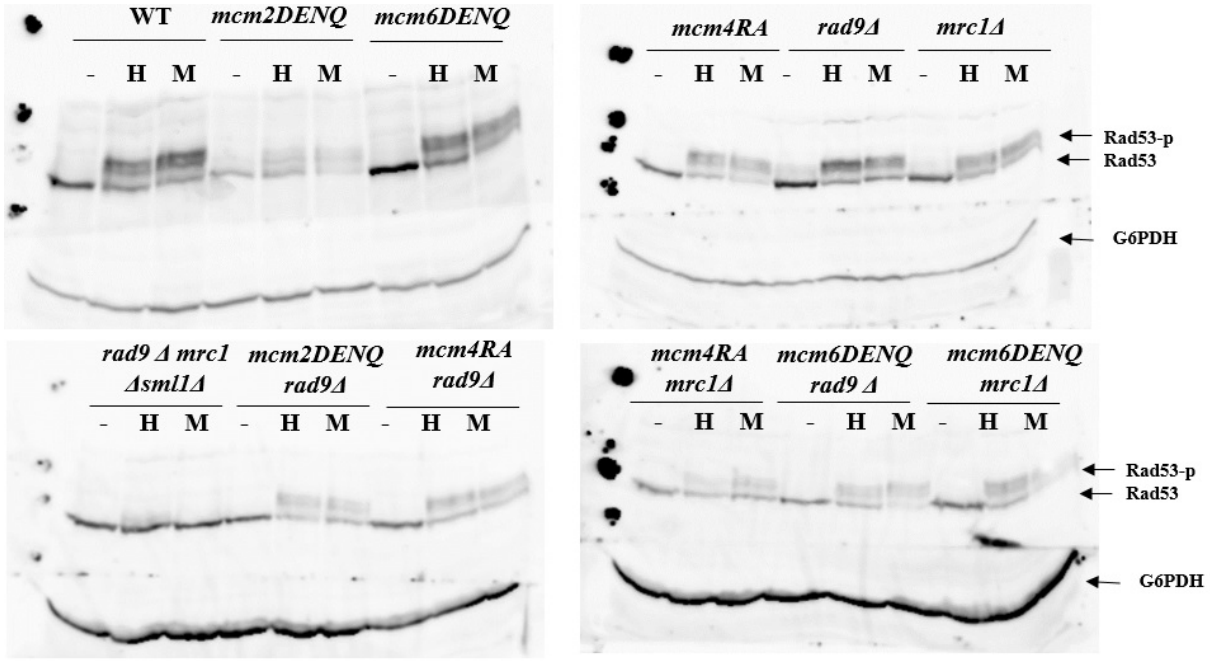

Figure 38. Rad53 phosphorylation in *mcm4RA* and *mcm6DENQ* mutants is normal

Same strains as Fig. 37, assayed for Rad53 phosphorylation after growing cultures ±0.2M HU or 0.033%MMS. Additional strains analyzed were *mcm2DENQ* (UPY499) and *mcm2DENQ rad*9Δ (UPY634).

A.2.5 Neither the *mcm4RA* nor the *mcm6DENQ* mutant has an appreciable DNA damage phenotype

We tested the *mcm4RA* and 6DENQ mutants for additional defects during unchallenged growth conditions. As mentioned earlier, the *mcm2DENQ* mutant accrues DNA damage in the G2 phase of the cell cycle, even in the absence of any chemical treatments. We similarly asked if the *mcm4RA* and *mcm6DENQ* had a DNA damage phenotype. We first tested asynchronous cultures for the presence of yH2A foci, which is a marker of DNA double strand breaks (DSBs). However,

we did not observe any enrichment in γH2A foci in either of these mutants, indicating that these mutations probably do not cause DSBs **(Figure 39)**. We subsequently tested these mutants for Rad52-YFP foci to check if other types are damage are present in these mutants. As noted earlier, although Rad52 is recruited to DSBs, it can bind to ssDNA, and is therefore additionally useful for the analysis of non-DSB related DNA damage phenomena. We could not observe any significant Rad52 foci formation in these mutants from either asynchronous or synchronized cultures, indicating these mutants do not grossly affect genome integrity.

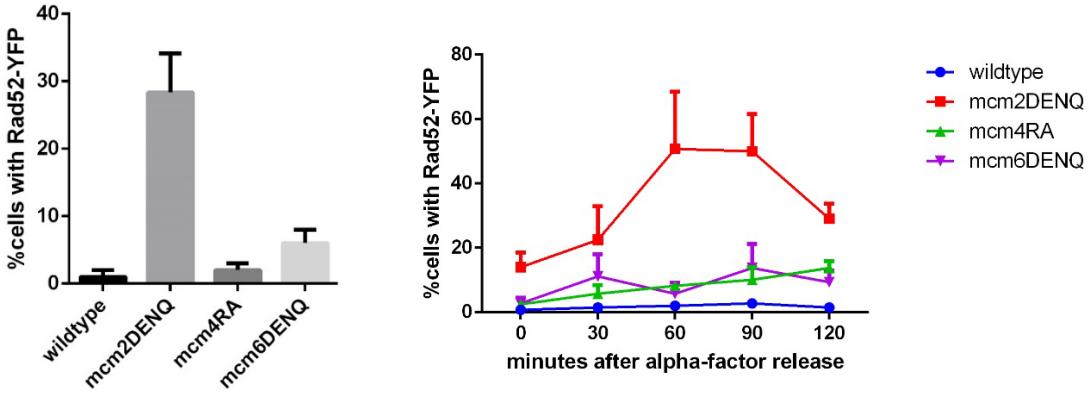

Figure 39. Neither of the Mcm4/6 active site mutants have a strong DNA damage phenotype

Wildtype (UPY938), *mcm2DENQ* (UPY1014), *mcm4RA* (UPY1022) and *mcm6DENQ* (UPY1017) strains were analyzed for Rad52-YFP foci in either asynchronous (left panel) or synchronized cultures. Data plotted as mean and SEM of n≥3 experiments.

A.2.6 *mcm4RA* and *mcm6DENQ* mutations do not affect protein levels or stability

It is reasonable to assume that the phenotypes seen with the above mcm mutants may occur if the mutant proteins are less stable or less abundant than wildtype proteins. This may further lead to the formation of less-productive Mcm complexes, which could result in Mcm misregulation.

We checked *mcm4RA* and *mcm6DENQ* mutants for protein stability by cycloheximide chase analysis and found that *Mcm4RA* and *Mcm6DENQ* proteins are relatively stable over the course of a cell cycle (**Figure 40)**. We additionally performed timecourse quantitative western blots on samples from synchronized mutant cultures (**Figure 40)** and observed no quantitative differences in protein levels over time, indicating that the mutations do not result in hypomorphic defects.

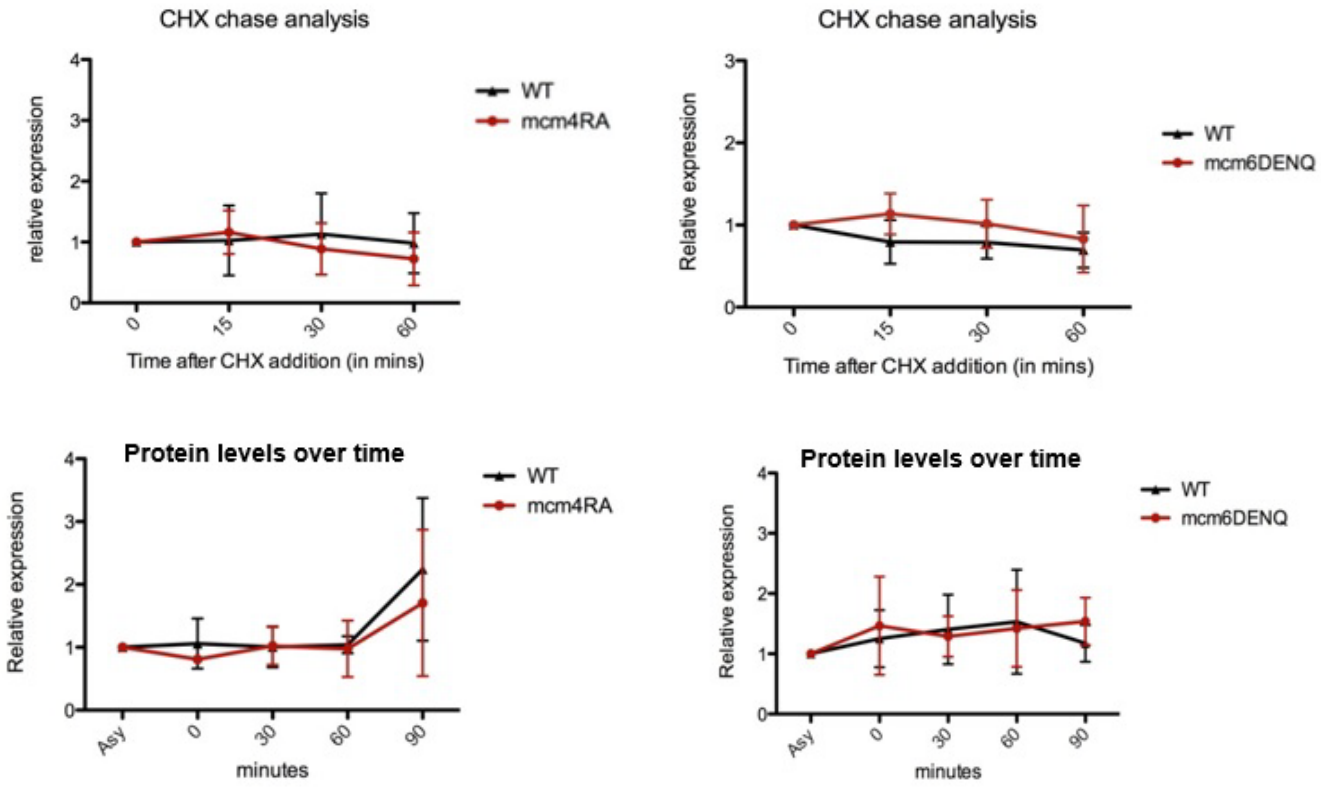

Figure 40. *mcm4RA* and *mcm6DENQ* mutations do not affect protein levels or stability

(Top panel) Cycloheximide chase analysis of wildtype (UPY 464), *mcm4RA* (UPY529) and *mcm6DENQ* (UPY525) strains. (Bottom panel)- strains from top panel synchronized in α-factor, released into YPD and samples from indicated timepoints analyzed through quantitative Western blots. Antibodies used were mouse anti-Mcm4 (AS 6.1) and mouse anti-Mcm6 (AS 3.1). Data plotted as mean and SEM of n≥3 experiments.

A.3 DISCUSSION

Mcm2-7 is a key player in eukaryotic DNA replication. It associates with replicative origins at the beginning of G1 phase, where it is maintained in an inactive state until S-phase. During S-phase, cell-cycle specific kinases activate the helicase, and allow it to bind several accessory factors which convert Mcm2-7 into a robust DNA unwinding motor as part of the CMG complex. Mcm regulation is crucial throughout the cell cycle to ensure that the genome replicates once and only once during each cell cycle. Consequently, misregulation of the Mcm complex can often lead to replicative defects. Following from this, one assumption underlying many of the defects seen with the above mcm mutants is that such defects arise simply as secondary consequences of inefficient DNA replication.

The *mcm2DENQ* mutant has a variety of *in vivo* phenotypes that implicate Mcm2-7, particularly the 6/2 active site, in various processes in addition to DNA unwinding during S phase, including the replication checkpoint and sister chromatid cohesion. Although most of our evidence suggests that these defects are specific to ATP hydrolysis at the 6/2 site, we sought separation-of-function mutants of the Mcm2-7 complex that can uncouple some of the *mcm2DENQ* defect. While the *mcm2DENQ* mutant has genomic instability, cell death, spontaneous DNA damage, improper checkpoint activation and aberrant sister chromatid cohesion, *mcm4RA* and *mcm6DENQ* show defects in only a subset of these processes. Therefore, we infer that it is possible to formally separate DNA replication defects from sister chromatid cohesion defects. While the *mcm6DENQ* mutant displays an SCC defect similar to *mcm2DENQ* and *mrc1* mutants, it displays relatively normal DNA replication. Conversely, the *mcmRA* mutant demonstrates a significant defect in replication initiation but no apparent SCC defects. Additionally, in contrast to *mcm2DENQ*

phenotypes, *mcm4RA* and *mcm6DENQ* strains do not seem to accumulate spontaneous DNA damage to any significant extent as measured by γH2AX immunofluorescence or Rad52-YFP assays, neither do they seem to overtly affect checkpoint activation in the presence or absence of genotoxic stress, as measured by Rad53 phosphorylation assays.

It should be noted that Mcm2-7 interacts with a plethora of factors during S-phase, and undergo cell-cycle specific phosphorylation on different subunits [29]. The multifactorial regulation of Mcm2-7 *in vivo* may, therefore, partially explain the discrepancies observed between the biochemical and genetic analyses of these mutants. A recent study also shows the involvement of Mcm4 in the DNA damage response [346]. In this study, the authors have shown the involvement of an N-terminal serine-rich domain within Mcm4 in restricting origin firing and fork progression under replication stress, and in activating the checkpoint response. Mutations within this domain resulted in aberrantly fired late origins and defective in Rad53 phosphorylation. Interestingly, this domain is targeted by many different cell cycle kinases such as CDK and DDK. Our study similarly shows that perturbations within Mcm4 in the C-terminal ATPase active site domains can lead to similar phenotypes, including defective initiation and sensitivity to genotoxic agents. Other studies have similarly found *in vivo* defects associated with mutating conserved domains within the ATPase active site of Mcm4 in *S. pombe* [347]. The analysis of Mcm6 Walker B mutants has also been previously shown to abolish *in vitro* helicase activity without affecting viability [348]. Our results are in good agreement with the above studies, and demonstrate specific ablation of ATPase active sites can give rise to many individually separable defects, highlighting the role of ATP hydrolysis at this active site in regulation of these processes.

We also show that a specific Mcm6 allele can destabilize sister chromatid cohesion without significantly affecting either DNA replication or checkpoint function. Interestingly, a previous study showed that Mcm6 can directly bind Mrc1 to coordinate checkpoint function and replication, with mutations in the Mrc1-binding domain resulting in sensitivity to DNA damaging agents [219]. It is possible that the *mcm6DENQ* mutant might also be partially compromised for certain interactions at the replication fork which may result in an SCC defect. More importantly, such interactions again seem to hinge on ATP hydrolysis at the Mcm4/6 active site, further outlining the *in vivo* importance of low turnover ATPase active sites in Mcm regulation.

It is possible that ATPase active sites might be coordinately regulating some of the same processes, which might explain similarities between the *mcm2DENQ* and *mcm4RA*/*6DENQ* mutant phenotypes. In this case, mutations at one active site might be causing an allosteric perturbation of the neighboring active site function. Alternatively, there might exist a certain level of functional pleiotropy within the Mcm complex *in vivo*, which probably allows various active sites to partially compensate for the loss of neighboring ATPase active site function. It should be pointed out that both the *mcm4RA* and *mcm6DENQ* mutations affect the same active site (Mcm4/6). However, the phenotypes associated with them are dissimilar. There could be several explanations for this discrepancy. Firstly, the various motifs within AAA+ ATPase active sites have subtle functional differences. Biochemically, it has been observed that Walker B mutant active sites usually behave as substrate traps that have the ability to bind substrates but are unable to release them. While arginine finger is also necessary for ATP hydrolysis, it is additionally required to propagate energy-dependent conformational changes to neighboring subunits (reviewed in[349]). Therefore, within the context of the Mcm complex, the *mcm4RA* mutation

could potentially affect communications between the gate and motor subunits. Secondly, it is possible that the mutations have similar effects on ATP hydrolysis, but different effects on protein conformation of Mcm4 and Mcm6, which may differentially alter their respective interactions with other factors, and give rise to different phenotypes.

Interestingly, we also noticed that it is possible to create *mcm4RA*/*mcm6DENQ* double mutants without losing viability (data not shown). Both the Mcm 4/6 active site mutants do however exhibit synthetic lethality with the *mcm2DENQ* mutation (data not shown). Although this indicates that the ATPase activity of the Mcm4/6 active site might be functionally redundant either with other sites in the complex or with other cellular factors, we have so far not tested the double mutants for any other informative phenotypes. Further work would be required to directly determine how the Mcm4/6 site regulates interactions of the Mcm2-7 complex with other cellular factors at replication forks.

APPENDIX B- EXPLORING THE GENETIC INTERACTIONS OF MCM MUTANTS VIA SGA ANALYSIS

As discussed in the previous sections, the Mcm2-7 complex is a central component of the replisome and its regulation is key to the precise coordination of not just replication during S-phase, but for other activities that occur in conjunction with replication such as sister chromatid cohesion and checkpoint activation. With its six distinct ATPase active sites, the Mcm complex can in theory serve as a portal for multifaceted regulation of several different processes coordinately. For example, we have already established that the Mcm6/2 active site and the Mcm4/6 active sites are playing key roles in coupling the replication machinery to checkpoint control, genome stability and sister chromatid cohesion. Because the above conclusions were derived from the analysis of ATPase active site mutants, it is assumed that ATP turnover at the listed active sites is key for coupling different processes through Mcm2-7. However, whether ATP hydrolysis is the sole determinant of Mcm regulation is a matter of speculation.

It is reasonable to assume that several additional factors may either directly or indirectly regulate ATP hydrolysis at one or more Mcm active sites, or may function redundantly with the Mcm complex under specific conditions. We have observed several synthetic lethal interactions have between our mcm mutants and other alleles including cohesion factors (*eco1-1*), checkpoint factors (*mrc1, tof1,csm3, mec1*), and transcription-related factors (*spt16*). Furthermore, as noted previously, the Mcm4RA and Mcm6DENQ mutant complexes lack *in vitro* helicase activity, suggesting that they play a role in DNA unwinding. However, these mutants are viable *in vivo*,

albeit with many subtle molecular phenotypes. This further raises the possibility that this active site might be functioning redundantly with other cellular factors.

Because the above studies were performed with a small set of mutants, we were interested in exploring the full range of genetic interactions of the Mcm complex on a genome-wide scale. Using our three viable mcm alleles (*mcm2DENQ, mcm4RA* and *mcm6DENQ*), we conducted a genome-wide synthetic lethal analysis using the synthetic genetic array (SGA) methodology [350]. The mutants were tested against two different mutant collections- the first set included knockouts of all non-essential yeast genes, and contains ~4600 mutants. The second collection consisted of temperature-sensitive alleles of a subset of all essential genes in yeast. Details of strain construction, screening and interaction scoring methodologies have been described in Methods.

Several interactions obtained from our screen results validate our previous observations. For example, as noted previously, the list of *mcm2DENQ* negative interactions included *mrc1*Δ, AND *csm3*Δ strains. The SCC establishment factor Eco1 (*eco1-1*) was also observed among the negative interactions with the *mcm2DENQ* mutant. However, we also obtained several contradictory results from the screen compared to our earlier observations. Many of the mutants listed under negative interactions (*e.g., cdc16*, *rad9*, cdc15) are viable in combination with *mcm2DENQ* in our hands. In other cases, the screen failed to pick up mutants such as *mec1* and *tof1*Δ which are synthetically lethal with *mcm2DENQ* in our analyses. We attribute many of these discrepancies to the methodology of scoring interactions (colony size), strain background differences (BY4741 vs W303) or on the effect of dominant marker cassettes on our genes of interest (all mcm mutants were marked with a C-terminal *NATMX4* cassette). The large number of

hits obtained from the *mcm2DENQ* screen could be attributed to the hybrid nature of the mutant strain, which may have resulted in more background noise. As mentioned previously, we were unable to introduce the *mcm2DENQ* mutation into the 'magic marker' strain background using the traditional pop-in/pop-out approach even after repeated attempts. Therefore, we created the appropriate test strain via several rounds of backcrossing between a *mcm2DENQ* mutant strain in a W303 background and the S288C magic marker strain. In contrast, we were easily able to introduce *mcm4RA* and *mcm6DENQ* mutations in the magic marker strains, which resulted in a cleaner strain background and presumably resulted in lesser hits on their respective screens.

Despite the vast scale of genetic interactions observed in all the seen outputs, certain unifying trends were observed among all mutants. We conducted Gene ontology (GO) searches on the results from the deletion collection and the temperature-sensitive (*ts*) mutant collection analyses to check which major categories of processes do the genetic interactions fall under. To further refine our search, we specified the categories in our ontology search to only include processes closely associated with chromatin metabolism (e.g. DNA replication, DNA repair, cohesion, transcription, DNA damage response, telomere processing), or the cell cycle (e.g. mitosis, regulation of cell cycle) (**Tables 4-7**).

We noticed that a high percentage of results from all the screens contained genes that were involved in DNA repair and the cellular response to DNA damage. (17% of the ~1100 hits in both deletion and *ts* screens for *mcm2DENQ*, negative interactions; 18% of the ~280 hits for *mcm6DENQ*; ~17% of the ~380 hits for *mcm4RA*) (**Tables 8-11**). This further highlights the involvement of Mcm ATPase active sites in regulating diverse nuclear processes that are closely

coordinated with replication. A significantly higher number of genes (>100) were observed in this category for *mcm2DENQ*, which is a good proof-of-principle for some of the results discussed in earlier chapters implicating the Mcm 6/2 active site in coordinating the DRC with replication.

Future directions: In line with the phenotypic characteristics of the various *mcm* mutants described in the earlier sections, we found that the Mcm2-7 complex has a broad range of genetic interactions, especially with factors that are involved in various forms of chromatin regulation (**Tables 4-7**). An obvious next step would be to test a subset of these genetic combinations individually to determine the precise nature of the process that is affected by such interactions. For example, among the positive interactions identified for *mcm2DENQ*, *EXO1*, which encodes a repair endonuclease, is an interesting candidate for further analysis, as it could provide a reasonable explanation for the DSB phenotypes seen in the *mcm2DENQ* mutant. Notably, as mentioned earlier, *exo1* mutations can suppress several growth defects associated with mutations of *rad53*, therefore studying these interactions may help us define some common mechanistic basis for various checkpoint mutant phenotypes. A preliminary analysis using this approach has already provided some promising results, whereby the *sac3* mutation–reported in this screen–was seen to suppress the induction of Rad52 foci in the *mcm2DENQ* mutant (Chapter 4). It is conceivable that many other interactions could be similarly useful in delineating the molecular basis of other *mcm* mutant phenotypes, especially the poorly-understood but intriguing SCC defects. Finally, many human diseases, especially cancer, contain mutations in multiple genes related to genome surveillance and DNA replication. A knowledge of specific Mcm negative interactions could be exploited to define the underlying molecular basis of disease susceptibility, by asking if specific combinations of such mutations are required for developing the disease.

Non essential genes-negative interactions	*mcm2DENQ*	*mcm4RA*	*mcm6DENQ*
GO term			
Cellular response to DNA damage stimulus	FUN30,MCM2,RAD16,DPB3,MRC1,MSH3,NHP10,BRE1,RAD28,PPH3,UBC13,BMH2,DPB4,RAD9,DIN7,RTT103,XRS2,DOT1,PTC2,MAG1,RAD24,BMH1,MMS2,SHU1,CSM2,RRD1,MPH1,RAD26,POL32,TOR1,IXR1,APN1,PCD1,RAD33,SUB1,CSM3,PSO2,MLH1,RAD14,YKU70,MSH2,ELG1,WTM2,RAD17,CHL1,RMI1,ELC1,DDC1,NHP6A	DCC1,MRC1,MSH3,NHP10,BRE1,RAD9,RTT103,MUS81,DOT1,PTC2,RAD24,BMH1,SAE2,RTF1,WSS1,SRS2,POL32,TOR1,EAF6,RAD27,APN1,NUP133,RTT109,CSM3,CTF18,MLH1,MRE11,SIN3,ELG1,ULS1,RAD17,DDC1,MCM4,CTF4	NUP60,MRC1,BRE1,RAD9,HTA1,RTT103,RAD24,BMH1,MCM6,SRS2,POL32,TOR1,IXR1,SUB1,CSM3,CTF18,MKT1,SIN3,ELG1,RAD17,CHL1,DDC1,CTF4
DNA repair	FUN30,MCM2,RAD16,DPB3,MRC1,MSH3,NHP10,BRE1,RAD28,PPH3,UBC13,DPB4,RAD9,DIN7,XRS2,DOT1,MAG1,RAD24,MMS2,SHU1,CSM2,RRD1,MPH1,RAD26,POL32,IXR1,APN1,PCD1,RAD33,SUB1,CSM3,PSO2,MLH1,RAD14,YKU70,MSH2,ELG1,RAD17,CHL1,ELC1,DDC1,NHP6A	MRC1,MSH3,NHP10,BRE1,RAD9,MUS81,DOT1,RAD24,SAE2,RTF1,SRS2,POL32,EAF6,RAD27,APN1,NUP133,RTT109,CSM3,CTF18,MLH1,MRE11,SIN3,ELG1,ULS1,RAD17,DDC1,MCM4,CTF4	NUP60,MRC1,BRE1,RAD9,HTA1,RAD24,MCM6,SRS2,POL32,IXR1,SUB1,CSM3,CTF18,SIN3,ELG1,RAD17,CHL1,DDC1,CTF4
Chromatin organization	SWC3,FUN30,MSI1,SWC5,DPB3,SGF29,NHP10,BRE1,PAA1,DPB4,CPR1,HST4,SWR1,DOT1,VPS72,JHD1,SPT2,CHD1,PUF4,SET2,RAD26,MSN4,ARP6,SWC7,VPS71,IOC4,RKR1,YKU70,FKH2,FPR1,HTZ1,YNG1,NHP6A,HPA2	MRC1,MSH3,NHP10,BRE1,RAD9,MUS81,DOT1,RAD24,SAE2,RTF1,SRS2,POL32,EAF6,RAD27,APN1,NUP133,RTT109,CSM3,CTF18,MLH1,MRE11,SIN3,ELG1,ULS1,RAD17,DDC1,MCM4,CTF4	SWC3,SIF2,BRE1,HTA1,SWR1,SPT3,VPS72,SPT2,CHD1,VPS71,SIN3,HTZ1,HST3,LGE1
Regulation of cell cycle	LTE1,AMN1,PCH2,KCC4,MRC1,BRE1,PCL2,RAD61,PPH3,CPR1,RAD9,DOT1,PTC2,DBF2,GIC1,PCL7,HOP1,MAD3,MAD2,FAR1,SET2,SWE1,BFA1,TOR1,IME1,SIS2,DCR2,BUB2,DMA2,MEK1,DDC1,OPY2,CLB2	FUS3,MRC1,BRE1,RAD9,GIC2,DOT1,PTC2,KIP3,DBF2,BUB1,KEL1,TOR1,BUD2,SIC1,VRP1,NUP53,BUB3,DDC1	FUS3,SIF2,MRC1,BRE1,RAD9,BUB1,STE20,TOR1,NUP53,BUB3,DDC1
DNA recombination	MCM2,PCH2,MSH3,NHP10,BRE1,MSH5,VMA1,PPH3,XRS2,DOT1,IES5,RAD51,RAD24,SHU1,REC104,CSM2,MPH1,SET2,NUC1,POL32,CST9,MLH1,YKU70,MSH2,ELG1,RAD17,HHO1,DDC1,REC8	MSH3,NHP10,BRE1,MUS81,DOT1,IRC4,RAD24,MSH4,SAE2,SRS2,POL32,RAD27,CST9,CTF18,MLH1,MRE11,HST1,ELG1,RAD17,DDC1,MCM4,CTF4	BRE1,RAD24,MCM6,SRS2,POL32,CTF18,ELG1,RAD17,DDC1,CTF4
DNA replication	MCM2,SLX1,DPB3,MRC1,BRE1,BMH2,DPB4,SUM1,CHD1,MPH1,SET2,POL32,CSM3,FKH2,ELG1,RFM1	MRC1,BRE1,CHD1,RRM3,POL32,RAD27,CSM3,CTF18,SIN3,DIA2,ELG1,MCM4,CTF4	MRC1,BRE1,CHD1,MCM6,POL32,CSM3,CTF18,SIN3,DIA2,ELG1,LGE1,CTF4
Chromosome segregation	GIP4,MRC1,RAD61,CSM2,MAD3,TUB3,CSM3,GLC8,ELG1,CHL1,RMI1,GIP3,VIK1,REC8	DCC1,MRC1,CSM1,MUS81,BUB1,RTT102,CTF8,CSM3,CTF18,ELG1,CTF4	MRC1,BUB1,CSM3,CTF18,ELG1,CHL1,CTF4
Telomere organization	PBP2,MRC1,NHP10,BRE1,XRS2,IES5,RAD51,YKU70,ELG1	MRC1,NHP10,BRE1,SAE2,ELG1	MRC1,BRE1,ELG1

Table 4. Gene Ontology (GO) term classification of *mcm* negative interactions with genes from YKO collection, sorted by processes

Non essential genes-positive interactions	***mcm2DENQ***	***mcm4RA***	***mcm6DENQ***
GO term			
Cellular response to DNA damage stimulus	SAW1,NUP60,RDH54,TDP1,HSM3, SNF5,POL4,SLX5,RPN4,SAC3, RAD34,ESC2,RAD30,SLX8,RAD4 ,RAD6,SOH1,SNF6,SAE3,RTT107, CKA1,RTT101,SRS2,DOA1,MLH2, MMS22,RAD10,YKU80,TPP1,PMS1, EAF7,SIN3,DDR2,DNL4,EXO1,ULS 1,RAD1,MLH3	APN2,TDP1,CHK1,SNF5, SLX5,SAC3,ESC2,SLX8, MMS22,MSH2,EXO1, MCM4	RFA1,MCM2,MCM7, MRC1,PDS1,CDC1,ACT1, NUP145,MCM6,SWC4, DNA2,MCM10,DPB11, POL32,TAH11,IXR1, RAD27,MCM5,SFH1, PDS5,CTF18,LEO1,ESA1, MCM4,CTF4
DNA repair	SAW1,NUP60,RDH54,TDP1,HSM3, SNF5,POL4,RPN4,SAC3,RAD34, ESC2,RAD30,RAD4,RAD6,SOH1, SNF6,SAE3,RTT107,SRS2,DOA1, MLH2,MMS22,RAD10,YKU80,TPP1 ,PMS1,EAF7,SIN3,DNL4,EXO1,ULS 1,RAD1,MLH3	APN2,TDP1,SNF5,SAC3, ESC2,MMS22,MSH2, EXO1,MCM4	CDC28,NSE4,RPO21, CDC1,NSE3,TFB1,ACT1, RPT6,MCM6,SSL1,NSE1, NSE5,RPT4
Chromatin organization	ACS1,SIF2,SWD3,HPC2,SHG1,SNF5 ,AHC2,BDF2,HMO1,UME6,PHO4, RAD6,SGF73,RTG2,SNF6,SDS3, HOS4,ASF1,CBF1,UTH1,NAP1, BUD6,YKU80,PHO23,EAF7,SIN3, TOP1,ULS1,HOS1	SWD3,SNF5,SIR1	ORC2,CKS1,SWR1,SPT3, RSP5,SPT2,ACT1,SWC4, SWD2,RSC58,MCM5, SFH1,VPS71,RCO1, LEO1,ESA1,LGE1,SGV1
Regulation of cell cycle	CLN3,SIF2,ASM4,UME6,ESC2, RIM15,RAD6,YBP2,RCK1,XRN1, RME1,CLB6,BUB1,SMI1,SPO13, SPO12,SPO16,HOS4,RTT101,ELM1, HSL1,SIC1,SWI6,VRP1,MIH1,GID8, CLN1,PHO80,RTS1,UME1	ESC2,XRN1,IME2,SWI6, DMA2,PHO80,ASE1, UME1	CDC24,CKS1,MRC1, MPS1,DBF4,CDC37,SKP1 ,CDC14,DBF2,ZPR1, MOB1,DPB11,SFH1,PSE1 ,CDC33,ESA1
DNA recombination	SAW1,RDH54,SNF5,RPS16B,EBS1, ZIP1,ESC2,RAD6,SOH1,SKI8,UPF3, MSC7,SAE3,SPO16,THP2,IRC8, SRS2,MLH2,SWI6,MMS22,MFT1, RAD10,YKU80,REC114,TOP1,IRC1 1,EXO1,IRC14,MSC6,RAD1,MLH3	SNF5,ESC2,SWI6,MMS22, MSH2,EXO1,MCM4	RFA1,MCM2,MCM7, PDS1,MCM6,MCM10, DPB11,POL32,TAH11, RAD27,MCM5,CTF18, MCM4,CTF4
DNA replication	RIM1,HUR1,CLB6,RRM3,RTT101, SBA1,MMS22,RIF2,SIN3,TOP1,TGS 1	CHK1,HUR1,MMS22, MCM4	RFA1,MCM2,ORC2, MCM7,MRC1,POL3,DBF 4,MCM6,ORC6,DNA2, MCM10,DPB11,CDC6, POL32,TAH11,RAD27, ORC3,MCM5,SFH1, ORC1,RCO1,CTF18,LGE1 ,MCM4,CTF4,ORC4
Chromosome segregation	KIN3,RDH54,IML3,MCM21,ESC2, RAD30,LRS4,MAM1,SOH1,BUB1, SPO13,CBF1,NKP2,MMS22,TOP1, RTS1	ESC2,MMS22	MRC1,MPS1,CDC48, PDS1,CDC14,DUO1,SFH1 ,PDS5,CTF18,CIK1,CTF4
Telomere organization	SWD3,GBP2,SLX5,SLX8,RAD6, SBA1,STM1,RIF2,YKU80,EXO1, TGS1	SWD3,SLX5,SLX8,EXO1	RFA1,MRC1,DNA2, SWD2

Table 5. Gene Ontology (GO) term classification of *mcm* positive interactions with genes from YKO collection, sorted by processes

ts **alleles-positive interactions**	***mcm2DENQ***	***mcm4RA***	***mcm6DENQ***
GO term			
Cellular response to DNA damage stimulus	CDC28,SUB2,NSE4,RPO21,CDC1, NSE3,TFB1,TFB3,SLX8,GLC7,ACT1, RPT6,STH1,SSL2,MCM10,RTT101, ABF1,SSL1,NSE1,SMC6,SPT5,NSE5, POL1,EAF7,RPT4	CDC28,NSE4,RPO21, CDC1,NSE3,TFB1,SLX8, SMC1,ACT1,RPT6,SSL2, SSL1,NSE1,SPT5,MCM4	CDC28,NSE4,RPO21, CDC1,NSE3,TFB1,SLX8, ACT1,RPT6,MCM6,SSL1, NSE1,NSE5,RPT4
DNA repair	CDC28,SUB2,NSE4,RPO21,CDC1, NSE3,TFB1,TFB3,ACT1,RPT6,STH1, SSL2,MCM10,ABF1,SSL1,NSE1, SMC6,SPT5,NSE5,POL1,EAF7,RPT4	CDC28,NSE4,RPO21, CDC1,NSE3,TFB1,SMC1, ACT1,RPT6,SSL2,SSL1, NSE1,SPT5,MCM4	CDC28,NSE4,RPO21, CDC1,NSE3,TFB1,ACT1, RPT6,MCM6,SSL1,NSE1, NSE5,RPT4
Chromatin organization	DEP1,CDC28,MSI1,TAF5,SGF29, TAF12,GLC7,ACT1,RPT6,SGF73, TAF6,STH1,ASF1,SWD2,ABF1, POB3,RNT1,EAF7,SGF11,RVB2, SGV1	CKS1,CDC28,TAF5,NOP1 ,TAF12,ACT1,RPT6,POB3	CDC28,TAF5,NOP1, TAF12,ACT1,RPT6, POB3,ARP7
Regulation of cell cycle	CDC24,CDC28,CDC39,DBF4,SKP1, GLC7,DBF2,ZPR1,SDA1,RTT101, ELM1,TOR2,CDC123,PHO80,CDC3 3,SGT1,IPL1	CKS1,CDC28,MPS1,DBF4 ,DBF2,CDC25,PSE1, PHO80,SGT1	CDC28,MPS1,DBF4, CDC14,DBF2,SDA1, CDC123,TEM1,PSE1, PHO80,SGT1
DNA recombination	CDC28,SKI8,SSL2,MCM10,SMC6	CDC28,SSL2,MSC1, MCM4	CDC28,MCM6
DNA replication	DEP1,CDC28,DBF4,GLC7,NOP7, IPI1,MET30,MCM10,RTT101,ABF1, NOC3,SMC4,CLF1,POB3,MCM1, POL1,TBF1	BRN1,CDC28,DBF4, MET30,SMC4,POB3, MCM1,TBF1,MCM4	BRN1,CDC28,DBF4, MCM6,NOP7,MET30, NOC3,SMC4,POB3, MCM1
Chromosome segregation	MTW1,CDC28,CDC48,YCG1,GLC7, SMC2,IRR1,STH1,CSE4,SMC4,YCS4 ,SMC6,NUF2,GPN2,IPL1	BRN1,CDC28,MPS1, CDC48,YCG1,SMC1,IRR1 ,SMC4,YCS4,SPC24,NUF 2	BRN1,CDC28,MPS1, CDC48,YCG1,CDC14, SMC2,DSN1,SMC4,SPC24 ,NUF2
Telomere organization	SLX8,SWD2,TBF1	SLX8,TBF1	SLX8

Table 6. Gene Ontology (GO) term classification of *mcm* negative interactions with genes from temperature-sensitive collection, sorted by processes

ts **alleles- negative interactions**			
	mcm2DENQ	***mcm4RA***	***mcm6DENQ***
GO term			
Cellular response to DNA damage stimulus	RFA1,CDC28,MCM7,DCC1,MRC1,NHP10,MCD1,CDC7, RPN4,NSE4,CDC9,PSF1,PDS1,NSE3,SLD5,GLC7,RAD3, SMC1,ACT1,ECO1,RSC8,NUP145,SLD3,RAD54,SWC4, DNA2,MCM10,PSF2,ARP4,DPB11,POL31,POL32,TAH1 1,RFC2,PRI2,ABF1,RAD27,RAD5,CDC45,MCM5,SFH1,S EN1,TSA1,RAD52,PDS5,CTF18,SGS1,MRE11,POL1, RFC4,LEO1,ESA1,MCM4,EAF3,CTF4,DPB2	RFA1,MCM2,MCM7,MRC1,PSF1,PDS1, CDC1,SLD5,ACT1,NUP145,SLD3,DNA2 ,MCM10,DPB11,POL32,TAH11,RFC2, IXR1,RAD27,NUP133,MCM5,SFH1,SEN 1,PDS5,POL1,LEO1,ESA1,MCM4,CTF4	HHT1,SLX5,ESC2,SLX8,MCM6, REV7,YLR235C,EXO1
DNA repair	RFA1,CDC28,MCM7,MRC1,NHP10,MCD1,CDC7,RPN4, NSE4,CDC9,PSF1,PDS1,NSE3,SLD5,RAD3,SMC1,ACT1, ECO1,RSC8,NUP145,SLD3,RAD54,SWC4,DNA2,MCM1 0,PSF2,ARP4,DPB11,POL31,POL32,TAH11,RFC2,PRI2, ABF1,RAD27,RAD5,CDC45,MCM5,SFH1,RAD52,PDS5, CTF18,SGS1,MRE11,POL1,RFC4,LEO1,ESA1,MCM4, EAF3,CTF4,DPB2	RFA1,MCM2,MCM7,MRC1,PSF1,PDS1, CDC1,SLD5,ACT1,NUP145,SLD3,DNA2 ,MCM10,DPB11,POL32,TAH11,RFC2, IXR1,RAD27,NUP133,MCM5,SFH1,PDS 5,POL1,LEO1,ESA1,MCM4,CTF4	HHT1,ESC2,MCM6,REV7,EXO1
Chromatin organization	SWC3,CKS1,CDC28,TAF5,NHP10,NOP1,RSC3,SWR1,S PT3,RSP5,GLC7,SPT2,ACT1,CDC26,RSC8,RAD54,SPT1 6,SWC4,SPT6,ARP4,SET2,ESS1,SWD2,ABF1,RSC58,MC M5,SFH1,VPS71,POB3,RSC9,RCO1,RNT1,HDA1,LEO1, ESA1,APC5,LGE1,RLF2,EAF3,SPN1,SGV1,DPB2,HDA3	ORC2,CKS1,SWR1,SPT3,RSP5,SPT2, ACT1,SDS3,SET2,SWD2,RSC58,MCM5, SFH1,POB3,RCO1,LEO1,ESA1,APC5	NUP170,HHT1,SHG1,HMO1,SIR1, TOP1
Regulation of cell cycle	CDC24,CKS1,SLI15,CDC28,MRC1,CDC7,MPS1,DBF4,C DC37,RSC3,GLC7,ECO1,CDC14,SPC105,CDC20,DBF2,E SP1,SMI1,MOB1,DPB11,SET2,CDC25,SFH1,SGS1,ESA1	CDC24,CKS1,MRC1,MPS1,DBF4,CDC3 7,CDC14,CDC20,DBF2,MOB1,DPB11, SET2,SFH1,ESA1	NUP170,HHT1,ESC2,IME2,SIC1, SWI6,ASE1
DNA recombination	RFA1,CDC28,MCM7,NHP10,CDC7,CDC9,PSF1,PDS1,S LD5,IES5,RAD3,SLD3,RAD54,MCM10,PSF2,SMC3,DPB 11,SET2,POL32,TAH11,RAD27,CDC45,MCM5,RAD52,C TF18,SGS1,MRE11,MCM4,CTF4	RFA1,MCM2,MCM7,PSF1,PDS1,SLD5, SLD3,MCM10,DPB11,SET2,POL32,TAH 11,RAD27,MCM5,MCM4,CTF4	ESC2,MCM6,SWI6,TOP1,EXO1
DNA replication	RFA1,RFC5,CDC28,MCM7,MRC1,MCD1,CDC7,POL3, CDC9,CDC13,PSF1,DBF4,RSC3,SUM1,SLD5,GLC7, ECO1,SLD3,SPT16,DNA2,MCM10,PRI1,PSF2,DPB11, SET2,CDC6,POL31,POL32,TAH11,RFC2,CDC16,PRI2, ABF1,RAD27,ORC3,CDC45,MCM5,SFH1,SEN1,ORC1, POB3,RCO1,CTF18,SGS1,POL1,RFC4,LGE1,MCM4, EAF3,CTF4,ORC4,DPB2	RFA1,MCM2,POL12,ORC2,MCM7, MRC1,POL3,PSF1,DBF4,SLD5,SLD3, ORC6,DNA2,MCM10,DPB11,SET2, CDC6,POL32,TAH11,RFC2,RAD27, ORC3,MCM5,SFH1,SEN1,ORC1,POB3, RCO1,POL1,MCM4,CTF4,ORC4	MCM6,RRM3,TOP1
Chromosome segregation	RFC5,SLI15,CDC28,AME1,DCC1,MRC1,MCD1,MPS1, DAD1,PDS1,SPC19,GLC7,SMC1,TUB2,ECO1,CDC14, DUO1,SPC105,ESP1,DAM1,CBF2,OKP1,CTF8,STS1, MPS3,SMC3,RFC2,NNF1,SDS22,SPC34,DAD2,SFH1, PDS5,CTF18,SPC24,SGS1,NUF2,RFC4,NSL1,CTF4, HDA3	MRC1,MPS1,CDC48,PDS1,CDC14, DUO1,DAM1,CTF8,MPS3,RFC2,SPC34, SFH1,PDS5,CTF4	NUP170,ESC2,TOP1
Telomere organization	RFA1,MRC1,NHP10,CDC13,IES5,ECO1,RAD54,DNA2, SWD2,RAD52,SGS1	RFA1,POL12,MRC1,DNA2,SWD2	SLX5,SLX8,EXO1

Table 7. Gene Ontology (GO) term classification of *mcm* positive interactions with genes from temperature-sensitive collection, sorted by processes

Non essential genes- negative interactions	*mcm2DENQ*		*mcm4RA*		*mcm6DENQ*	
GO term	**Cluster frequency**	**Genome frequency**	**Cluster frequency**	**Genome frequency**	**Cluster frequency**	**Genome frequency**
Cellular response to DNA damage stimulus	49 out of 801 genes, 6.1%	292 of 6335 genes, 4.6%	34 out of 235 genes, 14.5%	292 of 6335 genes, 4.6%	23 out of 142 genes, 16.2%	292 of 6335 genes, 4.6%
DNA repair	42 out of 801 genes, 5.2%	239 of 6335 genes, 3.8%	28 out of 235 genes, 11.9%	239 of 6335 genes, 3.8%	19 out of 142 genes, 13.4%	239 of 6335 genes, 3.8%
Chromatin organization	34 out of 801 genes, 4.2%	238 of 6335 genes, 3.8%	24 out of 235 genes, 10.2%	238 of 6335 genes, 3.8%	14 out of 142 genes, 9.9%	238 of 6335 genes, 3.8%
Regulation of cell cycle	33 out of 801 genes, 4.1%	184 of 6335 genes, 2.9%	18 out of 235 genes, 7.7%	184 of 6335 genes, 2.9%	11 out of 142 genes, 7.7%	184 of 6335 genes, 2.9%
DNA recombination	29 out of 801 genes, 3.6%	174 of 6335 genes, 2.7%	22 out of 235 genes, 9.4%	174 of 6335 genes, 2.7%	10 out of 142 genes, 7.0%	174 of 6335 genes, 2.7%
DNA replication	16 out of 801 genes, 2%	151 of 6335 genes, 2.4%	13 out of 235 genes, 5.5%	151 of 6335 genes, 2.4%	12 out of 142 genes, 8.5%	151 of 6335 genes, 2.4%
Chromosome segregation	14 out of 801 genes, 1.7%	146 of 6335 genes, 2.3%	11 out of 235 genes, 4.7%	146 of 6335 genes, 2.3%	7 out of 142 genes, 4.9%	146 of 6335 genes, 2.3%
Telomere organization	9 out of 801 genes, 1.1%	76 of 6335 genes, 1.2%	5 out of 235 genes, 2.1%	76 of 6335 genes, 1.2%	3 out of 142 genes, 2.1%	76 of 6335 genes, 1.2%

Table 8. Gene Ontology (GO) term frequency analysis of *mcm* negative interactions with genes from YKO collection, sorted by processes

ts alleles- negative interactions	*mcm2DENQ*		*mcm4RA*		*mcm6DENQ*	
GO term	**Cluster frequency**	**Genome frequency**	**Cluster frequency**	**Genome frequency**	**Cluster frequency**	**Genome frequency**
Cellular response to DNA damage stimulus	56 out of 294 genes, 19.0%	292 of 6335 genes, 4.6%	29 out of 141 genes, 20.6%	292 of 6335 genes, 4.6%	8 out of 162 genes, 4.9%	292 of 6335 genes, 4.6%
DNA repair	52 out of 294 genes, 17.7%	239 of 6335 genes, 3.8%	28 out of 141 genes, 19.9%	239 of 6335 genes, 3.8%	5 out of 162 genes, 3.1%	239 of 6335 genes, 3.8%
Chromatin organization	43 out of 294 genes, 14.6%	238 of 6335 genes, 3.8%	18 out of 141 genes, 12.8%	238 of 6335 genes, 3.8%	6 out of 162 genes, 3.7%	238 of 6335 genes, 3.8%
Regulation of cell cycle	25 out of 294 genes, 8.5%	184 of 6335 genes, 2.9%	14 out of 141 genes, 9.9%	184 of 6335 genes, 2.9%	7 out of 162 genes, 4.3%	184 of 6335 genes, 2.9%
DNA recombination	29 out of 294 genes, 9.9%	174 of 6335 genes, 2.7%	16 out of 141 genes, 11.3%	174 of 6335 genes, 2.7%	5 out of 162 genes, 3.1%	174 of 6335 genes, 2.7%
DNA replication	52 out of 294 genes, 17.7%	151 of 6335 genes, 2.4%	32 out of 141 genes, 22.7%	151 of 6335 genes, 2.4%	3 out of 162 genes, 1.9%	151 of 6335 genes, 2.4%
Chromosome segregation	41 out of 294 genes, 13.9%	146 of 6335 genes, 2.3%	14 out of 141 genes, 9.9%	146 of 6335 genes, 2.3%	3 out of 162 genes, 1.9%	146 of 6335 genes, 2.3%
Telomere organization	11 out of 294 genes, 3.7%	76 of 6335 genes, 1.2%	5 out of 141 genes, 3.5%	76 of 6335 genes, 1.2%	3 out of 162 genes, 1.9%	76 of 6335 genes, 1.2%

Table 9. Gene Ontology (GO) term frequency analysis of *mcm* negative interactions with genes from temperature-sensitive collection, sorted by processes

Non essential genes-positive interactions	*mcm2DENQ*		*mcm4RA*		*mcm6DENQ*	
GO term	**Cluster frequency**	**Genome frequency**	**Cluster frequency**	**Genome frequency**	**Cluster frequency**	**Genome frequency**
Cellular response to DNA damage stimulus	38 out of 1124 genes, 3.4%	292 of 6335 genes, 4.6%	12 out of 215 genes, 5.6%	292 of 6335 genes, 4.6%	25 out of 135 genes, 18.5%	292 of 6335 genes, 4.6%
DNA repair	33 out of 1124 genes, 2.9%	239 of 6335 genes, 3.8%	9 out of 215 genes, 4.2%	239 of 6335 genes, 3.8%	25 out of 135 genes, 18.5%	239 of 6335 genes, 3.8%
Chromatin organization	29 out of 1124 genes, 2.6%	238 of 6335 genes, 3.8%	3 out of 215 genes, 1.4%	238 of 6335 genes, 3.8%	18 out of 135 genes, 13.3%	238 of 6335 genes, 3.8%
Regulation of cell cycle	30 out of 1124 genes, 2.7%	184 of 6335 genes, 2.9%	8 out of 215 genes, 3.7%	184 of 6335 genes, 2.9%	16 out of 135 genes, 11.9%	184 of 6335 genes, 2.9%
DNA recombination	31 out of 1124 genes, 2.8%	174 of 6335 genes, 2.7%	7 out of 215 genes, 3.3%	174 of 6335 genes, 2.7%	14 out of 135 genes, 10.4%	174 of 6335 genes, 2.7%
DNA replication	11 out of 1124 genes, 1%	151 of 6335 genes, 2.4%	4 out of 215 genes, 1.9%	151 of 6335 genes, 2.4%	26 out of 135 genes, 19.3%	151 of 6335 genes, 2.4%
Chromosome segregation	16 out of 1124 genes, 1.4%	146 of 6335 genes, 2.3%	2 out of 215 genes, 0.9%	146 of 6335 genes, 2.3%	11 out of 135 genes, 8.1%	146 of 6335 genes, 2.3%
Telomere organization	11 out of 1124 genes, 1%	76 of 6335 genes, 1.2%	4 out of 215 genes, 1.9%	76 of 6335 genes, 1.2%	4 out of 135 genes, 3%	76 of 6335 genes, 1.2%

Table 10. Gene Ontology (GO) term frequency analysis of *mcm* positive interactions with genes from YKO collection, sorted by processes

ts alleles-positive interactions	*mcm2DENQ*		*mcm4RA*		*mcm6DENQ*	
GO term	**Cluster frequency**	**Genome frequency**	**Cluster frequency**	**Genome frequency**	**Cluster frequency**	**Genome frequency**
Cellular response to DNA damage stimulus	25 out of 357 genes, 7.0%	292 of 6335 genes, 4.6%	15 out of 181 genes, 8.3%	292 of 6335 genes, 4.6%	14 out of 177 genes, 7.9%	292 of 6335 genes, 4.6%
DNA repair	22 out of 357 genes, 6.2%	239 of 6335 genes, 3.8%	14 out of 181 genes, 7.7%	239 of 6335 genes, 3.8%	13 out of 177 genes, 7.3%	239 of 6335 genes, 3.8%
Chromatin organization	21 out of 357 genes, 5.9%	238 of 6335 genes, 3.8%	8 out of 181 genes, 4.4%	238 of 6335 genes, 3.8%	8 out of 177 genes, 4.5%	238 of 6335 genes, 3.8%
Regulation of cell cycle	17 out of 357 genes, 4.8%	184 of 6335 genes, 2.9%	9 out of 181 genes, 5%	184 of 6335 genes, 2.9%	11 out of 177 genes, 6.2%	184 of 6335 genes, 2.9%
DNA recombination	5 out of 357 genes, 1.4%	174 of 6335 genes, 2.7%	4 out of 181 genes, 2.2%	174 of 6335 genes, 2.7%	2 out of 177 genes, 1.1%	174 of 6335 genes, 2.7%
DNA replication	17 out of 357 genes, 4.8%	151 of 6335 genes, 2.4%	9 out of 181 genes, 5%	151 of 6335 genes, 2.4%	10 out of 177 genes, 5.6%	151 of 6335 genes, 2.4%
Chromosome segregation	15 out of 357 genes, 4.2%	146 of 6335 genes, 2.3%	11 out of 181 genes, 6.1%	146 of 6335 genes, 2.3%	11 out of 177 genes, 6.2%	146 of 6335 genes, 2.3%
Telomere organization	3 out of 357 genes, 0.8%	76 of 6335 genes, 1.2%	2 out of 181 genes, 1.1%	76 of 6335 genes, 1.2%	1 out of 177 genes, 0.6%	76 of 6335 genes, 1.2%

Table 11. Gene Ontology (GO) term frequency analysis of *mcm* positive interactions with genes from temperature-sensitive collection, sorted by processes

CONCLUSIONS AND FUTURE PERSPECTIVES

Regulation of genome stability is crucial for survival. Eukaryotes have consequently evolved multiple mechanisms to deal with situations that pose a threat to the integrity of their DNA. Obviously, regulation of factors that directly interact with DNA during specific times during a cell cycle is a common mechanism. The process of DNA replication is even more stringently controlled, as it involves processing of the entire genome within a limited time with great accuracy. Such a necessity puts added burden on the cells to ensure that errors in the process are kept to a minimum. While a large number of proteins are involved in this process, in some ways the regulation of this entire process critically hinges on the spatiotemporal control of the replicative helicase. As a factor that partakes in the licensing of replicative origins in G1, the initiation of DNA replication in early S-phase, and in elongation as an unwinding machine throughout S-phase, Mcm2-7 is an essential component of eukaryotic DNA replication.

We have shown that misregulation of the Mcm complex via perturbations to specific active sites is detrimental to many closely-related processes such as checkpoint signaling and chromosome segregation. We have further demonstrated that *mcm* mutations can affect many processes without overtly affecting DNA replication. The initial screen from which many members of the Mcm complex were first identified relied on using plasmid stability as a metric for determining that the Mcms had a role in replication. Since then, many studies have similarly shown that mutations in mcm subunits affect either complex assembly, helicase activity, or DNA replication [88, 291, 347, 351]. Other studies have similarly looked at segregation defects in *mcm* mutants [352]. These effects are almost invariably due to hypomorphic mutations that reduce Mcm

function. On the other hand, we were able to identify a mutant which has several specific defects *in vivo* without overt replication defects. Specifically, we show that the *mcm2DENQ* mutant, while having negligible effects on *in vitro* DNA unwinding, and *in vivo* complex assembly, protein stability or protein abundance, and early origin firing, can still short circuit the DNA replication checkpoint, and additionally lead to DNA damage even under unchallenged growth conditions. Additionally, with other mcm alleles, we were able to show that it is possible to genetically separate some of these defects. Therefore, unlike the previously held view in the field that most mcm mutations invariably affect DNA replication, and therefore spawn secondary defects, we show through our studies that this is not necessarily the case. In this manner, we identify novel *in vivo* roles for different ATPase active sites.

Because the mutants examined map to low turnover ATPase active sites, it explains why certain mutations do not affect bulk DNA unwinding in *in vitro* assays and permit viability but nevertheless are associated with many *in vivo* defects. This suggests that ATP turnover at these active sites is likely associated with key regulatory functions. *In vivo*, other factors associating with specific Mcm subunits might also be playing a role in regulating ATP hydrolysis at the Mcm6/2 and Mcm4/6 active sites. As mentioned previously, proteins such as Mrc1 directly associate with Mcm6 and seem like good candidates for such regulation. It is worth mentioning that nucleotide turnover of GTPases such as Ras are analogously regulated by proteins such as GAPs and GEFs [353].

While prokaryotic helicases (e.g. *E. coli* DnaB), and archael replicative helicases (*Sulfolobus* Mcm) usually rely on homohexameric complexes to unwind their DNA, the eukaryotic Mcm2-7 is unique as the only known heterohexameric replicative helicase. These multiple subunits offer Mcm2-7 several advantages over its primitive counterparts, including the ability to differentially control ATP hydrolysis at specific active sites, providing multiple points of regulation within the same complex, and the potential to interact with multiple additional factors at replication forks. As is apparent in the genetic screens of our ATPase active site mutants, the Mcm complex can functionally interface with a wide range of factors involved not just in replication but in cell cycle control, chromosome segregation and DNA repair to list a few examples.

Our findings also hold significance from a clinical point of view. We show that that the misregulation of specific mcm ATPase active sites give rise to phenotypes such as genomic instability, loss of sister chromatid cohesion, DNA damage and aberrant firing of dormant replication origins under conditions where the cell cycle should arrest. Almost all of these phenotypes are common features of different cancers [354, 355]. *mcm4Chaos3* is a well-studied recent example, whereby a change in a conserved amino acid (F345I) results in an unstable Mcm4 protein [356]. While mice bearing this mutation show an elevated incidence of adenocarcinomas, yeast strains engineered to contain the corresponding allele (resulting in an F391I change) also display a classical plasmid loss phenotype and severe genome instability. There are a variety of studies that further show how misregulation of Mcms either as overexpression, impaired subcellular localization, or decreased gene dosage can confer cancer susceptibility and cause chromosome instability [357, 358]. Additionally, monitoring Mcm2 and Mcm5 expression have

been proposed as a prognostic technique in colon cancer [359]. In the latter example, misregulation of Mcm subunits that constitute the regulatory 'gate' within the Mcm complex can have unfavorable consequences for cells, leading us to speculate that regulatory subunits play a key part in ensuring normal Mcm function. Furthermore, many cancer studies have shown the selective misregulation of specific Mcm subunits but not others. Notably, Mcm7 overexpression is correlated with various types of cancer include prostate and non-small lung cancer [360, 361]. Interestingly, Mcm7 has been known to bind several tumor suppressor proteins, most notably retinoblastoma protein Rb, and p130 [362], suggesting that selective overexpression of only certain Mcms may serve as a mechanism to titrate anti-cancer factors to allow proliferation.

Based on the above studies, Mcm regulation seems like an attractive target for designing cancer chemotherapeutics. While Mcms are expressed both by normally proliferating cells and cells with cancer potential, phenotypes arising from Mcm misregulation create basic physiological differences between such cells. For example, a study showed that a reduction of Mcm levels in human cell lines was still able to support replication for a considerable length of time. However, upon induction of replicative stress such cells became highly sensitive to replication inhibitors and showed genetic instability and DNA damage [363]. In principle, cancer cells represent 'stressed' replication environments and therefore it is possible to selectively target Mcms in cancer cells with minimal injury to normal cells. Future studies could also be aimed at exploring the wide range of Mcm interactions and design strategies to selectively target pathways involving Mcm misregulation rather than focusing on one or few factors. Our studies showing Mcm regulation as a common denominator of multiple genomic processes provide a sound theoretical framework for pursuing such avenues.

BIBLIOGRAPHY

1. Bell, S.P. and A. Dutta, *DNA replication in eukaryotic cells.* Annu Rev Biochem, 2002. **71**: p. 333-74.
2. Fachinetti, D., et al., *Replication termination at eukaryotic chromosomes is mediated by Top2 and occurs at genomic loci containing pausing elements.* Mol Cell, 2010. **39**(4): p. 595-605.
3. Cha, R.S. and N. Kleckner, *ATR homolog Mec1 promotes fork progression, thus averting breaks in replication slow zones.* Science, 2002. **297**(5581): p. 602-6.
4. Alzu, A., et al., *Senataxin associates with replication forks to protect fork integrity across RNA-polymerase-II-transcribed genes.* Cell, 2012. **151**(4): p. 835-46.
5. Bermejo, R., et al., *The Replication Checkpoint Protects Fork Stability by Releasing Transcribed Genes from Nuclear Pores.* Cell, 2011. **146**(2): p. 233-246.
6. Bermejo, R., et al., *Top1- and Top2-mediated topological transitions at replication forks ensure fork progression and stability and prevent DNA damage checkpoint activation.* Genes Dev, 2007. **21**(15): p. 1921-36.
7. Sundin, O. and A. Varshavsky, *Terminal stages of SV40 DNA replication proceed via multiply intertwined catenated dimers.* Cell, 1980. **21**(1): p. 103-14.
8. Vijayraghavan, S. and A. Schwacha, *The eukaryotic Mcm2-7 replicative helicase.* Subcell Biochem, 2012. **62**: p. 113-34.
9. Langston, L.D. and M. O'Donnell, *DNA replication: keep moving and don't mind the gap.* Mol Cell, 2006. **23**(2): p. 155-60.
10. Mechali, M., *Eukaryotic DNA replication origins: many choices for appropriate answers.* Nat Rev Mol Cell Biol, 2010. **11**(10): p. 728-38.
11. Eaton, M.L., et al., *Conserved nucleosome positioning defines replication origins.* Genes Dev, 2010. **24**(8): p. 748-53.
12. Sequeira-Mendes, J. and M. Gomez, *On the opportunistic nature of transcription and replication initiation in the metazoan genome.* Bioessays, 2012. **34**(2): p. 119-25.
13. Ge, X.Q., D.a. Jackson, and J.J. Blow, *Dormant origins licensed by excess Mcm2-7 are required for human cells to survive replicative stress.* Genes & development, 2007. **21**: p. 3331-41.
14. Woodward, A.M., et al., *Excess Mcm2-7 license dormant origins of replication that can be used under conditions of replicative stress.* The Journal of cell biology, 2006. **173**: p. 673-83.
15. Jacob, F. and S. Brenner, *[On the regulation of DNA synthesis in bacteria: the hypothesis of the replicon]*. C R Hebd Seances Acad Sci, 1963. **256**: p. 298-300.
16. Bell, S.P., *Eukaryotic replicators and associated protein complexes.* Curr Opin Genet Dev, 1995. **5**(2): p. 162-7.
17. Stinchcomb, D.T., K. Struhl, and R.W. Davis, *Isolation and characterisation of a yeast chromosomal replicator.* Nature, 1979. **282**(5734): p. 39-43.
18. Bell, S.P. and B. Stillman, *ATP-dependent recognition of eukaryotic origins of DNA replication by a multiprotein complex.* Nature, 1992. **357**(6374): p. 128-34.

19. Marahrens, Y. and B. Stillman, *A yeast chromosomal origin of DNA replication defined by multiple functional elements.* Science, 1992. **255**(5046): p. 817-23.
20. Zou, L. and B. Stillman, *Assembly of a complex containing Cdc45p, replication protein A, and Mcm2p at replication origins controlled by S-phase cyclin-dependent kinases and Cdc7p-Dbf4p kinase.* Mol Cell Biol, 2000. **20**(9): p. 3086-96.
21. Raghuraman, M.K., et al., *Replication dynamics of the yeast genome.* Science, 2001. **294**(5540): p. 115-21.
22. Cayrou, C., et al., *New insights into replication origin characteristics in metazoans.* Cell Cycle, 2012. **11**(4).
23. Aggarwal, B.D. and B.R. Calvi, *Chromatin regulates origin activity in Drosophila follicle cells.* Nature, 2004. **430**(6997): p. 372-6.
24. Eaton, M.L., et al., *Chromatin signatures of the Drosophila replication program.* Genome Res, 2011. **21**(2): p. 164-74.
25. Miotto, B., *Regulation of DNA licensing by targeted chromatin remodeling.* Cell Cycle, 2011. **10**(10): p. 1522.
26. Schaper, S. and W. Messer, *Interaction of the initiator protein DnaA of Escherichia coli with its DNA target.* J Biol Chem, 1995. **270**(29): p. 17622-6.
27. Duderstadt, K.E., et al., *Origin remodeling and opening in bacteria rely on distinct assembly states of the DnaA initiator.* J Biol Chem, 2010. **285**(36): p. 28229-39.
28. Grabowski, B. and Z. Kelman, *Archeal DNA replication: eukaryal proteins in a bacterial context.* Annu Rev Microbiol, 2003. **57**: p. 487-516.
29. Randell, J.C., et al., *Sequential ATP hydrolysis by Cdc6 and ORC directs loading of the Mcm2-7 helicase.* Mol Cell, 2006. **21**(1): p. 29-39.
30. Speck, C., et al., *ATPase-dependent cooperative binding of ORC and Cdc6 to origin DNA.* Nat Struct Mol Biol, 2005. **12**(11): p. 965-71.
31. Liu, S., et al., *Structural analysis of human Orc6 protein reveals a homology with transcription factor TFIIB.* Proc Natl Acad Sci U S A, 2011. **108**(18): p. 7373-8.
32. Fernandez-Cid, A., et al., *An ORC/Cdc6/MCM2-7 complex is formed in a multistep reaction to serve as a platform for MCM double-hexamer assembly.* Mol Cell, 2013. **50**(4): p. 577-88.
33. Houchens, C.R., et al., *Multiple mechanisms contribute to Schizosaccharomyces pombe origin recognition complex-DNA interactions.* J Biol Chem, 2008. **283**(44): p. 30216-24.
34. Kuo, A.J., et al., *The BAH domain of ORC1 links H4K20me2 to DNA replication licensing and Meier-Gorlin syndrome.* Nature, 2012. **484**(7392): p. 115-9.
35. Maine, G.T., P. Sinha, and B.K. Tye, *Mutants of S. cerevisiae defective in the maintenance of minichromosomes.* Genetics, 1984. **106**(3): p. 365-85.
36. Tye, B.K., *MCM proteins in DNA replication.* Annu Rev Biochem, 1999. **68**: p. 649-86.
37. Kubota, Y., et al., *Identification of the yeast MCM3-related protein as a component of Xenopus DNA replication licensing factor.* Cell, 1995. **81**(4): p. 601-9.
38. Chong, J.P., et al., *Purification of an MCM-containing complex as a component of the DNA replication licensing system.* Nature, 1995. **375**(6530): p. 418-21.
39. Ishimi, Y., *A DNA helicase activity is associated with an MCM4, -6, and -7 protein complex.* J Biol Chem, 1997. **272**(39): p. 24508-13.
40. Thommes, P., et al., *The RLF-M component of the replication licensing system forms complexes containing all six MCM/P1 polypeptides.* EMBO J, 1997. **16**(11): p. 3312-9.

41. Bochman, M.L., S.P. Bell, and A. Schwacha, *Subunit organization of Mcm2-7 and the unequal role of active sites in ATP hydrolysis and viability.* Mol Cell Biol, 2008. **28**(19): p. 5865-73.
42. Davey, M.J., C. Indiani, and M. O'Donnell, *Reconstitution of the Mcm2-7p heterohexamer, subunit arrangement, and ATP site architecture.* J Biol Chem, 2003. **278**(7): p. 4491-9.
43. Bochman, M.L. and A. Schwacha, *The Mcm complex: unwinding the mechanism of a replicative helicase.* Microbiol Mol Biol Rev, 2009. **73**(4): p. 652-83.
44. Erzberger, J.P. and J.M. Berger, *Evolutionary relationships and structural mechanisms of AAA+ proteins.* Annu Rev Biophys Biomol Struct, 2006. **35**: p. 93-114.
45. Chen, S., et al., *Mechanism of ATP-driven PCNA clamp loading by S. cerevisiae RFC.* J Mol Biol, 2009. **388**(3): p. 431-42.
46. Erzberger, J.P., M.L. Mott, and J.M. Berger, *Structural basis for ATP-dependent DnaA assembly and replication-origin remodeling.* Nat Struct Mol Biol, 2006. **13**(8): p. 676-83.
47. Liu, J., et al., *Structure and function of Cdc6/Cdc18: implications for origin recognition and checkpoint control.* Mol Cell, 2000. **6**(3): p. 637-48.
48. Takisawa, H., S. Mimura, and Y. Kubota, *Eukaryotic DNA replication: from pre-replication complex to initiation complex.* Curr Opin Cell Biol, 2000. **12**(6): p. 690-6.
49. Chen, S., M.A. de Vries, and S.P. Bell, *Orc6 is required for dynamic recruitment of Cdt1 during repeated Mcm2-7 loading.* Genes Dev, 2007. **21**(22): p. 2897-907.
50. Takara, T.J. and S.P. Bell, *Multiple Cdt1 molecules act at each origin to load replication-competent Mcm2-7 helicases.* EMBO J, 2011. **30**(24): p. 4885-96.
51. Davey, M.J., et al., *The DnaC helicase loader is a dual ATP/ADP switch protein.* EMBO J, 2002. **21**(12): p. 3148-59.
52. Tanaka, S. and J.F. Diffley, *Interdependent nuclear accumulation of budding yeast Cdt1 and Mcm2-7 during G1 phase.* Nat Cell Biol, 2002. **4**(3): p. 198-207.
53. Ferenbach, A., et al., *Functional domains of the Xenopus replication licensing factor Cdt1.* Nucleic Acids Res, 2005. **33**(1): p. 316-24.
54. You, Z. and H. Masai, *Cdt1 forms a complex with the minichromosome maintenance protein (MCM) and activates its helicase activity.* J Biol Chem, 2008. **283**(36): p. 24469-77.
55. Teer, J.K. and A. Dutta, *Human Cdt1 lacking the evolutionarily conserved region that interacts with MCM2-7 is capable of inducing re-replication.* J Biol Chem, 2008. **283**(11): p. 6817-25.
56. Whittaker, A.J., I. Royzman, and T.L. Orr-Weaver, *Drosophila double parked: a conserved, essential replication protein that colocalizes with the origin recognition complex and links DNA replication with mitosis and the down-regulation of S phase transcripts.* Genes Dev, 2000. **14**(14): p. 1765-76.
57. Remus, D., et al., *Concerted loading of Mcm2-7 double hexamers around DNA during DNA replication origin licensing.* Cell, 2009. **139**(4): p. 719-30.
58. Tsuyama, T., et al., *Licensing for DNA replication requires a strict sequential assembly of Cdc6 and Cdt1 onto chromatin in Xenopus egg extracts.* Nucleic Acids Res, 2005. **33**(2): p. 765-75.
59. Evrin, C., et al., *A double-hexameric MCM2-7 complex is loaded onto origin DNA during licensing of eukaryotic DNA replication.* Proc Natl Acad Sci U S A, 2009. **106**(48): p. 20240-5.

60. Perkins, G. and J.F. Diffley, *Nucleotide-dependent prereplicative complex assembly by Cdc6p, a homolog of eukaryotic and prokaryotic clamp-loaders.* Mol Cell, 1998. **2**(1): p. 23-32.
61. Evrin, C., et al., *The ORC/Cdc6/MCM2-7 complex facilitates MCM2-7 dimerization during prereplicative complex formation.* Nucleic Acids Res, 2013.
62. Seki, T. and J.F. Diffley, *Stepwise assembly of initiation proteins at budding yeast replication origins in vitro.* Proc Natl Acad Sci U S A, 2000. **97**(26): p. 14115-20.
63. Kang, S., M.D. Warner, and S.P. Bell, *Multiple Functions for Mcm2-7 ATPase Motifs during Replication Initiation.* Mol Cell, 2014.
64. Sun, J., et al., *Cryo-EM structure of a helicase loading intermediate containing ORC-Cdc6-Cdt1-MCM2-7 bound to DNA.* Nat Struct Mol Biol, 2013. **20**(8): p. 944-51.
65. Remus, D., et al., *Concerted loading of Mcm2-7 double hexamers around DNA during DNA replication origin licensing.* Cell, 2009. **139**: p. 719-30.
66. Fletcher, R.J., et al., *The structure and function of MCM from archaeal M. Thermoautotrophicum.* Nat Struct Biol, 2003. **10**(3): p. 160-7.
67. Gambus, A., et al., *MCM2-7 Form Double Hexamers at Licensed Origins in Xenopus Egg Extract.* J Biol Chem, 2011. **286**(13): p. 11855-64.
68. Frigola, J., et al., *ATPase-dependent quality control of DNA replication origin licensing.* Nature, 2013. **495**(7441): p. 339-43.
69. Coster, G., et al., *Origin Licensing Requires ATP Binding and Hydrolysis by the MCM Replicative Helicase.* Mol Cell, 2014.
70. Sheu, Y.J. and B. Stillman, *Cdc7-Dbf4 phosphorylates MCM proteins via a docking site-mediated mechanism to promote S phase progression.* Mol Cell, 2006. **24**(1): p. 101-13.
71. Sclafani, R.A., *Cdc7p-Dbf4p becomes famous in the cell cycle.* J Cell Sci, 2000. **113 (Pt 12)**: p. 2111-7.
72. Nougarede, R., et al., *Hierarchy of S-phase-promoting factors: yeast Dbf4-Cdc7 kinase requires prior S-phase cyclin-dependent kinase activation.* Mol Cell Biol, 2000. **20**(11): p. 3795-806.
73. Ilves, I., et al., *Activation of the MCM2-7 helicase by association with Cdc45 and GINS proteins.* Mol Cell, 2010. **37**(2): p. 247-58.
74. Gambus, A., et al., *GINS maintains association of Cdc45 with MCM in replisome progression complexes at eukaryotic DNA replication forks.* Nat Cell Biol, 2006. **8**(4): p. 358-66.
75. Moyer, S.E., P.W. Lewis, and M.R. Botchan, *a candidate for the eukaryotic DNA replication fork helicase.* PNAS, 2006.
76. Tercero, J.A., K. Labib, and J.F. Diffley, *DNA synthesis at individual replication forks requires the essential initiation factor Cdc45p.* EMBO J, 2000. **19**(9): p. 2082-93.
77. Aparicio, T., A. Ibarra, and J. Mendez, *Cdc45-MCM-GINS, a new power player for DNA replication.* Cell Div, 2006. **1**: p. 18.
78. Kubota, Y., et al., *A novel ring-like complex of Xenopus proteins essential for the initiation of DNA replication.* Genes Dev, 2003. **17**(9): p. 1141-52.
79. Pacek, M. and J.C. Walter, *A requirement for MCM7 and Cdc45 in chromosome unwinding during eukaryotic DNA replication.* EMBO J, 2004. **23**(18): p. 3667-76.
80. Takayama, Y., et al., *GINS, a novel multiprotein complex required for chromosomal DNA replication in budding yeast.* Genes Dev, 2003. **17**(9): p. 1153-65.

81. Moyer, S.E., P.W. Lewis, and M.R. Botchan, *Isolation of the Cdc45/Mcm2-7/GINS (CMG) complex, a candidate for the eukaryotic DNA replication fork helicase.* Proc Natl Acad Sci U S A, 2006. **103**(27): p. 10236-41.
82. Schwacha, A. and S.P. Bell, *Interactions between two catalytically distinct MCM subgroups are essential for coordinated ATP hydrolysis and DNA replication.* Mol Cell, 2001. **8**(5): p. 1093-104.
83. Kaplan, D.L., M.J. Davey, and M. O'Donnell, *Mcm4,6,7 Uses a "Pump in Ring" Mechanism to Unwind DNA by Steric Exclusion and Actively Translocate along a Duplex.* Journal of Biological Chemistry, 2003. **278**(49): p. 49171-49182.
84. Sato, M., et al., *Electron microscopic observation and single-stranded DNA binding activity of the Mcm4,6,7 complex.* J Mol Biol, 2000. **300**(3): p. 421-31.
85. Kanter, D.M., I. Bruck, and D.L. Kaplan, *Mcm subunits can assemble into two different active unwinding complexes.* J Biol Chem, 2008. **283**(45): p. 31172-82.
86. Ying, C.Y. and J. Gautier, *The ATPase activity of MCM2-7 is dispensable for pre-RC assembly but is required for DNA unwinding.* EMBO J, 2005. **24**(24): p. 4334-44.
87. Aparicio, O.M., D.M. Weinstein, and S.P. Bell, *Components and dynamics of DNA replication complexes in S. cerevisiae: redistribution of MCM proteins and Cdc45p during S phase.* Cell, 1997. **91**(1): p. 59-69.
88. Labib, K., J.A. Tercero, and J.F. Diffley, *Uninterrupted MCM2-7 function required for DNA replication fork progression.* Science, 2000. **288**(5471): p. 1643-7.
89. Leon, R.P., M. Tecklenburg, and R.A. Sclafani, *Functional conservation of beta-hairpin DNA binding domains in the Mcm protein of Methanobacterium thermoautotrophicum and the Mcm5 protein of Saccharomyces cerevisiae.* Genetics, 2008. **179**(4): p. 1757-68.
90. Bochman, M.L. and A. Schwacha, *Differences in the single-stranded DNA binding activities of MCM2-7 and MCM467: MCM2 and MCM5 define a slow ATP-dependent step.* J Biol Chem, 2007. **282**(46): p. 33795-804.
91. Liu, W., et al., *Structural analysis of the Sulfolobus solfataricus MCM protein N-terminal domain.* Nucleic Acids Res, 2008. **36**(10): p. 3235-43.
92. McGeoch, A.T., et al., *Organization of the archaeal MCM complex on DNA and implications for the helicase mechanism.* Nat Struct Mol Biol, 2005. **12**(9): p. 756-62.
93. Bochman, M.L. and A. Schwacha, *The Saccharomyces cerevisiae Mcm6/2 and Mcm5/3 ATPase active sites contribute to the function of the putative Mcm2-7 'gate'.* Nucleic Acids Res, 2010. **38**(18): p. 6078-88.
94. Bochman, M.L. and A. Schwacha, *The Mcm2-7 complex has in vitro helicase activity.* Mol Cell, 2008. **31**(2): p. 287-93.
95. Samel, S.A., et al., *A unique DNA entry gate serves for regulated loading of the eukaryotic replicative helicase MCM2-7 onto DNA.* Genes Dev, 2014. **28**(15): p. 1653-66.
96. Costa, A., et al., *The structural basis for MCM2-7 helicase activation by GINS and Cdc45.* Nat Struct Mol Biol, 2011.
97. Costa, A., et al., *The structural basis for MCM2-7 helicase activation by GINS and Cdc45.* Nat Struct Mol Biol, 2011. **18**(4): p. 471-7.
98. Takahashi, T.S., D.B. Wigley, and J.C. Walter, *Pumps, paradoxes and ploughshares: mechanism of the MCM2-7 DNA helicase.* Trends Biochem Sci, 2005. **30**(8): p. 437-44.
99. Wessel, R., J. Schweizer, and H. Stahl, *Simian virus 40 T-antigen DNA helicase is a hexamer which forms a binary complex during bidirectional unwinding from the viral origin of DNA replication.* J Virol, 1992. **66**(2): p. 804-15.

100. Yardimci, H., et al., *Uncoupling of sister replisomes during eukaryotic DNA replication.* Mol Cell, 2010. **40**(5): p. 834-40.
101. Fu, Y.V., et al., *Selective bypass of a lagging strand roadblock by the eukaryotic replicative DNA helicase.* Cell, 2011. **146**(6): p. 931-41.
102. Brewster, A.S., et al., *Mutational analysis of an archaeal minichromosome maintenance protein exterior hairpin reveals critical residues for helicase activity and DNA binding.* BMC Mol Biol, 2010. **11**: p. 62.
103. Brewster, A.S., et al., *Crystal structure of a near-full-length archaeal MCM: functional insights for an AAA+ hexameric helicase.* Proc Natl Acad Sci U S A, 2008. **105**(51): p. 20191-6.
104. Jenkinson, E.R. and J.P. Chong, *Minichromosome maintenance helicase activity is controlled by N- and C-terminal motifs and requires the ATPase domain helix-2 insert.* Proc Natl Acad Sci U S A, 2006. **103**(20): p. 7613-8.
105. Gai, D., et al., *Mechanisms of conformational change for a replicative hexameric helicase of SV40 large tumor antigen.* Cell, 2004. **119**(1): p. 47-60.
106. Sanchez-Pulido, L. and C.P. Ponting, *Cdc45: the missing RecJ ortholog in eukaryotes?* Bioinformatics, 2011. **27**(14): p. 1885-8.
107. Bruck, I. and D.L. Kaplan, *GINS and Sld3 compete with one another for Mcm2-7 and Cdc45 binding.* J Biol Chem, 2011.
108. Szambowska, A., et al., *DNA binding properties of human Cdc45 suggest a function as molecular wedge for DNA unwinding.* Nucleic Acids Res, 2013.
109. Tanaka, S., et al., *CDK-dependent phosphorylation of Sld2 and Sld3 initiates DNA replication in budding yeast.* Nature, 2007. **445**(7125): p. 328-32.
110. Sanchez-Pulido, L., J.F. Diffley, and C.P. Ponting, *Homology explains the functional similarities of Treslin/Ticrr and Sld3.* Curr Biol, 2010. **20**(12): p. R509-10.
111. Bruck, I. and D.L. Kaplan, *GINS and Sld3 compete with one another for Mcm2-7 and Cdc45 binding.* J Biol Chem, 2011. **286**(16): p. 14157-67.
112. Zegerman, P. and J.F. Diffley, *Phosphorylation of Sld2 and Sld3 by cyclin-dependent kinases promotes DNA replication in budding yeast.* Nature, 2007. **445**(7125): p. 281-5.
113. Kamimura, Y., et al., *Sld2, which interacts with Dpb11 in Saccharomyces cerevisiae, is required for chromosomal DNA replication.* Mol Cell Biol, 1998. **18**(10): p. 6102-9.
114. Masumoto, H., et al., *S-Cdk-dependent phosphorylation of Sld2 essential for chromosomal DNA replication in budding yeast.* Nature, 2002. **415**(6872): p. 651-5.
115. Muramatsu, S., et al., *CDK-dependent complex formation between replication proteins Dpb11, Sld2, Pol (epsilon}, and GINS in budding yeast.* Genes Dev, 2010. **24**(6): p. 602-12.
116. Zou, L. and B. Stillman, *Formation of a preinitiation complex by S-phase cyclin CDK-dependent loading of Cdc45p onto chromatin.* Science, 1998. **280**(5363): p. 593-6.
117. Bruck, I. and D.L. Kaplan, *Origin single-stranded DNA releases Sld3 from Mcm2-7, allowing GINS to bind Mcm2-7.* J Biol Chem, 2011.
118. Bramhill, D. and A. Kornberg, *Duplex opening by dnaA protein at novel sequences in initiation of replication at the origin of the E. coli chromosome.* Cell, 1988. **52**(5): p. 743-55.
119. Kanke, M., et al., *Mcm10 plays an essential role in origin DNA unwinding after loading of the CMG components.* EMBO J, 2012. **31**(9): p. 2182-94.

120. Ricke, R.M. and A.K. Bielinsky, *Mcm10 regulates the stability and chromatin association of DNA polymerase-alpha.* Mol Cell, 2004. **16**(2): p. 173-85.
121. Lou, H., et al., *Mrc1 and DNA polymerase epsilon function together in linking DNA replication and the S phase checkpoint.* Mol Cell, 2008. **32**(1): p. 106-17.
122. Nedelcheva, M.N., et al., *Uncoupling of unwinding from DNA synthesis implies regulation of MCM helicase by Tof1/Mrc1/Csm3 checkpoint complex.* J Mol Biol, 2005. **347**(3): p. 509-21.
123. Osborn, A.J. and S.J. Elledge, *Mrc1 is a replication fork component whose phosphorylation in response to DNA replication stress activates Rad53.* Genes Dev, 2003. **17**(14): p. 1755-67.
124. Numata, Y., et al., *Interaction of human MCM2-7 proteins with TIM, TIPIN and Rb.* J Biochem, 2010. **147**(6): p. 917-27.
125. Ryu, M.J., et al., *Direct interaction between cohesin complex and DNA replication machinery.* Biochem Biophys Res Commun, 2006. **341**(3): p. 770-5.
126. Balakrishnan, L. and R.A. Bambara, *Flap endonuclease 1.* Annu Rev Biochem, 2013. **82**: p. 119-38.
127. Bowers, J.L., et al., *ATP hydrolysis by ORC catalyzes reiterative Mcm2-7 assembly at a defined origin of replication.* Mol Cell, 2004. **16**(6): p. 967-78.
128. Donovan, S., et al., *Cdc6p-dependent loading of Mcm proteins onto pre-replicative chromatin in budding yeast.* Proc Natl Acad Sci U S A, 1997. **94**(11): p. 5611-6.
129. Mizushima, T., N. Takahashi, and B. Stillman, *Cdc6p modulates the structure and DNA binding activity of the origin recognition complex in vitro.* Genes Dev, 2000. **14**(13): p. 1631-41.
130. Wohlschlegel, J.A., et al., *Inhibition of eukaryotic DNA replication by geminin binding to Cdt1.* Science, 2000. **290**(5500): p. 2309-12.
131. Lee, C., et al., *Structural basis for inhibition of the replication licensing factor Cdt1 by geminin.* Nature, 2004. **430**(7002): p. 913-7.
132. Koepp, D.M., et al., *The F-box protein Dia2 regulates DNA replication.* Mol Biol Cell, 2006. **17**(4): p. 1540-8.
133. Li, J.M., M.T. Tetzlaff, and S.J. Elledge, *Identification of MSA1, a cell cycle-regulated, dosage suppressor of drc1/sld2 and dpb11 mutants.* Cell Cycle, 2008. **7**(21): p. 3388-98.
134. Kamimura, Y., et al., *Sld3, which interacts with Cdc45 (Sld4), functions for chromosomal DNA replication in Saccharomyces cerevisiae.* EMBO J, 2001. **20**(8): p. 2097-107.
135. Yabuuchi, H., et al., *Ordered assembly of Sld3, GINS and Cdc45 is distinctly regulated by DDK and CDK for activation of replication origins.* EMBO J, 2006. **25**(19): p. 4663-74.
136. Tanaka, S., et al., *Origin association of Sld3, Sld7, and Cdc45 proteins is a key step for determination of origin-firing timing.* Curr Biol, 2011. **21**(24): p. 2055-63.
137. Tanaka, T., et al., *Sld7, an Sld3-associated protein required for efficient chromosomal DNA replication in budding yeast.* EMBO J, 2011. **30**(10): p. 2019-30.
138. Muramatsu, S., et al., *CDK-dependent complex formation between replication proteins Dpb11, Sld2, Pol ϵ, and GINS in budding yeast.* Genes Dev, 2010. **24**(6): p. 602-12.
139. Tak, Y.S., et al., *A CDK-catalysed regulatory phosphorylation for formation of the DNA replication complex Sld2-Dpb11.* EMBO J, 2006. **25**(9): p. 1987-96.
140. Garcia, V., K. Furuya, and A.M. Carr, *Identification and functional analysis of TopBP1 and its homologs.* DNA Repair (Amst), 2005. **4**(11): p. 1227-39.

141. Aparicio, T., et al., *The human GINS complex associates with Cdc45 and MCM and is essential for DNA replication.* Nucleic acids research, 2009. **37**: p. 2087-95.
142. Costa, A., et al., *The structural basis for MCM2-7 helicase activation by GINS and Cdc45.* Nat Struct Mol Biol, 2011. **18**(4): p. 471-477.
143. Zou, L., J. Mitchell, and B. Stillman, *CDC45, a novel yeast gene that functions with the origin recognition complex and Mcm proteins in initiation of DNA replication.* Mol Cell Biol, 1997. **17**(2): p. 553-63.
144. Kunkel, T.A. and P.M. Burgers, *Dividing the workload at a eukaryotic replication fork.* Trends Cell Biol, 2008. **18**(11): p. 521-7.
145. Burgers, P.M., *Polymerase dynamics at the eukaryotic DNA replication fork.* J Biol Chem, 2009. **284**(7): p. 4041-5.
146. Muzi-Falconi, M., et al., *The DNA polymerase alpha-primase complex: multiple functions and interactions.* ScientificWorldJournal, 2003. **3**: p. 21-33.
147. Chowdhury, A., et al., *The DNA unwinding element binding protein DUE-B interacts with Cdc45 in preinitiation complex formation.* Mol Cell Biol, 2010. **30**(6): p. 1495-507.
148. Balestrini, A., et al., *GEMC1 is a TopBP1-interacting protein required for chromosomal DNA replication.* Nat Cell Biol, 2010. **12**(5): p. 484-91.
149. Homesley, L., et al., *Mcm10 and the MCM2-7 complex interact to initiate DNA synthesis and to release replication factors from origins.* Genes Dev, 2000. **14**(8): p. 913-26.
150. van Deursen, F., et al., *Mcm10 associates with the loaded DNA helicase at replication origins and defines a novel step in its activation.* EMBO J, 2012. **31**(9): p. 2195-206.
151. Wohlschlegel, J.A., et al., *Xenopus Mcm10 binds to origins of DNA replication after Mcm2-7 and stimulates origin binding of Cdc45.* Mol Cell, 2002. **9**(2): p. 233-40.
152. Maiorano, D., et al., *MCM8 is an MCM2-7-related protein that functions as a DNA helicase during replication elongation and not initiation.* Cell, 2005. **120**: p. 315-28.
153. Lutzmann, M. and M. Mechali, *MCM9 binds Cdt1 and is required for the assembly of prereplication complexes.* Mol Cell, 2008. **31**(2): p. 190-200.
154. Gambus, A., et al., *A key role for Ctf4 in coupling the MCM2-7 helicase to DNA polymerase alpha within the eukaryotic replisome.* EMBO J, 2009. **28**(19): p. 2992-3004.
155. Zhu, W., et al., *Mcm10 and And-1/CTF4 recruit DNA polymerase alpha to chromatin for initiation of DNA replication.* Genes Dev, 2007. **21**(18): p. 2288-99.
156. Duncker, B.P., et al., *Cyclin B-cdk1 kinase stimulates ORC- and Cdc6-independent steps of semiconservative plasmid replication in yeast nuclear extracts.* Mol Cell Biol, 1999. **19**(2): p. 1226-41.
157. Masuda, T., S. Mimura, and H. Takisawa, *CDK- and Cdc45-dependent priming of the MCM complex on chromatin during S-phase in Xenopus egg extracts: possible activation of MCM helicase by association with Cdc45.* Genes Cells, 2003. **8**(2): p. 145-61.
158. Schwob, E. and K. Nasmyth, *CLB5 and CLB6, a new pair of B cyclins involved in DNA replication in Saccharomyces cerevisiae.* Genes Dev, 1993. **7**(7A): p. 1160-75.
159. Wilmes, G.M., et al., *Interaction of the S-phase cyclin Clb5 with an "RXL" docking sequence in the initiator protein Orc6 provides an origin-localized replication control switch.* Genes Dev, 2004. **18**(9): p. 981-91.
160. Chuang, L.C., et al., *Phosphorylation of Mcm2 by Cdc7 promotes pre-replication complex assembly during cell-cycle re-entry.* Mol Cell, 2009. **35**(2): p. 206-16.
161. Donaldson, A.D., W.L. Fangman, and B.J. Brewer, *Cdc7 is required throughout the yeast S phase to activate replication origins.* Genes Dev, 1998. **12**(4): p. 491-501.

162. Dowell, S.J., P. Romanowski, and J.F. Diffley, *Interaction of Dbf4, the Cdc7 protein kinase regulatory subunit, with yeast replication origins in vivo.* Science, 1994. **265**(5176): p. 1243-6.
163. Duncker, B.P. and G.W. Brown, *Cdc7 kinases (DDKs) and checkpoint responses: lessons from two yeasts.* Mutat Res, 2003. **532**(1-2): p. 21-7.
164. Jares, P., A. Donaldson, and J.J. Blow, *The Cdc7/Dbf4 protein kinase: target of the S phase checkpoint?* EMBO Rep, 2000. **1**(4): p. 319-22.
165. Sheu, Y.J. and B. Stillman, *The Dbf4-Cdc7 kinase promotes S phase by alleviating an inhibitory activity in Mcm4.* Nature, 2010. **463**(7277): p. 113-7.
166. Swaminathan, S., et al., *Yra1 is required for S phase entry and affects Dia2 binding to replication origins.* Mol Cell Biol, 2007. **27**(13): p. 4674-84.
167. Wold, M.S., *Replication protein A: a heterotrimeric, single-stranded DNA-binding protein required for eukaryotic DNA metabolism.* Annu Rev Biochem, 1997. **66**: p. 61-92.
168. Dionne, I., et al., *On the mechanism of loading the PCNA sliding clamp by RFC.* Mol Microbiol, 2008. **68**(1): p. 216-22.
169. Kumar, R., et al., *Stepwise loading of yeast clamp revealed by ensemble and single-molecule studies.* Proc Natl Acad Sci U S A, 2010. **107**(46): p. 19736-41.
170. Trakselis, M.A. and S.J. Benkovic, *Intricacies in ATP-dependent clamp loading: variations across replication systems.* Structure, 2001. **9**(11): p. 999-1004.
171. Kubota, T., et al., *The Elg1 replication factor C-like complex functions in PCNA unloading during DNA replication.* Mol Cell, 2013. **50**(2): p. 273-80.
172. Shiomi, Y., et al., *A second proliferating cell nuclear antigen loader complex, Ctf18-replication factor C, stimulates DNA polymerase eta activity.* J Biol Chem, 2007. **282**(29): p. 20906-14.
173. Bylund, G.O. and P.M. Burgers, *Replication protein A-directed unloading of PCNA by the Ctf18 cohesion establishment complex.* Mol Cell Biol, 2005. **25**(13): p. 5445-55.
174. Wang, J.C., *Cellular roles of DNA topoisomerases: a molecular perspective.* Nat Rev Mol Cell Biol, 2002. **3**(6): p. 430-40.
175. Baxter, J. and J.F. Diffley, *Topoisomerase II inactivation prevents the completion of DNA replication in budding yeast.* Mol Cell, 2008. **30**(6): p. 790-802.
176. Nishiyama, A., L. Frappier, and M. Mechali, *MCM-BP regulates unloading of the MCM2-7 helicase in late S phase.* Genes Dev, 2011. **25**(2): p. 165-75.
177. Ayyagari, R., et al., *Okazaki fragment maturation in yeast. I. Distribution of functions between FEN1 AND DNA2.* J Biol Chem, 2003. **278**(3): p. 1618-25.
178. Storici, F., et al., *The flexible loop of human FEN1 endonuclease is required for flap cleavage during DNA replication and repair.* EMBO J, 2002. **21**(21): p. 5930-42.
179. Bando, M., et al., *Csm3, Tof1, and Mrc1 form a heterotrimeric mediator complex that associates with DNA replication forks.* J Biol Chem, 2009. **284**(49): p. 34355-65.
180. Katou, Y., et al., *S-phase checkpoint proteins Tof1 and Mrc1 form a stable replication-pausing complex.* Nature, 2003. **424**(6952): p. 1078-83.
181. Randell, J.C., et al., *Mec1 is one of multiple kinases that prime the Mcm2-7 helicase for phosphorylation by Cdc7.* Mol Cell, 2010. **40**(3): p. 353-63.
182. Haering, C.H., et al., *Molecular architecture of SMC proteins and the yeast cohesin complex.* Mol Cell, 2002. **9**(4): p. 773-88.
183. Nasmyth, K. and C.H. Haering, *Cohesin: its roles and mechanisms.* Annu Rev Genet, 2009. **43**: p. 525-58.

184. Toth, A., et al., *Yeast cohesin complex requires a conserved protein, Eco1p(Ctf7), to establish cohesion between sister chromatids during DNA replication.* Genes Dev, 1999. **13**(3): p. 320-33.
185. Kenna, M.A. and R.V. Skibbens, *Mechanical link between cohesion establishment and DNA replication: Ctf7p/Eco1p, a cohesion establishment factor, associates with three different replication factor C complexes.* Mol Cell Biol, 2003. **23**(8): p. 2999-3007.
186. Ciosk, R., et al., *Cohesin's binding to chromosomes depends on a separate complex consisting of Scc2 and Scc4 proteins.* Mol Cell, 2000. **5**(2): p. 243-54.
187. Gordon, G.S. and A. Wright, *DNA segregation in bacteria.* Annu Rev Microbiol, 2000. **54**: p. 681-708.
188. Fukuura, M., et al., *CDK promotes interactions of Sld3 and Drc1 with Cut5 for initiation of DNA replication in fission yeast.* Mol Biol Cell, 2011. **22**(14): p. 2620-33.
189. Weinreich, M., et al., *Binding of cyclin-dependent kinases to ORC and Cdc6p regulates the chromosome replication cycle.* Proc Natl Acad Sci U S A, 2001. **98**(20): p. 11211-7.
190. Chen, S. and S.P. Bell, *CDK prevents Mcm2-7 helicase loading by inhibiting Cdt1 interaction with Orc6.* Genes & development, 2011.
191. Perkins, G., L.S. Drury, and J.F. Diffley, *Separate SCF(CDC4) recognition elements target Cdc6 for proteolysis in S phase and mitosis.* EMBO J, 2001. **20**(17): p. 4836-45.
192. Nguyen, V.Q., et al., *Clb/Cdc28 kinases promote nuclear export of the replication initiator proteins Mcm2-7.* Curr Biol, 2000. **10**(4): p. 195-205.
193. Nguyen, V.Q., C. Co, and J.J. Li, *Cyclin-dependent kinases prevent DNA re-replication through multiple mechanisms.* Nature, 2001. **411**(6841): p. 1068-73.
194. Bousset, K. and J.F. Diffley, *The Cdc7 protein kinase is required for origin firing during S phase.* Genes Dev, 1998. **12**(4): p. 480-90.
195. Masai, H., et al., *Phosphorylation of MCM4 by Cdc7 kinase facilitates its interaction with Cdc45 on the chromatin.* J Biol Chem, 2006. **281**(51): p. 39249-61.
196. Francis, L.I., et al., *Incorporation into the prereplicative complex activates the Mcm2-7 helicase for Cdc7-Dbf4 phosphorylation.* Genes & development, 2009. **23**: p. 643-54.
197. Weinreich, M. and B. Stillman, *Cdc7p-Dbf4p kinase binds to chromatin during S phase and is regulated by both the APC and the RAD53 checkpoint pathway.* EMBO J, 1999. **18**(19): p. 5334-46.
198. Harper, J.W. and S.J. Elledge, *The DNA damage response: ten years after.* Mol Cell, 2007. **28**(5): p. 739-45.
199. Cimprich, K.A. and D. Cortez, *ATR: an essential regulator of genome integrity.* Nat Rev Mol Cell Biol, 2008. **9**(8): p. 616-27.
200. Lopes, M., et al., *The DNA replication checkpoint response stabilizes stalled replication forks.* Nature, 2001. **412**(6846): p. 557-61.
201. Barbour, L., et al., *DNA damage checkpoints are involved in postreplication repair.* Genetics, 2006. **174**(4): p. 1789-800.
202. Foiani, M., et al., *DNA damage checkpoints and DNA replication controls in Saccharomyces cerevisiae.* Mutat Res, 2000. **451**(1-2): p. 187-96.
203. Alcasabas, A.A., et al., *Mrc1 transduces signals of DNA replication stress to activate Rad53.* Nat Cell Biol, 2001. **3**(11): p. 958-65.
204. Santocanale, C. and J.F. Diffley, *A Mec1- and Rad53-dependent checkpoint controls late-firing origins of DNA replication.* Nature, 1998. **395**(6702): p. 615-8.

205. Branzei, D. and M. Foiani, *The Rad53 signal transduction pathway: Replication fork stabilization, DNA repair, and adaptation.* Exp Cell Res, 2006. **312**(14): p. 2654-9.
206. Vialard, J.E., et al., *The budding yeast Rad9 checkpoint protein is subjected to Mec1/Tel1-dependent hyperphosphorylation and interacts with Rad53 after DNA damage.* EMBO J, 1998. **17**(19): p. 5679-88.
207. Naylor, M.L., et al., *Mrc1 phosphorylation in response to DNA replication stress is required for Mec1 accumulation at the stalled fork.* Proc Natl Acad Sci U S A, 2009. **106**(31): p. 12765-70.
208. Szyjka, S.J., et al., *Rad53 regulates replication fork restart after DNA damage in Saccharomyces cerevisiae.* Genes Dev, 2008. **22**(14): p. 1906-20.
209. Fiorentini, P., et al., *Exonuclease I of Saccharomyces cerevisiae functions in mitotic recombination in vivo and in vitro.* Mol Cell Biol, 1997. **17**(5): p. 2764-73.
210. Tsubouchi, H. and H. Ogawa, *Exo1 roles for repair of DNA double-strand breaks and meiotic crossing over in Saccharomyces cerevisiae.* Mol Biol Cell, 2000. **11**(7): p. 2221-33.
211. Segurado, M. and J.F. Diffley, *Separate roles for the DNA damage checkpoint protein kinases in stabilizing DNA replication forks.* Genes Dev, 2008. **22**(13): p. 1816-27.
212. Smolka, M.B., et al., *Proteome-wide identification of in vivo targets of DNA damage checkpoint kinases.* Proc Natl Acad Sci U S A, 2007. **104**(25): p. 10364-9.
213. Chen, S.H., et al., *A proteome-wide analysis of kinase-substrate network in the DNA damage response.* J Biol Chem, 2010. **285**(17): p. 12803-12.
214. Albuquerque, C.P., et al., *A multidimensional chromatography technology for in-depth phosphoproteome analysis.* Mol Cell Proteomics, 2008. **7**(7): p. 1389-96.
215. Cheung, H.C., et al., *An S/T-Q cluster domain census unveils new putative targets under Tel1/Mec1 control.* BMC Genomics, 2012. **13**: p. 664.
216. Jossen, R. and R. Bermejo, *The DNA damage checkpoint response to replication stress: A Game of Forks.* Front Genet, 2013. **4**: p. 26.
217. Randell, J.C.W., et al., *Mec1 Is One of Multiple Kinases that Prime the Mcm2-7 Helicase for Phosphorylation by Cdc7.* Molecular Cell, 2010. **40**: p. 353-363.
218. Ilves, I., N. Tamberg, and M.R. Botchan, *Checkpoint kinase 2 (Chk2) inhibits the activity of the Cdc45/MCM2-7/GINS (CMG) replicative helicase complex.* Proc Natl Acad Sci U S A, 2012. **109**(33): p. 13163-70.
219. Komata, M., et al., *The direct binding of Mrc1, a checkpoint mediator, to Mcm6, a replication helicase, is essential for the replication checkpoint against methyl methanesulfonate-induced stress.* Mol Cell Biol, 2009. **29**(18): p. 5008-19.
220. Lou, H., et al., *Mrc1 and DNA polymerase epsilon function together in linking DNA replication and the S phase checkpoint.*, in *Molecular cell*. 2008. p. 106-17.
221. Hashimoto, Y., F. Puddu, and V. Costanzo, *RAD51- and MRE11-dependent reassembly of uncoupled CMG helicase complex at collapsed replication forks.* Nat Struct Mol Biol, 2012. **19**(1): p. 17-24.
222. Forsburg, S.L., *Eukaryotic MCM proteins: beyond replication initiation.* Microbiol Mol Biol Rev, 2004. **68**(1): p. 109-31.
223. Pacek, M., et al., *Localization of MCM2-7, Cdc45, and GINS to the site of DNA unwinding during eukaryotic DNA replication.* Mol Cell, 2006. **21**(4): p. 581-7.

224. Kulczyk, A.W., et al., *An interaction between DNA polymerase and helicase is essential for the high processivity of the bacteriophage T7 replisome.* J Biol Chem, 2012. **287**(46): p. 39050-60.
225. Kim, S., et al., *Coupling of a replicative polymerase and helicase: a tau-DnaB interaction mediates rapid replication fork movement.* Cell, 1996. **84**(4): p. 643-50.
226. Georgescu, R.E., et al., *Mechanism of asymmetric polymerase assembly at the eukaryotic replication fork.* Nat Struct Mol Biol, 2014.
227. Patel, S.S., M. Pandey, and D. Nandakumar, *Dynamic coupling between the motors of DNA replication: hexameric helicase, DNA polymerase, and primase.* Curr Opin Chem Biol, 2011. **15**(5): p. 595-605.
228. Sengupta, S., et al., *Dpb2 integrates the leading-strand DNA polymerase into the eukaryotic replisome.* Curr Biol, 2013. **23**(7): p. 543-52.
229. Kang, Y.H., et al., *Properties of the human Cdc45/Mcm2-7/GINS helicase complex and its action with DNA polymerase epsilon in rolling circle DNA synthesis.* Proc Natl Acad Sci U S A, 2012. **109**(16): p. 6042-7.
230. Duggin, I.G., et al., *The replication fork trap and termination of chromosome replication.* Mol Microbiol, 2008. **70**(6): p. 1323-33.
231. Brewer, B.J. and W.L. Fangman, *A replication fork barrier at the 3' end of yeast ribosomal RNA genes.* Cell, 1988. **55**(4): p. 637-43.
232. Lambert, S., et al., *Gross chromosomal rearrangements and elevated recombination at an inducible site-specific replication fork barrier.* Cell, 2005. **121**(5): p. 689-702.
233. Admire, A., et al., *Cycles of chromosome instability are associated with a fragile site and are increased by defects in DNA replication and checkpoint controls in yeast.* Genes Dev, 2006. **20**(2): p. 159-73.
234. Greenfeder, S.A. and C.S. Newlon, *Replication forks pause at yeast centromeres.* Mol Cell Biol, 1992. **12**(9): p. 4056-66.
235. Sundin, O. and A. Varshavsky, *Arrest of segregation leads to accumulation of highly intertwined catenated dimers: dissection of the final stages of SV40 DNA replication.* Cell, 1981. **25**(3): p. 659-69.
236. Hashash, N., A.L. Johnson, and R.S. Cha, *Topoisomerase II- and condensin-dependent breakage of MEC1ATR-sensitive fragile sites occurs independently of spindle tension, anaphase, or cytokinesis.* PLoS Genet, 2012. **8**(10): p. e1002978.
237. Sakwe, A.M., et al., *Identification and characterization of a novel component of the human minichromosome maintenance complex.* Mol Cell Biol, 2007. **27**(8): p. 3044-55.
238. Nishiyama, A., L. Frappier, and M. Méchali, *MCM-BP regulates unloading of the MCM2-7 helicase in late S phase.* Genes & development, 2010.
239. Schmidt, K.H. and R.D. Kolodner, *Suppression of spontaneous genome rearrangements in yeast DNA helicase mutants.* Proc Natl Acad Sci U S A, 2006. **103**(48): p. 18196-201.
240. Ivessa, A.S., et al., *Saccharomyces Rrm3p, a 5' to 3' DNA helicase that promotes replication fork progression through telomeric and subtelomeric DNA.* Genes Dev, 2002. **16**(11): p. 1383-96.
241. Marston, A.L., *Chromosome segregation in budding yeast: sister chromatid cohesion and related mechanisms.* Genetics, 2014. **196**(1): p. 31-63.
242. Ng, T.M., et al., *Pericentromeric sister chromatid cohesion promotes kinetochore biorientation.* Mol Biol Cell, 2009. **20**(17): p. 3818-27.

243. Gruber, S., et al., *Evidence that loading of cohesin onto chromosomes involves opening of its SMC hinge.* Cell, 2006. **127**(3): p. 523-37.
244. Gruber, S., C.H. Haering, and K. Nasmyth, *Chromosomal cohesin forms a ring.* Cell, 2003. **112**(6): p. 765-77.
245. Haering, C.H., et al., *Structure and stability of cohesin's Smc1-kleisin interaction.* Mol Cell, 2004. **15**(6): p. 951-64.
246. Burmann, F., et al., *An asymmetric SMC-kleisin bridge in prokaryotic condensin.* Nat Struct Mol Biol, 2013. **20**(3): p. 371-9.
247. Onn, I., et al., *Sister chromatid cohesion: a simple concept with a complex reality.* Annu Rev Cell Dev Biol, 2008. **24**: p. 105-29.
248. Kogut, I., et al., *The Scc2/Scc4 cohesin loader determines the distribution of cohesin on budding yeast chromosomes.* Genes Dev, 2009. **23**(19): p. 2345-57.
249. Guacci, V., D. Koshland, and A. Strunnikov, *A direct link between sister chromatid cohesion and chromosome condensation revealed through the analysis of MCD1 in S. cerevisiae.* Cell, 1997. **91**(1): p. 47-57.
250. Laloraya, S., V. Guacci, and D. Koshland, *Chromosomal addresses of the cohesin component Mcd1p.* J Cell Biol, 2000. **151**(5): p. 1047-56.
251. Fernius, J. and A.L. Marston, *Establishment of cohesion at the pericentromere by the Ctf19 kinetochore subcomplex and the replication fork-associated factor, Csm3.* PLoS Genet, 2009. **5**(9): p. e1000629.
252. Heidinger-Pauli, J.M., E. Unal, and D. Koshland, *Distinct targets of the Eco1 acetyltransferase modulate cohesion in S phase and in response to DNA damage.* Mol Cell, 2009. **34**(3): p. 311-21.
253. Rolef Ben-Shahar, T., et al., *Eco1-dependent cohesin acetylation during establishment of sister chromatid cohesion.* Science, 2008. **321**(5888): p. 563-6.
254. Sutani, T., et al., *Budding yeast Wpl1(Rad61)-Pds5 complex counteracts sister chromatid cohesion-establishing reaction.* Curr Biol, 2009. **19**(6): p. 492-7.
255. Unal, E., et al., *A molecular determinant for the establishment of sister chromatid cohesion.* Science, 2008. **321**(5888): p. 566-9.
256. Borges, V., et al., *Hos1 deacetylates Smc3 to close the cohesin acetylation cycle.* Mol Cell, 2010. **39**(5): p. 677-88.
257. Heck, M.M., *Condensins, cohesins, and chromosome architecture: how to make and break a mitotic chromosome.* Cell, 1997. **91**(1): p. 5-8.
258. Hirano, T., *Condensins: organizing and segregating the genome.* Curr Biol, 2005. **15**(7): p. R265-75.
259. Renshaw, M.J., et al., *Condensins promote chromosome recoiling during early anaphase to complete sister chromatid separation.* Dev Cell, 2010. **19**(2): p. 232-44.
260. Baxter, J. and L. Aragon, *A model for chromosome condensation based on the interplay between condensin and topoisomerase II.* Trends Genet, 2012. **28**(3): p. 110-7.
261. Nezi, L. and A. Musacchio, *Sister chromatid tension and the spindle assembly checkpoint.* Curr Opin Cell Biol, 2009. **21**(6): p. 785-95.
262. Thomas, B.J. and R. Rothstein, *Elevated recombination rates in transcriptionally active DNA.* Cell, 1989. **56**(4): p. 619-30.
263. Hogan, E. and D. Koshland, *Addition of extra origins of replication to a minichromosome suppresses its mitotic loss in cdc6 and cdc14 mutants of Saccharomyces cerevisiae.* Proc Natl Acad Sci U S A, 1992. **89**(7): p. 3098-102.

264. Goldstein, A.L. and J.H. McCusker, *Three new dominant drug resistance cassettes for gene disruption in Saccharomyces cerevisiae.* Yeast, 1999. **15**(14): p. 1541-53.
265. Longtine, M.S., et al., *Additional modules for versatile and economical PCR-based gene deletion and modification in Saccharomyces cerevisiae.* Yeast, 1998. **14**(10): p. 953-61.
266. Guldener, U., et al., *A new efficient gene disruption cassette for repeated use in budding yeast.* Nucleic Acids Res, 1996. **24**(13): p. 2519-24.
267. Funakoshi, M. and M. Hochstrasser, *Small epitope-linker modules for PCR-based C-terminal tagging in Saccharomyces cerevisiae.* Yeast, 2009. **26**(3): p. 185-92.
268. Nakamura, A., et al., *Techniques for gamma-H2AX detection.* Methods Enzymol, 2006. **409**: p. 236-50.
269. Straight, A.F., et al., *GFP tagging of budding yeast chromosomes reveals that protein protein interactions can mediate sister chromatid cohesion.* Curr Biol., 1996. **6**(12): p. 1599-1608.
270. Wright, A.P., M. Bruns, and B.S. Hartley, *Extraction and rapid inactivation of proteins from Saccharomyces cerevisiae by trichloroacetic acid precipitation.* Yeast, 1989. **5**(1): p. 51-3.
271. Bhamidipati, A., et al., *Exploration of the Topological Requirements of ERAD Identifies Yos9p as a Lectin Sensor of Misfolded Glycoproteins in the ER Lumen.* Mol Cell, 2005. **19**(6): p. 741-751.
272. Tong, A.H., et al., *Systematic genetic analysis with ordered arrays of yeast deletion mutants.* Science, 2001. **294**(5550): p. 2364-8.
273. Megee, P.C. and D. Koshland, *A Functional Assay for Centromere-Associated Sister Chromatid Cohesion.* Science, 1999. **285**(5425): p. 254-257.
274. Vernis, L., J. Piskur, and J.F.X. Diffley, *Reconstitution of an efficient thymidine salvage pathway in Saccharomyces cerevisiae.* Nucleic Acids Res, 2003. **31**(19): p. e120.
275. Desany, B.A., et al., *Recovery from DNA replicational stress is the essential function of the S-phase checkpoint pathway.* Genes Dev, 1998. **12**(18): p. 2956-70.
276. Paulovich, A.G. and L.H. Hartwell, *A checkpoint regulates the rate of progression through S phase in S. cerevisiae in response to DNA damage.* Cell, 1995. **82**(5): p. 841-7.
277. Kastan, M.B. and J. Bartek, *Cell-cycle checkpoints and cancer.* Nature, 2004. **432**(7015): p. 316-23.
278. Savitsky, K., et al., *A single ataxia telangiectasia gene with a product similar to PI-3 kinase.* Science, 1995. **268**(5218): p. 1749-1753.
279. Sanchez, Y., et al., *Regulation of RAD53 by the ATM-like kinases MEC1 and TEL1 in yeast cell cycle checkpoint pathways.* Science, 1996. **271**(5247): p. 357-60.
280. Mordes, D.A., E.A. Nam, and D. Cortez, *Dpb11 activates the Mec1-Ddc2 complex.* Proc Natl Acad Sci U S A, 2008. **105**(48): p. 18730-4.
281. Zou, L. and S.J. Elledge, *Sensing DNA damage through ATRIP recognition of RPA-ssDNA complexes.* Science, 2003. **300**(5625): p. 1542-8.
282. Kawabata, T., et al., *Stalled Fork Rescue via Dormant Replication Origins in Unchallenged S Phase Promotes Proper Chromosome Segregation and Tumor Suppression.* Mol Cell, 2011. **41**(5): p. 543-53.
283. Andreson, B.L., et al., *The ribonucleotide reductase inhibitor, Sml1, is sequentially phosphorylated, ubiquitylated and degraded in response to DNA damage.* Nucleic Acids Res, 2010. **38**(19): p. 6490-501.

284. Bochman, M.L. and A. Schwacha, *The Saccharomyces cerevisiae Mcm6/2 and Mcm5/3 ATPase active sites contribute to the function of the putative Mcm2-7 'gate'.* Nucleic acids research, 2010. **38**: p. 6078-88.
285. Gilbert, C.S., et al., *The budding yeast Rad9 checkpoint complex: chaperone proteins are required for its function.* EMBO Rep, 2003. **4**(10): p. 953-8.
286. Redon, C., D.R. Pilch, and W.M. Bonner, *Genetic analysis of Saccharomyces cerevisiae H2A serine 129 mutant suggests a functional relationship between H2A and the sister-chromatid cohesion partners Csm3-Tof1 for the repair of topoisomerase I-induced DNA damage.* Genetics, 2006. **172**(1): p. 67-76.
287. Zhao, X., et al., *The ribonucleotide reductase inhibitor Sml1 is a new target of the Mec1/Rad53 kinase cascade during growth and in response to DNA damage.* EMBO J, 2001. **20**(13): p. 3544-53.
288. Nyberg, K.A., et al., *Toward maintaining the genome: DNA damage and replication checkpoints.* Annu Rev Genet, 2002. **36**: p. 617-56.
289. Poli, J., et al., *dNTP pools determine fork progression and origin usage under replication stress.* EMBO J, 2012. **advance online publication**.
290. Crabbe, L., et al., *Analysis of replication profiles reveals key role of RFC-Ctf18 in yeast replication stress response.* Nat Struct Mol Biol, 2010. **17**(11): p. 1391-1397.
291. Shima, N., et al., *A viable allele of Mcm4 causes chromosome instability and mammary adenocarcinomas in mice.* Nat Genet, 2007. **39**(1): p. 93-8.
292. Li, X.C. and B.K. Tye, *Ploidy dictates repair pathway choice under DNA replication stress.* Genetics, 2011. **187**(4): p. 1031-40.
293. Stead, B.E., et al., *ATP Binding and Hydrolysis by Mcm2 Regulate DNA Binding by Mcm Complexes.* J Mol Biol, 2009. **391**(2): p. 301-313.
294. De Piccoli, G., et al., *Replisome stability at defective DNA replication forks is independent of S phase checkpoint kinases.* Mol Cell, 2012. **45**(5): p. 696-704.
295. Bermejo, R., et al., *The replication checkpoint protects fork stability by releasing transcribed genes from nuclear pores.* Cell, 2011. **146**(2): p. 233-46.
296. Lou, H., et al., *Mrc1 and DNA Polymerase Epsilon Function Together in Linking DNA Replication and the S Phase Checkpoint.* Mol Cell, 2008. **32**(1): p. 106-117.
297. Tsubouchi, T. and G.S. Roeder, *A synaptonemal complex protein promotes homology-independent centromere coupling.* Science, 2005. **308**(5723): p. 870-3.
298. San Filippo, J., P. Sung, and H. Klein, *Mechanism of eukaryotic homologous recombination.* Annu Rev Biochem, 2008. **77**: p. 229-57.
299. Moore, J.K. and J.E. Haber, *Cell cycle and genetic requirements of two pathways of nonhomologous end-joining repair of double-strand breaks in Saccharomyces cerevisiae.* Mol Cell Biol, 1996. **16**(5): p. 2164-73.
300. Mao, Z., et al., *DNA repair by nonhomologous end joining and homologous recombination during cell cycle in human cells.* Cell Cycle, 2008. **7**(18): p. 2902-6.
301. Lisby, M., R. Rothstein, and U.H. Mortensen, *Rad52 forms DNA repair and recombination centers during S phase.* Proc Natl Acad Sci U S A, 2001. **98**(15): p. 8276-82.
302. Pilch, D.R., et al., *Characteristics of gamma-H2AX foci at DNA double-strand breaks sites.* Biochem Cell Biol, 2003. **81**(3): p. 123-9.
303. Moreau, S., E.A. Morgan, and L.S. Symington, *Overlapping functions of the Saccharomyces cerevisiae Mre11, Exo1 and Rad27 nucleases in DNA metabolism.* Genetics, 2001. **159**(4): p. 1423-33.

304. Lisby, M., et al., *Choreography of the DNA damage response: spatiotemporal relationships among checkpoint and repair proteins.* Cell, 2004. **118**(6): p. 699-713.
305. Aylon, Y. and M. Kupiec, *DSB repair: the yeast paradigm.* DNA Repair (Amst), 2004. **3**(8-9): p. 797-815.
306. Assenmacher, N. and K.P. Hopfner, *MRE11/RAD50/NBS1: complex activities.* Chromosoma, 2004. **113**(4): p. 157-66.
307. Hopfner, K.P., et al., *Structural biochemistry and interaction architecture of the DNA double-strand break repair Mre11 nuclease and Rad50-ATPase.* Cell, 2001. **105**(4): p. 473-85.
308. Lobachev, K.S., D.A. Gordenin, and M.A. Resnick, *The Mre11 complex is required for repair of hairpin-capped double-strand breaks and prevention of chromosome rearrangements.* Cell, 2002. **108**(2): p. 183-93.
309. Wu, D., L.M. Topper, and T.E. Wilson, *Recruitment and dissociation of nonhomologous end joining proteins at a DNA double-strand break in Saccharomyces cerevisiae.* Genetics, 2008. **178**(3): p. 1237-49.
310. Clerici, M., et al., *The Saccharomyces cerevisiae Sae2 protein promotes resection and bridging of double strand break ends.* J Biol Chem, 2005. **280**(46): p. 38631-8.
311. Mimitou, E.P. and L.S. Symington, *Sae2, Exo1 and Sgs1 collaborate in DNA double-strand break processing.* Nature, 2008. **455**(7214): p. 770-4.
312. Rogakou, E.P., et al., *DNA double-stranded breaks induce histone H2AX phosphorylation on serine 139.* J Biol Chem, 1998. **273**(10): p. 5858-68.
313. Huyen, Y., et al., *Methylated lysine 79 of histone H3 targets 53BP1 to DNA double-strand breaks.* Nature, 2004. **432**(7015): p. 406-11.
314. Barlow, J.H., M. Lisby, and R. Rothstein, *Differential regulation of the cellular response to DNA double-strand breaks in G1.* Mol Cell, 2008. **30**(1): p. 73-85.
315. Navadgi-Patil, V.M. and P.M. Burgers, *Cell-cycle-specific activators of the Mec1/ATR checkpoint kinase.* Biochem Soc Trans, 2011. **39**(2): p. 600-5.
316. Yang, X.H. and L. Zou, *Recruitment of ATR-ATRIP, Rad17, and 9-1-1 complexes to DNA damage.* Methods Enzymol, 2006. **409**: p. 118-31.
317. Sugiyama, T., et al., *Rad52-mediated DNA annealing after Rad51-mediated DNA strand exchange promotes second ssDNA capture.* EMBO J, 2006. **25**(23): p. 5539-48.
318. Barlow, J.H. and R. Rothstein, *Rad52 recruitment is DNA replication independent and regulated by Cdc28 and the Mec1 kinase.* EMBO J, 2009. **28**(8): p. 1121-30.
319. Lee, S.E., et al., *Yeast Rad52 and Rad51 recombination proteins define a second pathway of DNA damage assessment in response to a single double-strand break.* Mol Cell Biol, 2003. **23**(23): p. 8913-23.
320. Symington, L.S., *Role of RAD52 epistasis group genes in homologous recombination and double-strand break repair.* Microbiol Mol Biol Rev, 2002. **66**(4): p. 630-70, table of contents.
321. Shcheprova, Z., et al., *A mechanism for asymmetric segregation of age during yeast budding.* Nature, 2008. **454**(7205): p. 728-34.
322. Henderson, K.A. and D.E. Gottschling, *A mother's sacrifice: what is she keeping for herself?* Curr Opin Cell Biol, 2008. **20**(6): p. 723-8.
323. Xu, H., C. Boone, and G.W. Brown, *Genetic dissection of parallel sister-chromatid cohesion pathways.* Genetics, 2007. **176**(3): p. 1417-29.

324. Noble, D., et al., *Intersection between the regulators of sister chromatid cohesion establishment and maintenance in budding yeast indicates a multi-step mechanism.* Cell Cycle, 2006. **5**(21): p. 2528-36.
325. Strom, L., et al., *Postreplicative formation of cohesion is required for repair and induced by a single DNA break.* Science, 2007. **317**(5835): p. 242-5.
326. Unal, E., J.M. Heidinger-Pauli, and D. Koshland, *DNA double-strand breaks trigger genome-wide sister-chromatid cohesion through Eco1 (Ctf7).* Science, 2007. **317**(5835): p. 245-8.
327. Lyons, N.A., et al., *Sequential primed kinases create a damage-responsive phosphodegron on Eco1.* Nat Struct Mol Biol, 2013. **20**(2): p. 194-201.
328. Peters, J.M., *The anaphase promoting complex/cyclosome: a machine designed to destroy.* Nat Rev Mol Cell Biol, 2006. **7**(9): p. 644-56.
329. Alexandru, G., et al., *Phosphorylation of the cohesin subunit Scc1 by Polo/Cdc5 kinase regulates sister chromatid separation in yeast.* Cell, 2001. **105**(4): p. 459-72.
330. Vanoosthuyse, V. and K.G. Hardwick, *Bub1 and the multilayered inhibition of Cdc20-APC/C in mitosis.* Trends Cell Biol, 2005. **15**(5): p. 231-3.
331. Alani, E., et al., *Characterization of DNA-binding and strand-exchange stimulation properties of y-RPA, a yeast single-strand-DNA-binding protein.* J Mol Biol, 1992. **227**(1): p. 54-71.
332. Blobel, G., *Gene gating: a hypothesis.* Proc Natl Acad Sci U S A, 1985. **82**(24): p. 8527-9.
333. Ünal, E., et al., *A Molecular Determinant for the Establishment of Sister Chromatid Cohesion.* Science, 2008. **321**(5888): p. 566-569.
334. Lisby, M. and R. Rothstein, *Choreography of recombination proteins during the DNA damage response.* DNA Repair (Amst), 2009. **8**(9): p. 1068-76.
335. Pacek, M. and J.C. Walter, *A requirement for MCM7 and Cdc45 in chromosome unwinding during eukaryotic DNA replication.* EMBO J, 2004. **23**(18): p. 3667-3676.
336. Sabatinos, S.A., M.D. Green, and S.L. Forsburg, *Continued DNA synthesis in replication checkpoint mutants leads to fork collapse.* Mol Cell Biol, 2012. **32**(24): p. 4986-97.
337. Steinacher, R., et al., *The DNA helicase Pfh1 promotes fork merging at replication termination sites to ensure genome stability.* Genes Dev, 2012. **26**(6): p. 594-602.
338. Osman, F. and M.C. Whitby, *Exploring the roles of Mus81-Eme1/Mms4 at perturbed replication forks.* DNA Repair (Amst), 2007. **6**(7): p. 1004-17.
339. Kai, M., et al., *Replication checkpoint kinase Cds1 regulates Mus81 to preserve genome integrity during replication stress.* Genes Dev, 2005. **19**(8): p. 919-32.
340. Murfuni, I., et al., *Survival of the replication checkpoint deficient cells requires MUS81-RAD52 function.* PLoS Genet, 2013. **9**(10): p. e1003910.
341. Gilson, E. and V. Geli, *How telomeres are replicated.* Nat Rev Mol Cell Biol, 2007. **8**(10): p. 825-38.
342. Tsolou, A. and D. Lydall, *Mrc1 protects uncapped budding yeast telomeres from exonuclease EXO1.* DNA Repair (Amst), 2007. **6**(11): p. 1607-17.
343. Megee, P.C. and D. Koshland, *A functional assay for centromere-associated sister chromatid cohesion.* Science, 1999. **285**(5425): p. 254-7.
344. Ishimi, Y., et al., *Identification of MCM4 as a target of the DNA replication block checkpoint system.* The Journal of biological chemistry, 2003. **278**: p. 24644-50.

345. Ishimi, Y., et al., *Levels of MCM4 phosphorylation and DNA synthesis in DNA replication block checkpoint control.* Journal of Structural Biology, 2004. **146**(1-2): p. 234-41.
346. Sheu, Y.J., et al., *Domain within the helicase subunit Mcm4 integrates multiple kinase signals to control DNA replication initiation and fork progression.* Proc Natl Acad Sci U S A, 2014. **111**(18): p. E1899-908.
347. Gomez, E.B., M.G. Catlett, and S.L. Forsburg, *Different phenotypes in vivo are associated with ATPase motif mutations in Schizosaccharomyces pombe minichromosome maintenance proteins.* Genetics, 2002. **160**(4): p. 1305-18.
348. You, Z., Y. Komamura, and Y. Ishimi, *Biochemical analysis of the intrinsic Mcm4-Mcm6-mcm7 DNA helicase activity.* Mol Cell Biol, 1999. **19**(12): p. 8003-15.
349. Hanson, P.I. and S.W. Whiteheart, *AAA+ proteins: have engine, will work.* Nat Rev Mol Cell Biol, 2005. **6**(7): p. 519-29.
350. Tong, A.H. and C. Boone, *Synthetic genetic array analysis in Saccharomyces cerevisiae.* Methods Mol Biol, 2006. **313**: p. 171-92.
351. Ishimi, Y., et al., *Biochemical function of mouse minichromosome maintenance 2 protein.* J Biol Chem, 1998. **273**(14): p. 8369-75.
352. Takahashi, K., H. Yamada, and M. Yanagida, *Fission yeast minichromosome loss mutants mis cause lethal aneuploidy and replication abnormality.* Molecular Biology of the Cell, 1994. **5**(10): p. 1145-58.
353. Bos, J.L., H. Rehmann, and A. Wittinghofer, *GEFs and GAPs: critical elements in the control of small G proteins.* Cell, 2007. **129**(5): p. 865-77.
354. Barber, T.D., et al., *Chromatid cohesion defects may underlie chromosome instability in human colorectal cancers.* Proc Natl Acad Sci U S A, 2008. **105**(9): p. 3443-8.
355. Negrini, S., V.G. Gorgoulis, and T.D. Halazonetis, *Genomic instability--an evolving hallmark of cancer.* Nat Rev Mol Cell Biol, 2010. **11**(3): p. 220-8.
356. Li, X.C., J.C. Schimenti, and B.K. Tye, *Aneuploidy and improved growth are coincident but not causal in a yeast cancer model.* PLoS Biol, 2009. **7**(7): p. e1000161.
357. Chuang, C.H., et al., *Incremental genetic perturbations to MCM2-7 expression and subcellular distribution reveal exquisite sensitivity of mice to DNA replication stress.* PLoS Genet, 2010. **6**(9): p. e1001110.
358. Ishimi, Y., et al., *Enhanced expression of Mcm proteins in cancer cells derived from uterine cervix.* Eur J Biochem, 2003. **270**(6): p. 1089-101.
359. Giaginis, C., et al., *Clinical significance of MCM-2 and MCM-5 expression in colon cancer: association with clinicopathological parameters and tumor proliferative capacity.* Dig Dis Sci, 2009. **54**(2): p. 282-91.
360. Ren, B., et al., *MCM7 amplification and overexpression are associated with prostate cancer progression.* Oncogene, 2006. **25**(7): p. 1090-8.
361. Toyokawa, G., et al., *Minichromosome Maintenance Protein 7 is a potential therapeutic target in human cancer and a novel prognostic marker of non-small cell lung cancer.* Mol Cancer, 2011. **10**: p. 65.
362. Sterner, J.M., et al., *Negative regulation of DNA replication by the retinoblastoma protein is mediated by its association with MCM7.* Mol Cell Biol, 1998. **18**(5): p. 2748-57.
363. Ibarra, A., E. Schwob, and J. Mendez, *Excess MCM proteins protect human cells from replicative stress by licensing backup origins of replication.* Proc Natl Acad Sci U S A, 2008. **105**(26): p. 8956-61.